

Non-invasive Peripheral Perfusion Monitoring using Photoplethysmography

Musabbir Khan

A thesis submitted for the degree of

Doctor of Philosophy

in

Bioengineering

at the

University of Canterbury,

Christchurch, New Zealand

September 2016

Acknowledgements

It is my great pleasure to thank a number of people and organization who have made my time working on this research during the last few years a rewarding experience.

My supervisors, Distinguished Prof. Geoff Chase, Dr Chris Pretty, and Dr Geoff Shaw, thank you for all of your support, patience, guidance and wisdom over the past few years. I have learnt a lot from you both and I appreciate the time you have given me.

Alexander, Joel, and Lachlan, thanks a lot for their technical support and assistance to make the MOOSE study happen and beyond. Thank you all for providing your contributions and sharing your knowledge.

St George's Hospital, thanks for sponsoring the MOOSE study. In particular, thanks to Nikki Wood and all the staffs in the hospital ICU for their help, time, and support.

Rodney Elliott for providing his technical expertise and being patient at times. Thank you very much for your guidance and troubleshooting problems with my research equipment time to time.

All the colleagues in the Centre for Bioengineering, thanks for creating an amazing and friendly environment to work in, and organizing delicious potlucks. You all made life at work really nice. In particular, thanks to Guo, Azlan, Salwa, Alex, Shun, Hina, and Melanie for their friendship.

My parents, siblings, and my wife Ludmila, thank you all for your unconditional love, comfort, and encouragement throughout the duration of my studies. I could not have completed this work without the support you all have provided me outside of university.

Finally, thanks to almighty god, Allah, for everything I am and everything I achieved. Please, always guide me in the right path.

Contents

Acknowledgements	3
Contents	5
List of Figures.....	12
List of Tables	16
Nomenclature	Error! Bookmark not defined.
Abstract.....	19
Chapter 1: Introduction.....	23
1.1 Research overview.....	34
1.1.1 Clinical significance of this research	34
1.1.2 Research goals	35
1.2 Preface.....	37
Chapter 2: Background and literature review.....	40
2.1 Pulse oximetry and photoplethysmography.....	40
2.1.1 History of pulse oximetry	41
2.1.2 Photoplethysmography origin.....	42
2.1.3 Pulse oximetry principles	43
2.1.4 Beer-Lambert model	45
2.1.5 Empirical calibration to determine oxygen saturation	46
2.1.6 Calibration free methods of SpO ₂ estimation.....	49
2.2 Photoplethysmography signal and modes	50
2.2.1 PPG signal components	50
2.2.2 PPG waveform and shape	51
2.2.3 Transmission and Reflectance mode photoplethysmography	53
2.3 Applications of PPG and its limitations.....	54
2.3.1 Blood flow and perfusion monitoring	54
2.3.2 Heart rate variability.....	55
2.3.3 Cardiac output and pulse transit time	55

2.3.4 Blood Pressure estimation.....	56
2.3.5 Peripheral and systemic resistance assessment	57
2.3.6 Aging and vascular disease assessment.....	57
2.3.7 Vasopastic conditions assessment	58
2.3.8 Limitations.....	58
2.4 Perfusion monitoring	25
2.4.1 Definition.....	25
2.4.2 Peripheral perfusion monitoring	25
2.5 Perfusion and sepsis	26
2.5.1 Epidemiology of sepsis	27
2.5.2 Microvascular perfusion dysfunction in sepsis	30
2.5.3 Assessment of peripheral perfusion during sepsis	32
2.5.4 Peripheral blood flow and SvO_2 evaluation in sepsis	33
2.6 Venous physiology and SvO_2 assessment	59
2.6.1 Physiology of peripheral venous compartment.....	60
2.6.2 Methods to assess tissue perfusion and SvO_2	61
2.7 Existing research into non-invasive methods to assess SvO_2	63
2.7.1 Venous pulsation using mechanical ventilation to assess SvO_2 .	63
2.7.2 Estimation of SvO_2 using natural venous pulsation	64
2.7.3 External venous pulsation to assess SvO_2	65
2.7.4 Venous occlusion dependent peripheral SvO_2 estimation using NIRS	66
2.7.5 Peripheral SvO_2 estimation using NIRS.....	68
2.8 Discussion and integration	69
2.9 Summary.....	71
Chapter 3: Design and development of a novel pulse oximeter system	72
3.1 Introduction.....	72
3.2 System Background.....	73
3.3 Signal Acquisition	74
3.3.1 Sensor principles	74
3.3.2 Intensity control.....	75
3.3.3 Signal conditioning	78

3.3.4 Signal sampling and recording	80
3.4 Firmware and user interface development.....	81
3.4.1 Firmware and Finite state machine development.....	81
3.4.2 Pulse oximeter user interface	83
3.5 Summary.....	87
Chapter 4: PPG processing and analysis	88
4.1 Introduction.....	88
4.2 Data and signal processing.....	89
4.2.1 Processing interface.....	89
4.2.2 Filter design and implementation	89
4.3 Peak-trough detection.....	92
4.3.1 Zero-crossing method.....	93
4.3.2 Trough-thresholding method	94
4.3.3 Crossing-crossing method.....	95
4.3.4 Comparison tests between the three methods.....	96
4.4 SpO ₂ assessment.....	99
4.4.1 R value estimation.....	99
4.4.2 SpO ₂ estimation.....	100
4.5 HR assessment.....	102
4.5.1 Frequency domain method.....	103
4.5.2 Time domain method	103
4.5.3 Comparison between the two methods.....	104
4.6 Summary.....	105
Chapter 5: Effect of temperature on PPG signal quality	106
5.1 Introduction.....	106
5.2 Related studies, test equipment and ethics.....	107
5.2.1 Related study	107
5.2.2 Equipment set up for Study 1.....	108
5.2.3 Ethics approval for Studies 1 and 2	109
5.3 Experimental Protocol	109
5.3.1 Study 1	109

5.3.2 Study 2	111
5.4 PPG signal analysis	112
5.4.1 Signals of interest	112
5.4.2 Metric for SNR	112
5.4.3 Statistical analysis	113
5.5 Results.....	113
5.5.1 RMS data comparison	113
5.5.2 Tri-linear model.....	114
5.5.3 Amplitude data comparison	116
5.5.4 Statistical differences	117
5.5.5 Correlation between pulse oximeters.....	118
5.5.6 Main outcome from Study 2	119
5.6 Discussion.....	120
5.6.1 Overall outcome	120
5.6.2 Inaccuracy of the commercial pulse oximeter.....	124
5.6.3 Study limitation and validation.....	125
5.7 Summary.....	125
Chapter 6: Monitoring peripheral blood flow changes using photoplethysmography	127
6.1 Introduction.....	127
6.2 Vascular Doppler Ultrasound.....	129
6.2.1 Technology Fundamentals	129
6.2.2 Doppler Velocity Waveform.....	130
6.2.3 Other features and modification	132
6.2.4 Preliminary tests	133
6.3 Main Study.....	134
6.3.1 Ethics Approval.....	134
6.3.2 Experimental Protocol.....	134
6.3.3 Signal Analysis.....	136
6.4 Results.....	137
6.4.1 Blood flow change detection	137
6.4.2 Median PPG and Doppler data analysis	139

6.4.3 Correlation between the two measurements.....	142
6.4.4 Heart rate assessment.....	143
6.5 Discussion.....	144
6.5.1 Blood flow trends	144
6.5.2 Vasodilation during post occlusion hyperemia	146
6.5.3 Overall outcome	147
6.5.4 Study Limitations	148
6.6 Summary.....	149
Chapter 7: Estimation of peripheral venous saturation and oxygen extraction using a novel pulse oximeter method	150
7.1 Introduction.....	150
7.2. Artificial venous blood modulation using the compliance difference principle 151	
7.2.1 Arterial-venous compartment compliance difference principle151	
7.2.2 Artificial pulse generation system development	153
7.2.3 APG pressure control and selection test.....	154
7.2.4 APG frequency selection test.....	155
7.2.5 GUI to operate APG.....	156
7.3 Study protocol and data processing	157
7.3.1 Ethics approval	157
7.3.2 Study protocol	157
7.3.3 Data processing and analysis	158
7.4 Results and discussion.....	160
7.4.1 Venous pulse detection	160
7.4.2 Instantaneous saturation estimation	162
7.4.3 SpO ₂ assessment by the two pulse oximeters.....	163
7.4.4 Main Outcome.....	163
7.4.5 Limitations and future work.....	165
7.5 Summary.....	166
Chapter 8: Clinical validation trial of a novel pulse oximeter concept for non-invasive estimation of peripheral venous saturation	167
8.1 Introduction.....	167

8.1.1 MOOSE trial Background.....	168
8.2 Improvements to the APG system and PPG processing	168
8.2.1 Pressure regulation with ITV001	169
8.2.2 Pressure regulation interface.....	170
8.2.3 Additional filter to extract APG signals	171
8.3 Ethics approval and study cohort	172
8.3.1 HDEC ethics approval	172
8.3.2 Study cohort.....	172
8.4 Methodology, trial protocol and modifications	173
8.4.1Additional equipment employed.....	173
8.4.2 Study set up procedure	174
8.4.3 Experimental protocol.....	175
8.4.4 Problems encountered and changes in study procedure.....	179
8.5 Data processing and Analysis	181
8.5.1 Data processing	181
8.5.2 Statistical analysis	182
8.5.3 Error propagation analysis	182
8.6 Results.....	186
8.6.1 Detection of AC and APG signals from PPG.....	186
8.6.2 Interesting findings in Test 4	188
8.6.3 Correlation between R _{Ven} and SvO ₂	190
8.6.4 Study Measurements	192
8.7 Discussion.....	195
8.7.1 Main outcome.....	195
8.7.2 Difference between R _{Art} and R _{Ven} modulation ratios	196
8.7.3 Low oxygen saturation detection using PPG	197
8.7.4 Limitations.....	200
8.8 Summary.....	201
Chapter 9: Conclusions	203
9.1 Outcomes from Thesis: Part 1	203
9.2 Outcomes from Thesis: Part 2	205

9.3 Overall outcome	207
Chapter 10: Future Work.....	209
10.1 Improvements to the PO system	209
10.2 Modifications to the sensor and clinical applicability.....	210
10.3 Assessment of absolute blood flow.....	211
10.4 Further testing and application of the SvO_2 estimation model	211
References	213
Appendix	230

List of Figures

FIGURE 1.1: CRITERIA FOR SIRS, SEPSIS, SEVERE SEPSIS, AND SEPTIC SHOCK ACCORDING TO THE 1991 ACCP/SCCM CONSENSUS CONFERENCE. ADAPTED FROM: BONE ET AL. (1992).	27
FIGURE 1.2: SEPSIS HAVING THE HIGHEST NUMBER OF INCIDENCES IN US/EUROPE RECEIVING THE LOWEST AMOUNT RESEARCH FUNDING COMPARED TO OTHER MEDICAL CONDITIONS. SOURCE: KUNZ (2012).....	29
FIGURE 1.3: RELATIONSHIP BETWEEN SUBLINGUAL MICRO CIRCULATION AND ICU MORTALITY IN 252 PATIENTS WITH SEVERE SEPSIS. THE PATIENTS WERE GROUPED INTO QUARTILES IN PROPORTION OF PERFUSED CAPILLARIES. SOURCE: DE BACKER ET AL. (2014).	31
FIGURE 2.1: ABSORPTION SPECTRA OF THE FOUR TYPES OF HAEMOGLOBIN, SHOWING THE EXTINCTION COEFFICIENTS ($\text{LMMOL}^{-1}\text{CM}^{-1}$) AT RED AND INFRARED WAVELENGTHS. REPRODUCED FROM TREMPER AND BARKER (1989).	44
FIGURE 2.2: TYPICAL PULSE OXIMETER CALIBRATION CURVE ALSO SHOWING THE BEER-LAMBERT MODEL. SOURCE: ROSS (1999).	47
FIGURE 2.3: DYNAMIC LIGHT ABSORPTION OF VASCULAR BED DURING CARDIAC CYCLE. SOURCE: TAMURA ET AL. (2014).....	51
FIGURE 2.4: A TYPICAL PPG WAVEFORM PULSE SHOWING SOME FEATURES.	52
FIGURE 2.5: TRANSMISSION VS REFLECTION MODE PHOTOPLETHYSMOGRAPHY	53
FIGURE 3.1: HARDWARE CIRCUITRY OF PO SYSTEM, ALONG WITH THE SENSOR.....	73
FIGURE 3.2: BLOCK DIAGRAM FOR THE PO SYSTEM.....	74
FIGURE 3.3: SENSOR LED TIMING DIAGRAM	75
FIGURE 3.4: LED SWITCHING AND INTENSITY CONTROL CIRCUIT DIAGRAM, WHERE TRANSISTORS Q1 AND Q4 ARE THE CONTROLLING THE IR LED, AND Q2 AND Q3 ARE CONTROLLING THE RD LED.	76
FIGURE 3.5: RELATIONSHIP BETWEEN LED CURRENT VS DAC COUNT, THUS LED INTENSITY CHARACTERISTICS.....	77
FIGURE 3.6: RELATIONSHIP BETWEEN BEAM POWER AND DAC COUNT FOR RD AND IR LEDs.....	78

FIGURE 3.7: TRANSIMPEDANCE AMPLIFIER CIRCUIT, WHERE U1 REPRESENTS STAGE 1 AND U2 REPRESENTS STAGE 2 AMPLIFIERS, RESPECTIVELY.....	79
FIGURE 3.8: BLOCK DIAGRAM SHOWING THE LED CURRENT CONTROL, THE TRANSIMPEDANCE AMPLIFIER STAGES, AND THE ADC END OF THE PULSE OXIMETER'S FRONT-END.....	80
FIGURE 3.9: PO SYSTEM FIRMWARE TOP LEVEL BLOCK DIAGRAM.....	82
FIGURE 3.10: FSM STATES AND TRANSITIONS FOR LED INTENSITY CONTROL.....	82
FIGURE 3.11: FLOWCHART FOR THE PPG ACQUISITION AND MONITORING GUI.....	85
FIGURE 3.12: PULSE OXIMETER LABVIEW GUI, SHOWING THE MONITORING TAB IN THE FRONT PANEL.....	86
FIGURE 4.1: FILTER DESIGN OF THE FIRST STAGE LOW PASS FILTER, WHICH REMOVES HIGH FREQUENCY NOISE FROM THE PPG.....	91
FIGURE 4.2: AN EXAMPLE OF PPG DATA WITH IDENTIFIED PEAKS AND TROUGHS.....	93
FIGURE 4.3: THREE PEAK-TROUGH DETECTION METHODS WERE APPLIED FOR A GIVEN PPG SIGNAL; ZERO-CROSSING (TOP), TROUGH-BASED THRESHOLDING (MIDDLE), CROSSING-CROSSING (BOTTOM). INCORRECT OR MISSED PEAKS/TROUGHS ARE HIGHLIGHTED WITH DASHED BLUE CIRCLE.....	97
FIGURE 4.4: AMPLITUDE $ AC $ AND CORRESPONDING DC_{MEAN} VALUES DETERMINED FROM IR AC AND DC SIGNALS, RESPECTIVELY, AS AN EXAMPLE.....	99
FIGURE 4.5: INSTANTANEOUS AND OVERALL SPO_2 ESTIMATED FOR A TEST PPG DATA USING EQUATION 4.5.....	102
FIGURE 4.6: POWER SPECTRAL DENSITY OF THE IR PPG, WITH THE DC COMPONENT REMOVED, AS AN EXAMPLE. ALL THE CARDIAC FREQUENCIES ARE LABELLED. THE HIGHEST PEAK MAGNITUDE, AT ABOUT 1 Hz, IS THE HR.....	103
FIGURE 4.7: PPG BASED HR ASSESSMENT USING THE TWO METHODS; FFT BLOCK METHOD (TOP) AND PEAK-PEAK BLOCK METHOD (BOTTOM).....	104
FIGURE 5.1: FLOWCHART OF THE EXPERIMENTAL PROTOCOL, SHOWING THE STEP-BY-STEP PROCESS. THE OVERALL SERIES OF TEST CAPTURES NORMAL, RELATIVELY COLD AND RELATIVELY WARM TEMEPRATURES.....	110
FIGURE 5.2: AC SIGNAL RMS VERSUS TEMPERATURE FROM THE THREE DIFFERENT EXPERIMENTS: IR (LEFT), RD (RIGHT).....	115
FIGURE 5.3: MEDIAN AC SIGNAL AMPLITUDE FOR THE COHORT FROM THE THREE TESTS.....	116

FIGURE 5.4: AC SIGNALS FROM THE 3 TESTS FOR SUBJECTS 19 (LEFT) AND 20 (RIGHT): COLD (A), BASELINE (B), AND WARM (C).....	117
FIGURE 5.5: FRONT PANEL OF NPB-75 DISPLAYING PPG SIGNAL AND DATA FOR SUBJECT 20: COLD (LEFT), BASELINE (MIDDLE) AND WARM (RIGHT).	118
FIGURE 6.1: TYPICAL APPEARANCE OF A DIRECTIONAL DOPPLER WAVEFORM FROM A NORMAL COMMON FEMORAL ARTERY (A), SHOWING THE FLOW ENVELOPE AT VARIOUS PHASES OF THE FLOW CYCLE (B) AND RELATED VELOCITIES. ADAPTED FROM (VOWDEN AND VOWDEN, 2004)	131
FIGURE 6.2: MOUNTING DESIGNED TO ASSIST IN HOLDING THE BV-520T PROBE AT FIXED 30° ANGLE OF INSONATION	132
FIGURE 6.3: THE BV-520T AND PO SENSORS SET UP DURING THE STUDY.....	135
FIGURE 6.4: PEAK-TROUGH DETECTION ALGORITHM, TO EXTRACT AC AMPLITUDE ($ AC $) INFORMATION FROM THE AC SIGNAL OF RD AND IR PPGs.....	137
FIGURE 6.5: BLOOD FLOW CHANGE TREND CAPTURED FOR ONE SUBJECT DURING THE WHOLE EXPERIMENT WITH PPG (TOP) AND DOPPLER (BOTTOM).....	138
FIGURE 6.6: TRAJECTORY OF THE MEDIAN AC SIGNAL AMPLITUDE AND DOPPLER VELOCITY VALUES FOR THE WHOLE STUDY; PHASE 1 – BASELINE, PHASE 2 – PARTIAL OCCLUSION, PHASE 3 – FULL OCCLUSION, PHASE 4 – RECOVERY1, PHASE 5 – RECOVERY 2.	141
FIGURE 6.7: CORRELATION BETWEEN MEAN PULSE AMPLITUDE AND VELOCITY OF BLOOD FLOW FOR THE WHOLE COHORT	142
FIGURE 6.8: DETECTED HR TREND USING THE PPG SENSOR TREND FOR SUBJECT 2 DURING THE EXPERIMENT, WITH NO HR DETECTED DURING FULL OCCLUSION.	143
FIGURE 7.1: CROSS SECTION VIEW OF A TYPICAL ARTERY AND VEIN, DEPICTING THE DIFFERENCE IN VESSEL ELASTICITY. ADAPTED FROM: WESTER ET AL. (2013).	151
FIGURE 7.2: THE RELATIONSHIP BETWEEN VOLUME AND PRESSURE WITHIN BOTH THE ARTERIAL AND VENOUS SYSTEMS. ADAPTED FROM: (WARDHAN AND SHELLEY (2009); MOHRMAN ET AL. (2006); KLABUNDE (2011); WESTER ET AL. (2013); HALL (2006)).....	152
FIGURE 7.3: PPG SENSOR AND DIGIT CUFF PLACEMENT	153
FIGURE 7.4: APG SYSTEM FUNCTIONAL BLOCK DIAGRAM ILLUSTRATING OVERALL OPERATION....	155
FIGURE 7.5: LABVIEW GUI USED TO CONTROL THE APG SYSTEM	156

FIGURE 7.6: DERIVED COMPONENTS FROM WALTON'S TIME DOMAIN EQUATIONS, IN TERMS OF THE AC AND DC PPG SIGNALS.	159
FIGURE 7.7: PPG SIGNALS OF SUBJECT 6: DC (TOP), AC (MIDDLE) AND RAW (BOTTOM) FOR EACH SUBJECT.	161
FIGURE 7.8: PPG SIGNALS OF SUBJECT 9: DC (TOP), AC (MIDDLE) AND RAW (BOTTOM) FOR EACH SUBJECT.	161
FIGURE 7.9: INSTANTANEOUS SAO_2 AND SVO_2 CALCULATED FOR SUBJECTS 6 AND 9, FOR AN ILLUSTRATIVE PORTION OF THE BASELINE AND APG PERIODS.....	162
FIGURE 7.10: POWER SPECTRUM OF IR PPG SIGNAL FOR SUBJECT 4, WITH LABELLED HARMONICS.	165
FIGURE 8.1: BLOCK DIAGRAM OF THE ITV001 PRESSURE REGULATOR WORKING PRINCIPLE.	169
FIGURE 8.2: LABVIEW BASED APG PRESSURE CONTROL GUI.	171
FIGURE 8.3: TYPICAL EQUIPMENT SET UP FOR THE MOOSE STUDY. ALL COMPONENTS ARE INDIVIDUALLY LABELLED.	175
FIGURE 8.4: CLINICIANS DRAWING VENOUS BLOOD SAMPLE FROM THE PERIPHERAL VEIN OF A SUBJECT VIA THE VENOUS LINE IV CATHETER.	177
FIGURE 8.5: A SUBJECT EXERCISING THE HAND USING A SQUASHABLE TOY DURING TEST 3.....	179
FIGURE 8.6: BASELINE PPG SIGNALS SHOWING PRE APG AND POST APG PHASES FOR SUBJECT 7; STARTING FROM THE TOP 1) AC SIGNAL, 2) APG SIGNAL, 3) DC SIGNAL, AND 4) RAW SIGNAL.	186
FIGURE 8.7: FREQUENCY POWER SPECTRUMS FOR SUBJECT 7 FROM TEST 1 WITH LABELLED FREQUENCIES; (A) AC SIGNAL AT RD, (B) AC SIGNAL AT IR, (C) APG SIGNAL AT RD, (D) APG SIGNAL AT IR, (E) DC SIGNAL AT RD, AND (F) DC SIGNAL AT IR.....	188
FIGURE 8.8: PPG SIGNALS FOR SUBJECT 7 IN TEST 4; STARTING FROM THE TOP 1) AC SIGNAL, 2) APG SIGNAL, 3) DC SIGNAL, AND 4) RAW SIGNAL.	189
FIGURE 8.9: CORRELATION ($R^2 = 0.9515$) BETWEEN ALL ESTIMATED R_{VEN} AND MEASURED SVO_2 SAMPLES ACROSS THE WHOLE COHORT FROM THE 3 TESTS. THE SOLID BLUE LINE IS THE PROPOSED SPVO_2 CALIBRATION MODEL AND THE DASHED RED LINE IS THE EMPIRICAL SPO_2 CALIBRATION MODEL (WEBSTER, 2002).	191

List of Tables

TABLE 1.1: WORLDWIDE INCIDENCES OF SEPSIS AND RELATED MORTALITY AS DETERMINED IN 8 STUDIES.....	28
TABLE 4.1: SPECIFICITY AND SENSITIVITY RATINGS FOR ASSESSED PEAK-TROUGH DETECTION ALGORITHMS	97
TABLE 5.1: DEMOGRAPHICS, PPG SIGNAL RMS, AND MEDIAN TEMPERATURE DATA FOR ALL SUBJECTS FROM THE STUDY	114
TABLE 5.2: RESULTS OF NON-PARAMETRIC STATISTICAL TEST COMPARISON BETWEEN EXPERIMENTAL DATA SETS	117
TABLE 5.3: MEDIAN SPO ₂ DATA OF ALL SUBJECTS FROM THE EXPERIMENT	119
TABLE 5.4: PPG SIGNAL RMS AND MEDIAN DIGIT SKIN TEMPERATURE VALUES FOR ALL SUBJECTS IN STUDY 2	120
TABLE 6.1: PSV MEASUREMENTS FROM THE PRELIMINARY TEST, S1 MEANS SET 1 AND S2 MEANS SET 2	133
TABLE 6.2: MEDIAN [IQR] AC SIGNAL AMPLITUDE (V) AND DOPPLER ULTRASOUND VELOCITY (CM/S) DATA FROM THE STUDY	140
TABLE 7.1: SUBJECT DEMOGRAPHICS AND SAO ₂ ESTIMATION COMPARISON BY TWO PULSE OXIMETERS.....	163
TABLE 7.2: SUBJECT ESTIMATED SATURATION VALUES FROM THE EXPERIMENT	164
TABLE 8.1: ESTIMATED R _{VEN} , MEASURED SvO ₂ , AND RELATED UNCERTAINTIES FOR EACH SUBJECT FROM THE WHOLE STUDY	190
TABLE 8.2: BASELINE PPG AND BLOOD GAS MEASUREMENTS FOR ALL THE SUBJECTS	192
TABLE 8.3: PPG AND BLOOD GAS MEASUREMENTS FOR ALL THE SUBJECTS FROM TEST 2	193
TABLE 8.4: PPG AND BLOOD GAS MEASUREMENTS FOR ALL THE SUBJECTS FROM TEST 4	194
TABLE 8.5: MEASURED AND ESTIMATED OXYGEN SATURATION DIFFERENCES FOR ALL SUBJECTS, ACROSS THE THREE TESTS. NO MEASURED OR ESTIMATED ARTERIAL OXYGEN SATURATIONS FOR SOME SUBJECTS ARE PRESENTED AS EXPLAINED IN SECTION 8.4.4.	195

Nomenclature

<i>AC</i>	High frequency component of the PPG signal
<i>ADC</i>	Analog-to-digital converter
<i>APG</i>	Artificial pulse generation
<i>BP</i>	Blood pressure
<i>BF</i>	Blood flow
<i>BV</i>	Blood velocity
<i>CO</i>	Cardiac output
<i>COM</i>	Communication (port)
<i>CSA</i>	Cross sectional area
<i>DAC</i>	Digital-to-analog converter
<i>DAQ</i>	Data acquisition
<i>DC</i>	Low frequency component of the PPG signal
<i>DSP</i>	Digital signal processor
<i>ECG</i>	Electrocardiogram
<i>EDV</i>	End diastolic velocity
<i>FFT</i>	Fast Fourier Transform
<i>FIR</i>	Finite impulse response
<i>FSM</i>	Finite state machine
<i>GUI</i>	Graphical user interface
<i>Hb</i>	De-oxygenated haemoglobin
<i>HbO₂</i>	Oxygenated haemoglobin
<i>HCO₃</i>	Bicarbonate
<i>HDEC</i>	Health and Disability Ethics Committee
<i>HR</i>	Heart rate
<i>HRV</i>	Heart rate variability
<i>ICU</i>	Intensive care unit
<i>IIR</i>	Infinite impulse response
<i>IR</i>	Infrared light/wavelength
<i>IV</i>	Intravenous

<i>LED</i>	Light emitting diode
<i>MCU</i>	Microcontroller unit
<i>MOOSE</i>	Monitoring Oxygen for Saturation and Extraction
<i>NIRS</i>	Near infrared spectroscopy
<i>O₂E</i>	Oxygen extraction
<i>PCO₂</i>	Partial pressure of carbon dioxide
<i>PD</i>	Photo diode/Photodetector
<i>pH</i>	Acidity (of blood)
<i>PI</i>	Perfusion Index
<i>PPG</i>	Photoplethysmograph
<i>PO</i>	Pulse oximeter
<i>PO₂</i>	Partial pressure of oxygen
<i>PSV</i>	Peak systolic velocity
<i>PTT</i>	Pulse transit time
<i>PTTR</i>	Pulse time reflection ratio
<i>R</i>	Modulation ratio
<i>R_{Art}</i>	R value derived from AC and DC signals
<i>R_{Ven}</i>	R value derived from APG and DC signals
<i>RBC</i>	Red blood cell
<i>RD</i>	Red light/wavelength
<i>RMS</i>	Root mean squares
<i>RPO</i>	Reflectance mode PPG
<i>SaO₂</i>	Arterial blood oxygen saturation
<i>SpO₂</i>	Pulse oximeter estimated SaO ₂
<i>SO₂</i>	Oxygen saturation
<i>SpaO₂</i>	Custom pulse oximeter estimated SaO ₂
<i>SNR</i>	Signal-to-noise ratio
<i>SvO₂</i>	Venous blood oxygen saturation
<i>SpyO₂</i>	Custom pulse oximeter estimated SvO ₂
<i>StO₂</i>	Tissue oxygen saturation
<i>T</i>	Temperature
<i>TPO</i>	Transmission mode PPG
<i>VOT</i>	Vascular Occlusion Test

Abstract

In the intensive care unit (ICU), cardiovascular disease and sepsis are major drivers of morbidity, mortality, and cost. Microcirculatory dysfunction during sepsis and cardiac failure is known to significantly impair perfusion in major organs and peripheral tissues, resulting in poor patient outcome if not corrected early. Arterial oxygen saturation (SaO_2), venous oxygen saturation (SvO_2), and their difference, or oxygen extraction (O_2E), in association with blood flow, are key parameters necessary to assess tissue perfusion. Although, SaO_2 can be reliably estimated by non-invasive optical technologies, such as pulse oximetry in terms of SpO_2 , there are no established, easy, or non-invasive methods to assess SvO_2 , and thus O_2E . Therefore, real-time, low-cost, and non-invasive assessment of SvO_2 , O_2E , and blood flow could significantly advance the diagnosis, management, and of care sepsis or cardiovascular disease in the ICU.

This research focuses on the development of a novel pulse oximeter based concept to non-invasively and more completely assess tissue perfusion in peripheral extremities, such as the finger. A transmittance pulse oximeter sensor was used as the basis of a device to estimate and monitor peripheral SvO_2 , O_2E , and blood flow changes. Robustness of perfusion assessment methods at various digit skin temperatures was also investigated to improve accuracy and define the limits of sensor accuracy.

A custom built pulse oximeter (PO) device and graphical user interface (GUI) were developed to access and acquire all photoplethysmograph (PPG) signals, including the raw PPG signals. A two

stage digital filter system was implemented to extract useful signals from the PPG. Time and frequency domain methods, including peak-trough detection algorithms, were developed to analyse the PPG data and estimate parameters, such as SaO_2 and heart rate. This system was thus used as the basis for developing SvO_2 and blood flow monitoring methods, and also the investigation of temperature effects on PPG measurements.

A study was conducted with healthy adult volunteers ($n = 20$) to investigate the effect of a range of digit skin temperatures on pulse oximeter performance using a transmittance pulse oximeter sensor. It was hypothesized that cold digits can significantly reduce PPG signal quality and the resulting accuracy of SpO_2 measurements, due to the likely reduction in blood flow of the periphery at these temperatures. PPG data were recorded at cold, normal, and baseline skin temperatures, using the PO system as well as a commercial pulse oximeter for reference. Results show warm skin temperatures improved PPG signal quality up to 64.4% compared to baseline, and provided SpO_2 estimation of 96.5[96.1 – 97] % in the expected range for healthy adults. At baseline conditions, the majority of subjects showed a good PPG signal and expected SpO_2 estimate of 95.8[93.2 – 96.8] %. PPG signal quality degraded significantly up to 54.0% at cold conditions and SpO_2 estimates of 88.5[87.1 – 92.8] % were unreliable when compared to baseline. The main outcome is a tri-linear model quantifying PPG signal quality as a function of temperature, suggesting warm skin temperature conditions (approximately 33°C) should be maintained for reliable transmittance pulse oximetry.

In circulatory dysfunction, peripheral blood flow can be reduced, adding error to assessment of SvO_2 and O_2E using typical models and assumptions. Relative volumetric blood flow change

assessments using the PO sensor were performed in a study using 7 human adult volunteers. The signal amplitude of the high frequency PPG component, which is related to the pulsatile arterial blood flow, was used as an indicator of blood flow change. A vascular Doppler ultrasound sensor was used as a reference measurement. Changes in blood flow conditions were induced by a series of vascular occlusion tests. Good correlation ($R^2 = 0.69$) and trend agreement was obtained between median PPG amplitude and Doppler ultrasound velocity, particularly at normal and clinically important low flow conditions. Thus, PPG amplitude monitoring can be a potential surrogate or alternative to vascular Doppler ultrasound based blood velocity monitoring, and can provide continuous and reliable measurements, ensuring flow conditions can be included in assessing SvO_2 .

A novel artificial pulse generation system (APG) was developed to cause low frequency and low pressure modulations of venous blood in the finger using a pneumatic digit cuff. The APG system used a feedback controlled pressure regulator and solenoid valve to inflate/deflate the pressure cuff. This system was designed to exploit the significant arterial-venous compliance difference and make the peripheral venous blood pulsatile, while having negligible impact on arterial blood flow. Ten healthy human adults were recruited for proof-of-concept testing of this device. Modulation ratio (R) values derived from the artificially modulated PPG signals were used to estimate venous oxygen saturation ($SpvO_2$) using an empirical calibration equation developed for arterial blood. Conventional empirical calibration model estimated arterial and venous saturations of 96.95[96.1 – 97.4] % and 93.15[91.1 – 93.9] % agree with published literature values. Median O_2E was 3.6%, with a statistically significant and expected difference ($p = 0.002$) between pairs of measurements in each subject.

The APG system in association with the pulse oximeter device to assess SvO_2 was then validated in a clinical study with healthy adult volunteers ($n = 8$). A range of physiologically realistic SvO_2 values were induced using vascular occlusion tests. Gold standard, arterial and venous blood gas measurements were used as reference measurements. Modulation ratios related to arterial and venous systems were determined using a frequency domain analysis of the PPG signals. A strong, linear correlation ($R^2 = 0.95$) was found between estimated venous modulation ratio and measured SvO_2 , providing a calibration curve relating measured modulation ratio of venous blood to oxygen saturation. Median venous and arterial oxygen saturation accuracies from paired measurements were 0.29% and 0.65%, respectively, showing good accuracy of the pulse oximeter system. Investigations also revealed the empirical calibration model used to estimate SpaO_2 cannot be used to estimate SpvO_2 because of the difference in optical absorption caused by artificial perturbations. In particular, there is a significant difference in gradient between the SpvO_2 estimation model ($\text{SpvO}_2 = 111 - 40.5 * R$) and the empirical SpaO_2 estimation model of ($\text{SpaO}_2 = 110 - 25 * R$). The main outcome of this study presents a novel pulse oximeter based calibration model that can be used to assess peripheral SvO_2 , and thus O_2E , using the device developed in this work.

Overall, this thesis successfully develops and demonstrates a non-invasive, pulse oximeter based method to assess peripheral tissue perfusion in terms of SaO_2 , SvO_2 , O_2E and volumetric blood flow changes. This novel sensor may potentially detect peripheral perfusion alterations in real-time during microvascular and/or overall circulatory dysfunction, such as in sepsis or cardiac failure. Future work will follow the application of the novel sensor in a comprehensive clinical study with a larger, more diverse, cohort.

Chapter 1: Introduction

Healthcare economics are getting increasingly difficult. Costs are increasing rapidly, driven largely by rising demands due to aging populations and chronic diseases (Dorman and Pauldine, 2007; Bloomfield, 2003). These trends are unsustainable, eroding the quality, access, and equity of healthcare for all. In addition, the future of healthcare is broadly regarded as personalised, predictive, preventive and participatory (Hood and Friend, 2011), as well the demand to be more productive, and thus more economically affordable. In particular, better quality, more productive, and cost effective care are the primary demands and expectations of future healthcare.

The intensive care unit (ICU) is a leading source of hospital admission, mortality and cost. In the ICU, cardiovascular and circulatory failure and management are major drivers of morbidity, mortality, and cost. Alterations in oxygen transport and use can influence development of septic shock (Trzeciak et al., 2007), cardiovascular diseases (Rostand et al., 1984), and multiple organ failure (Moore et al., 1992). Prospective trials have reported positive outcomes when early treatment is directed towards restoration of adequate tissue perfusion (Vincent et al., 2003). Thus, the primary objective of circulatory resuscitation and management is to re-establish effective tissue perfusion and oxygenation, and thus cellular metabolism.

The main clinical endpoints or goals in monitoring circulatory functions and its response to care during circulatory management and resuscitation include, but are not limited to:

- The heart’s ability as a pump in terms cardiac output or accurate beat to beat stroke volume (SV) measurements (Uzzan et al., 2006), where recent surveys and consensus statements indicate that SV might be more preferred (Cecconi et al., 2014).
- The heart and circulatory systems ability to perfuse organs via determination of stressed blood volume using a model-based metric (Matson et al., 1991).
- The circulatory systems ability to exchange oxygen with tissues as a measure of arterial oxygen saturation (SaO_2), which is commonly done non-invasively (Jubran, 2015), venous oxygen saturation (SvO_2), which is commonly done invasively, (Chan and Gu, 2011), and the difference between the two saturations or oxygen extraction (O_2E).

However, treatment end points remain significantly controversial because of the difficulties in determining what is constituted to be “optimal” in terms of these values. Information obtained from global, whole-body monitoring may not identify regional organ blood flow and oxygenation, or perfusion, abnormalities until they are severe. Equally, the ideal “canary” organ that is easily accessible for monitoring tissue perfusion, and thus can work as an early and sensitive marker of tissue abnormalities, remains to be established. Hence, there is a need for better measurements, preferably that are not invasive or make use of existing standard measurements.

Perfusion monitoring can be the key to promptly diagnose and manage possible organ dysfunction or tissue abnormalities. This monitoring is considered integral to determine postoperative outcomes after cardiac surgery (Kuttila and Niinikoski, 1989). In particular, peripheral perfusion monitoring can be used to determine abnormalities in tissue microcirculation, independent of systemic haemodynamics parameters (Ait-Oufella et al., 2011; van Genderen et al., 2014; van Genderen et al., 2012a), and is considered for investigation in this thesis.

1.1 Perfusion monitoring

1.1.1 Definition

The word perfusion is derived from the French verb "perfuser", which means to "pour over or through" (Keane and Toole, 2003). In physiology, perfusion is the process by which blood is delivered to a capillary bed, in biological tissue, for tissue oxygenation and cellular metabolism. The concept of tissue perfusion has been linked to blood flow and oxygen delivery, or a combination of flow and nutritional supply, including oxygen. Overall, the transportation of oxygen to tissues and its absorption by the cells could be defined as tissue oxygen perfusion (Gottrup, 1994). Thus, the assessment of tissue blood flow and oxygen consumption lies at the core of tissue oxygen perfusion monitoring.

1.1.2 Peripheral perfusion monitoring

Peripheral tissues are sensitive to alterations in perfusion. Hypoperfusion in peripheral tissues is associated with the severity of organ dysfunction and outcome, and is independent of systemic haemodynamics (Lima et al., 2009; Lima et al., 2011; Cohn et al., 2007). In addition, prolonged peripheral capillary refill time was strongly correlated with reduced perfusion assessed by increased proven tissue infection in previous studies (Bohnhorst et al., 2012; Van den Bruel et al., 2010). Thus, the assessment of peripheral perfusion can be used as an early indicator of systemic haemodynamic disorder (van Genderen et al., 2012b).

In various patient categories, more severe and persistent alterations in peripheral perfusion have been associated with poor outcomes, and these correlations were independent of systemic haemodynamic parameters (Ait-Oufella et al., 2011; van Genderen et al., 2014; van Genderen et

al., 2012a). In addition, interventions directed at systemic parameters can have an unpredictable effect on peripheral circulation parameters, especially during hyperdynamic conditions (Bonanno, 2011; Lima and Bakker, 2015). Thus, it appears that changes in peripheral perfusion can reflect changes in regional vasomotor tone, rather than systemic perfusion, which requires invasive procedures for perfusion monitoring with typical available methods.

Peripheral circulation deterioration has frequently been observed in critically ill patients using subjective assessment and optical techniques. In a prospective study of 108 healthy volunteers and 37 critically ill patients, peripheral perfusion was assessed and compared between the two groups using a peripheral perfusion index (PFI) based on the analysis of non-invasive pulse oximetry (Lima et al., 2002). The variation of the PFI in both groups was related to the central-to-toe temperature difference and capillary refill time after changes were detected in clinical signs of peripheral perfusion. It was concluded that changes in PFI strongly correlated to changes in core-to-toe temperature difference in critically ill patients, but not in healthy subjects ($r^2 = 0.52$, $p < 0.001$). However, although their research measured oxygen supply, no measurement for blood flow or oxygen consumption was provided, which would have strengthened the result.

1.2 Perfusion and sepsis

Sepsis is a major public health risk associated with high morbidity and mortality. It is a complex medical condition characterised by a system inflammatory response syndrome (SIRS) in association with presumed or proven infection. In 1991, the American College of Chest Physicians and Society of Critical Care Medicine Consensus developed a framework to define SIRS, sepsis and severe sepsis (Bone et al., 1992), outlined in Figure 1.1. The criteria were later revised to

include infection and the presence of any diagnostic criteria, based on clinical or laboratory parameters, that are particularly sensitive or specific to diagnose sepsis (Levy et al., 2003). This section details the clinical significance and impact of reliable perfusion monitoring in sepsis, as a high morbidity and mortality example.

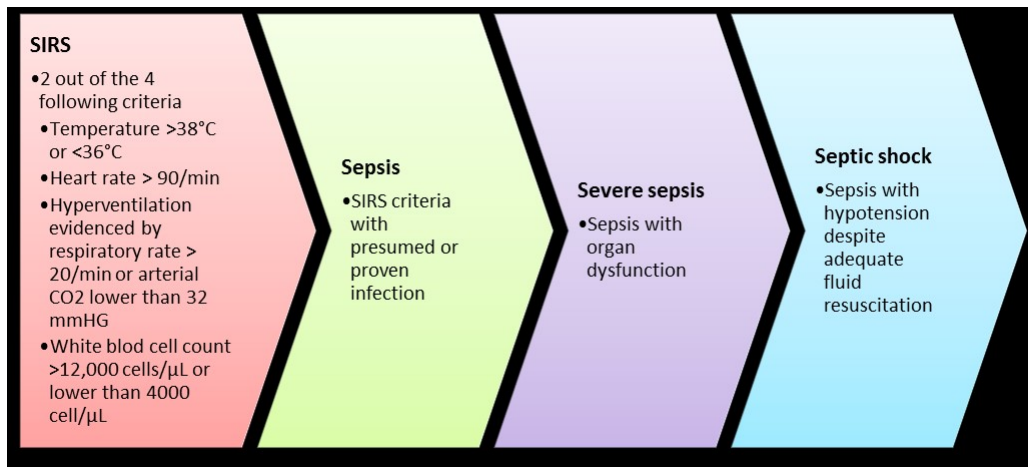


Figure 1.1: Criteria for SIRS, sepsis, severe sepsis, and septic shock according to the 1991 ACCP/SCCM Consensus Conference. Adapted from: Bone et al. (1992).

1.2.1 Epidemiology of sepsis

In general, sepsis occurs in approximately 2% of all hospital cases across Europe and in most developed countries. Sepsis related incidences may occur in between 6 – 30% of all ICU patients, with considerable discrepancy due to the heterogeneity between ICUs (Vincent et al., 2006; Alberti et al., 2002). Between 1997 – 2005, a study in Australia and New Zealand reported 7649 admitted patients having sepsis or septic shock, with an ICU and hospital mortality of 20.9% and 27.6%, respectively (Moran et al., 2007). Table 1.1 shows incidences of sepsis and related mortality reported in several major worldwide studies. However, it should be noted, incidences of sepsis, severe sepsis, and septic shock are less known in the developing world (Adhikari et al., 2010).

Table 1.1: Worldwide incidences of sepsis and related mortality as determined in 8 studies.

Study by	Country or countries	Study period	Study design	Incidences (per 100,000 population)	Mortality (%)
Angus et al. (2001b)	USA	1995	Examination of state databases	300	29
Martin et al. (2003)	USA	1997 - 2002	Examination of national databases	91	34
Padkin et al. (2003)	England and Wales	1997	Examination of national databases	51	47
EPISEPSIS and Group (2004)	France	2001	Multicenter cohort study	95	38
Finfer et al. (2004)	Australia and New Zealand	1999	Multicenter cohort study	77	35
Silva et al. (2004)	Brazil	2001 - 2002	Multicenter cohort study	614	34
Flaatten (2004)	Norway	1999	Examination of national databases	149	14
Hoa et al. (1998)	Vietnam	1993 - 1994	Examination of state databases	204	6

Sepsis presents a serious medical problem in the adult ICU, with a 11 – 15% incidence of severe sepsis, 30 – 80% mortality rate, US\$22,100 average cost per case, US\$16.7B annual total cost, and 1.5% projected annual incidence increase (Angus et al., 2001a; Dellinger et al., 2008). Sepsis patients are typically more severely ill, stay longer in hospital, more expensive to treat, and at greater risk of death when compared to hospitalised patients diagnosed with other medical condition. In one study, the mean hospitalization length of stay and costs for patients with severe sepsis were 16 days and US\$26,820, respectively, with 1-year inpatient and outpatient costs totaling US\$48,996 (Braun et al., 2004). Figure 1.2 gives an example of the high cost related treatment and low research funding for sepsis in US and Europe, compared to other medical conditions and diseases.

Elderly people, aged ≥ 65 years, are at higher risk of being diagnosed with sepsis than younger people (Wester et al., 2013; Starr and Saito, 2014). However, race, ethnicity, and gender may also be associated to the variable risks of developing sepsis (Martin et al., 2003; Mayr et al., 2010; Dombrovskiy et al., 2007). For example, men are typically more susceptible to developing sepsis compared to women (Esper et al., 2006; Martin et al., 2003; Moss, 2005). Other studies claim people of black origin are at the highest risk of developing sepsis followed by other non-white and white origins (Esper et al., 2006; Barnato et al., 2008), although they have been contradicted by a more recent study (Moore et al., 2015).

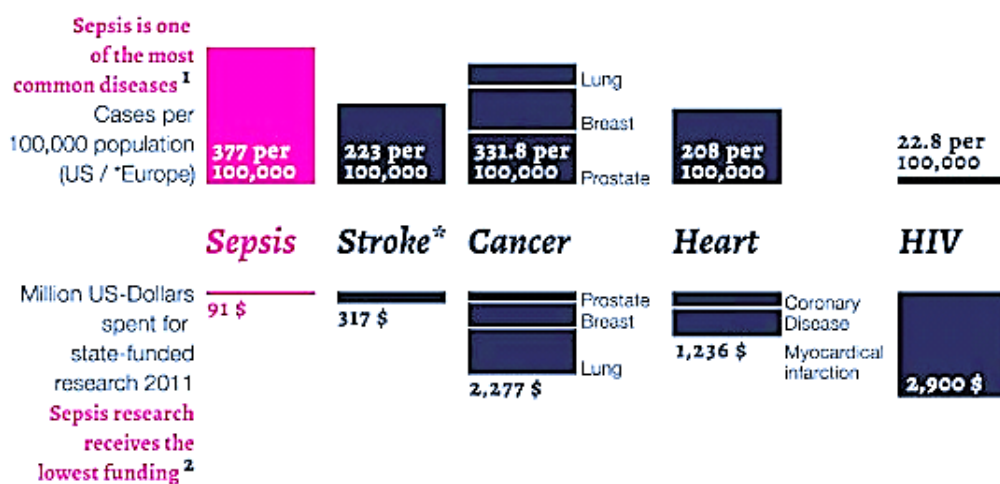


Figure 1.2: Sepsis having the highest number of incidences in US/Europe receiving the lowest amount research funding compared to other medical conditions. Source: Kunz (2012)

Currently, blood cultures are considered the gold standard for confirmation of the infection component of sepsis. However, the culturing process can take between 24 – 48 hours and only 51% of sepsis cases are positively identified by this method, while the others denoted “culture-negative sepsis” (Martin et al., 2003; Carrigan et al., 2004). Biomarkers can aid sepsis diagnosis by producing results in 2 – 3 hours, with varying levels of clinical accuracy (Carrigan et al., 2004).

However, biomarkers are yet to be adopted as a standard of care due to low sensitivity and specificity demonstrated in clinical trials (Uzzan et al., 2006; Matson et al., 1991; Chan and Gu, 2011; Drucker and Krapfenbauer, 2013).

Sepsis treatment guidelines and patient management protocols recommend early goal-directed resuscitation of the septic patient during the first 6 hours after infection recognition (Dellinger et al., 2008). Early interventions have been documented to reduce mortality from 46.5% to 30.5% (Rivers et al., 2001). Hence, a rapid, early diagnostic with reasonable sensitivity and specificity could significantly improve diagnosis, care, and outcomes.

1.2.2 Microvascular perfusion dysfunction in sepsis

Sepsis fundamentally functions as a disease of the microcirculation, where alterations in microvascular perfusion have been recognized in severe sepsis and septic shock (De Backer et al., 2002), and the severity of these alterations is connected with a poor outcome (Sakr et al., 2004; De Backer et al., 2013). Microvascular dysfunction is a pivotal element in the pathogenesis of sepsis and septic shock, which can lead to reduced tissue extraction of oxygen and organ failure (Trzeciak and De Backer, 2007; Spronk et al., 2004; Ince, 2005). This dysfunction involves all three elements of microcirculation: arterioles, capillaries, and venules (Lush and Kvietys, 2000; Bauer, 2002). Under such circumstances, the microvascular blood flow is altered (De Backer et al., 2002) hampering oxygen transport to tissues in organs (Ince, 2005; Ellis et al., 2002; Bateman et al., 2003). As a result, microvascular tissues become hypoxic, which can result in cellular loss, organ failure, and death.

Healthy individuals have a dense network of capillaries with good perfusion. In contrast, septic individuals have a less dense network of capillaries, which is associated with an increase in heterogeneity of perfusion (De Backer et al., 2014). This effect occurs due to the existence of intermittently or not-perfused capillaries in close vicinity to well perfused capillaries (Croner et al., 2006; Secor et al., 2010; Verdant et al., 2009; Farquhar et al., 1996). The reduction in vascular density results in a greater distance for oxygen to diffuse (Bateman et al., 2007). In a large study with 252 septic patients, shown in Figure 1.3, it was seen that capillary density and perfusion was an independent factor associated with survival rate.

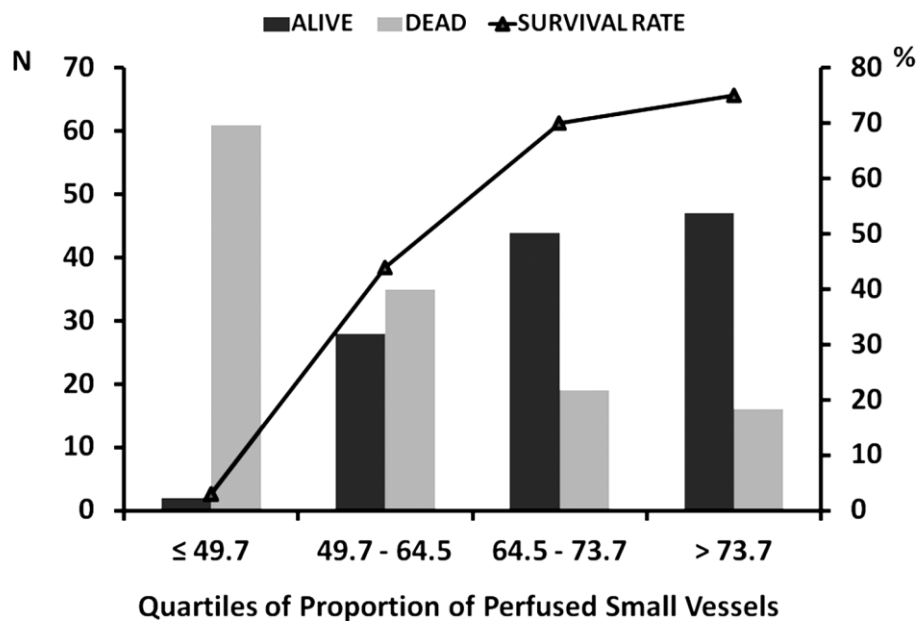


Figure 1.3: Relationship between sublingual microcirculation and ICU mortality in 252 patients with severe sepsis. The patients were grouped into quartiles in proportion of perfused capillaries. Source: De Backer et al. (2014).

In addition, sepsis also impairs capillary autoregulation mechanisms. A recent study has shown that impairment of capillary autoregulation is manifested by impaired capillary stopped-flow, increased capillary response time within hypoxic capillaries, decreased oxygen supply rate and

decreased RBC oxygen dependent adenosine tri-phosphate efflux (Bateman et al., 2015). This compromise of local microvascular control is partially influenced by increased capillary RBC supply rate and is correlated with increased oxidized metabolites of nitric oxide in blood plasma. Furthermore, these microvascular alterations play an important role in the development of organ dysfunction and are not just an indication of the severity of sepsis.

More importantly and as a result, the heterogeneity of microvascular perfusion during sepsis is associated with alterations in tissue oxygenation and altered oxygen extraction ability. O₂E is the quantity of oxygen being absorbed by tissues from circulating blood. In other words, O₂E is related to the difference between SaO₂ of the blood supplying the tissues and SvO₂ of the blood leaving the tissues (Gutierrez and Theodorou, 2012; Vincent and De Backer, 2004; Lifesciences, 2002). In experimental models and studies of sepsis, microvascular flow impairment have, as a result, been shown to impair tissue O₂E (Ellis et al., 2002; Trzeciak et al., 2007; Mesquida et al., 2011; Sair et al., 2001). Hence, the ability to assess O₂E directly would provide a good surrogate of perfusion and microvascular condition.

1.2.3 Assessment of peripheral perfusion during sepsis

Although sepsis causes blood flow alterations in different central regions, several studies reported resting forearm blood flow is relatively high in septic patients compared to non-septic controls (Kirschenbaum et al., 2000; Astiz et al., 1995; Astiz et al., 1991). Peripheral vascular response can be assessed by examining reactive hyperaemia, such as during vascular occlusion tests (VOT), which can provide a measure of the integrity of the microvascular responses to hypoxia.

Several studies reported that the response to reactive hyperaemia is attenuated in septic patients during VOTs (Kirschenbaum et al., 2000; Astiz et al., 1995; Astiz et al., 1991; Neviere et al., 1996). Reactive hyperaemia is defined as the transient increase in tissue blood flow, that typically occurs after a brief period of ischemia (Klabunde, 2011). The peak blood flow is decreased during reactive hyperaemia phase in septic patients compared to healthy subjects (Kirschenbaum et al., 2000; Neviere et al., 1996; Astiz et al., 1991; Sair et al., 2001; Astiz et al., 1995), thereby increasing the restoration time of tissues to be saturated with oxygen (Skarda et al., 2007; Neviere et al., 1996).

Hence, failure of the microvasculature to increase blood flow in the face of tissue hypoxia may be associated with compromised vasodilation or a loss of capillary cross-sectional area (Kirschenbaum et al., 2000) and diminished RBC deformability (Astiz et al., 1995). This malfunction is related to the slow rate of tissue deoxygenation during stagnant ischemia in septic patients compared to healthy controls (Mesquida et al., 2011; Pareznik et al., 2006; Sair et al., 2001). Thus, the microvascular response to tissue hypoxia is attenuated in sepsis, as evidenced by a diminution of reactive hyperaemia. The ability to measure O_2E and/or local blood flow would capture this attenuation, and thus provide a marker of microvascular dysfunction.

1.2.4 Peripheral blood flow and SvO_2 evaluation in sepsis

The heterogeneity of microvascular blood flow needs to be accounted when considering compromised oxygen extraction capabilities that occur in sepsis (De Backer et al., 2002). Some studies indicated that peripheral blood flow, especially in the skin, increases significantly during sepsis (Young and Cameron, 1995; Kirschenbaum et al., 2000) accompanied with impaired or low

tissue O₂E (De Backer et al., 2002; Ellis et al., 2002; Walley, 1996; Doerschug et al., 2007). In addition, a rise in SvO₂, due to low O₂E, is common during sepsis despite tissue oxygen deprivation (Zaja, 2007; Lifesciences, 2002; Cecconi et al., 2014). Thus, independent monitoring of SvO₂ can also serve as an indicator for microvascular dysfunction and reduced O₂E in sepsis diagnosis.

However, investigating SvO₂, O₂E, and blood flow in organs is less feasible than in the periphery, as it typically requires invasive procedures. The currently available literature is unclear about any relationship between peripheral versus core (organ) blood flow and O₂E, with progressive severity of sepsis (Di Giantomasso et al., 2003; Chung et al., 2001; Wang et al., 1998; Hart et al., 2003). In particular, the literature is unclear whether high or low organ blood flow and O₂E is associated with high or low peripheral blood flow and O₂E in septic conditions. Since the reported results are often contradictory, this issue creates an open area of research where this thesis aims to make a contribution by assessing peripheral perfusion in terms of SaO₂, SvO₂, O₂E, and blood flow in the periphery using non-invasive technologies.

1.3 Research overview

1.3.1 Clinical significance of this research

This research focuses to develop accurate, continuous, and noninvasive methods that can easily assess peripheral tissue perfusion under clinical conditions. Microcirculatory distress not corrected for 24 hours has been shown to be the single independent factor predicting patient outcome in septic patients (Sakr et al., 2004). Furthermore, there are no established, easy, or non-invasive methods to assess SvO₂. Therefore, real-time, low-cost, and non-invasive detection of SvO₂, tissue

O_2E , and blood flow would transform sepsis or cardiovascular disease diagnosis, monitoring and care, by providing an early, real-time measure of a key negative outcome that can be monitored and managed directly. Such a development could significantly aid in early-goal directed therapy in sepsis (Rivers et al., 2001) and circulatory failure.

1.3.2 Research goals

In this research, the primary objective is the development of a novel pulse oximeter system that can enable real-time, non-invasive, estimation of peripheral SvO_2 and O_2E using photoplethysmograph (PPG) signals. It is hypothesized that the peripheral venous bed can be predominantly modulated with respiration-like excitations using a pneumatic pressure cuff and control system, to transform the non-pulsatile peripheral venous system into a pulsatile system. These modulations can be detected by a PPG based sensor and analysis of the relevant spectral component can enable continuous and non-invasive assessment of SvO_2 , and thus O_2E using the PPG derived SaO_2 .

This research includes hardware and software development of a custom pulse oximeter, design of methodology and experimental protocols, proof of concept testing, and validation of the concept against gold standard comparators in a clinical study. The development of a custom pulse oximeter system that can provide access to the raw PPG signals for processing, unlike conventional pulse oximeters (Shelley et al., 2014), is equally integral to this research for reasons discussed in Section 2.6.

Blood flow change assessment using the PPG signal is second to SvO_2 and O_2E estimation in this research. A true measure of tissue extraction also needs a measure of blood flow so that flow

limited states don't appear the same as those with higher/normal blood flow (Podbregar and Mozina, 2007). However, current blood flow monitoring methods are reliant on laser or ultrasound based Doppler technologies, which do not provide a measure of oxygen saturation. It is hypothesized that the PPG pulse amplitude can be used to continuously monitor volumetric blood flow changes in peripheral extremities, such as the finger. Equally, an alternate or surrogate measurement for Doppler technologies can be developed using this method, to provide an accurate, reliable surrogate for blood flow.

Parallel to peripheral perfusion monitoring, an independent study was conducted to investigate the effect of temperature on PPG signal quality to ensure robustness of the pulse oximeter system. The success of this research is dependent on obtaining good quality PPG signals for data analysis. Cold skin temperatures at extremities, such as the finger, can severely degrade PPG signal quality and local heating can improve conditions and PPG signal quality, as discussed in Chapter 5. This study thus investigates and quantifies the strength of the PPG signal quality at cold, warm, and normal skin temperatures and their impact on the accuracy of PPG based measurements.

Overall, the main outcome of this research is a novel, robust, low-cost, and non-invasive perfusion monitoring system for SaO_2 , peripheral SvO_2 , local tissue O_2E , and local blood flow. The results of this research can be beneficial in early diagnosis and management of circulatory and cardiac dysfunctions. Challenges remain with the technology itself, including the standardization of measurements, improving repeatability, and establishing comprehensive normative data ranges for comparison with critically ill patients, preferably septic, and for evaluating responses to diagnostic.

1.4 Preface

This thesis is separated in two major parts. Part 1, Chapters 2 – 5, discusses the fundamental principles of pulse oximetry and PPG technology, the development of a novel pulse oximeter system, PPG analysis and testing involved, and the effects of different temperatures on pulse oximeter signal quality and measurement accuracy. Part 2, Chapters 6 – 8, discusses application of the novel pulse oximeter system in perfusion monitoring, in particular blood flow change detection and SvO_2 estimation, in experimental settings. The following chapters of this thesis are arranged as follows:

Chapter 2: Background and literature review. First, this chapter discusses the fundamental principles of pulse oximetry and PPG, and presents the various applications of PPG. Second, background on perfusion monitoring and its significance in sepsis diagnosis is presented. Finally, the peripheral venous physiology and a review of the shortcomings of available non-invasive methods to assess local SvO_2 are discussed.

Chapter 3: Design and development of a novel pulse oximeter system. This chapter presents all the design, hardware specifications, and development of a custom pulse oximeter system that provides access to the raw PPG signals. In addition, the firmware and interface used for PPG data acquisition are also detailed.

Chapter 4: PPG processing and analysis. This chapter introduces the digital filtering environment used to extract useful PPG signals and the methods used to estimate physiological parameters from

extracted signals. In addition, it investigates 3 peak detection algorithms used to compute amplitude information from the PPG signals.

Chapter 5: Effect of temperature on PPG signal quality. This chapter analyses the effect of cold, normal, and warm digits on transmittance pulse oximetry, with regards to PPG signal quality and measurement accuracy. In addition, results from a clinical validation study are also included.

Chapter 6: Monitoring peripheral blood flow changes using photoplethysmography. This chapter presents how the PPG signal amplitude can be used to monitor peripheral blood flow changes and its application as a surrogate to vascular Doppler ultrasound technology.

Chapter 7: Estimation of peripheral venous saturation and oxygen extraction using a novel pulse oximeter method. This chapter introduces the development and initial proof of concept testing of a novel respiration-like pulse generation system that can be used to predominantly modulate the venous system. The artificial modulations can be detected by PPG and the spectral components can be analysed to estimate SvO_2 and O_2E .

Chapter 8: Clinical validation trial of a novel pulse oximeter concept for non-invasive estimation of peripheral SvO_2 . This chapter further investigates the concept in Chapter 7, and the correlation of the PPG based measurements to gold standard measurements. In addition, improvements made to the hardware and development of a new experimental protocol are also discussed in this chapter.

Chapter 9: Conclusions. This chapter summarizes all the outcomes from this research in a nut shell.

Chapter 10: Future work. This chapter discusses the potential shortcomings of this research and proposes several improvements that can be made to overcome them.

Chapter 2: Background and literature review

2.1 Pulse oximetry and photoplethysmography

Pulse oximeters are ubiquitous devices in hospital wards, operating rooms, and intensive care units. They are used to non-invasively estimate arterial blood oxygen saturation and monitor heart rate, and are a standard of care for patient oxygenation monitoring (Ortega et al., 2011; Haynes et al., 2009; Jubran, 2015; Tremper and Barker, 1989). Pulse oximetry uses photoplethysmograph signals produced by an optical sensor, typically mounted on a finger, toe, or ear-lobe, to detect blood volume changes. It is generally accepted that the PPG waveform results from the pulsatile variation in the tissue optical density produced by significant arterial pulsations (Daly and Leahy, 2013; Aoyagi, 2003). Conventional pulse oximetry relies on the pulsatile nature of arterial blood and differential absorption of oxyhaemoglobin and de-oxyhaemoglobin at red (RD) and infrared (IR) wavelengths to estimate SaO_2 and HR (Aoyagi, 2003; Mendelson, 1992; Jubran, 2009; Severinghaus, 2007).

Typical transmittance pulse oximeter probes consist of two high output RD and IR light emitting diodes (LEDs) and a sensitive photo-detector (PD). Light energy transmitted through tissue is detected by the PD, which generates the PPG signal. The PPG signal is separated into two parts; the rapidly changing (AC) and the slowly changing (commonly referred to as DC) components. By taking the appropriate AC/DC ratios and calibration values, SaO_2 can be reliably estimated (Jubran, 2009; Goldman et al., 2000).

2.1.1 History of pulse oximetry

In 1940, J. R. Squire was the first to recognize that changes in RD and IR light transmission caused by pneumatic tissue compression permitted oxygen saturation to be computed (Squire, 1940). During the Second World War, Glen Allen Millikan invented the term ‘oximeter’ for an ear based, light-weight, optical device he developed to continuously measure SaO_2 in humans, as part of aviation research (Millikan, 1942). In 1949, Earl Wood used this idea to compute absolute saturation continuously from the ratios of optical density changes with pressure in an ear oximeter (Wood et al., 1950).

In 1972, an electrical engineer at the Nihon Kohden company in Tokyo, named Takuo Aoyagi, was interested in measuring cardiac output non-invasively (Aoyagi, 2003). He was using the dye dilution method using a commercially available ear oximeter and balanced the RD and IR signals to cancel the pulse noise, which had prevented accurate dye washout measurements (Severinghaus, 2007). It was discovered that changes in oxygen saturation voided his pulse cancellation. From this discovery, it was concluded that these pulsatile changes could be used to compute oxygen saturation from the ratio of ratios of pulse changes in the RD and IR wavelengths (Aoyagi, 2003; Severinghaus, 2007). Takuo Aoyagi’s pulse oximeter was improved and successfully marketed by Minolta in 1978, stimulating other firms to further improve and market pulse oximeters worldwide from the mid 1980’s. Notable success of the development of pulse oximetry include reductions in anesthesia-related fatalities by 90% (Severinghaus, 2007), as well as their almost ubiquitous hospital use.

In the early 1990s, pulse oximetry became the standard of care for perfusion monitoring during anaesthesia (Allen, 2007), and is now one of the most commonly employed monitoring modalities in the critical care setting. During the past 20 years, several studies focused on the technical aspects of pulse oximeters and concluded that this technology has a good degree of accuracy (Jubran, 2009). This accuracy and non-invasive nature, coupled with the ease of operation, led to the widespread use of pulse oximetry for patient monitoring in hospital units. SpO₂ measurement by pulse oximeters has widespread application in many different clinical settings, including operating rooms, ICUs, post-anesthesia care units, and emergency departments (Ortega et al., 2011). Outside clinical settings, SpO₂ measurement has significance in sports medicine, domiciliary use, and in veterinary clinics.

2.1.2 Photoplethysmography origin

The word “plethysmograph” is derived from two ancient Greek words “plethysmos” and “grapho” which mean “to increase” and “write” (Shelley, 2007; Alnaeb et al., 2007), respectively. Plethysmography is a technique typically used to determine and record variations in tissue blood volume or flow due to heartbeat (Elgendi, 2012). In general, there are 4 different varieties of plethysmography; air plethysmography, impedance plethysmography, strain gauge plethysmography, and photoplethysmography.

Photoplethymography is an optical technique used by pulse oximeters for peripheral blood volume change monitoring and was developed by Alrick Hertzman in 1938 (Hertzman, 1938). Since then, clinicians have widely used photoplethysmography in the study and monitoring of the cardiovascular pulse wave associated with changes in blood volume in the peripheral vascular bed

(Roberts, 1982; Dorlas and Nijboer, 1985; Higgins and Fronek, 1986). The convenience, simplicity, and non-invasive nature of this technology have resulted in the dominance of this optical method as a desired technology in several biomedical monitoring situations. PPG fundamentals are detailed in the Section 2.2, since the research presented in this thesis relies on PPG based pulse oximetry.

2.1.3 Pulse oximetry principles

The principles of pulse oximetry are based on the differential absorption characteristics of emitted light by oxygenated (HbO_2) and deoxygenated haemoglobin (Hb) species. Two separate wavelengths, typically IR and RD, are used to distinguish between the two species of haemoglobin and illuminate the vascular bed. The oxygen chemically combined with haemoglobin inside the red blood cells (RBC) makes up for the majority of the oxygen present in the blood. Functional SaO_2 is defined as the ratio of oxyhaemoglobin to the total concentration of haemoglobin present in the arterial blood stream:

$$SaO_2 = \frac{\text{Oxygenated Haemoglobin}}{\text{Total haemoglobin}} = \frac{HbO_2}{HbO_2 + Hb} \quad (2.1)$$

Figure 2.1 shows the extinction coefficients as a function of wavelengths of these two types of haemoglobin. The extinction coefficient relates to the strength of light absorption by haemoglobin at a given wavelength, per mass density or per molar concentration. The typical wavelength band for RD is 600 – 750 nm and for IR is 850 – 1000 nm.

At the isosbestic point (approximately 806 nm), both HbO_2 and Hb have the same extinction coefficients, and thus absorption. Oxygenated haemoglobin greatly absorbs IR light, while allowing more RD light to pass through. In contrast, deoxygenated (or reduced) haemoglobin absorbs more RD light, while allowing more IR light to pass through. The values for RD and IR wavelengths are chosen such that the absorption by the two haemoglobin species is significantly different at the two points.

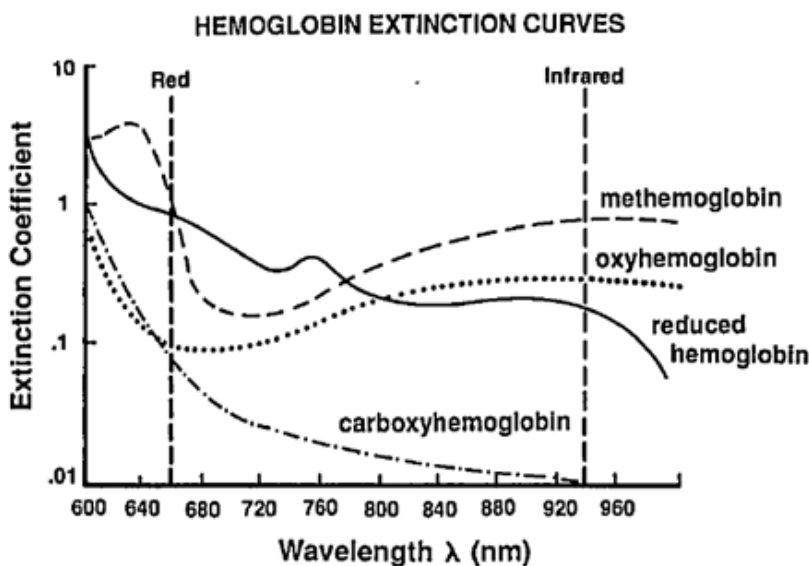


Figure 2.1: Absorption spectra of the four types of haemoglobin, showing the extinction coefficients ($\text{Lmmol}^{-1}\text{cm}^{-1}$) at red and infrared wavelengths. Reproduced from Tremper and Barker (1989).

The amount of light absorbed is proportional to the Hb concentration in the blood vessel. Thus, the greater the Hb per unit area of the vessel, the greater is the amount of light absorbed. This property is described by “Beer’s Law” (Miller et al., 2009). The following section details the application of this law in pulse oximetry.

2.1.4 Beer-Lambert model

The basic mathematics of pulse oximetry can be derived through an algebraic manipulation of the Beer-Lambert model (Webster, 2002). This spectroscopy principle considers how light intensity exponentially decreases as it passes through non-scattering, light-absorbing tissues comprised of one or multiple components. The intensity of light passing through the medium decreases exponentially with respect to distance, in accordance to the following equation (Tremper and Barker, 1989):

$$I_{out} = I_{in} e^{-\varepsilon(\lambda)cd} \quad (2.2)$$

Where:

- I_{in} is the incident light intensity
- I_{out} is the transmitted light intensity
- ε is the extinction coefficient of the absorbing substance at a specific wavelength λ
- c the concentration of the absorbing substance, which is constant in the medium
- d is the optical path length through the medium

Thus, taking the ratio of the transmitted and incident light at the two wavelengths gives:

$$R = \frac{\log(I_{out}/I_{in})_{\lambda_1}}{\log(I_{out}/I_{in})_{\lambda_2}} \quad (2.3)$$

The modulation ratio (R), a ratio of ratios, is defined as the ratio of the absorbance of blood at the two illuminating wavelengths. SaO_2 may be determined from the measured R and knowledge of extinction coefficient of haemoglobin species using:

$$SaO_2 = \frac{\varepsilon_{Hb}(\lambda_1) - R\varepsilon_{Hb}(\lambda_2)}{R[\varepsilon_{HbO_2}(\lambda_2) - \varepsilon_{Hb}(\lambda_2)] + [\varepsilon_{Hb}(\lambda_1) - \varepsilon_{HbO_2}(\lambda_1)]} \times 100\% \quad (2.4)$$

Where ε_{Hb} is the extinction coefficient of reduced haemoglobin and ε_{HbO_2} is the extinction coefficient of oxygenated haemoglobin. Early pulse oximeters used this concept to operate, as it was originally engineered by Aoyagi and Miyasaka (2002) in the first generation of pulse oximeters. However, in reality, human blood is a highly scattering medium (Roggan et al., 1999; Mannheimer, 2007). Thus, the photons in the transmitted beam of light will not travel all in a straight path before reaching the PD. The actual path length of the detected light is a complicated function of both the scattering and absorption properties of the tissue medium (Mannheimer et al., 1997). Since it was proven that light no longer travels in a straight path, conventional pulse oximetry cannot completely rely on the Beer-Lambert model.

2.1.5 Empirical calibration to determine oxygen saturation

Modern pulse oximeters use a calibration function to correct for errors due to scattering. A test pulse oximeter is calibrated against whole arterial blood gas data, measured from healthy, normothermic, human subjects, during *in vitro* clinical studies (Schnapp and Cohen, 1990; Webster, 2002). The effective haemoglobin extinction coefficients are usually based upon an empirical calibration through the employment of induced hypoxia experiments (Kamat, 2002; Schnapp and Cohen, 1990). Hence, errors encountered due to the assumptions implicit in the Beers-Lambert model are able to be corrected.

Figure 2.2 shows a typical pulse oximeter calibration curve versus the Beer-lambert model, depicting the relation between the ratio of ratios (R) and measured SaO_2 . The Beer-lambert model

is an exponential curve representing the exponential decrease of transmitted light as it passes through layers of light absorbing tissue medium, not considering any light scattering by the tissues. The Empirical Calibration model has a curve between $R = 0.5 – 1.25$ as a result of modulation ratio derived from Oxygen Saturation: 100 – 70% during hypoxic experiments. However, the data in the range of $R = 1.25 – 2.5$ is linearly extrapolated from the experimental data.

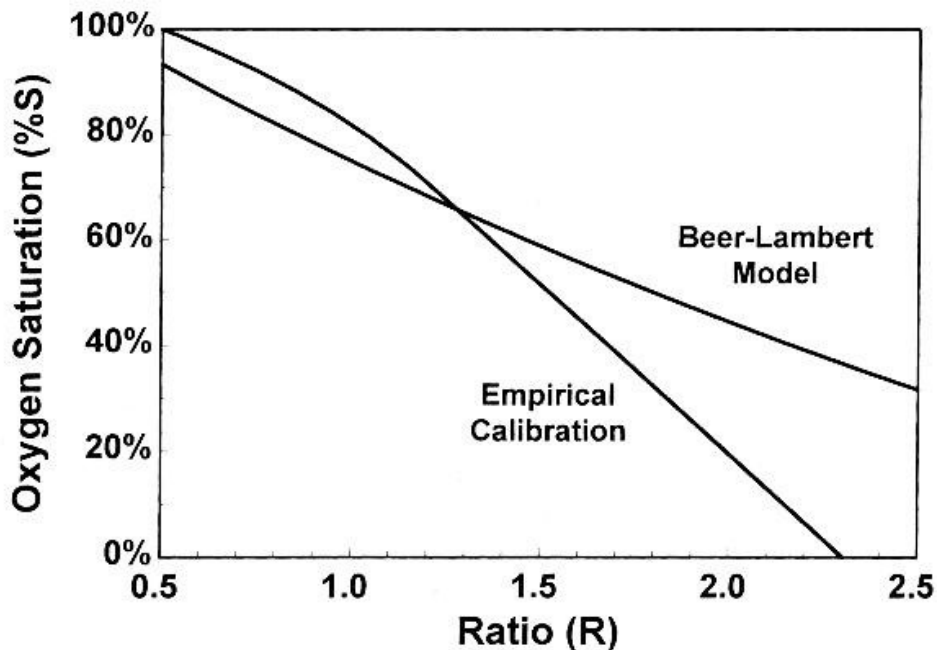


Figure 2.2: Typical pulse oximeter calibration curve also showing the Beer-Lambert Model. Source: Ross (1999).

To relate the estimated R values to the pulse oximeter's reading, the equation of the theoretical calibration curve based on Beer's law can be modified as Mendelson and Kent (1989) defined:

$$SaO_2 = SpO_2 = \frac{k_1 - k_2 R}{k_3 - k_4 R} \quad (2.5)$$

In Equation 2.5, the extinction coefficients from Equation 2.4 are replaced by constants k_1 , k_2 , k_3 , and k_4 , which are calculated from clinical studies to provide the curve a best fit to the *in vitro* measured data (Webster, 2002). The term SpO_2 means the SaO_2 estimate determined by pulse oximetry (Philips, 2003).

Pulse oximetry determines SpO_2 by illumination of RD and IR light through vascular tissue, with rapid switching between two separate light sources. AC signals of RD and IR PPG are sensitive to changes in SpO_2 because of the variance in the light absorption of HbO_2 and Hb at these two wavelengths. Using the AC signal's amplitude ratio and corresponding DC components for each wavelength, Equation 2.3 can be transformed to calculate R value using:

$$R = (AC_{RD}/DC_{RD})/(AC_{IR}/DC_{IR}) \quad (2.6)$$

Since the absolute intensity of the transmitted beam is not known, the transmitted RD and IR signals are normalized by dividing the pulsatile transmitted light (AC component) by the non-pulsatile transmitted light (DC component) (Goldman et al., 2000). This normalization also accounts for light path length variations through the measured tissue. Equation 2.5 can be simplified and SpO_2 can be easily calculated as a linear function of R (Mendelson, 1992):

$$\text{SpO}_2 = K_1 + K_2R \quad (2.7)$$

Where, K_1 and K_2 are constants derived from the calibration curve (Webster, 2002; de Kock and Tarassenko, 1993; Sinex; Mendelson, 1992; Yang et al., 1998).

2.1.6 Calibration free methods of SpO₂ estimation

Several studies developed methods to compute SpO₂ independent of any calibration. Recently, a calibration-free method based on two wavelengths that are close to each other, 780 and 808 nm, was reported (Nitzan and Taitelbaum, 2008; Nitzan et al., 2014a). When the wavelengths are less different, the effective optical path-lengths differences and blood concentration change are also small (Nitzan et al., 2000). These studies developed a model that utilizes R value and haemoglobin extinction coefficients to estimate SpO₂:

$$SpO_2 = \frac{\varepsilon_{d1} - R\varepsilon_{d2}}{R(\varepsilon_{o2} - \varepsilon_{d2}) + (\varepsilon_{d1} - \varepsilon_{o1})} \quad (2.8)$$

Where ε_o and ε_d are extinction coefficients for HbO₂ and Hb, respectively, which are available in literature (Wieben, 1997; Mannheimer et al., 1997; Laing et al., 1975).

Reddy et al. (2011) developed a model based on light attenuation to estimate SpO₂. They demonstrated that, after applying the natural logarithm, the AC components alone are sufficient to compute SpO₂ values without the need for any calibration constants derived from data obtained from volunteers. Their model used the peak to peak values of the AC signal and published haemoglobin extinction coefficients (Wieben, 1997; Mannheimer et al., 1997; Laing et al., 1975) to estimate SpO₂:

$$SpO_2 \% = \frac{\hat{V}_{IR}\varepsilon_{HbRD} - \hat{V}_{RD}\varepsilon_{HbIR}}{(\hat{V}_{IR}\varepsilon_{HbRD} - \hat{V}_{RD}\varepsilon_{HbIR}) + (\hat{V}_{RD}\varepsilon_{HbOIR} - \hat{V}_{IR}\varepsilon_{HbORD})} \times 100\% \quad (2.9)$$

Where, V_{RD} and V_{IR} are peak to peak values of the AC component for the RD and IR signals, respectively. Although their method used available extinction coefficients, similar to Nitzan and Taitelbaum (2008) model, they did not require any R-value estimation. However, these calibration free models are not used in this research due to the lack of reliability and robustness as discussed in Sections 2.7.4 and 4.4.2.

2.2 Photoplethysmography signal and modes

2.2.1 PPG signal components

PPG systems distinguish between light absorption due to blood volume and that of other tissue constituents by considering arterial blood to be dynamic (pulsatile), while everything else is considered static (non-pulsatile). Therefore, there are two components in the PPG signal: the AC component due to pulsatile arterial blood; and the DC component due to non-pulsatile blood, tissues, and bones. The AC component is related to high frequency signals (>0.5 Hz) and is synchronous with HR. In contrast, the DC component is related to very low frequency signals (<0.5 Hz) and captures the slowly varying tissue absorption and light scattering. The PPG signal components and light absorption by vascular bed are illustrated in Figure 2.3.

The AC portion of the PPG arises due to cardiac activity pulsating arterial blood in the vasculature. The frequency components of the AC signal can vary, depending on the heart rate of the individual. This AC signal is superimposed on a large and relatively static DC signal, which is related to average non-pulsatile blood volume and tissues. The DC signal varies very slowly due to respiration, vasomotor activity, and thermoregulation, among other factors (Nitzan et al., 1998). Depending on the physiological state of the microvascular bed, the pulsatile component accounts

for a small percentage (approximately 0.05 – 1%) of the total light intensity, either transmitted through or back scattered from the tissue or skin (Mendelson and Ochs, 1988).

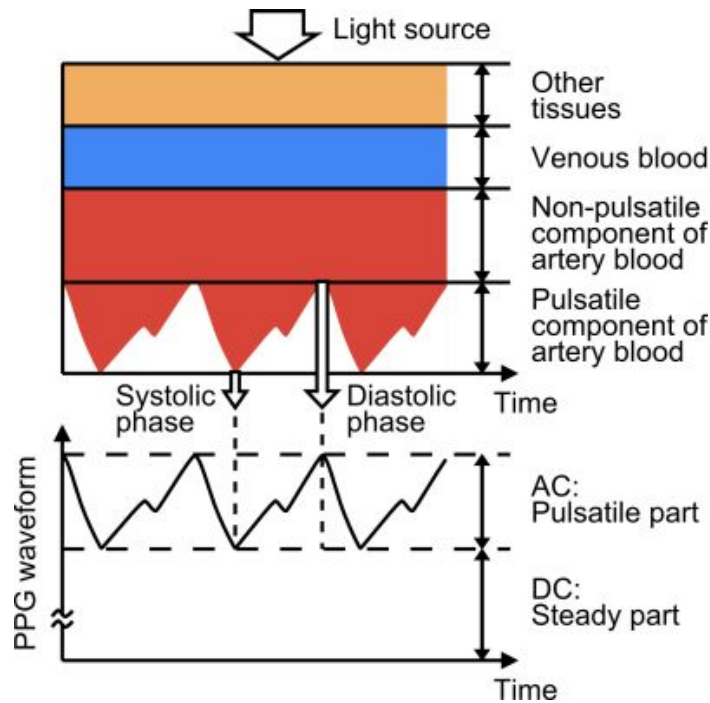


Figure 2.3: Dynamic light absorption of vascular bed during cardiac cycle. Source: Tamura et al. (2014).

2.2.2 PPG waveform and shape

The PPG waveform results from the time-varying amount of blood pushed into the arterial vascular bed during systole and diastole of the heart's cardiac cycle. A typical PPG waveform is shown in Figure 2.4. During systole (anacrotic phase), the blood volume in the arteries increases, increasing light absorption and thereby reducing the received intensity. This phase is seen as an ascending limb on a PPG wave. During diastole (catacrotic phase), the blood volume in the arteries decreases, thus reducing light absorption and increases received intensity. This phase is seen as a descending limb on the PPG. Thus, the PPG signal appears pulsatile in nature with this pulsatility matching the HR. On clinical monitors (and Figure 2.4), the PPG waveform is always displayed inverted so that

it agrees with the movement of the arterial pressure waveform, increasing in systole and decreasing in diastole, and is thus simply interpreted (Alian and Shelley, 2014; Jonsson, 2006).

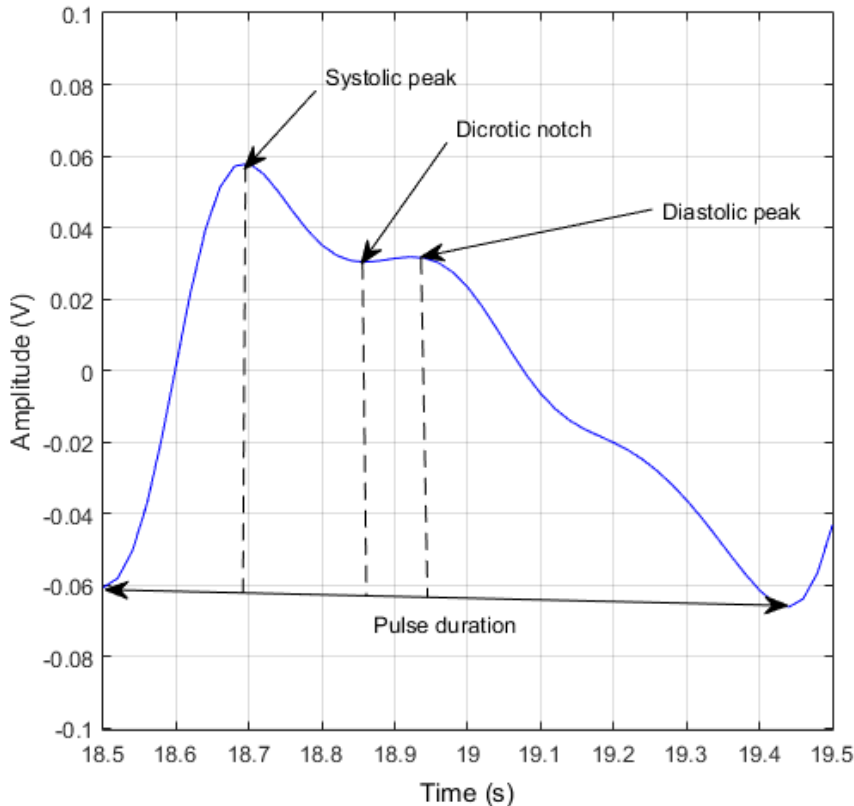


Figure 2.4: A typical PPG waveform pulse showing some features.

A characteristic notch is typically visible in descending limb of a PPG pulse (Murray and Foster, 1996; Jubran, 2015; Allen, 2007), and is due to pressure wave reflection at bifurcations of the arterial tree (Sherebrin and Sherebrin, 1990). This notch resembles the dicrotic notch feature seen in an aortic pressure waveform, indicating the closure of the heart's aortic valve, which causes a similar interruption to flow. This dicrotic notch feature is labelled in Figure 2.4.

2.2.3 Transmission and Reflectance mode photoplethysmography

PPG signals can be acquired by a sensor in either transmission (TPO) or reflection (RPO) mode, as shown in Figure 2.5. In TPO mode, light transmitted through the tissue is detected by a PD on the opposite side of the LED source. TPO sensors are capable of obtaining a relatively strong signal, across the whole transmitted path length. This high signal-to-noise ratio (SNR) is mainly due to a larger fraction of the emitted light reaching the PD. However, in this mode the measurement site is limited to a few locations, such as the fingertip, earlobe, toe, and tongue, where transmitted light can be easily detected in order to be effective (Tamura et al., 2014).

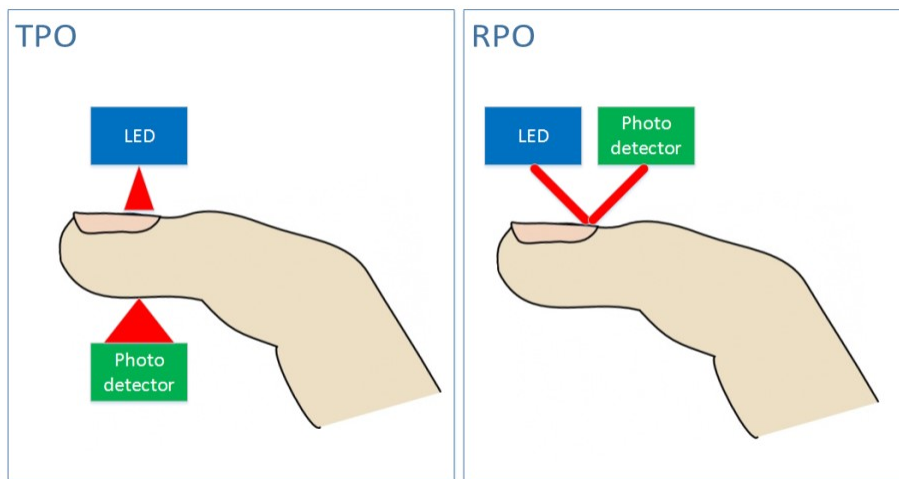


Figure 2.5: Transmission vs Reflection mode photoplethysmography

In RPO mode, the LED source and PD are placed adjacently on the same side, allowing the PD to detect the light that is back-scattered or reflected from the tissue. This mode provides much more flexibility with sensor placement, and a variety of measurement sites can be used, such as the forehead, chest, and forearm, which are not possible with TPO. In RPO mode, a small fraction of the emitted light reaches the detector, and is mostly scattered, which results in low SNR and pulse

amplitude (Dassel et al., 1997). This shortcoming can make RPO sensors much more prone to motion artifacts and pressure disturbances (Tamura et al., 2014). In addition, the path length in RPO mode is much shorter than that in TPO mode as it uses low power LED, thus can provide less in depth information. (Huang et al., 2011).

2.3 Applications of PPG and its limitations

SpO₂ measurement has been the predominant application of PPG technology in clinical settings. However, the PPG signal is rich in physiological information (Shelley, 2007), and can be used in monitoring of various physiological parameters. Other examples of PPG based assessments include blood flow and perfusion monitoring, heart rate variability, cardiac output and pulse transit time, blood pressure, and systemic and peripheral resistances. In addition, PPG can also be used in clinical diagnosis, such as vasospastic conditions and vascular diseases. This section briefly reviews each of these areas to demonstrate the widespread dominance of this optical technology in medical science, and thus its considerable potential for further innovation and application.

2.3.1 Blood flow and perfusion monitoring

Non-invasive assessment of blood flow changes in muscle and bone using PPG has been previously reported (Bergstrand et al., 2009; Naslund et al., 2006; Zhang et al., 2001). These studies showed that the AC component of the PPG corresponds to blood flow, while the DC component corresponds to the blood volume change. Monitoring AC pulse amplitude can reliably estimate blood flow changes at different locations.

Perfusion Index (PI) is a relative assessment of the PPG pulse strength at the monitoring site, and can be used as an indicator of perfusion (Masimo, 2007). PI is measured as a ratio of AC to DC components of the IR signal, corresponding to the pulsatile and the non-pulsatile amounts of blood. Lima et al. (2002) demonstrated that the PI measurements can be used to non-invasively monitor peripheral perfusion in critically ill patients. Another study reported that the PI can accurately indicate sympathectomy-induced vasodilatation that can affect perfusion (Ginosar et al., 2009).

2.3.2 Heart rate variability

The distance between two systolic peaks (peak-peak interval) can be used to reliably monitor HR (Fu et al., 2008; Cennini et al., 2010). In addition, this PPG feature can also be used to estimate heart rate variability (HRV) overtime. Several studies compared HRV derived from R-R intervals in electrocardiogram (ECG) signal to HRV derived from PPG pulse interval and peak-peak interval in healthy cohort and hospital patients (Chuang et al., 2015; Selvaraj et al., 2008; Gil et al., 2010). All of these studies found a strong correlation between the HRV's calculated from the two methods. Another study showed that the PPG pulse interval can also be used to determine HRV (Lu et al., 2008). HRV determined from PPG signals can be a potential surrogate for its ECG counterpart (Gil et al., 2010; Chuang et al., 2015), due to the simpler measurement procedure and ease of access, since PPG devices uses only one probe to record the complete waveform.

2.3.3 Cardiac output and pulse transit time

Cardiovascular monitoring is not only essential for hospitalised critically ill patients, but also for patients at home and those undergoing cardiopulmonary exercise testing. Wang et al. (2010) developed a tube model that can derive a cardiac output (CO) index, based on the pulse time

reflection ratio (PTRR) from an electrocardiogram and PPG based measurements. With appropriate calibration, the PTRR can be used to estimate beat-to-beat CO. Lee et al. (2013) extracted spectral and morphological features from a finger based PPG sensor, and added to HR and mean arterial pressure as input features to a multivariate regression model to estimate CO and systemic vascular resistance. They developed a stepwise feature search algorithm to select statistically significant features. Myint et al. (2014) used PPG sensors at finger and wrist to measure pulse transit time (PTT), which is the time between the two maxima of two PPG waveforms at two sensor locations. PTT is derived from the difference between the wrist PPG sensor and the finger PPG sensor, by calculating the arrival time's difference of a corresponding point of identity on each of the PPG waveforms.

2.3.4 Blood Pressure estimation

Nitzan et al. (2009) presented a pressure cuff based technique for automatic measurement of systolic blood pressure, based on simultaneous measurement of PPG signals from fingers of both hands. They inflated a pressure cuff to a level above systolic blood pressures at a relatively slow rate, resulting in loss of PPG signal. The pressure cuff was then deflated, and the pressure at which the PPG signal reappeared was taken as the systolic blood pressure. Their results agreed well with sphygmomanometry measurements. In contrast, Song et al (Song et al., 2009) demonstrated that both the systolic and diastolic blood pressure can be estimated by studying the changes in morphology of the PPG , using a similar pressure cuff method.

2.3.5 Peripheral and systemic resistance assessment

The PPG pulse width and area has been previously used to determine peripheral and systemic resistances. Awad et al. (2007) reported that the pulse width of finger and ear PPG tracings correlates well with changes in systemic vascular resistance, ($r = 0.56$ and 0.62 , respectively). In another study, (Wang et al., 2009) split the pulse area at the dicrotic notch, and found that the ratio of the two areas as a potential indicator of total peripheral resistance. This ratio is called the inflection point area ratio.

2.3.6 Aging and vascular disease assessment

PPG technology can be clinically important in aging and vascular disease assessment. Yousef et al. (2012) reported that parameters derived from PPG contour analysis have a close relation with age. Aging affects the contour of PPG signals which accelerates the disappearance of PPG's dicrotic notch and PPG's inflection point as well. Peripheral arterial diseases, such as vascular atherosclerosis, prevail with the increase in age and can result in the occlusion of the arteries. Under such diseased conditions, the PPG pulse usually becomes damped, delayed, and diminished with increasing severity of disease (Heck and Hall, 1974; Osmundson et al., 1985; Kvernebo et al., 1989), and thus can be diagnosed using PPG (Shelley and Shelley, 2001). In addition, PPG signal derivatives can be useful in vascular disease determination. Alty et al. (2007) demonstrated that the peak-peak interval, crest time, and stiffness index derived from the first derivative of the PPG were ideal features for cardiovascular disease classification.

2.3.7 Vasospastic conditions assessment

PPG sensors have been previously used to investigate vasospastic or cold sensitivity condition called Raynaud's phenomenon. Cooke et al. (1985) characterized the PPG pulse shape in healthy subjects and Raynaud's patients and found that both the pulse amplitude and the slope of the rising edge are good markers for the condition. Loss of the PPG dicrotic notch in affected patients secondary to systemic sclerosis was also reported, in association with reductions in vessel compliance. Variation in pulse amplitude with cold exposure have shown prospects for diagnosing 'vibration white finger', also known as hand arm vibration syndrome, using multi-channel finger based PPG assessments (Dyszkiewicz and Tendera, 2006).

2.3.8 Limitations

Conventional pulse oximetry may provide erroneous readings due to poor signal strength (low SNR), resulting from many physiological conditions, such as low perfusion, skin temperature, vasoconstriction, and skin pigmentation (Feiner et al., 2007; Khan et al., 2015a; Njoum and Kyriacou, 2013; Sinex, 1999; Talke and Stapelfeldt, 2006; Fouzas et al., 2011). Poor peripheral perfusion triggered by clinical conditions, such as hypovolaemia, hypothermia, and vasoconstriction during surgery, may result in pulse oximeter error or failure (Kyriacou et al., 2002). These clinical conditions often arise due to the administration of anaesthetic agents and/or muscle relaxants (Nakajima et al., 2000). Other external circumstances can also reduce SNR of pulse oximeter, such as motion artefacts, electromagnetic interferences, environmental noise, strong ambient light, and finger nail polish (Fluck et al., 2003; Hanning and Alexander-Williams, 1995; Petterson et al., 2007; Sinex, 1999; Fouzas et al., 2011; Hartmut Gehring et al., 2002). All these limitations can result in inaccurate SpO₂ readings and/or cause false alarms.

In addition to the physiological drawbacks, conventional pulse oximetry has several design limitations. Being highly dependent on the pulsatile component of the PPG restricts its operation to SaO_2 assessment and cannot measure SvO_2 . Typical pulse oximeter derived waveforms presented to the clinician are highly filtered and processed from the original PPG signal. Manufacturers use adaptive noise reduction-based signal conditioning and advanced digital signal processing techniques (NTS, 2011), which enable separation of sources and noise signals (Goldman et al., 2000; Bennett, 1998; Rheineck-Leyssius and Kalkman, 1999). Thus, with minimum access to the raw PPG waveform and the overriding clinical importance of monitoring oxygen saturation, various other potential uses for the PPG waveform have been largely neglected or not possible (Shelley et al., 2014).

In conventional pulse oximeters, the process of amplifying the AC signal for a clearly detectable pulse, removes bulk of the DC component. Complex algorithms are used to evaluate the shape of each potential pulses and extract useful pulses from noisy signals (Rheineck-Leyssius and Kalkman, 1999; Bennett, 1998). While such signal processing may help in SpO_2 estimation, it often compromises valuable physiological information. Preservation of the DC signal in the raw PPG has the potential to enable other parameters, such as SvO_2 , to be determined. Thus, the development of a pulse oximeter system, which gives access to both the raw and amplified signal, is a necessary part of extending potential uses and for perfusion assessment in this research.

2.4 Venous physiology and SvO_2 assessment

Arterial oxygen saturation, SaO_2 , can be reliably determined using non-invasive pulse oximetry due to the pulsatile nature of arterial blood. SaO_2 is a global parameter, and thus the body's

regulatory systems maintain the same systemic and peripheral saturation levels. In contrast to SaO_2 , peripheral SvO_2 is different to central SvO_2 due to the difference in oxygen demand and consumption between peripheral and central tissues. Neither peripheral nor central SvO_2 can be determined using conventional pulse oximetry.

If regional SvO_2 can be reliably estimated non-invasively, the degree of local O_2E can also be determined from the difference to SaO_2 . This difference would reflect, at least locally, the adequacy of regional tissue perfusion. In addition, SvO_2 has been reported as an early indicator of increased oxygen consumption and inadequate oxygen delivery in patients undergoing cardiac surgery (Kamshilin et al., 2015), further validating the potential of this measure. This section discusses the venous physiology and the currently applied or investigated methods used to assess SvO_2 .

2.4.1 Physiology of peripheral venous compartment

In the peripheral regions, venous blood exhibits a non-pulsatile, constant flow. As arteries lead to arterioles and capillaries, the resistance to blood flow decreases due to a significant increase in the total cross sectional area (CSA) of the vasculature before entering veins (Patton, 2015). The reduction in peripheral resistance has been associated with the transition from pulsatile flow in the arteries to constant flow in the veins (Walton et al., 2010). In addition, the venous pathways linking peripheral veins with the heart are interrupted by series of valves. These valves significantly attenuate the retrograde pressure waves emerging from the right heart (Walton et al., 2010; Caro et al., 2012), which thus prevent any natural pulsation in the peripheral veins. Therefore, conventional pulse oximetry cannot estimate SvO_2 since the technology relies on the pulsatile nature of blood.

2.4.2 Methods to assess tissue perfusion and SvO_2

Current methods of measuring peripheral SvO_2 in clinical settings involve fibre optic catheterization, such as peripheral IV catheters or via direct blood draw (Bloos and Reinhart, 2005), both of which are intrusive and come with risk of complications. Previous studies have shown that peripheral perfusion can be assessed non-invasively under clinical conditions using technologies such as laser Doppler based blood flow measurements (Briers, 2001; Cutolo et al., 2010; Humeau et al., 2007) and capillary microscopy (Jacobs et al., 1990; Carpentier, 1998), or by monitoring the central-to-toe temperature difference (Vincent et al., 1988; Boerma et al., 2008; Boerma et al., 2005), although these technologies or methods cannot measure SaO_2 or SvO_2 . In contrast, several studies have previously shown that optical technologies, such as near infrared spectroscopy (NIRS) and photoplethysmography can be employed to detect changes in peripheral perfusion and estimate oxygen saturation (Lima et al., 2002; Van Beekvelt et al., 2001; Lipcsey et al., 2012; Nioka et al., 2006; Shelley, 2007).

NIRS is a non-invasive, optical technique that allows determination of tissue oxygen saturation (StO_2) based on spectro-photometric quantification of oxygenated and deoxygenated hemoglobin within a tissue. Typically, NIRS sensors use three or more wavelengths to measure StO_2 . However, the StO_2 determined by NIRS devices cannot distinguish between arterial, capillary, and venous blood (Petrov et al., 2012; Colquhoun et al., 2012; Sørensen et al., 2013). As a result, NIRS cannot precisely measure SvO_2 . Hence, while some NIRS based studies have provided reasonable SvO_2 measurements within physiological range (Colquhoun et al., 2012; Franceschini et al., 2002), there are several concerns over their methods and outcomes, which are explicitly discussed in the following section. In addition, it is difficult to assess blood flow continuously using NIRS as it

requires vascular occlusion procedures (Lima and Bakker, 2011; Van Beekvelt et al., 2001), that also significantly interrupt care.

Several researchers have previously tried to measure SvO_2 in the central vasculature using PPG. Recent PPG studies on the central vasculature have shown that the PPG waveform is influenced by positive pressure ventilation and respiratory variations (Natalini et al., 2006; Phillips et al., 2012; Walton et al., 2010; Wardhan and Shelley, 2009; Cannesson et al., 2007; Nilsson et al., 2003; Leung et al., 2008). Respiratory variations impart a periodic oscillation on the PPG signal, which is dominated by venous blood, rather than arterial blood. (Lynch et al., 2014; Walton et al., 2010; Phillips et al., 2012; Cannesson et al., 2007; Nilsson et al., 2003; Wardhan and Shelley, 2009; Shafqat et al., 2015; Colquhoun et al., 2012). This variable and large pulsatile artefact in the PPG has been analysed to estimate central or peripheral SvO_2 using PPG based sensors.

While some of these studies reported a reasonable SvO_2 estimate (Walton et al., 2010; Shafqat et al., 2015; Colquhoun et al., 2012), outcome of their study has several concerns, which are discussed in detail in the subsequent section. Equally, none of these methods addressed the measurement of O_2E and blood flow, or their significance in determining regional perfusion. Other approaches to non-invasively estimate SvO_2 are also discussed in the following section, but these too have significant limitations that do not address all the needs outlined in this chapter.

2.5 Existing research into non-invasive methods to assess SvO_2

2.5.1 Venous pulsation using mechanical ventilation to assess SvO_2

Previous studies investigated the periodic oscillations of PPG signals induced in the thoracic cavity by pressure changes due to mechanical ventilation or normal respiratory cycles (Walton et al., 2010; Phillips et al., 2012; Shafqat et al., 2015). The positive pressure changes were mediated by volume changes in the central venous compartment. These modulated PPG signals were analyzed to evaluate SvO_2 . However, the methods used in these studies are invasive, and/or required positive pressure ventilation, and/or are not applicable to measurements in the peripheral regions.

Specifically, Walton et al. (2010) used a reflectance PPG sensor in the oesophagus to assess central SaO_2 and SvO_2 in cardiac surgery patients. They investigated the influence of positive pressure ventilation on the PPG waveform. They extracted low and high frequency components from the PPG signals. Several algorithms were proposed to estimate the ratio of ratios (R value) from the filtered PPG signals in both the time and frequency domains. Median SaO_2 estimates were approximately 100% and SvO_2 estimates were approximately 80%, while the differences between them were statistically significant ($n = 10, p < 0.0071$).

In a subsequent study, Shafqat et al. (2015) used the same experimental data and improved the method of estimating instantaneous SvO_2 using a smoothed-pseudo Wigner-Ville distribution. A statistically significant difference was found between instantaneous SaO_2 and SvO_2 estimates ($n = 12, p \leq 0.001$). However, both methods required insertion of a PPG probe inside the oesophagus and examined sedated patients undergoing positive pressure mechanical ventilation. In addition,

neither study validated their results against a gold standard, such as blood gas measurements of venous blood.

Phillips et al. (2012) conducted a similar study on healthy volunteers, but used a forced respiratory inspiration method. They investigated the effect of negative airway pressure on the blood volume within the tissue bed of the finger, and the subsequent modulation of the PPG signals. Estimated mean SvO_2 was determined to be 3.1% ($\pm 4.2\%$) below estimated mean SaO_2 . The reason for the small difference between the two saturations was suggested to be due to the lack of skeletal muscles in the finger. However, 50% of their SaO_2 estimates were below expected values of 95 – 100% for healthy adults. In addition, some of their SvO_2 estimates were greater than the corresponding estimated SaO_2 values, which is not physiologically possible. Like the prior two related studies, there was also no validation against a gold standard in this study.

2.5.2 Estimation of SvO_2 using natural venous pulsation

Colquhoun et al. (2012) compared SvO_2 measured via NIRS and reflectance PPG with blood gas data from blood samples obtained from the internal jugular vein. Venous drainage of the brain occurs almost exclusively through the relatively superficial internal jugular veins. Being close to the core, it is expected that the venous blood there gets naturally pulsed by respiration. Frequency components due to respiration (approx. 0.2 Hz) and cardiac activity (approx. 1 Hz) were identified using FFT. Walton's ResDC algorithm (Walton et al., 2010) was applied to estimate SvO_2 from the PPG signals. NIRS assessed SvO_2 showed a weak, but statistically significant, correlation to measured SvO_2 ($r^2 = 0.28, p = 0.03$), with a mean bias of 2% and limits of agreement of -15.5% to 19.5%. In contrast, the reflectance PPG measurements showed no statistically significant

correlation ($r^2 = 0.00$, $p = 0.98$), with a mean bias of 4.3% and limits of agreement of -49.8% to 58.3%. They also posed concerns over the blood gas analyzer's accuracy at low saturations and the penetration depth of reflectance PPG. Thus, they were not able to assess any changes in jugular SvO_2 using NIRS or PPG.

2.5.3 External venous pulsation to assess SvO_2

Schoevers et al. (2009) developed an artificial pulse oximeter with pulse generation system to modulate the arterial and venous compartments simultaneously at very high pressures of 660 mmHg, which are well above systolic blood pressures. The study used 3 separate digit pressure cuffs, which were sequentially inflated to induce a pulsatile component in the PPG signal by peristaltic action. Their idea was to use Shelley's arterial to venous compliance ratio (Shelley et al., 2011) to estimate SaO_2 and SvO_2 from the PPG signals. However, Schoevers et al.'s results were determined to be neither comprehensive nor conclusive in a further study by Cloete et al. (2013). In addition, using a modulation pressure above systolic blood pressure interrupts normal arterial blood flow to the finger. Thus for these reasons, it is also not be possible to make continuous oxygen saturation measurements using this method.

In 2003, (Chan, 2002) developed the Venox concept to estimate SvO_2 in the periphery from PPG signal and filed a patent (Chan et al., 2007). This concept used high frequency (7.5 Hz) modulations to rapidly pulse the venous bed at low pressures of 40 mmHg, below typical diastolic pressures and thus not interrupting arterial flow, using a digit pressure cuff. The resulting PPG waveform was decomposed into relevant spectral components based on cardiac (approximately 1 Hz) and pressure cuff (7.5 Hz) frequencies. The rapid pulsations were expected to separately excite

the venous bed that can be observed in the PPG signals for SvO_2 estimation. Echiadis et al. (2007) implemented the Venox concept in a study with patients undergoing heart bypass surgery. However, their research did not appear to provide data suitable for clinical use, as scrutinized in another study by Thiele et al. (Thiele et al., 2011). The SvO_2 determined from the PPG signals was compared to central venous oxygen saturation (ScvO_2) measured by a cardiopulmonary bypass (CPB) machine. Since the PPG measurements were peripheral and the CPB provided central measurements, the author reported that it was not possible to infer ScvO_2 from PPG assessed SvO_2 , which is also not the goal in this research. In addition, no SvO_2 estimates were specified for healthy human subjects, not allowing any comparison to expected values.

2.5.4 Venous occlusion dependent peripheral SvO_2 estimation using NIRS

The volume of blood in a venous compartment can be increased by occluding the venous outflow with a pressure cuff, in a given limb. During such procedures, the pressure applied to the pressure cuff is much lower than arterial diastolic pressures to maintain perfusion, but higher than venous blood pressures (approximately 10 mmHg). As a result, blood pools in the venous compartment, increasing the venous blood volume. The spectral absorbance can be compared before and after venous occlusion at two or more wavelengths to assess SvO_2 in the venous compartment. Previously, researchers used NIRS and PPG technology to demonstrate this approach (Yoxall and Weindling, 1997; Nitzan et al., 2000).

Yoxall and Weindling (1997) compared the SvO_2 measured via NIRS with that obtained by co-oximetry, an *in vitro* reference measurement method, and venous occlusion on blood samples drawn from superficial veins. A significant correlation between the two measurements was

reported ($n = 19$, $r^2 = 0.49$, $p < 0.0001$). However, the linear correlation explained only 50% of the observed trends. They observed a systematic bias dependent on the lateral spacing between the light source and photo detector, adjacently positioned in RPO mode. It was concluded that the more distant the source and detector, the deeper light beams can travel, allowing detection of more desaturated blood or lower SvO_2 .

Nitzan et al. (2000) used two wavelengths close to each other, at 767 nm and 811 nm, and near to the isosbestic wavelength of 805 nm to measure SvO_2 via NIRS and venous occlusion. This choice of wavelengths can reduce the error of neglecting the difference in scattering constant between two wavelengths (Mannheimer et al., 1997). In addition, the difference of the effective optical path length and of the blood concentration change between the two wavelengths can be neglected. NIRS at the hand and finger of healthy volunteers ($n = 17$) resulted in mean SvO_2 values of 86.2% ($\pm 4.1\%$) and 80% ($\pm 8.2\%$), respectively. They modified an available SaO_2 model involving hemoglobin extinction coefficients to make these saturation estimates, as discussed in Section 2.1.6.

The venous occlusion technique used in both of these studies has two common downsides. First, continuous SvO_2 measurements cannot be made, since the method relies on discrete interventions isolated by sufficient time for the tissue to reach equilibrium. Second, prolonged disturbance to the venous compartment may lead to potential complications, such as venous stasis and venous thrombosis (Eberhardt and Raffetto, 2005), as well as interference to any intravenous access in clinical settings. Although Nitzan et al's SvO_2 estimates fall within reasonable physiological ranges for healthy subjects, the mean SaO_2 estimate of 94.5% ($\pm 3.0\%$) was below the expected

range of 95 – 100% for healthy subjects. This inaccuracy thus also questions the reliability of the SvO_2 estimates obtained with that sensor.

2.5.5 Peripheral SvO_2 estimation using NIRS

Franceschini et al. (2002) used 6 different wavelengths in a NIRS sensor and natural respiration induced oscillations of near infrared absorption in tissues to estimate peripheral SvO_2 . Experiments included investigations in the hind legs of pigs ($n = 3$) and upper thigh of human subjects ($n = 8$). Their study involved complex data processing and analysis to estimate SvO_2 . First, they computed the amplitude of absorption oscillations at the respiratory frequency at each wavelength. Second, the spectrum of the absorption amplitude was fitted with the hemoglobin absorption. In addition, the effective optical path length from the light source to the light detection point was determined, which is dependent on a frequency-domain multi-distance method (Alberti et al., 2002). Outcomes from the pig experiment showed good agreement between blood gas data and NIRS estimated SvO_2 values, with a mean difference of 1% ($\pm 5.8\%$). In addition, outcomes from the human experiments showed good agreement between NIRS estimates of SvO_2 from natural peripheral pulsation to those obtained using venous occlusion method, with an average deviation of 0.8% and maximum discrepancies of 24.2% and 15.8%.

However, there are several concerns about this study. No whole blood sample was taken from human subjects for blood gas analysis and comparison of estimates, and there was thus no reference standard comparator. There are also concerns about the measurements made in human subjects being affected by arterial pulsations, where it is typically recommended that the site of the NIRS sensor be distant from any arteries in proximity, which is not the case in this research.

Section 2.3.1 discussed how peripheral venous blood has constant flow, and is typically not subjected to any natural pulsation. Therefore, their study, assumptions, and outcome are contradictory to this information, and are thus not necessarily applicable in extremities like the hand or finger.

2.6 Discussion and integration

Available non-invasive methods, using PPG and NIRS sensors, to assess SvO_2 have several concerns. Some of these methods provided physiologically realistic SvO_2 estimates, but did not validate their results against gold standard measurements and used some invasive procedures (Walton et al., 2010; Phillips et al., 2012; Shafqat et al., 2015). No reference measurement and the invasive nature of these studies makes their method less reliable and less applicable, respectively, in peripheral perfusion monitoring. Colquhoun et al. (2012) could not detect any change in local SvO_2 using PPG and NIRS sensors, which is important to determine changes in perfusion. Being able to monitor changes in SvO_2 is very important to distinguish between normal and high/low levels of SvO_2 . In particular, sepsis patients are likely to experience blood flow alterations and significant changes in peripheral SvO_2 levels, due to impaired tissue oxygen extraction capability. Two other studies attempted to assess SvO_2 using PPG sensors by inducing pulsations to the venous system, but failed to provide a physiologically realistic estimate of SvO_2 (Schoevers et al., 2009; Echiadis et al., 2007). Accurate monitoring of SvO_2 is integral to consider this parameter as an indicator of perfusion alterations in sepsis diagnosis. In addition, they did not validate their method using gold-standard reference.

Yoxall and Weindling (1997) and Nitzan et al. (2000) reported some correlation of SvO_2 estimates with reference measurements and physiologically realistic SvO_2 estimates, respectively. However, their methods provide a measurement every 40 seconds, and thus continuous assessment of SvO_2 is not possible. In addition, their method employs venous occlusion procedures, which if prolonged may harm the vascular bed (Eberhardt and Raffetto, 2005). Finally, the study by Franceschini et al. (2002) showed some good outcomes, although, they did not validate their human subject data using blood gas analysis data. Their NIRS sensor often cannot provide accurate measurements due to artefacts caused by arterial pulsations. Hence, continuous and simultaneous assessment of local SaO_2 and SvO_2 to determine tissue O_2E or perfusion changes is not possible using this method.

Reliable SvO_2 monitoring is integral to perfusion monitoring as a necessary measure to determine tissue oxygen extraction capability, and as a clinical marker of microcirculatory failures. In addition to reliability, continuous monitoring of SvO_2 can track alterations in tissue perfusion in real-time, as such alterations are very common in sepsis patients. Pulse oximeters can continuously monitor SaO_2 , and thus continuous monitoring of SvO_2 will enable real-time assessment of tissue O_2E and perfusion changes. Hence, there is a need of a monitoring system that can provide reliable and continuous and simultaneous measurements of both SaO_2 and SvO_2 , which can lead to improved diagnosis of clinical conditions, such as sepsis.

Conventional pulse oximeters cannot assess peripheral venous blood due to its non-pulsatile nature. Available perfusion monitoring systems cannot reliably and/or continuously monitor SvO_2 using PPG or NIRS. This research aims to address these shortcomings of conventional pulse oximeters and available perfusion monitoring technologies in the context of defining the problem

and delineating how this research can improve its potential in perfusion assessment, in particular SvO_2 , using reliable, low cost, and non-invasive pulse oximetry.

2.7 Summary

Pulse oximeters are commonly used in clinical settings. They use photoplethysmography to detect changes in blood volume, which can be used to assess SpO_2 and HR. SvO_2 is a useful parameter to assess perfusion completely, and can be used as a marker in sepsis diagnosis. Conventional pulse oximetry cannot measure SvO_2 and other pulse oximeter based methods have several shortcomings, some of which are taken into consideration for the studies presented in Chapters 7 and 8. The following chapter discusses the design and development of a custom built pulse oximeter system, but also some novel technological aspects that are not demonstrated by current commercial offerings, for peripheral SaO_2 , SvO_2 , O_2E , and blood flow assessment in this thesis.

Chapter 3: Design and development of a novel pulse oximeter system

3.1 Introduction

Commercial sensitivity has limited access to raw PPG signal data, and thus the rate of new pulse oximeter applications has diminished significantly (Shelley, 2007). Although conventional pulse oximeters use two wavelengths, only the infrared PPG waveforms are typically presented to the user or clinician on screen. In addition, the filtering of a majority of the DC signal removes valuable physiological data, including venous blood absorption information. In this research, the primary goal is to measure tissue oxygen extraction, which is dependent on venous blood oxygen saturation data. Thus, the development of a pulse oximeter system that preserves all the original PPG signals is essential to extend its potential.

A custom pulse oximeter system (PO) was developed to provide access to the raw and amplified PPG signals for both RD and IR wavelengths. The final product meets the technical specification and functionality of a typical pulse oximeter (Markandey, 2010; Webster, 2002). The device provides extra flexibilities, such as control of LED intensity, complete PPG data monitoring, and recording data for post processing and analysis. The design specifications, control mechanics, PPG signal acquisition, and all other parameters of this PO system are presented in this chapter. Details of the PPG signal processing and analysis techniques employed are also included in this chapter.

3.2 System Background

The PO system was developed using a CY8CKIT-050 PSoC 5LP (Cypress Semiconductor, San Jose, CA, USA) Development Kit (CDK), as shown in Figure 3.1. This system uses an ARM Cortex M3 microcontroller unit (MCU). The overall design is based on the openly available pulse oximeter implementation on the TMS320C5515 (Texas Instruments, Dallas, TX, USA) DSP Medical Development Kit (Markandey, 2010), and uses the same electronics circuitry.

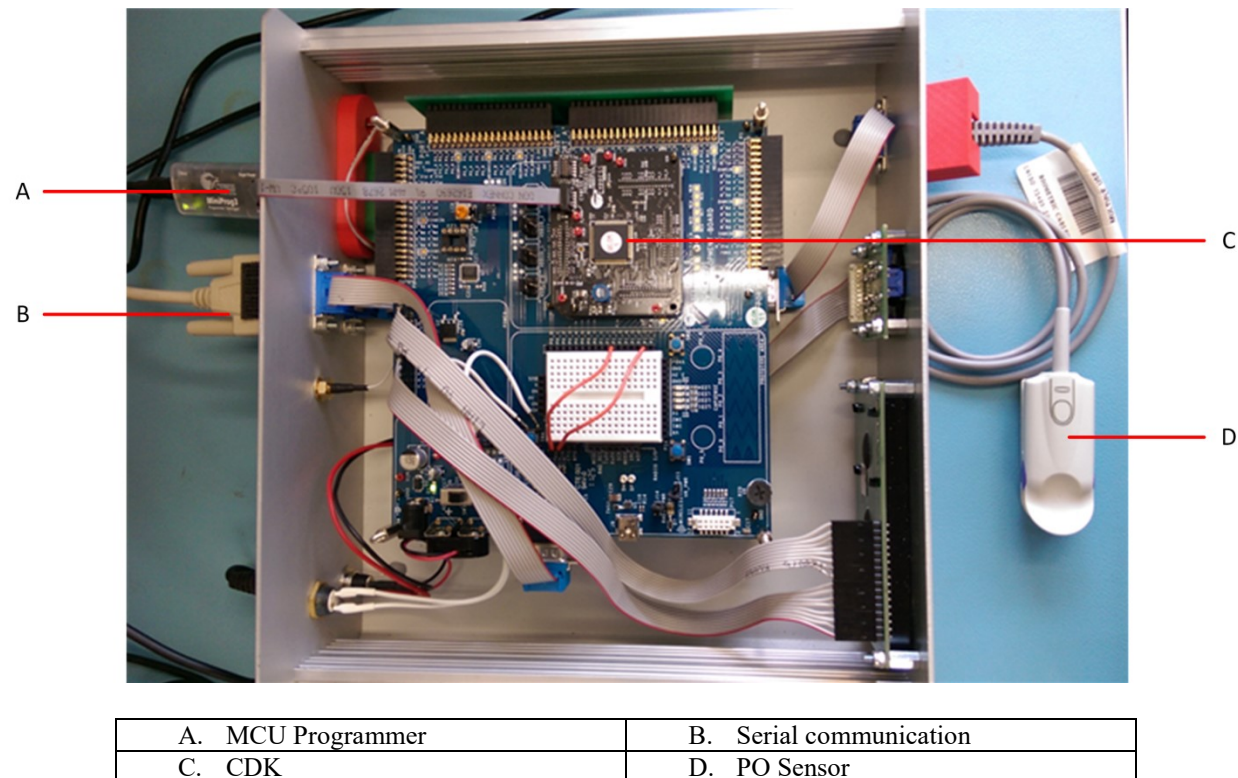


Figure 3.1: Hardware circuitry of PO system, along with the sensor

The sensor LEDs transmit RD and IR light through the finger, which is detected by the PD, in a TPO mode application. Light energy received at the PD end is converted to a current signal, which is passed through a transimpedance amplifier. A de-multiplexer extracts the conditioned raw PPG

signal from the transimpedance amplifier output, so that the RD and IR PPGs can be processed independently. Separated analog PPG signals are then passed through an analog-to-digital converter (ADC) for logging, storage, and post processing. The block diagram showing the major components of the PO system is presented in Figure 3.2.

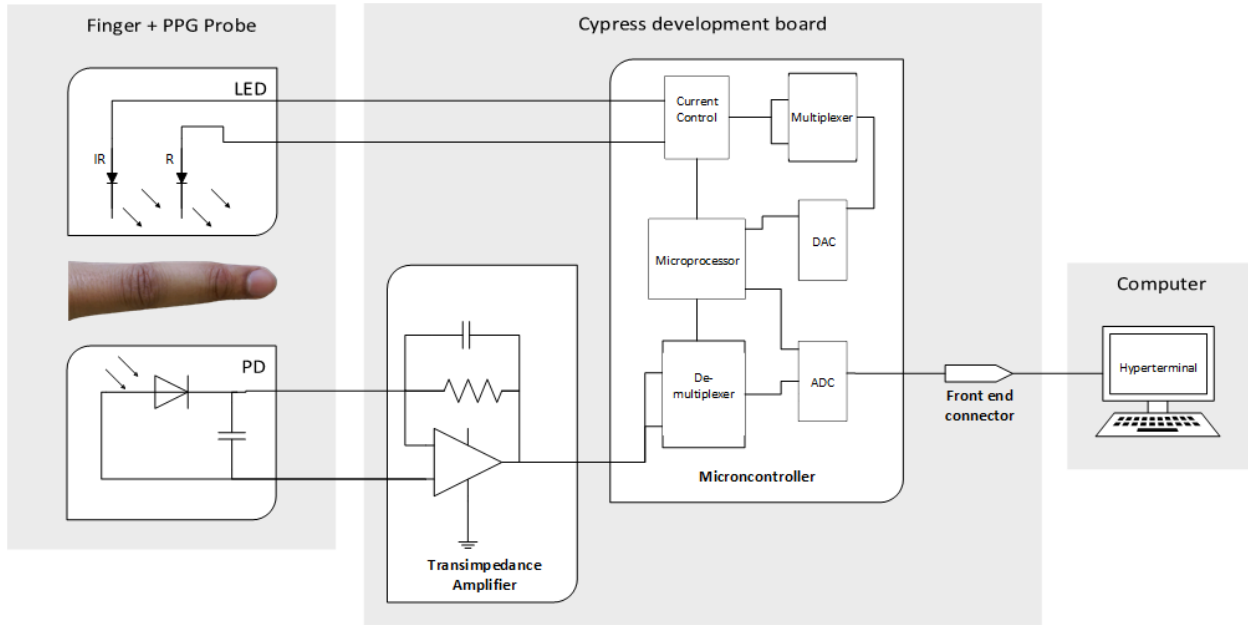


Figure 3.2: Block diagram for the PO system.

3.3 Signal Acquisition

3.3.1 Sensor principles

A standard transmission mode sensor (model: 320701001, Biometric Cables, Guindy, Chennai, India) is used to acquire PPG data from a finger. The dual LED sensor produces 660 nm and 940 nm wavelength light for the RD and IR modes, respectively, and contains a high sensitivity PD. This pair of wavelengths is widely used in pulse oximeter sensors (Ortega et al., 2011; Mendelson, 2003; Wang and Liu, 2011). The PD is optimized for reliable performance at both wavelengths, and exhibits low capacitance and residual currents (Optoelectronics, 2013). Detailed LED and PD

specifications can be found on the manufacturer's datasheet (Optoelectronics, 2013). The RD and IR LEDs are switched on and off alternately. A switching frequency of 500 Hz with a duty cycle of 29% is used to operate the LED switching, as shown in Figure 3.3. The software on the MCU of the development board controls the switching of the RD and IR LEDs.

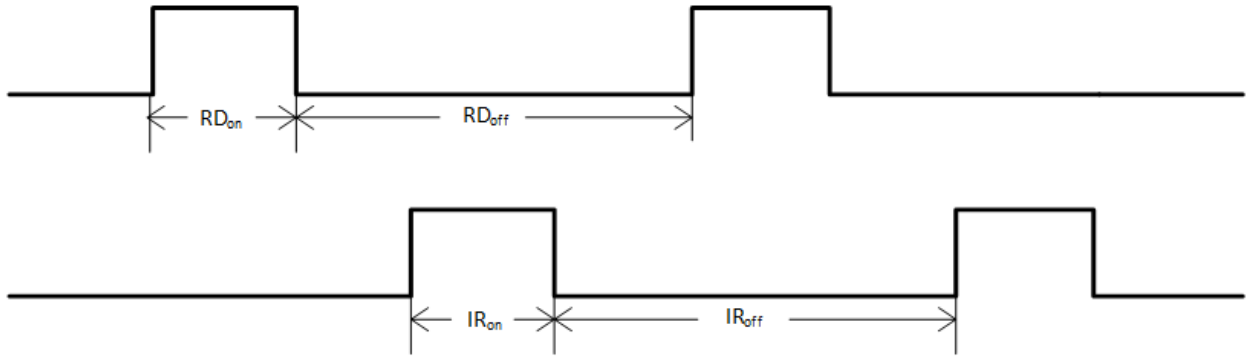


Figure 3.3: Sensor LED timing diagram

3.3.2 Intensity control

Humans have variable finger thickness and skin color. Thus, every finger will cause a different amount of light absorption and scattering. To compensate for this variation the LED light intensity needs to be adjusted specific to each finger, to optimize light transmission and reception. This section details how the LEDs are adjusted by the MCU of the PO system.

The output signal from the transimpedance amplifier is fed to the LED intensity control logic, and is kept within a fixed voltage range of 2.7 – 5.5V to be compatible with the ADC. The intensity control unit sends a feedback signal, based on the raw PPG signal strength, to a digital-to-analog converter (DAC) on the front-end board through the inter-integrated circuit (I2C) bus. This

feedback signal is of 12-bit resolution. The output voltage of the DAC is controlled by the MCU to change current through the LED, and thus intensity, using the circuit in Figure 3.4.

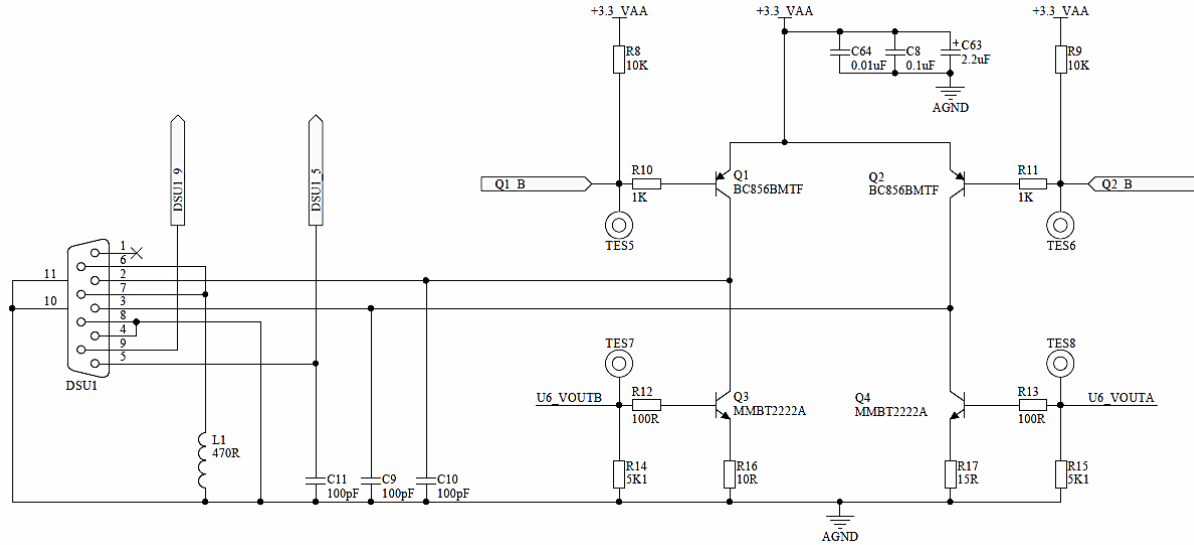


Figure 3.4: LED switching and intensity control circuit diagram, where transistors Q1 and Q4 are the controlling the IR LED, and Q2 and Q3 are controlling the RD LED.

Figure 3.5 shows the relationship between the DAC count and the driving LED current. The raw signal received for RD and IR wavelengths are used to control the intensity control of RD and IR LEDs, respectively. The control mechanism automatically increases or decreases the LED intensity to maximise the PPG signal amplitude without saturating the PD, thus maximising the SNR. The LED current is controlled by the DAC driven by the MCU, depending on the RD and IR intensity. The intensity level is thus automatically adjusted with respect to the finger's thickness and blood flow of the subject.

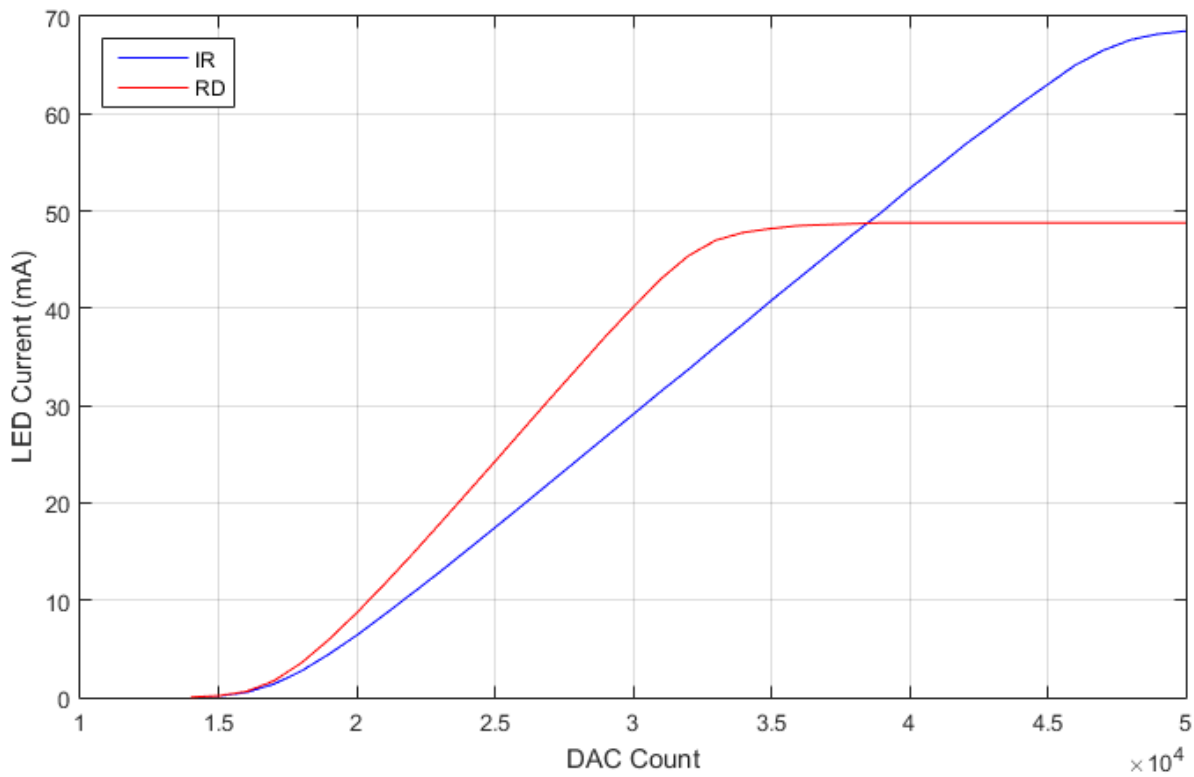


Figure 3.5: Relationship between LED Current vs DAC Count, thus LED intensity characteristics.

The relationship between the DAC count and beam power was validated in a test using a laser power meter (Handheld Laser Power Meter, Edmund Optics, Barrington, NJ, USA). During the test, the pulse oximeter firmware was modified to allow only the red LED to transmit light. The DAC count was increased in steps of 2000 from 19000 to 31000. At each step, the beam strength was measured using the power meter. The same procedure was repeated with the infrared LED. It was observed that the beam power (intensity) increases proportionally with DAC count for at both wavelengths, as shown in Figure 3.6. In addition, the IR radiant flux was found to be much more powerful than the RD radiant flux.

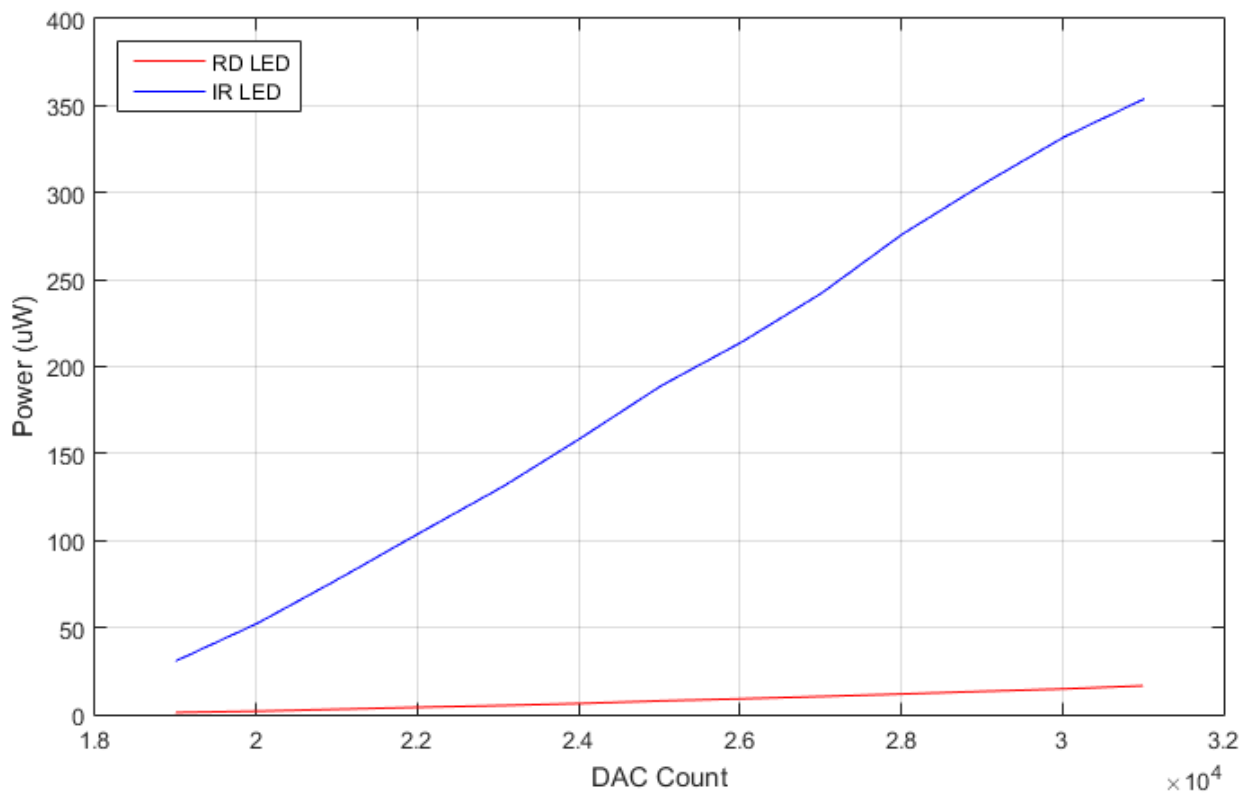


Figure 3.6: Relationship between beam power and DAC count for RD and IR LEDs

3.3.3 Signal conditioning

Light energy received at the PD is converted to current signals and passed through a transimpedance amplifier circuit for signal conditioning. The transimpedance amplifier is composed of two stages as shown in Figure 3.7. Stage 1 converts the current signal to voltage, and adds a gain of 5 to amplify the output. A $5.1\text{ M}\Omega$ feedback resistor converts the input current to an output voltage. Parallel to the resistor, a 2.7 pF capacitor is used to minimize peak gain and improve stability of the signal. This feedback capacitor limits bandwidth, and thus, reduces noise.

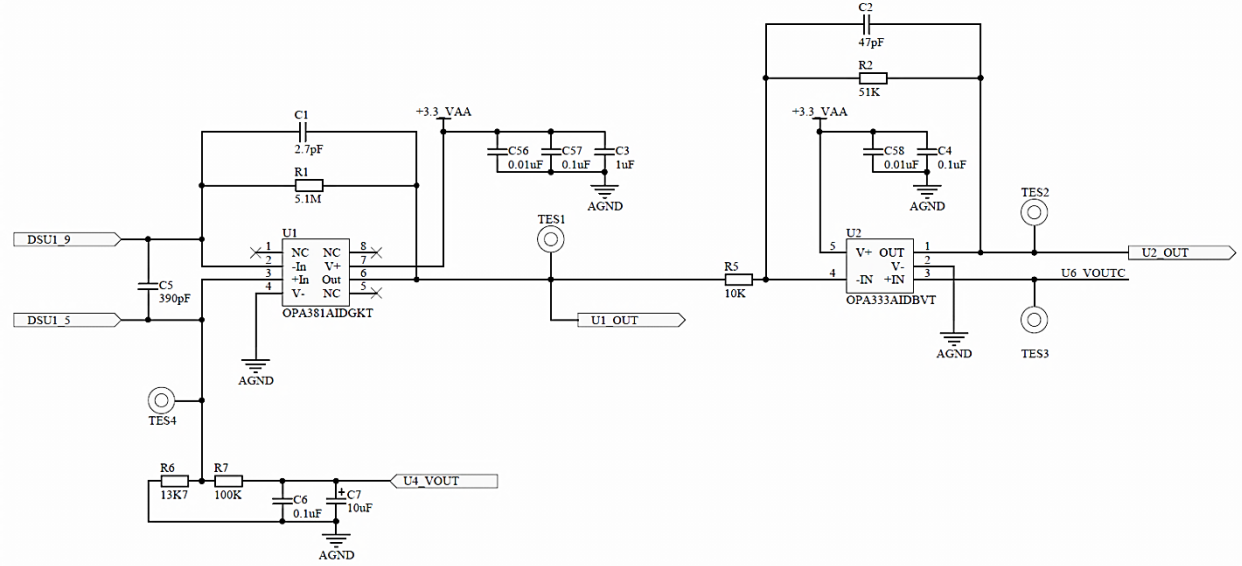


Figure 3.7: Transimpedance amplifier circuit, where U1 represents Stage 1 and U2 represents Stage 2 amplifiers, respectively.

Stage 2 of the transimpedance removes majority the of the DC signal from the raw PPG signal, using a DC correction mechanism highlighted in Figure 3.8, and amplifies the remaining AC signal. The non-inverting input of this amplifier is fed with a DC voltage of ~ 0.3 V, generated by MCU programmed DAC. This DC voltage ensures the output signal contains the complete AC component within the operational range of the ADC. This amplifier also provides a gain of 5 to the AC component.

Output from both Stage 1 and Stage 2 of the transimpedance amplifier are passed through a de-multiplexer, shown in Figure 3.2. The de-multiplexer splits the analog PPG signal to equivalent IR and RD components for independent processing. De-multiplexed analog PPG signals are then sent to the ADC for digitization through 2 separate channels.

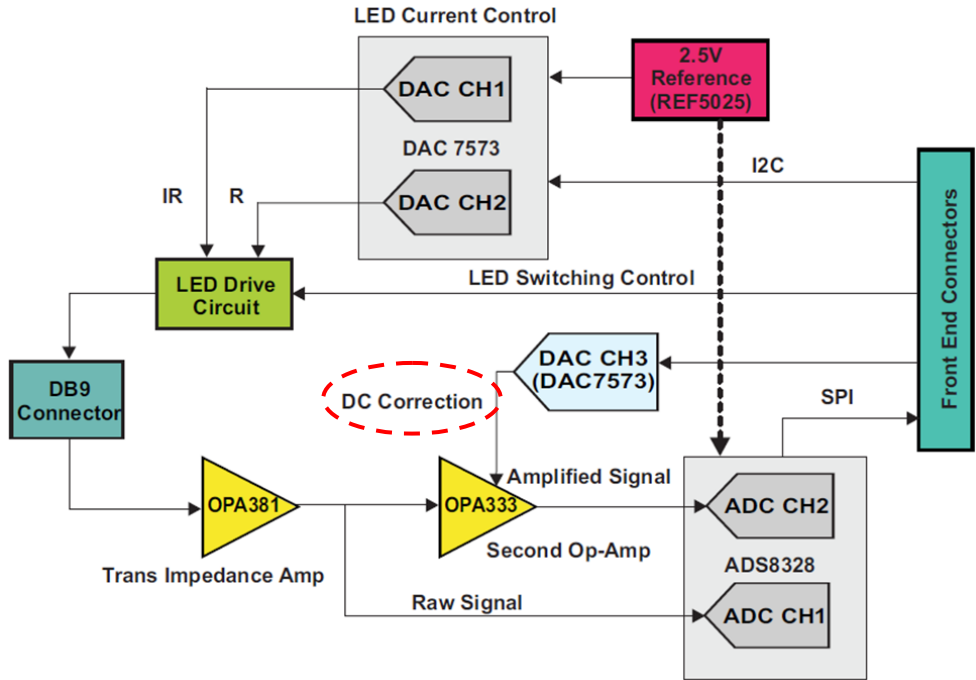


Figure 3.8: Block diagram showing the LED current control, the transimpedance amplifier stages, and the ADC end of the pulse oximeter’s front-end.

Only the output from Channel 1 of the ADC, shown in Figure 3.8 as ADC CH1, is considered for extraction of the complete DC component from the raw PPG signal during post processing. This channel connects directly to the output of the Stage 1 of the transimpedance amplifier, which contains the raw PPG signal. In parallel, the AC signal is extracted from the amplified PPG signal received at ADC Channel 2, also shown in Figure 3.8 as ADC CH2. The amplified signal provides a more reliable number for post processing of AC signal.

3.3.4 Signal sampling and recording

Analog PPG signals are sampled at 50 Hz by a manual mode 16-bit linear ADC, with a 2.5 V reference voltage, on the development board. The PO system’s design can reject 50 Hz mains noise, using several decoupling capacitors. This ability was confirmed during a hardware test, in

which no visible 50 Hz noise was detected by an oscilloscope anywhere in the system, including the transimpedance amplifier stage and the ADC input. This test outcome suggests any potential interference or noise from mains at 50 Hz is attenuated by the PO system.

Sampled data are recorded as ADC counts and transferred to the DSP of the MCU using a serial peripheral interface bus. ADC counts can be logged to a PC by a serial communication based interface. All PPG data are stored as text files on the PC, for offline signal processing and analysis in MATLAB (R2014a, MathWorks, Natick, MA, USA).

3.4 Firmware and user interface development

3.4.1 Firmware and Finite state machine development

The PO system's firmware source code was written using the C# programming language (AT&T and Bell Labs, NJ, USA). The source code controls the read/write functionality to/from ADC and DAC channels, LED intensity control, signal conditioning, signal transmission and streaming output from the ADC as schematically shown in Figure 3.9. A finite state machine (FSM) was developed and implemented to the firmware to enable LED intensity control.

Figure 3.10 shows a flowchart of all the states and transitions of the FSM. More specifically, the FSM allows two types of intensity adjustment; automatic and manual. In the automatic mode, the LED intensity is automatically adjusted according to the finger's thickness and blood flow using a control algorithm. In contrast, the manual mode allows the user to set the LED intensity value, which enables repeatable measurements to be made with the defined intensity.

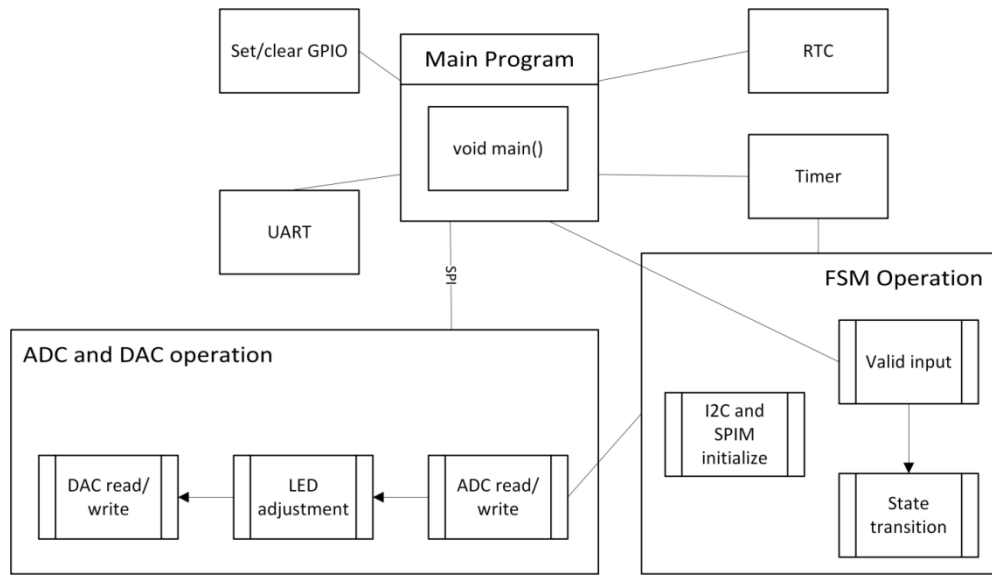


Figure 3.9: PO system firmware top level block diagram.

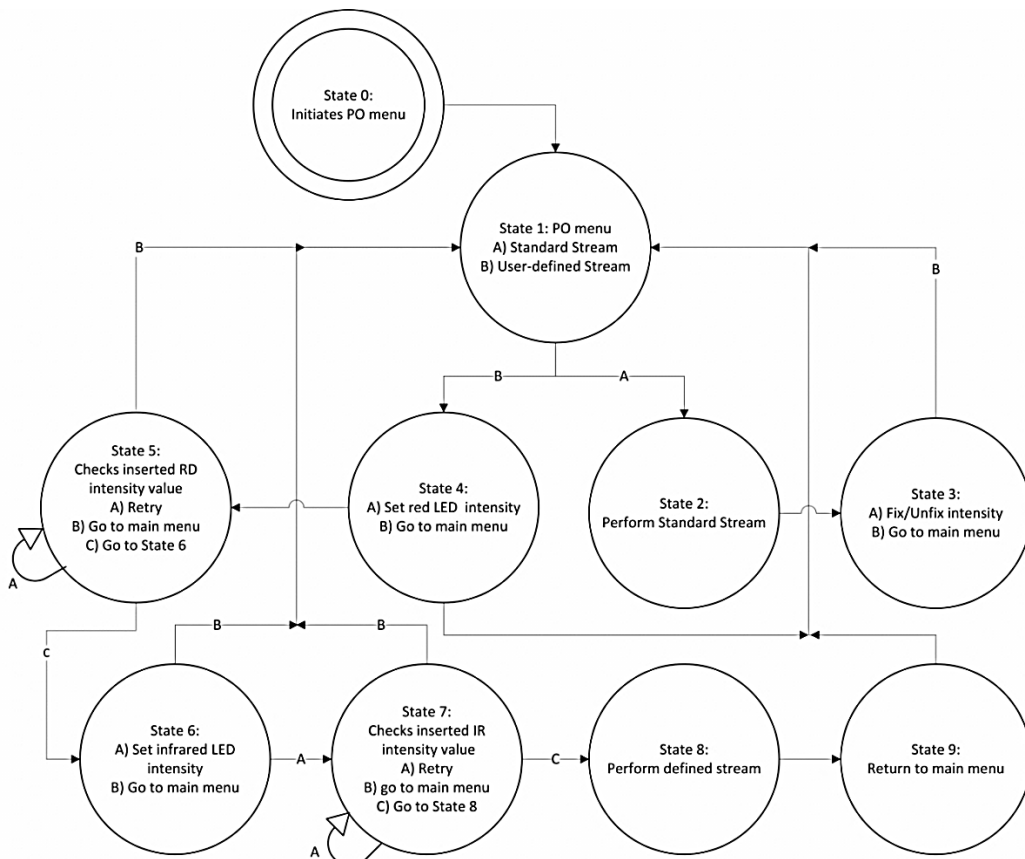


Figure 3.10: FSM states and transitions for LED intensity control

3.4.2 Pulse oximeter user interface

A majority of the PPG data presented in this thesis was acquired using open source serial communication software, such as HyperTerminal. However, such method of PPG data acquisition had several drawbacks. The typical serial interface does not provide any real time monitoring of the PPG waveform or timing feature. Thus, simple test errors were not found until after one or many data sets had been post-processed. Hence, the need for easy operation and real time signal monitoring of the PO system was essential.

To improve PPG data acquisition and operation, a graphical user interface (GUI) interface was developed in LabVIEW. The front panel of this GUI is composed of 4 tabs to simplify operation and display:

- 1) **Configuration** – Set communication (COM) port, control LED intensity, record the PPG data (default is text file format), and view the streaming data in different channels as in terminal software.
- 2) **Monitoring** – Monitor red and infrared PPG waveforms (AC, Raw, and DC signals), SpO₂ and HR, and data recording run-time.
- 3) **Protocol timing and notes** - Record the start and end time of a protocol, and make notes.
- 4) **Error Indicators** – Help to troubleshoot any error that may result while running the software, such as reading/writing from/to serial port, file processing, and filtering.

The configuration tab allows the user to select automatic or manual intensity control and set up serial communication. The following COM port settings are used to configure serial communication:

- COM port: Identified from the computers Device Manager application
- Baud rate: 57600
- Data bits: 8
- Parity: None
- Stop bits: 1
- Flow control: Hardware

Figure 3.11 illustrates the various features of the GUI using a flowchart. The GUI takes a complete line of 16-bit integer (50 characters long) PPG data and stores them in an array. The array contains 8 columns representing RD and IR component data as; RD intensity, RD raw signal, RD DC offset, RD amplified data, IR intensity, IR raw signal, IR DC offset, and IR amplified signal. A circular buffer is used to store the array for processing and collecting new array samples.

Real time filtering removes noise from the raw PPG but extracts the AC and DC components. Extracted AC and DC components are used to determine instantaneous SpO₂ and HR in real-time, using the peak detection algorithm and R value calculation discussed in Chapter 4. Displaying of such important parameters helps to identify the subject's perfusion and cardiovascular status but also the PPG signal quality.

A screen shot of the monitoring tab in the front panel of the GUI is shown in Figure 3.12. This tab displays PPG signals and calculated parameters in real-time, and also enables identification of weak PPG signals. Without real time waveform monitoring, it is not possible to determine whether the data recorded is of good quality until later post-processing. Real-time monitoring of PPG parameters is helpful when recording several hours length of PPG data, such as during clinical trials as discussed in Chapter 8.

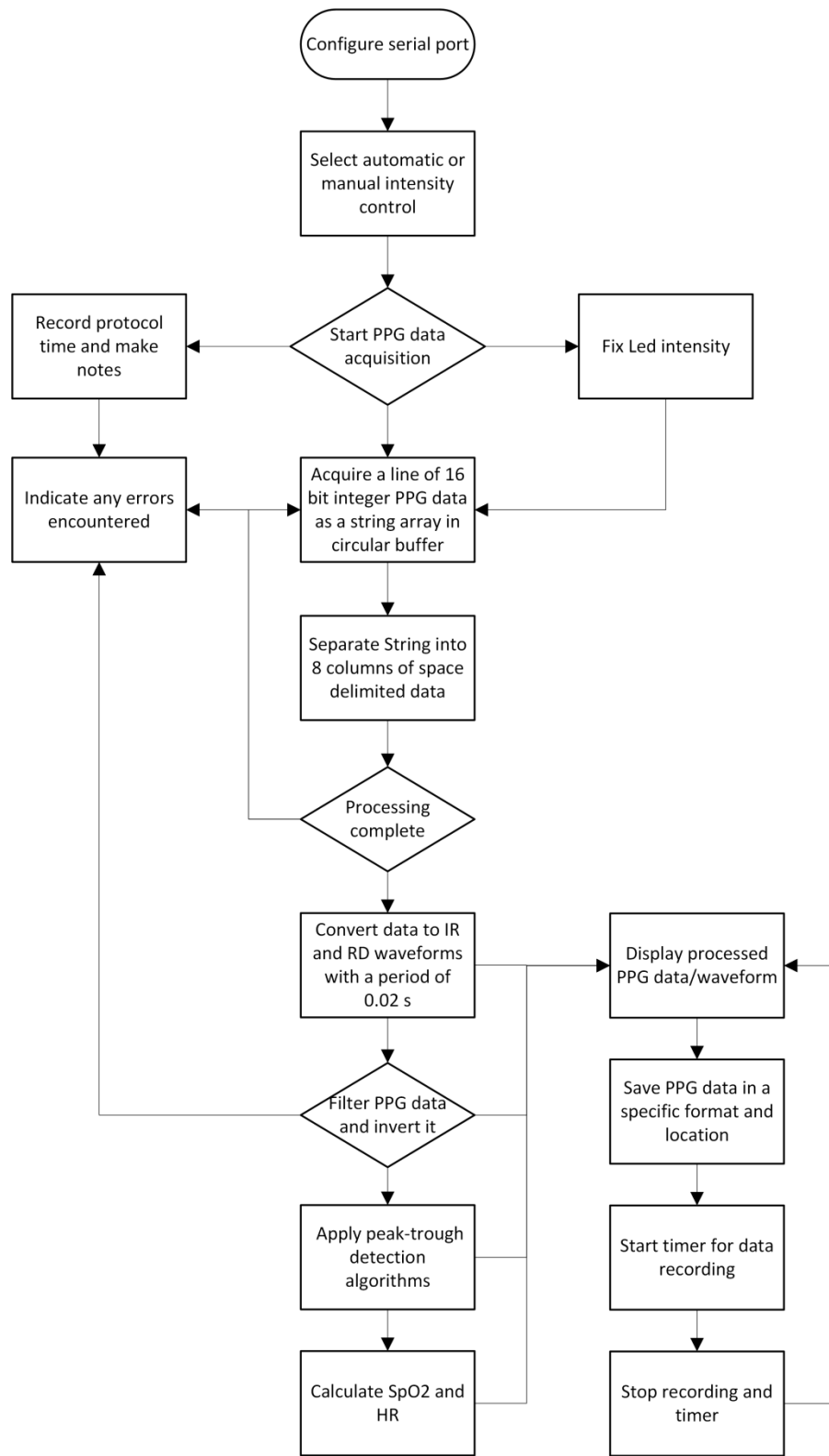


Figure 3.11: Flowchart for the PPG acquisition and monitoring GUI

Event logs feature in the Protocol timing and notes tab can be used to mark the start or end time of a particular protocol/test, to capture PPG data separately for that protocol/test, and also to easily separate PPG data between tests and/or subjects. In summary, this interface overcame all the short comings of open source serial communication software, while providing additional benefits, and was thus used during later studies (Chapter 6) and the clinical validation trial (Chapter 8). Photos for the other tabs are provided in the Appendix 3.1.

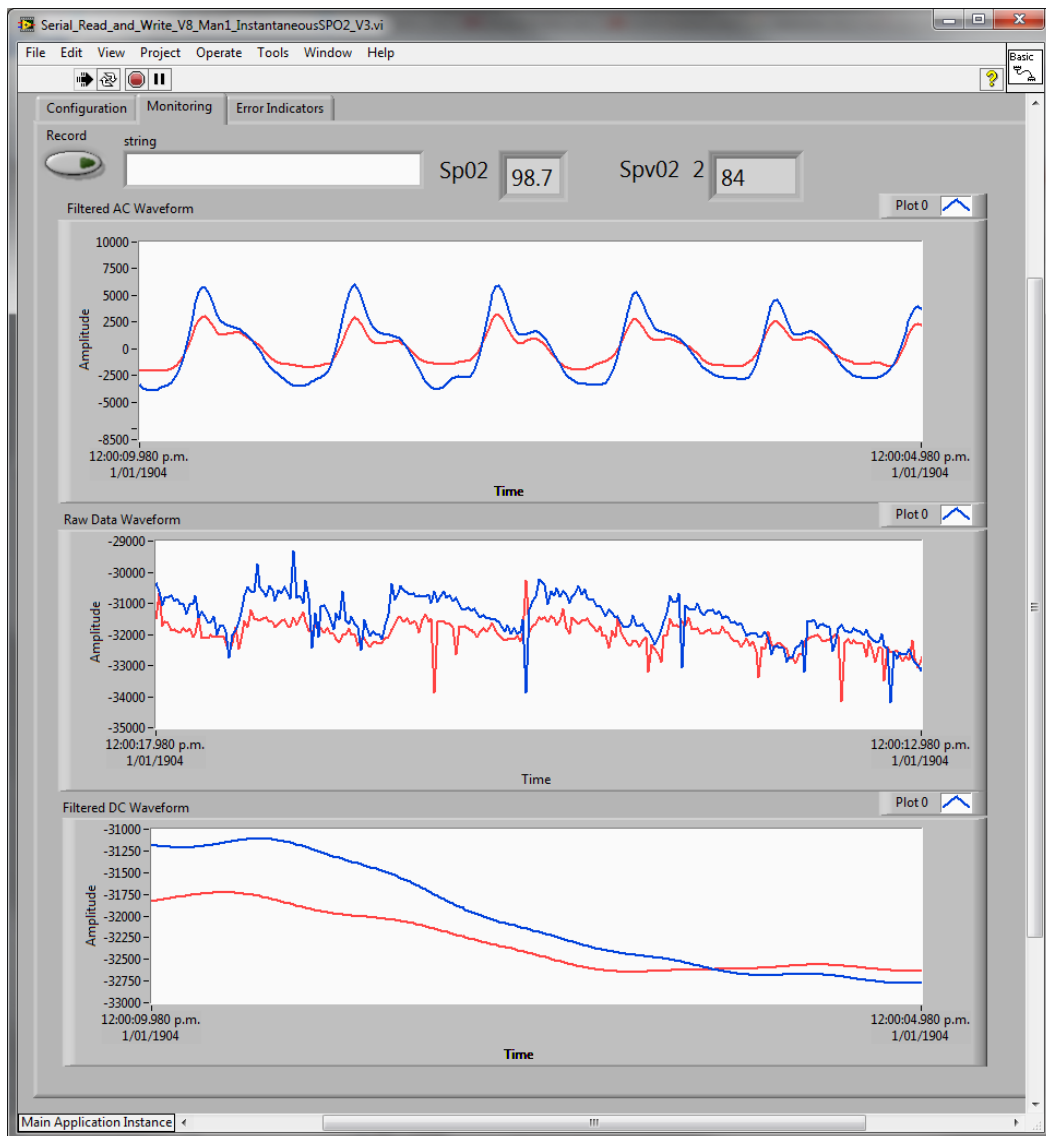


Figure 3.12: Pulse oximeter LabVIEW GUI, showing the monitoring tab in the front panel

3.5 Summary

Light energy detected by the PPG sensor is converted and conditioned by the PO system to a relative voltage signal. IR and RD signals of the raw and amplified PPG are processed and acquired separately. All analog PPG signals are sampled at 50 Hz, and interfaced to a PC via serial communication. The GUI presented in this chapter allows logging, real-time monitoring, and storing of PPG data for post processing. A FSM was developed for automatic or manual intensity control of the sensor. In addition, the GUI determines real-time SpO_2 and HR, from filtered AC and DC values using methods which will be discussed in the next chapter. Hence the system design presented covers the full technological functionality and how it captures all current PPG monitoring functions.

This chapter presents the basic design and specifications of the custom pulse oximeter system used in this research. The end product is a complete PPG acquisition and monitoring system. However this chapter does not discuss the additional modifications done to the PO system and equipment used to assess SvO_2 and O_2E , which are unique and will be covered in later chapters.

Chapter 4: PPG processing and analysis

4.1 Introduction

PPG data acquisition using the PO system is followed by post processing of the complete PPG data in an offline environment. This procedure is important for comprehensive analysis of patient data and to identify variations in PPG based measurements and their impact, in particular, since the PPG signal can be affected by physiological or external influences. This chapter introduces the post processing, methods, filter design, implementation, filtering, and signal processing involved to extract the AC and DC signals from the sampled raw and amplified PPG data. In addition, the methods and analysis used to estimate SpO₂ and HR parameters from the AC and DC signals are also presented in this chapter.

A two stage filter system was designed and implemented to extract the AC and DC signals from the amplified and raw PPG signals, respectively. Three peak-trough detection algorithms were investigated and compared to extract amplitude information from the filtered PPG signals. Modulation ratios of PPG signals, R values, are calculated from the extracted amplitude information with respect to the DC offset signal, and applied to mathematical models to estimate SpO₂. In addition, time and frequency domain methods were used to assess HR over time from the AC signals of the PPG, which are also discussed and compared in this chapter.

4.2 Data and signal processing

4.2.1 Processing interface

A PPG data processing function was developed in MATLAB. The function organizes the PPG data by checking file content of the raw data folder, determining existing files in the directory, making an identical copy of the name for the processed files, and importing the raw data for processing. A text processing function is also incorporated to the PPG script to remove any corrupt data. The module identifies and removes any data line that is not in the expected format. A data line is a set of data from the ADC output for one sample time.

The PPG data collected during data acquisition is in terms of ADC counts. Thus, the arbitrary count values are converted to equivalent voltage value, by multiplying with the reference voltage (2.5 V) of the ADC and then dividing by the number of bits, which in this case is 16 bits ($2^{16} - 1$). All data were also inverted, multiplying by -1 , to match visual representation of PPG waveforms in commercial devices. Data processing is followed by filtering, signal processing, data analysis, and plotting. All computed data (MATLAB workspace variables) and figures are automatically saved upon termination of the script.

4.2.2 Filter design and implementation

Sampled PPG data are filtered digitally after the data have been imported. The primary advantage of using digital filters is the flexibility to add/remove filters and modify configurations at any time, according to demand. A two-stage digital filter system was implemented for offline processing of amplified and raw PPG signals. MATLAB's Filter Design Tools (FDATools)

application was used to design and test the stability of the filters, as illustrated in Figure 4.1 for the first stage low pass filter as an example.

The first filter stage is used to remove any high frequency noise from the PPG signals, and the second stage is used to extract AC and DC signals from the filtered signals. The sampling frequency for both filtering stages is set at 50 Hz, to be compatible with the ADC's sampling rates (Sections 3.3.3 and 3.3.4). Zero phase filtering is applied at each filter stage to prevent any phase distortion and maintain PPG waveform shape.

Stage 1 of the two stage filter system consists of a finite impulse response (FIR), equiripple, low-pass filter. An FIR type filter ensures all frequencies in the PPG signal are delayed by the same duration of time, giving a linear phase response (Ifeachor and Jervis, 2002; Diniz et al., 2010), and thus providing a very stable output signal. The equiripple design method is selected to minimise maximum error between the chosen filter response and the digital approximation, since the filter coefficient values are adjusted to create an optimal filter, with ripples of equal amplitude. This filter design technique minimizes the transition width along the stopband and passband ripple using an efficient optimization procedure (Diniz et al., 2010). A 170th order filter with a cut-off frequency of 10 Hz and attenuation of 50 dB effectively remove any unwanted, high frequency noise from the PPG signals (Markandey, 2010), where high frequency is defined as above 10 Hz and practically above.

Stage 2 of the two stage filter system is composed of two parallel infinite impulse response (IIR) Butterworth filters. The IIR filter type provides a sharp frequency cut-off, and thus a steeper

transition region, with high PPG signal throughput (Ifeachor and Jervis, 2002; Diniz et al., 2010). The Butterworth design method is ideal to make the passband signals ripple free. One of the IIR filter is an empirically derived 6th order low-pass filter, which extracts the slowly changing DC signals, below a cut-off frequency of 0.67 Hz. The lower threshold of 0.67 Hz is chosen because the HR of any individual will not typically be less than 40 beats per minute (bpm). Therefore, pulsatility effects due to the heart's pumping blood and cardiac frequencies will be excluded from the DC signal, as desired.

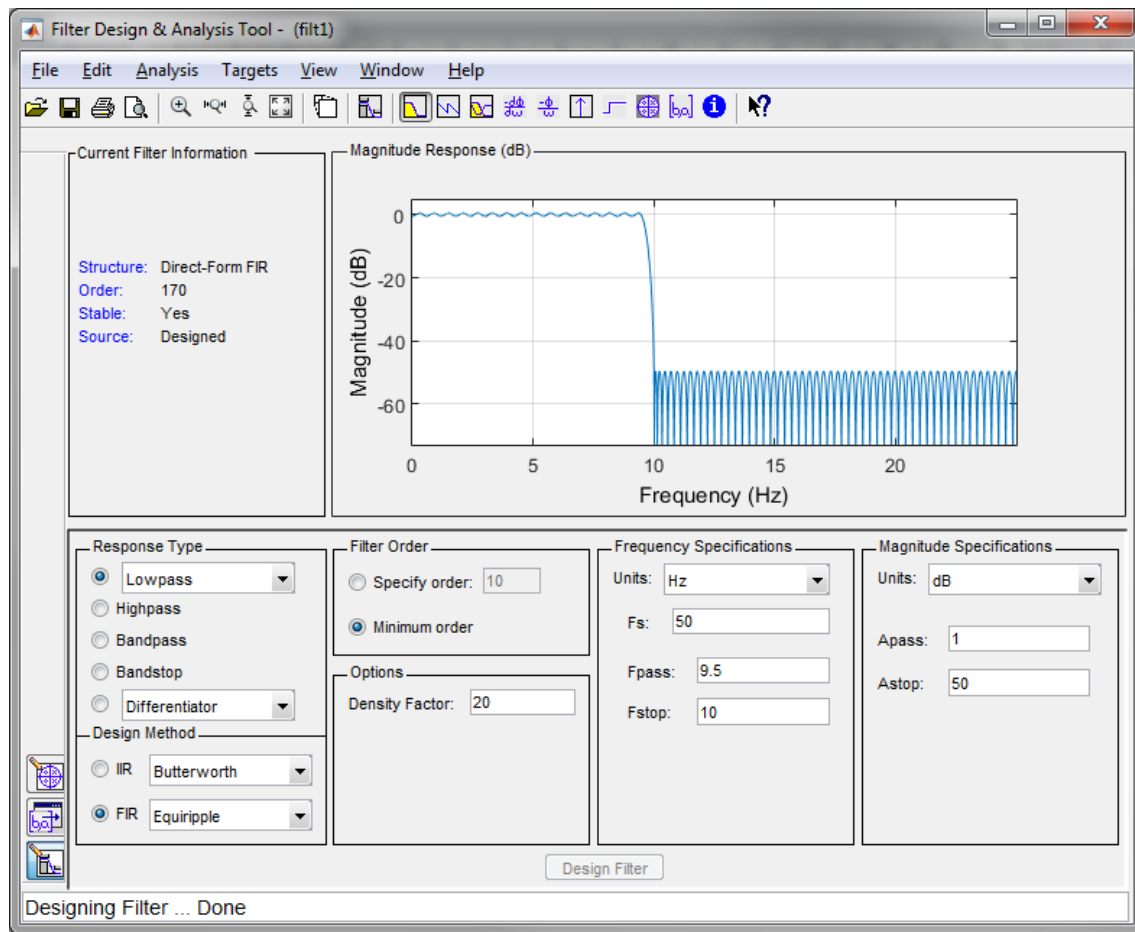


Figure 4.1: Filter design of the first stage low pass filter, which removes high frequency noise from the PPG

The second parallel IIR filter is an empirically derived 4th order band-pass filter. This filter extracts rapidly changing AC signals, such as the cardiac frequencies, with pass band frequencies 0.67 – 4.5 Hz. The upper threshold of 4.5 Hz captures HR and harmonics to a maximum of 135 bpm, which is well above the expected HRs for this research. This filter is used to extract AC signals from the both the raw and amplified PPG signals for analysis and comparison.

4.3 Peak-trough detection

R values must be determined from the filtered PPG data for SpO₂ estimation. Typically, in pulse oximetry, the R value from IR and RD PPG signals is estimated by time domain analysis of PPG signals. Applications of peak-trough detection algorithms on time domain PPG signals are seen in several studies to extract amplitude information (Bagha and Shaw, 2011; Shafique, 2011). Peak detection is also helpful in determination of HR (Allen, 2007; Nakajima et al., 1996). However, detecting peaks and troughs in a PPG signal can be difficult due a number of factors, such as presence of a dicrotic notch, varying signal amplitude, and poor SNR signal. This problem can result in incorrect or loss of AC pulse determination and amplitude calculation, and thus erroneous SpO₂ and HR estimation.

In this section, 3 peak-trough detection methods developed in this research are discussed and compared; Zero-crossing, Trough-thresholding, and Crossing-crossing. All peak-trough detection algorithms were developed and applied to the extracted AC and DC signals to determine the amplitudes relating to each heartbeat and the corresponding DC offset value, respectively. Figure 4.2 gives an example of the how peak-trough detection algorithm identifies amplitude

information from PPG. The amplitude of the rising edge of an AC beat is the difference between the corresponding peak and the trough.

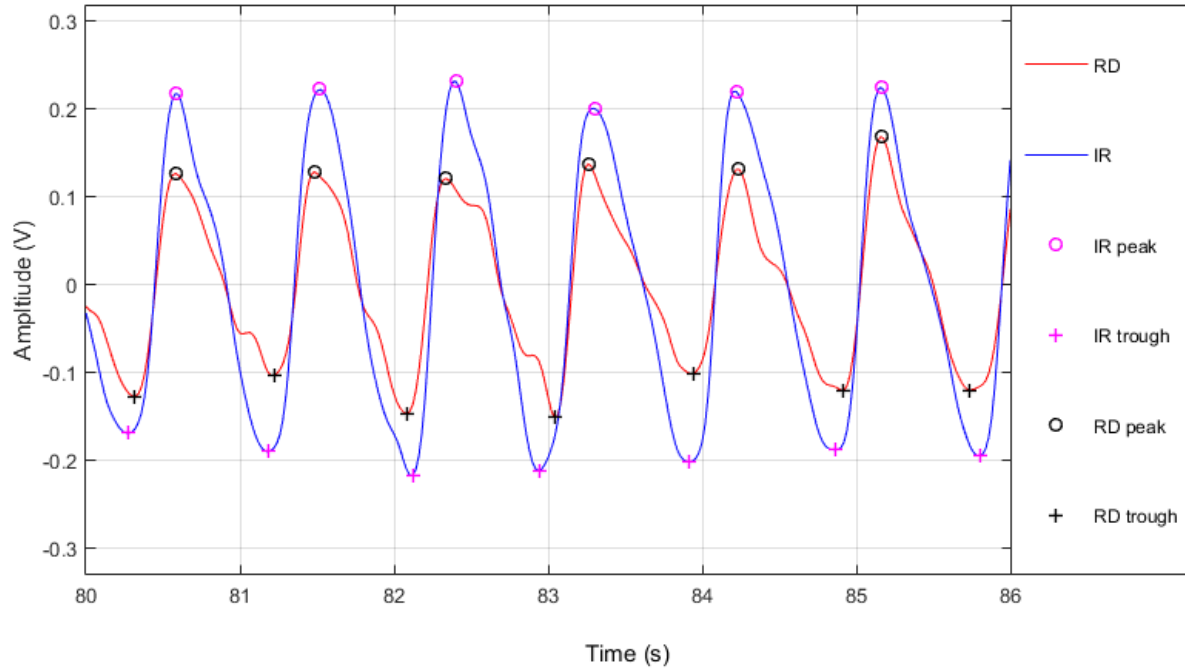


Figure 4.2: An example of PPG data with identified peaks and troughs.

4.3.1 Zero-crossing method

The Zero-crossing method iterates through the RD and IR AC signals in turn, and counts instances of signals transitioning from a positive to a negative voltage. A single pulse is defined as a time period in which a signal has transitioned from a negative voltage to a positive voltage, and vice versa. For each identified pulse, the local maximum and minimum are taken to find the corresponding peak and trough, respectively. In addition, a thresholding process is used to ensure that erroneous transitions due to noise or dicrotic notch are not counted as signal transitions. Essentially, this process adds hysteresis to the Zero-crossing counter. An empirically derived

thresholding factor, based on several test PPG data, is used to provide optimum peak and trough detection.

Some of the research PPG data presented in this thesis, such as in Chapters 5 and 7, used this method as a part of PPG processing and analysis. However, the Zero-crossing method is not very robust. The algorithm often misplaces or ignores peaks/troughs if the PPG data is not of good quality (low SNR and/or amplitude), such as during bad perfusion. Hence, other robust peak detection algorithms were investigated to overcome the shortcomings of this method.

4.3.2 Trough-thresholding method

The Trough-thresholding algorithm initially uses the troughs identified in the Zero-crossing module to create a series of linear thresholds for a given data set. A linear threshold gradient is empirically calculated between any two adjacent troughs, as originally detected. In addition, a vertical offset is calculated, based on the difference between the amplitudes of troughs and the relative DC value. This offset is then scaled until a desirable threshold height is obtained based on the AC pulse amplitude.

Using the calculated gradient and offset data, the linear threshold is divided between the determined trough positions and interpolated over the full range of the data set. The following criteria are used to search for peaks in this method:

1. Initiate search from the beginning of the array, until a rising edge crosses with the threshold line.

2. Iterate through the array from this point until a peak is found, identified as point which is larger than its immediate neighbours.
3. Scan ahead for a number of data points for any larger peaks. If a larger peak is found, move to this index and repeat this step. This is to prevent detection of any false peak due to noise or other artefacts.
4. Once the peak position has been confirmed, skip a number of data points and subsequently start search for crossings again. This is to avoid any false crossings being identified, specifically around the diastolic peak/ dicrotic notch area.
5. Repeat the Steps 2 – 4 to detect peaks for the whole AC waveform of the PPG.

To search for troughs a similar procedure is executed, except this time the algorithm searches for falling edge crossings and for a minimum point.

4.3.3 Crossing-crossing method

The Crossing-crossing algorithm is an adaptation of the Trough-thresholding method, and utilises the identified positive crossing location information. The time period between each crossing is assessed based on an empirically derived minimum period assumption of 0.35 s. In particular, if the interval between the current crossing and the next is smaller than the minimum time specified, it is assumed to be falsely detected, such as when a false positive is generated through detection of the diastolic peak. The minimum period is evaluated as average over the previous six crossing periods. If the minimum period criteria are not met, the crossing point is removed. Otherwise, properties such as the peak and trough are determined between the two crossings, by calculating the local maximum and minimum, respectively, over the crossing interval.

4.3.4 Comparison tests between the three methods

A test to determine the accuracy of the 3 peak-trough detection algorithm was devised. Four different data sets, taken from 3 different Subjects, were analysed using the 3 peak-trough detection algorithms. For each data set, approximately 5 min long, a period of 50 seconds were selected at random. The reference peak and trough positions for the AC waveforms were identified visually. Corresponding peak and troughs from each algorithm were then compared to the reference positions. The specificity and sensitivity ratios are identified as:

$$Specificity = \frac{True\ Positive}{True\ Positive + False\ Positive} \quad (4.1)$$

$$Sensitivity = \frac{True\ Positive}{True\ Positive + False\ Negative} \quad (4.2)$$

For Equations 4.1 and 4.2, a true positive reading is a peak or trough correctly matched with the previously identified “true” peak or trough. A false positive occurs when a peak or trough is identified but doesn’t coincide with the reference points. Finally, a false negative occurs where a peak or trough is not identified but should be. Table 4.1 presents the average specificity and sensitivity ratings for the 3 algorithms over the analysed AC waveform periods.

Figure 4.3 shows an example of the comparison test when the three peak-trough detection techniques were applied for a given AC signal from one of the tested data sets. The Zero-crossing method correctly identified all the troughs, however failed to detect the highlighted peak between 60 – 61 s. The Trough-thresholding method detected all the peaks, but erroneously determined

extra troughs between 57 – 58 s and 59.5 – 60.5 s. In contrast, the Crossing-crossing method outperformed the other two methods by accurately identifying all the peaks and troughs. For illustration purpose, only the RD PPG signal is shown. The outcome for the IR signal, although not shown in this figure, was exactly the same.

Table 4.1: Specificity and Sensitivity ratings for assessed peak-trough detection algorithms

Methods	PEAK		TROUGH		Average score
	Specificity	Sensitivity	Specificity	Sensitivity	
Zero-crossing	0.951	0.809	0.980	0.839	0.895
Trough-thresholding	0.869	0.940	0.964	0.936	0.928
Crossing-crossing	0.955	0.939	0.968	0.972	0.959

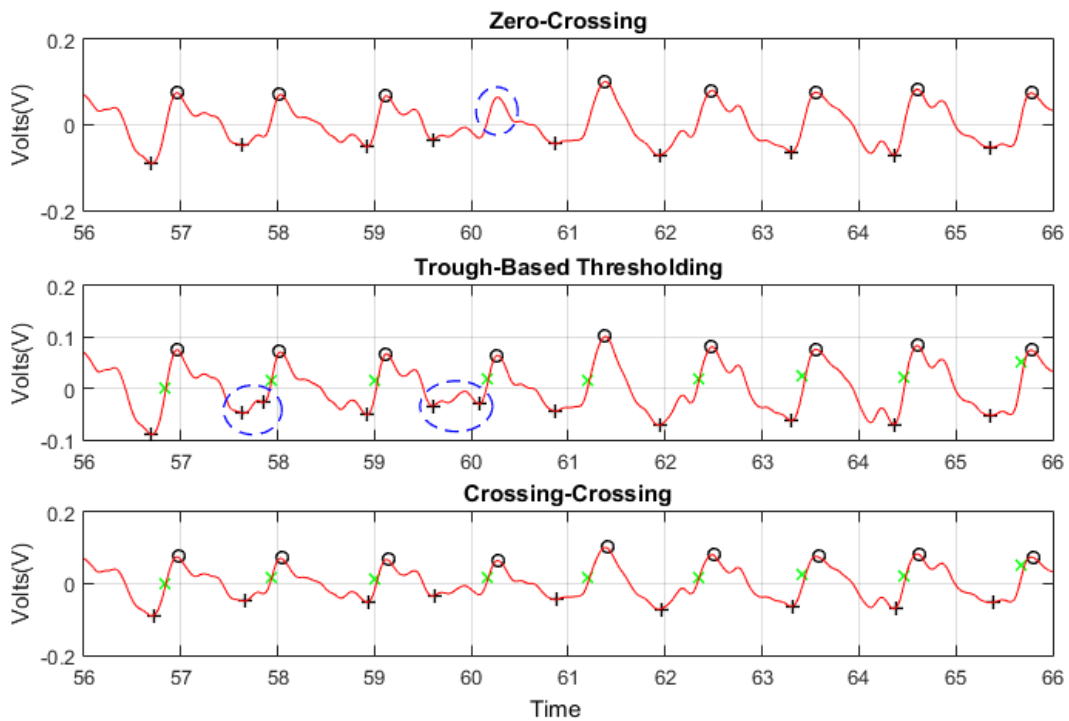


Figure 4.3: Three peak-trough detection methods were applied for a given PPG signal; zero-crossing (top), trough-based thresholding (middle), crossing-crossing (bottom). Incorrect or missed peaks/troughs are highlighted with dashed blue circle.

Although, the Zero-crossing method rates high under the specificity criterion compared to the other 2 algorithms, it lacks sensitivity and can only perform well with a good quality PPG. This issue is most likely due to the non-adaptive nature of the thresholding used and the lack of logic to prevent or minimise false crossing identification. As a result, the algorithm tends to skip actual peaks/troughs, so when it finds them it is correct, but loses sensitivity in these cases.

The Trough-thresholding method performs poorly under the specificity criteria compared to the other 2 methods. Although the algorithm utilises an adaptive threshold, based on the troughs identified by the original algorithm, and contains logic to counter false crossings, the variation in signal quality, shape, and form is not fully taken into consideration by this algorithm. It has been found that manual tuning of the threshold and logic is needed for optimization of the algorithm, with respect to each waveform, which is time consuming and lacks robustness. The specificity ratio for this method is high for trough detection. However, the relative sensitivity of the method is low. As the function bases the threshold on peaks identified in the original algorithm, if the original algorithm fails to detect a trough there is a chance that the adaptive threshold will not intersect the waveform near the trough. This issue often occurs where one trough's amplitude is higher than its neighbours.

Upon viewing the average specificity and sensitivity scores for each peak detection algorithm in Table 4.1 and their application in Figure 4.3, it is clear that the Crossing-crossing method performs the most accurately and consistently over the tested data sets. This method overcomes the shortcomings of the other two, and is thus, considered more versatile and robust. However, this

comparison test was done at a later stage of this research project, and was applied only in the processing and analysis of data presented in Chapters 6.

4.4 SpO_2 assessment

4.4.1 R value estimation

AC signal amplitude, $|\text{AC}|$, information obtained using the peak and trough detection are used for SpO_2 assessment. Additionally, for each identified AC pulse, the corresponding DC value was determined by calculating the mean DC offset, DC_{mean} , between peak and trough indices for each amplitude calculation. The ratio of the $|\text{AC}|$ to DC_{mean} values for each of the RD to IR signals, as illustrated in Figure 4.4, is used to calculate R value for each heartbeat, defined as (Walton et al., 2010):

$$R = \frac{(|\text{AC}|/\text{DC}_{\text{mean}})_{\text{RD}}}{(|\text{AC}|/\text{DC}_{\text{mean}})_{\text{IR}}} \quad (4.3)$$

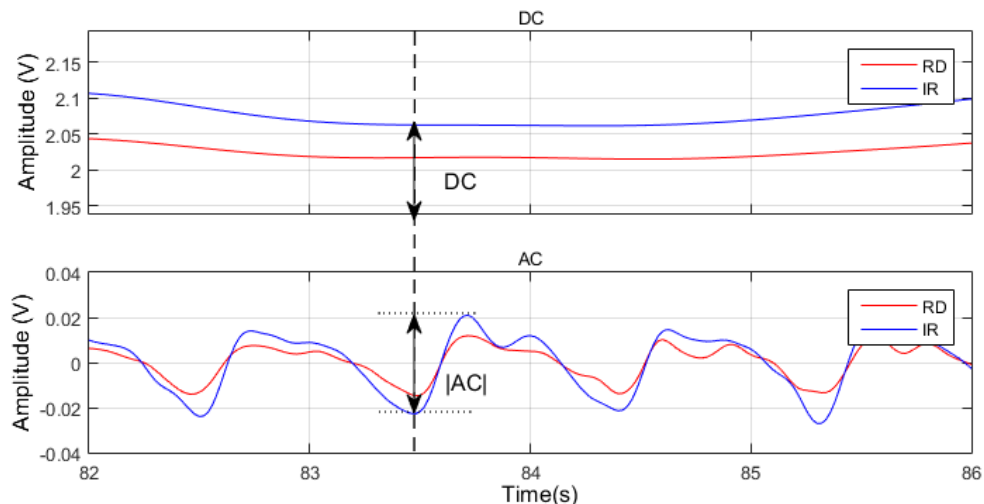


Figure 4.4: Amplitude $|\text{AC}|$ and corresponding DC_{mean} values determined from IR AC and DC signals, respectively, as an example.

R values can also be estimated by using the root mean square (RMS) of the AC signal and the DC offset signal (Oak and Aroul, 2015; Markandey, 2010). Using this method generates an array of RMS value AC_{RMS} elements. Dividing each of these elements with the corresponding DC element will give a ratio, which is also referred to as the perfusion index. Similar to the peak-trough detection, taking the AC to DC ratio of ratios of the RD and IR waveform, the R value can be easily estimated:

$$R = \frac{(AC_{RMS}/DC)_{RD}}{(AC_{RMS}/DC)_{IR}} \quad (4.4)$$

The advantage of using the RMS method is that it can provide an effective value of the varying AC signal, without depending on amplitude information. RMS is a measure of the magnitude of a set of numbers, by squaring every element in the AC signal and taking the square root of the average. This process overcomes some of the shortcomings in peak-trough detection algorithms, particularly if an incorrect peak is identified. However, this method has a few drawbacks. In particular, since it relies on the mean power of the signal it can provide erroneous R values, such as in the case of a PPG signal that has regions of no pulsatility. In addition, beat-to-beat (instantaneous) SpO_2 or HR cannot be calculated using this method. Thus, RMS based SpO_2 assessment was excluded from this research project.

4.4.2 SpO₂ estimation

The PO system was not calibrated against whole blood data and thus cannot directly estimate oxygen saturation. Therefore, published empirical calibration equations, such as in Chapter 2,

and data are used for SpO₂ estimation after analysing the PPG captured by the PO sensor. Estimated SpO₂ should agree with published SaO₂ values for healthy adults using this approach.

More specifically, instantaneous SpO₂ is computed using Webster's linear empirical calibration equation (Webster, 2002), for each R value, applied to a given section of a signal:

$$SpO_2 = 110 - 25 \times R \quad (4.5)$$

For Equation 4.5, an R value of 0.4 equates to approximately 100% SpO₂, R value of 1.00 equates to 85% SpO₂, R value of 2.40 equates to 50% SpO₂, while R value of 4.40 will be approximately 0% SpO₂. It is understood that Equation 4.5 is used (Rusch et al., 1996; Phillips et al., 2012) to calibrate Nellcor commercial pulse oximeters and is a linear approximation of empirical data obtained from volunteer studies (Rusch et al., 1996). The mean or median of the saturation values is calculated over a given time window, typically 120 s, to provide the overall SpO₂ value as shown in Figure 4.5. The average SpO₂ value is about 97% (± 1.90), which is within the normal SaO₂ range of 95 – 100% in healthy adults (Crapo et al., 1999; Williams, 1998).

In this research, the calibration free methods described in Chapter 2.4.2 are not applicable. First, the paired LED wavelengths of the sensor used in this research are not close to each other (660 – 940 nm), as opposed to Nitzan et al.'s LED wavelengths (780 – 808 nm). Second, Reddy et al.'s model (Equation 2.9) significantly underestimated SpO₂, by 6% in general, when tested compared to literature values. Thus, neither of these well-known calibration free methods are feasible for SpO₂ estimation in this research.

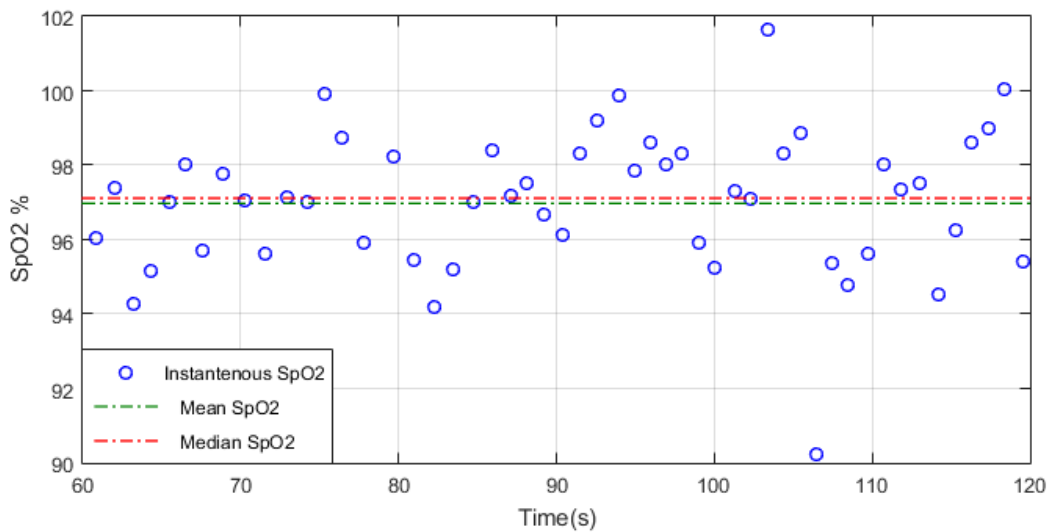


Figure 4.5: Instantaneous and overall SpO₂ estimated for a test PPG data using equation 4.5.

4.5 HR assessment

Heart rate, typically measured in beats per minute (bpm), is a very useful physiological parameter that can be reliably determined from the PPG, by using the peak to peak time intervals. HR information can be used as to monitor cardiovascular activity, which is important in this research. Initially, HR was extracted by applying Fast Fourier Transform (FFT) to a given PPG signal. The FFT can successfully capture the fundamental HR frequency and all related cardiac harmonics, as shown in the FFT power spectrum in Figure 4.6.

This simple FFT analysis provides a single frequency value for each cardiac component, labelled in Figure 4.6, for the whole PPG data set. However, PPG data can be very long and HR can vary over time. Thus it is important to estimate HR reliably throughout the duration of a study. Two methods were investigated to estimate HR reliably; a frequency domain method and a time domain

method, where one is a modification of an FFT-based method and the other relies on the time interval between each peak.

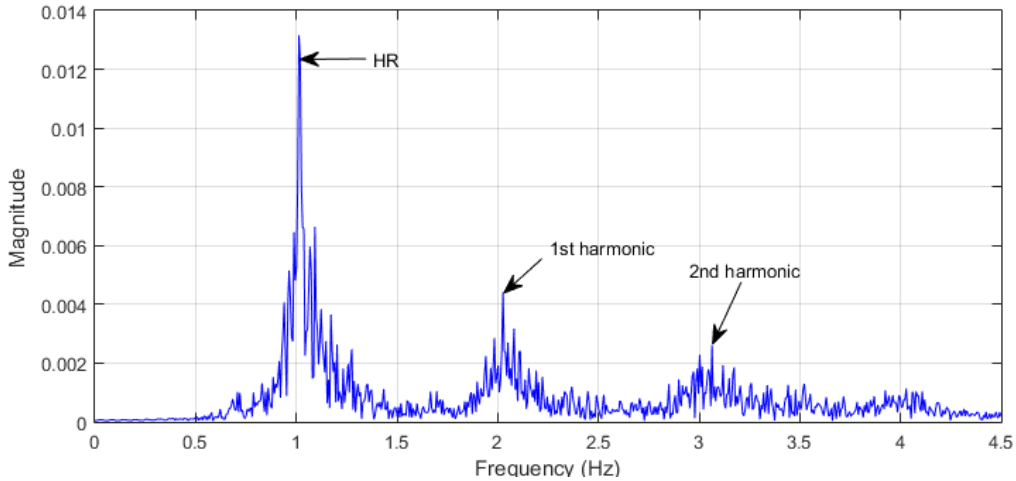


Figure 4.6: Power spectral density of the IR PPG, with the DC component removed, as an example. All the cardiac frequencies are labelled. The highest peak magnitude, at about 1 Hz, is the HR.

4.5.1 Frequency domain method

This technique will step through a PPG signal by a specified moving window size of 5 s. The peak frequency for the window block with the maximum amplitude is determined as the cardiac frequency. All HRs are calculated in bpm, as the standard unit for HR. Any bpm values that are outside the 40 – 140 bpm range are removed from the data set as outliers.

4.5.2 Time domain method

This method utilises the peak time values obtained through the IR trough thresholding module for the AC signal. The HR period is calculated as the time interval between adjacent peaks of the waveform. Similar to the FFT block methodology, a moving time window of 5 s is applied. The

peak-peak time array is iterated through, while the HR periods for each time window are averaged and transformed into HR readings in bpm.

4.5.3 Comparison between the two methods

HR was estimated using the two methods using 5 test data sets, each 120 s long, for comparison. Figure 4.7 provides an example of the application of the two methods, for a given PPG signal from the data of one of the data set. The average bpm over 120 s for the FFT block method was 61.2 (SD = 5.4 bpm) compared to the Peak-peak block method's 61.5 (SD = 5.8 bpm). The overall trend and of both methods was very similar throughout the duration of the PPG. In addition, tests for other test data sets showed good agreement between the two methods.

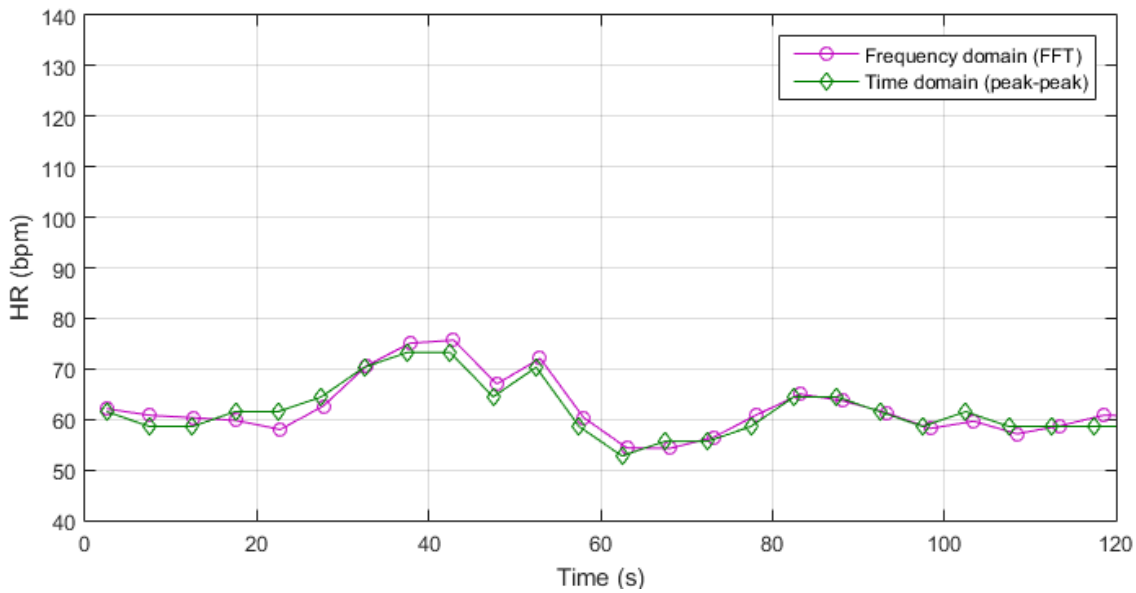


Figure 4.7: PPG based HR assessment using the two methods; FFT block method (top) and Peak-peak block method (bottom)

Under normal circumstances and with a good quality PPG signal (good SNR), the two methods agree well. However, the Peak-peak block method is favored in general, as it determines the HR from each individual pulse intervals and can capture HR variability information more reliably. In contrast, the FFT block method is more useful in cases of noisy or weak PPG signals, where a true peak can be hard to determine.

4.6 Summary

SpO₂ and HR evaluation is essential to meet the goal of this thesis. This chapter presented the PPG signal processing and analysis techniques used in this research to assess these two parameters. The digital filtering techniques implemented proved to be adequate to acquire the signals of interest from raw and amplified PPG. A 10 Hz low pass filters is used to remove all high frequency noise from the PPG signals. Subsequent low pass filtering below 0.67 Hz and band pass filtering of the range 0.67 – 4.5 Hz extracts DC and AC components, respectively, from PPG signals.

Three peak and trough detection algorithms are discussed and a test was conducted to compare their performance. The Crossing-crossing detection algorithm is found to be the best choice to determine amplitude information, and thus, R value. Calculated R values are used to estimate SpO₂, using published and derived calibration equations. Test data shows that estimated SpO₂ falls within the expected published SaO₂ range of 95 – 100% for healthy human individuals. In addition, two methods to monitor HR over time from PPG are also discussed and compared, showing good agreement in general. Certain data processing modifications and development to estimate SvO₂ from the processed PPG signals are unique and will be covered in following chapters.

Chapter 5: Effect of temperature on PPG signal quality

5.1 Introduction

Temperature is another, often overlooked, limiting factor when using pulse oximetry. It is generally accepted that cold digits may provide inaccurate pulse oximeter readings (DeMeulenaere, 2007; Fahy et al., 2007), and simple solutions like rubbing the hands together may solve the problem. However, people with naturally cold fingers or ICU patients with poor circulatory function and perfusion, where room temperature is typically maintained at $20 \pm 2^{\circ}\text{C}$ (TIC, 1997), are examples of cases where this problem can be exacerbated, as well as pass unnoticed.

Poor PPG signal quality can produce erroneous readings in pulse oximeters that can result in false alarms (Jubran, 2015). This problem was initially encountered during preliminary tests of the PO system. Healthy subjects who had cold fingers, provided below normal SpO₂ readings due to low PPG signal quality, which made analysis difficult and results variable and poor. This chapter presents two separate studies, Study 1 and Study 2, conducted to investigate the effect of temperature on PPG signal quality in finger using TPO based sensor. In addition, it is a first step to ameliorate this issue and its impact on this research.

The initial hypothesis of Study 1 was that PPG signal quality is severely degraded in cold digits, resulting in inaccurate SpO₂ readings, and thus limits the application of PPG. In response, a continuous heat source close to the sensor site was tested to assess improvement in PPG signal

quality and reliable SpO₂ estimation as a function of temperature. The overall goal is the delineation of signal quality and sensor reliability as a function of temperature to guide further use of the PO system. In addition, this chapter presents a further study, Study 2, where the effects of cold temperatures on SaO₂ were investigated using blood gas comparators to further verify the underlying issue that led to Study 1.

5.2 Related studies, test equipment and ethics

5.2.1 Related study

Previously, Njoum and Kyriacou (2013) investigated the effects of local sympathetic tone on healthy volunteers using a custom built pulse oximeter with a finger based RPO sensor. They used a cold pressor test to induce a drop in temperature of the right hand for 30 s. Outcomes of their research showed PPG signal pulse amplitude degraded significantly, up to 73%, in both hands during the ice water immersion, with an associated increase in pulse repetition time and HR.

Budidha and Kyriacou (Budidha and Kyriacou, 2014) conducted a similar cold pressor test investigation. They also included an ear canal based reflectance sensor as a comparator. Their finger based PPG devices reported a substantial drop in PPG signal pulse amplitude, up to 58%, and reported inaccuracy in SpO₂ estimation at low temperatures of approximately 8 °C.

However, neither of these studies investigated the effect on PPG signal quality in naturally cold fingers at warm room temperatures. They also did not present any subject specific data. In addition, neither study provided advice on how to improve PPG signal quality in such cases. Finally, neither

study considered TPO sensor. Thus, there is a need to determine the effect of practical, modestly reduced digit skin temperatures on PPG signal quality.

5.2.2 Equipment set up for Study 1

The PPG acquisition system for this study was the custom PO system presented in Chapter 3. In this study, AC and DC signals were extracted from the raw PPG signal, and the amplified signal was ignored. A serial communication based interface, presented in Section 3.4, was used for recording the PPG data for post processing. A commercial pulse oximeter and a temperature sensor were employed as a comparator and a control sensor, respectively.

A Nellcor NPB-75 (Covidien, Minneapolis, MN, USA) pulse oximeter was employed for comparison with the PO system. This hospital grade commercial pulse oximeter can provide continuous SpO₂ and HR readings. In addition, this device can display the real-time PPG signal for qualitative comparison. The NPB-75 sensor was attached to an alternate finger, index or middle, of the same hand. The device can only display PPG measurements, and thus, photos of the displayed measurements were recorded for analysis.

A Type-T surface mount thermocouple probe (SA1XL, Omega, Stamford, CT, USA) was taped to the surface of the skin, next to the PO sensor, to obtain temperature data from the surface of the skin. The probe was nominally accurate to ± 0.5 °C above 0 °C (Guyancourt, 2014). Temperature data was continuously logged for the duration of the study using a PC running LabVIEW via an NI cDAQ-9172 (National Instruments, Austin, TX, USA) multifunction data acquisition device.

5.2.3 Ethics approval for Studies 1 and 2

Study 1 and use of data were approved by the Human Ethics Committee (HEC), University of Canterbury (Ref: HEC 2015/04/LR-PS). Volunteers were included in the study after informed, and signed, consent was received. Data were de-identified and securely stored. The information sheet and consent form of Study 1 are included in Appendix 5.1. For Study 2, ethics approval (Reference: 15/CEN/141) was obtained from the NZ Human Ethics and Disability Committee (HDEC). More details on the Study 2 ethics application can be found in Chapter 8.

5.3 Experimental Protocol

Healthy adults with no pre-existing medical conditions were recruited for both studies. Healthy volunteers are easy to recruit, and are likely to demonstrate understandable responses subjected to induced changes. In contrast, critically ill-subjects can show changes that are challenging to explain, which can make test standardization and validation difficult.

5.3.1 Study 1

Twenty healthy adults, aged 24.9 [23.0 – 27.5] years were recruited in this study. Subjects were asked to refrain from smoking, caffeinated hot drinks, and strenuous physical activities for at least 2 hours prior to the experiment. This resting time is necessary for the subjects cardiac function to become normal. The experiment was conducted inside an air-conditioned room regulated at 20 [19.5 – 20.9] °C, which is a typical ICU room temperature.

Subjects were comfortably seated, while resting their left or right hand on a flat surface at approximately the same height as their heart with minimum movement. In addition, subjects were

asked to breathe normally for the duration of the experiment. The following three tests were then implemented, with 5 min intervals in between, as illustrated in Figure 5.1.

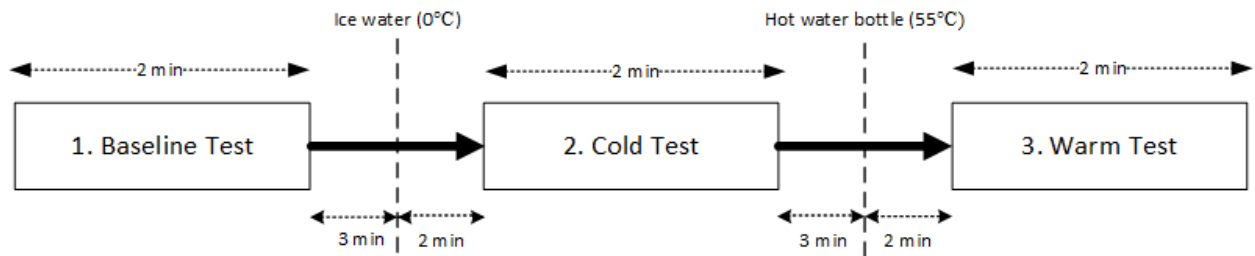


Figure 5.1: Flowchart of the experimental protocol, showing the step-by-step process. The overall series of test captures normal, relatively cold and relatively warm temperatures.

1. Baseline test

Two minutes of baseline PPG data, at a normal digit skin temperature of 28.9 [26.9 – 30.2] °C, were recorded using the PO system at the beginning of the experiment. Temperature data were logged from the thermocouple sensor site, adjacent to the PO sensor. NPB-75 measurements were also taken from an alternate finger of the same hand.

2. Cold test

Subjects removed the PO and NPB-75 sensors and immersed their hand up to the wrist in an ice-water bucket maintained at a temperature of 0 °C for approximately 2 min, resulting in a skin temperature of 19.8 [18.5 – 21.3] °C. After 2 min, subjects were asked to take their hand out of the bucket and quickly dry their hand. PO and NPB-75 sensors were then re-attached to the fingers and PPG data were logged for approximately 2 min.

3. Warm test

Subjects rested their hand with the palm placed upon a hot water bottle maintained at a temperature of 55 [53 – 57] °C for approximately 5 min, resulting in a skin temperature of 33.1 [32 – 34.6] °C. PPG, temperature, and NPB-75 data were then logged for 2 min. During PPG acquisition, subjects kept their hand on the hot water bottle, but not the fingers, to prevent rapid temperature drops during this phase of the test.

5.3.2 Study 2

Five healthy human volunteers with typical core temperature of 37 °C were recruited for this validation study. The study was conducted in an ICU environment, maintained at a room temperature of 21 °C. The PO system sensor was clipped to the left index/middle finger of the subject. A commercial Masimo SET pulse oximeter (Masimo Corporation, Irvine, CA, USA) was used and clipped on the left ring finger, for comparison. Finger skin temperature was measured by the same thermocouple probe used in Study 1. Subjects were comfortably seated, while resting their left or right hand on a flat surface at approximately the same height as their heart with minimum movement. In addition, subjects were asked to breathe normally for the duration of the experiment.

Two min of baseline PPG data were initially recorded at room temperature, and the finger skin temperature across the subjects was measured to be 32 °C [31.2 – 33.6]. The left hand was then cooled down to approximately 20 °C, using ice water bucket similar to the other study. Two min of PPG data were recorded at this low temperature before terminating the test.

Arterial blood samples per subject ($n = 2$) were drawn for blood gas analysis, using iStat1 blood gas analyser (Abbott, Princeton, NJ, USA), during the test: 1) at baseline temperature; and 2) when the finger skin temperature was approximately 20 °C. These blood gas measurements serve as gold standard reference comparators. The aim of this test was to prove the hypothesis that cold temperatures significantly reduces PPG signal quality, and thus can provide erroneous SpO₂ estimates as assessed by comparison to the gold standard.

5.4 PPG signal analysis

5.4.1 Signals of interest

In both studies, the AC portion of the IR and RD PPG signals were analysed using the PPG processing methods presented in Chapter 4. This choice was based on the fact that AC component of the PPG is the primary signal of interest in conventional pulse oximetry, dominates the SNR, and is directly related to arterial blood flow (Bergstrand et al., 2009; Naslund et al., 2006; Zhang et al., 2001; Zhang et al., 2004). Thus, the AC signal is most affected by any temperature induced change in perfusion. In addition, the DC component of the PPG is filtered in conventional pulse oximetry to remove low frequency artefacts. Equally, no apparent changes were observed in the DC portion of the PPG in either study.

5.4.2 Metric for SNR

A surrogate metric for SNR is required to meet the goals of both studies. The root mean square (RMS) value of the AC signals was calculated for each subject in Studies 1 and 2 to provide a surrogate measure of signal quality and SNR. Low energy signals result in low RMS values, thus providing a measure of poor SNR and vice versa.

The subject specific RMS data for each test in Study 1 were fit to a linear line. This procedure generates a tri-linear model of RMS, and thus SNR, as a function of temperature. As a result, the overall function of signal RMS over temperature can be seen for each test. In addition to RMS, the median PPG amplitude was calculated for each temperature test, per subject. The median amplitudes were calculated to provide a measure of the overall PPG pulse magnitude for each test condition (baseline, cold, and warm).

5.4.3 Statistical analysis

Kruskal-Wallis one way analysis of variance on ranks was performed on the PPG RMS and amplitude data from the Cold, Baseline, and Warm tests of Study 1 to determine any statistically significant difference for the RMS values and median PPG amplitude across these three test conditions. Significance was set at $p < 0.05$. Non-parametric tests were used because some of the data were not normally distributed. All statistical analysis was performed using MATLAB (The Mathworks, Natick, MA, USA).

5.5 Results

5.5.1 RMS data comparison

Individual subject demographics, PPG derived signal RMS values, and corresponding temperature data are presented in Table 5.1. During the cold test, the median signal RMS dropped by 9.4 mV (54.0%) for IR and 3 mV (30.6%) for RD from the baseline values. In contrast, signal RMS increased by 11.2 mV (64.4%) and 5.9 mV (60.2%) for RD and IR, respectively, during the warm test. The median difference between the warm and cold tests RMS values were 20.6 mV (112.6%

of warm value) for IR and 8.9 mV (79.1% of warm value) for RD. All of these differences were statistically significant ($p < 0.001$).

Table 5.1: Demographics, PPG signal RMS, and median temperature data for all subjects from the study

Subject	Gender	Age	Baseline			Cold Test			Warm Test		
			IR_{RMS} (mV)	RD_{RMS} (mV)	T (°C)	IR_{RMS} (mV)	RD_{RMS} (mV)	T (°C)	IR_{RMS} (mV)	RD_{RMS} (mV)	T (°C)
1	M	26	26.9	13.9	30.1	4.8	3.7	20.1	25.2	13.2	33.8
2	M	23	38.7	21.1	30.4	11.2	9.7	18.0	32.0	17.1	31.0
3	M	23	16.0	10.1	31.5	5.6	5.4	18.0	37.1	20.5	31.9
4	M	29	10.5	5.9	26.8	5.8	4.6	17.0	41.2	21.7	32.5
5	M	23	14.5	8.1	28.5	5.7	5.8	19.0	29.1	15.6	33.1
6	F	21	5.8	5.3	26.2	4.7	4.1	19.6	13.1	7.3	31.5
7	F	23	12.8	6.7	29.0	5.1	4.9	22.0	31.0	16.3	32.7
8	F	23	6.4	6.3	25.0	3.9	3.8	19.5	24.6	14.1	32.0
9	M	27	27.1	15.1	30.0	11.7	8.0	20.5	56.2	31.2	32.0
10	F	23	34.5	19.0	30.1	7.9	7.4	23.0	29.3	15.6	35.0
11	M	35	26.3	15.0	28.7	18.3	10.6	19.0	28.6	15.7	33.0
12	M	35	36.7	21.3	28.0	11.7	8.2	20.0	28.6	16.1	35.0
13	M	22	8.2	5.6	27.0	5.7	5.4	21.6	28.0	14.2	31.4
14	M	27	32.9	16.9	29.5	15.6	8.8	21.9	28.6	15.1	34.5
15	M	30	10.3	8.0	30.2	10.4	7.2	22.0	25.8	14.1	32.0
16	F	24	25.9	13.3	30.4	7.5	7.1	18.5	27.8	14.7	35.2
17	F	25	18.7	9.4	30.5	13.8	8.0	21.0	22.0	12.4	35.0
18	M	27	9.3	8.6	25.8	8.0	6.8	18.4	26.5	16.2	34.2
19	M	28	30.0	15.9	27.8	8.3	4.8	20.1	44.1	23.7	33.8
20	F	21	13.9	7.6	25.5	8.7	6.8	17.0	30.2	16.0	34.6
Median		24.5	17.4	9.8	28.9	8.0	6.8	19.8	28.6	15.7	33.1
Interquartile Range (IQR)		23.0	10.4	7.2	26.9	5.7	4.9	18.5	26.2	14.2	32.0
		—	—	—	—	—	—	—	—	—	—
		27.5	28.6	15.5	30.2	11.5	8.1	21.3	31.5	16.7	34.6

5.5.2 Tri-linear model

Figure 5.2 shows the PPG signal RMS (IR and RD) versus temperatures ranging over 17 – 35 °C for all subjects from each test. All the data points for the cold test were below 20 mV for IR and 11 mV for RD. In contrast, data points for the baseline test were scattered over a wide RMS range of 5 – 40 mV for IR and 5 – 23 mV for RD. The wide baseline test spread indicates how any given subject may have good or poor PPG signal quality as a function of their subject specific digit

temperature at baseline. However, for the warm test all the data points were between an elevated range of 12.5 – 60 mV and 7 – 32 mV for IR and RD, respectively. A clear separation between the cold and warm states as a function of RMS signal quality was evident ($p < 0.001$). Hence, while the baseline test was subject dependant, controlled temperatures were achieved for all subjects in cold and warm tests, leading to clearly separated results.

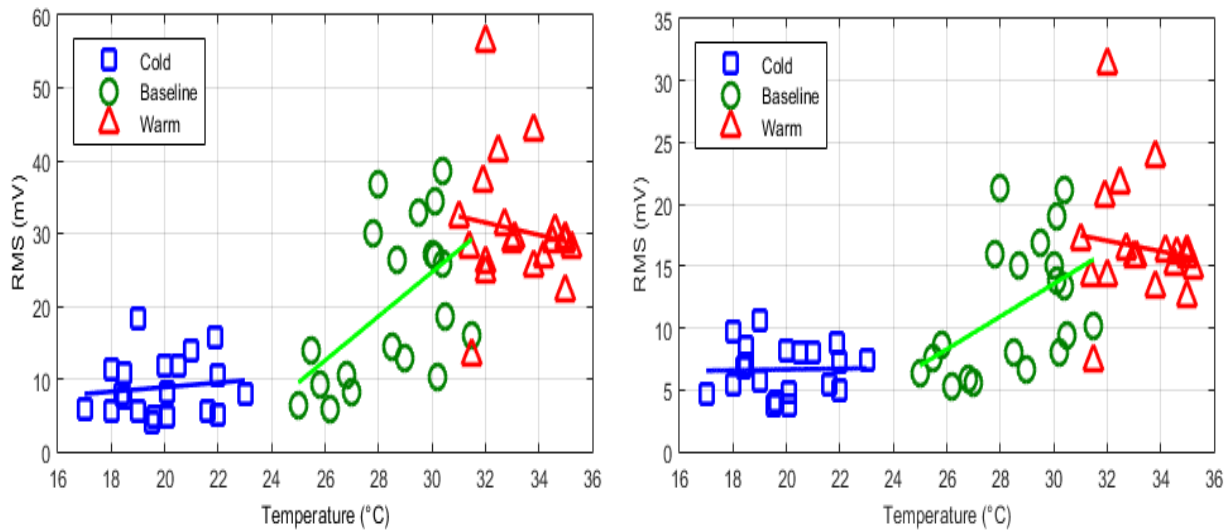


Figure 5.2: AC signal RMS versus temperature from the three different experiments: *IR* (left), *RD* (right).

Piecewise linear least-squares fitting resulted in a low, relatively flat fit for cold test data, a steeper gradient for the mixed Baseline test data and a higher, relatively flat fit for the warm test data for both IR and RD channels. Both channels showed similar features, except the IR channel had greater range. The tri-linear fits provide an outline for a simple model of signal RMS and quality as a function of temperature.

5.5.3 Amplitude data comparison

The per test median PPG amplitude values for the cohort at all three conditions are shown in Figure 5.3. During the cold state, the median signal amplitude reduced by 21.2 mV (55.3%) for IR and 7 mV (30.9%) for RD from the Baseline state. In contrast, the median signal amplitude improved by 41.7 mV (108.7%) for IR and 20.3 mV (89.4%) for RD during the warm state. Finally, the median amplitude difference between the cold and warm states was 62.9 mV and 27.25 mV for IR and RD, respectively. All of these differences were statistically significant ($p < 0.001$).

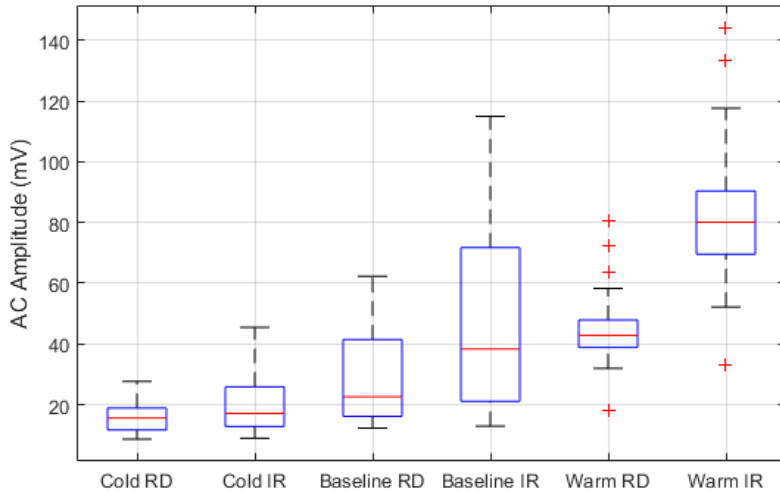


Figure 5.3: Median AC signal amplitude for the cohort from the three tests.

Figure 5.4 shows the IR and RD PPG signals of Subjects 19 and 20 recorded for each test, as an example. The cold test PPG waveforms were almost flat, with a substantial decrease in signal pulse amplitude compared to the baseline test. PPG amplitude was highest during the warm test, almost double the baseline test values. Clear dicrotic notches, indicated in Figure 5.4, were observed occasionally in the baseline test, but regularly in warm test PPG waveforms for all subjects. The typical PPG signal pulse used to determine HR was only clearly evident, despite filtering, in these

latter two cases. Hence, the reduced quality noted in other studies with low temperatures (Njoum and Kyriacou, 2013; Budidha and Kyriacou, 2014) is apparent here, as well as in Table 5.1 and Figures 5.2 – 5.3.

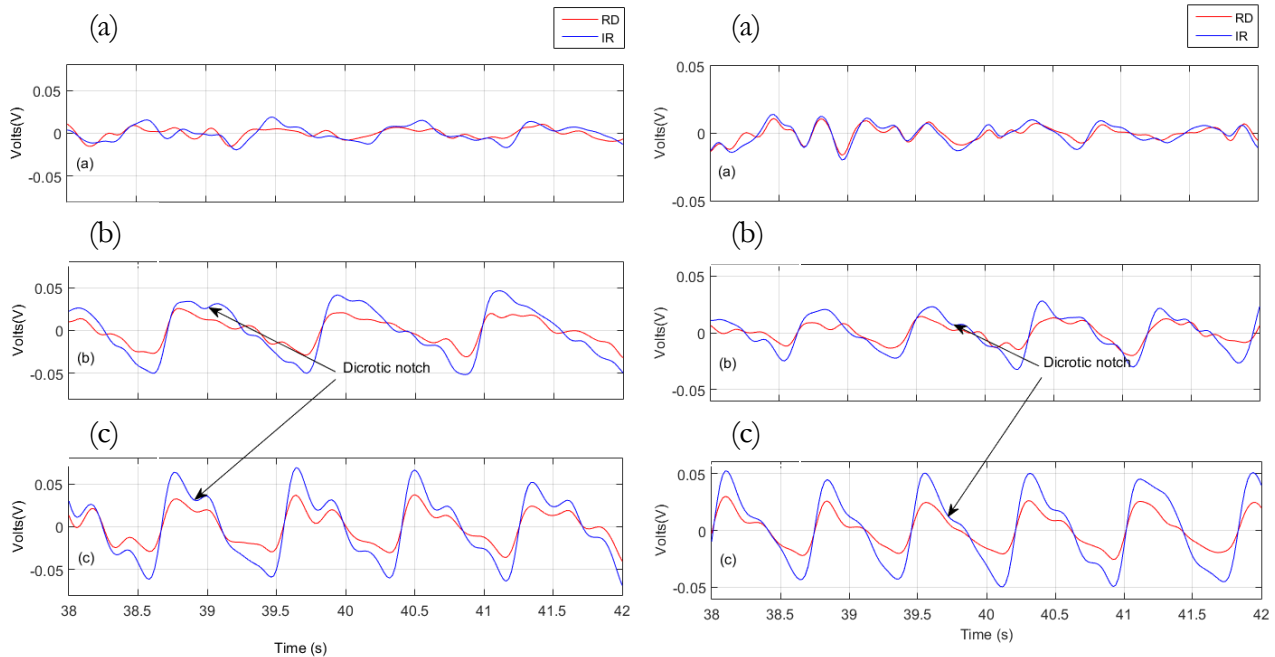


Figure 5.4: AC signals from the 3 tests for Subjects 19 (Left) and 20 (Right): Cold (a), Baseline (b), and Warm (c).

5.5.4 Statistical differences

All of these differences in median RMS and amplitude data between the PPG signals of the three tests were statistically significant ($p < 0.001$). The median values of the PPG signals were considered for statistical analysis. The results are presented in Table 5.2.

Table 5.2: Results of non-parametric statistical test comparison between experimental data sets

Signal	Parameter	Median [IQR] (mV)			<i>p</i> value (Kruskal Wallis)
		Cold	Baseline	Warm	
IR	RMS	8.0 [5.7 - 11.5]	17.4 [10.4 - 28.6]	28.6 [26.2 - 31.5]	<0.001
	Median Amplitude	17.2 [12.9 - 26.1]	38.4 [21.2 - 71.8]	80.1 [69.6 - 90.4]	<0.001
RD	RMS	6.8 [4.9 - 8.1]	9.8 [7.2 - 15.5]	15.7 [14.2 - 16.7]	<0.001
	Median Amplitude	15.7 [11.7 - 19.1]	24.6 [18.4 - 44.5]	42.9 [38.9 - 47.9]	<0.001

5.5.5 Correlation between pulse oximeters

For comparison to Figures 5.4, Figure 5.5 shows the PPG waveform displayed by the Nellcor NPB-75 pulse oximeter for Subject 20, as an example, for all the three tests. The cold test waveform was almost flat, with very low-amplitude and no visible dicrotic notch. Baseline test measurements had relatively high-amplitude waveforms with occasional dicrotic notches. In contrast to the previous two cases, the warm test data shows high-amplitude waveforms with clear dicrotic notches. The PPG waveform trends for the NPB-75 match what was observed with the custom pulse oximeter in Figure 5.4.

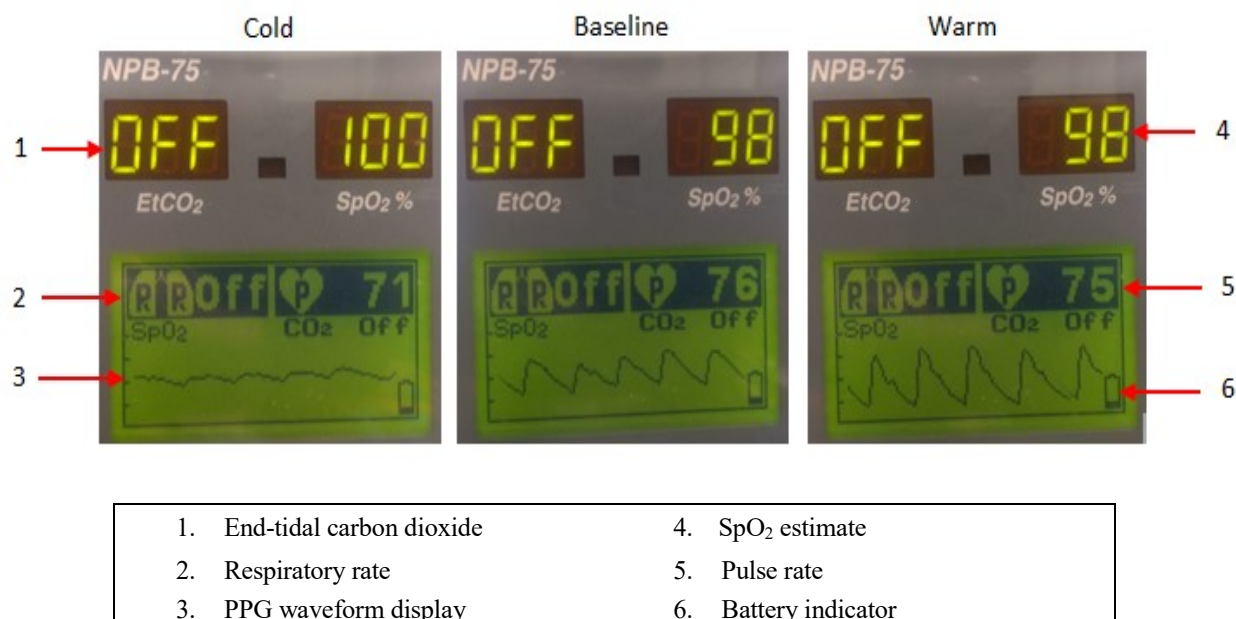


Figure 5.5: Front panel of NPB-75 displaying PPG signal and data for Subject 20: Cold (left), Baseline (middle) and Warm (right).

Table 5.3 compares the estimated SpO₂ data measured by the PO system and the NPB-75. The two pulse oximeters showed good agreement in the Warm test, where SNR of signal was high, with a median SpO₂ difference of 1.5%. Confidence in SpO₂ estimation between the two pulse

oximeters was marginally reduced in the baseline test, increasing the median SpO₂ difference to 2.2% when compared to the warm test. However, a poor association was observed between the PO system and the NPB-75 in the cold test, with a large median SpO₂ difference of 11%.

Table 5.3: Median SpO₂ data of all subjects from the experiment

Subject	Baseline SpO ₂ (%)			Cold Test SpO ₂ (%)			Warm Test SpO ₂ (%)		
	NPB-75*	PO†	Δ	NPB-75*	PO†	Δ	NPB-75*	PO†	Δ
1	98.0	96.8	1.2	99.0	90.9	8.1	98.0	96.9	1.1
2	98.0	96.4	1.6	97.0	87.4	9.6	98.0	96.8	1.2
3	98.0	93.1	4.9	100.0	86.2	13.8	98.0	96.6	1.4
4	100.0	95.8	4.2	100.0	89.1	10.9	99.0	96.5	2.5
5	97.0	95.3	1.7	89.0	84.6	4.4	98.0	96.1	1.9
6	100.0	86.8	13.2	100.0	87.8	12.2	98.0	96.3	1.7
7	98.0	96.9	1.1	100.0	87.5	12.5	98.0	97.1	0.9
8	96.0	86.5	9.5	95.0	86.3	8.7	97.0	95.7	1.3
9	98.0	96.0	2.0	98.0	92.4	5.6	98.0	96.1	1.9
10	97.0	95.8	1.2	87.0	86.9	0.1	99.0	97.4	1.6
11	97.0	95.3	1.7	98.0	94.4	3.6	98.0	96.2	1.8
12	99.0	95.7	3.3	97.0	93.2	3.8	98.0	96.0	2.0
13	99.0	93.3	5.7	99.0	86.9	12.1	99.0	97.6	1.4
14	99.0	97.1	1.9	100.0	94.0	6.0	99.0	97.0	2.0
15	97.0	88.6	8.4	100.0	92.4	7.6	99.0	96.1	2.9
16	98.0	97.0	1.0	100.0	87.3	12.7	98.0	96.8	1.2
17	98.0	97.8	0.2	100.0	93.9	6.1	99.0	95.9	3.1
18	100.0	86.9	13.1	99.0	87.3	11.7	96.0	94.8	1.2
19	97.0	96.6	0.4	100.0	93.8	6.2	98.0	96.4	1.6
20	98.0	96.7	1.3	100.0	90.0	10.0	98.0	97.0	1.0
Median	98.0	95.8	1.8	99.5	88.5	8.4	98.0	96.5	1.6
IQR	97.0 – 99.0	93.2 – 96.8	1.2 – 5.3	98.0 – 100.0	87.1 – 92.8	5.8 – 11.9	98.0 – 99.0	96.1 – 97.0	1.2 – 2.0

* NPB-75 refers to the commercial pulse oximeter SpO₂ readings

† PO refers to the custom pulse oximeter SpO₂ readings

Δ SpO₂ difference between NPB-75 and PO

5.5.6 Main outcome from Study 2

Table 5.4 shows 4 out of 5 subjects demonstrated a significant degradation in PPG signal quality of up to 0.3x, when the skin temperature was cold compared to baseline conditions, as detected by the

PO system. These results from Study 2 are in agreement to the corresponding results from Study 1. The compromise in PPG signal quality at low digit temperatures resulted in low median SpO₂ estimates of ≤89% across the subjects by the PO system. However, the Masimo SET pulse oximeter showed a median SpO₂ value of 100% across 4 out of 5 subjects, even with low quality PPG signal.

Table 5.4: PPG signal RMS and median digit skin temperature values for all subjects in Study 2.

Subject	Gender	Age	Baseline			Cold Test		
			IR _{RMS} (mV)	RD _{RMS} (mV)	T (°C)	IR _{RMS} (mV)	RD _{RMS} (mV)	T (°C)
1	M	30.0	92.4	53.1	35.7	23.4	16.9	19.2
2	M	24.0	103.9	63.8	31.0	31.0	28.4	20
3	M	37.0	95.5	54.0	32.7	29.9	18.2	21.5
4	M	23.0	51.5	33.9	25.0	23.7	20.3	19.8
5	M	25.0	74.7	46.5	33.3	61.8	40.2	20.3
Median		25.0	92.4	53.1	32.7	29.9	20.3	20.0
IQR		24.0 - 30.0	74.7 - 95.5	46.5 - 54	31.0 - 33.3	23.7 - 31.0	18.2 - 28.4	19.8 - 20.3

In contrast to both pulse oximeter measurements, true blood gas measurement showed a median value within the normal range (96 – 98%) across all the subjects. Thus, it can be concluded from this clinical validation trial that local cold temperature conditions only affect PPG signal quality and not the true SaO₂, as expected. In addition, there are processing differences between the PO system and the Masimo SET pulse oximeter leading to different results.

5.6 Discussion

5.6.1 Overall outcome

The controlled warm condition during the warm test significantly improved the quality of the PPG signals, up to 4x, as shown in Tables 5.1 – 5.2. This improved quality was associated with a closer

match between the SpO₂ values in Table 5.3 estimated by the PO system and the NPB-75. The only potential outlier was Subject 6. However, the signal RMS was still 2.8x and 2.3x better compared to the cold and baseline test measurements, respectively, for this subject.

Lesser inter-subject variability was observed with the results of SpO₂ values from the warm test as a result of variability in signal quality (RMS) seen in Figure 5.2. However, greater variability in SpO₂ outcome at baseline and cold tests occurred because of individual variability in the probable physiological response of blood flow to local temperature (O'Brien and Montain, 2003; Dickson et al., 2014). Hence, the warm condition provided consistency that was not evident in typical cohorts at and below room temperature.

In particular, for the warm test, the PPG quality was good, in general, across the cohort, with high signal RMS, while maintaining an expected and recognisable waveform shape. This improvement in quality was likely a result of enhanced perfusion at warm temperatures (Barcroft and Edholm, 1943; Gallen and Macdonald, 1990; Bornmyr et al., 1997). Local heat stimulation leads to an increase in vasodilation of peripheral blood vessels in the vicinity, even in naturally cold digits (Huizenga et al., 2004). The increase in cross sectional area of blood vessels due to increase in vasodilation, reduces peripheral vascular resistance and promotes enhanced peripheral blood flow to the digits, resulting in PPG signals with good SNR.

Cold temperatures tend to reduce peripheral blood flow in digits (Thorsson et al., 1985; Gregson et al., 2011; Bornmyr et al., 1997). The reduction in blood flow is predominantly due to vasoconstriction of the peripheral blood vessels, and can cause a rise in both systolic and diastolic

blood pressure from changes in sympathetic tone (Njoum and Kyriacou, 2013; Budidha and Kyriacou, 2014). When a hand at baseline temperature is immersed into ice water, the sudden drop in temperature causes the thermoregulatory system to stimulate the sympathetic nervous system to maintain homeostasis. Consequently, an increase in peripheral blood vessel resistance, volumetric elasticity, and wall stiffness follows, all of which reduce flow and perfusion, and thus signal quality, strength, and reliability of SpO₂ estimation.

Subject 20, as an example, had naturally low baseline skin temperature and thus likely lower peripheral blood flow, resulting in relatively poor baseline PPG quality, as seen in Figures 5.4 and 5.6. During the cold test, the PPG signal quality was further reduced. In fact, the RMS signal strength for every individual during the cold test was much lower compared to their Baseline and Warm test counterparts, as shown in Table 5.1 ($p < 0.0001$ in all cases). The drop in IR_{RMS} was about 1.6x greater than for RD_{RMS} for the median PPG value. Possible changes in blood pressure and flow during induced sympathetic tone may alter the optical path length and the tissue absorption coefficients during blood circulation (Njoum and Kyriacou, 2013), and thus can further affect signal quality.

During the warm and baseline tests, the average PPG amplitude was typically high, resulting in acceptable SpO₂ values matching those for healthy adults (Valdez-Lowe et al., 2009; Nitzan et al., 2014b). These results also agreed well with the commercial pulse oximeter's results in Table 5.3. However, the PPG amplitude was low during the cold test as shown in Figure 5.3. The agreement between the two pulse oximeters diminished for this test, as shown by significant deviation in SpO₂ estimation in Table 5.3.

A normal arterial PPG waveform seen in typical pulse oximeter monitors may vary greatly, but typically includes a sharp ascending systolic phase and descending diastolic phase limbs, which form a complete pulse. A characteristic notch on the descending limb is often visible in a good PPG waveform (Murray and Foster, 1996; Jubran, 2015), as shown in Figure 5.4. This notch resembles the dicrotic notch feature seen in an aortic pressure waveform, indicating the closure of the heart's aortic valve.

The dicrotic notch appeared regularly for the warm test PPG waveforms, and was occasionally visible in the baseline test PPG waveforms, as seen in Figure 5.4. When the peripheral perfusion is low, such as at very low temperatures, the PPG signal amplitude can be low and may miss this dynamic and suppress other features. In addition, the PPG waveform's shape can become inconsistent and non-uniform. Such abnormalities in the PPG waveform can cause the peak-trough detection algorithm to determine incorrect peaks and troughs, thus affecting any SpO₂, HR, or other estimations that rely on this value.

At normal or high arterial oxygen saturation conditions, the IR PPG signal amplitude is much greater than the RD PPG (NTS, 2011). However, at low SaO₂ conditions the RD pulse amplitude becomes larger than its IR counterpart (NTS, 2011). Since SaO₂ is a global variable, it is unlikely to vary generally from site to site for the healthy subjects in this study. Thus, low SaO₂ was not a factor. In addition, both RD and IR signals changed correspondingly in all the tests. Therefore, the median PPG amplitude degradation for both RD and IR signals during the cold test points to overall compromised signal quality, rather than any actual change in SaO₂ as evidenced by Study 2 results.

5.6.2 Inaccuracy of the commercial pulse oximeter

It should be noted that the typical pulse oximeter waveform presented, as in the case of NPB-75, is a highly filtered and processed version of the original PPG signal to aid in SpO₂ estimation. However, commercial pulse oximeters can still provide inaccurate readings with a highly processed signal, especially in low perfusion scenarios. For example, the NPB-75 SpO₂ estimates for Subjects 5 and 10 from the Cold test were below the reported minimum of 95% for healthy adults (Valdez-Lowe et al., 2009; Nitzan et al., 2014b), and far closer to the SpO₂ estimates by the PO system. In addition, SpO₂ of 100% was reported by the NPB-75 for Subjects 3, 7, 14 – 17, 19 and 20 with significantly low PPG amplitude. These estimates of 100% SpO₂ were actually higher than the corresponding Baseline and Warm test measurements on the same subjects, presented in Table 5.3. Such inaccuracy is typically due to the digit sensor signal being prone to vasoconstriction effects and a failure to detect adequate pulsatile signals during low perfusion (NTS, 2011).

Commercial pulse oximeters are typically calibrated with well perfused, normothermic healthy volunteers. Manufacturers use adaptive noise reduction based signal conditioning and advanced digital signal processing techniques (NTS, 2011), which enable the pulse oximeter to separate source and noise signals (Goldman et al., 2000; Bennett, 1998; Rheineck-Leyssius and Kalkman, 1999). Complex algorithms are used to evaluate the shape of each potential pulse and extract useful pulses from noisy signals (Rheineck-Leyssius and Kalkman, 1999; Bennett, 1998). In addition, auto-centering and auto-gain routines are applied to the displayed waveforms to minimize variations in the displayed signal (Shelley, 2007; Cannesson and Talke, 2009). Although such signal processing techniques may be useful in certain cases to estimate SpO₂, it often comes at the

expense of losing valuable physiological data (Shelley et al., 2014). Thus, its constraints may be finding signal shapes where they do not necessarily exist, as in Figure 5.4 for the Cold test.

5.6.3 Study limitation and validation

The primary limitation of Study 1 was that it was not possible to obtain a true reference for blood gas data during any of the three tests at the time of the experiment. Thus, it could not be validated that there is no significant change in actual SaO_2 in the Cold test during Study 1. However, the outcomes of that study justified the need to have arterial reference measurements in Study 2. In Study 2, arterial blood gas measurements were made to overcome the primary limitation of Study 1 and validate the initial hypothesis about the adverse effects of cold skin temperatures on PPG signal quality. Although a resting period was recommended prior to study, a subject experiencing stress and anxiety may have elevated HR or low BP, which can impact the subject's CO and thus peripheral blood flow. However, these factors cannot be controlled or assessed, and is also not the goal of this research.

5.7 Summary

This chapter investigated the effects of local skin temperature conditions on PPG signal quality as applied to pulse oximeters using TPO sensors. Cold temperature conditions significantly reduce PPG signal quality, as shown by reduced signal RMS and amplitude, and thus the accuracy of the resulting SpO_2 estimate, as shown in both studies. This degradation in signal quality is interrelated with decrease in blood volume and blood flow, due to induced vasoconstriction (sympathetic tone). Baseline measurements from naturally cold digits also showed poor PPG quality and inaccurate SpO_2 estimation.

Warm temperature conditions significantly improved the quality of the PPG signals, up to 4x, as well as SpO₂ estimation. This improvement in signal quality can be correlated with increase in blood volume and blood flow, due to induced vasodilation. Warming of the hand increased the confidence in accuracy of SpO₂ estimation for subjects with naturally cold fingers. The overall experimental outcomes from this research suggest that warm skin temperature conditions of approximately 33 °C should be maintained for reliable transmittance pulse oximetry, and any further clinical use of these signals in monitoring or measuring parameters related to peripheral O₂E and circulation.

Chapter 6: Monitoring peripheral blood flow changes using photoplethysmography

6.1 Introduction

Peripheral tissues are sensitive to alterations in perfusion. Perfusion monitoring is thus an essential part of monitoring oxygenation and extraction in the periphery. Currently, there is no gold standard for measuring local tissue perfusion, and available methods are typically invasive or time consuming. Hence, non-invasive monitoring of peripheral perfusion could be used as a surrogate measure, and thus as an early marker of systemic haemodynamic derangement and tissue hypoperfusion (van Genderen et al., 2012b; Lima and Bakker, 2005).

Blood flow information is necessary to determine oxygen extraction rate at different perfusion conditions. Non-invasive assessment of blood flow changes in peripheral regions using PPG has been previously reported by several studies. (Bergstrand et al., 2009; Naslund et al., 2006; Zhang et al., 2001). These studies show the AC signals of the PPG corresponds to blood flow, while the DC signals of the PPG corresponds to blood volume change. It is suggested that the AC component is linked to the pulsatile blood volume changes due to varying lumen of the vessel (Aoyagi, 2003; Cohn et al., 2007) and changes in red blood cell orientation during each cardiac cycle (Graaff et al., 1993; Lindberg and Oberg, 1993).

However, these assessments used reflection mode PPG sensors and focused on the anterior tibial muscles, patellar bone, and sacrum regions. None of these studies were done using a transmission

mode PPG sensor, and nor were they performed at accessible extremities like the finger. Hence, there is an opportunity to use such PPG signals to estimate flow changes in the finger and assess venous oxygen saturation, as well as O₂E, using simple the same and simple low cost sensors.

Sandberg et al. (2005) evaluated a specially developed PPG technique using green and near-infrared light sources, for simultaneous, non-invasive monitoring of skin and muscle perfusion in the lower leg. As a reference measurement, they used a pulsed Doppler ultrasound sensor over the femoral artery, to obtain blood velocity and vessel cross sectional diameter. Absolute blood flow was estimated using the ultrasound images for comparison. Evaluation was based on assessment of relative changes in PPG in response to various provocations, such as post-exercise hyperemia and hyperemia following the application of liniment. Their study showed that both the Doppler ultrasound and PPG sensors measured a similar hyeraemic response directly after dynamic contractions.

This chapter presents a TPO sensor based blood flow assessment in the finger, conducted using the PO system. A series of partial and full VOTs were designed to provoke changes in blood flow conditions in the forearm using a conventional sphygmomanometer and pressure cuff. The PPG was analysed to extract relative volumetric flow change information in terms of changes in the AC signal amplitude. A BV-520T (Shenzhen Bestman Instrument Co. Ltd, Nanshan Disc., Shenzhen, China) vascular Doppler ultrasound sensor was used as a reference sensor, for comparison and monitoring of blood velocity change. The overall goal of this study is to demonstrate and assess the correlation between Doppler ultrasound measured blood velocity and AC amplitude in the periphery.

6.2 Vascular Doppler Ultrasound

Velocity of blood flow in a limb can be measured using Doppler ultrasound techniques, which measures the arterial in-flow to the limb (Gill, 1985). In this research, the BV-520T vascular Doppler ultrasound sensor was employed to assess the radial arterial blood supply to the wrist as a reference measurement. This device can monitor perfusion in real-time by measuring blood flow velocity every 3 second. During this study, the blood velocity measurements were analysed for blood flow change estimation and monitoring. This section describes the fundamental principles of vascular Doppler ultrasound technique and how it assesses peripheral perfusion in terms of blood velocity.

6.2.1 Technology Fundamentals

The vascular Doppler ultrasound sensor transmits high frequency (8MHz) sound waves through ultrasound transmission gel on the skin surface, and transcutaneously reaches all the way to the blood vessels. Ultrasound gel is used as a conducting medium between the ultrasound device and skin, because ultrasound technology does not operate through air. The transmitted beam hits the moving cells in the blood stream, experiences a frequency shift, and reflects back to the receiver at a different frequency. The reflected ultrasound frequency is proportional to the velocity of the blood flow (AbuRahma and Bandyk, 2012). The difference between the transmitted and received frequency is the Doppler shift frequency (Thrush and Hartshorne, 1999; AbuRahma and Bandyk, 2012), defined:

$$\Delta F = \frac{2F_0 V \cos\theta}{C} \quad (6.1)$$

Where,

ΔF = Doppler shift frequency (MHz)

F_0 = Ultrasound transmission frequency (MHz)

V = Blood cell velocity (cm/s)

$\cos \theta$ = Angle of insonation

C = Speed of sound in soft tissue (154000 cm/s)

Doppler ultrasound technology works best with a small angle of insonation (Thrush and Hartshorne, 1999; Thrush and Hartshorne, 2009), typically $<45^\circ$ (Thrush and Hartshorne, 1999).

The insonation angle is the angle between the ultrasound probe and the direction of blood flow.

The error in Doppler ultrasound measurement is proportional to the insonation angle between $10 - 45^\circ$, with an increase in error by 2% per 10° . Measurement errors increase exponentially with an angle $>45^\circ$, such as an error of 19% at an insonation angle of 60° (Thrush and Hartshorne, 1999; Thrush and Hartshorne, 2009).

6.2.2 Doppler Velocity Waveform

A typical Doppler arterial velocity waveform has tri-phasic features (Donnelly et al., 2000), as shown in Figure 6.1. It starts with rapid antegrade flow during systole, reaching a peak, known as peak systolic velocity (PSV). A transient flow reversal is followed during early diastole, identified as a low diastolic velocity (LDV). Finally, it ends with a slow antegrade flow during late diastole, denoted end diastolic velocity (EDV). Some vascular Doppler ultrasound devices can use all the 3 phases to calculate the mean flow velocity (MFV). However, under conditions of stenosis, arterial velocity waveforms can take a bi-phasic form with increased velocity and little or no flow reversal (Donnelly et al., 2000).

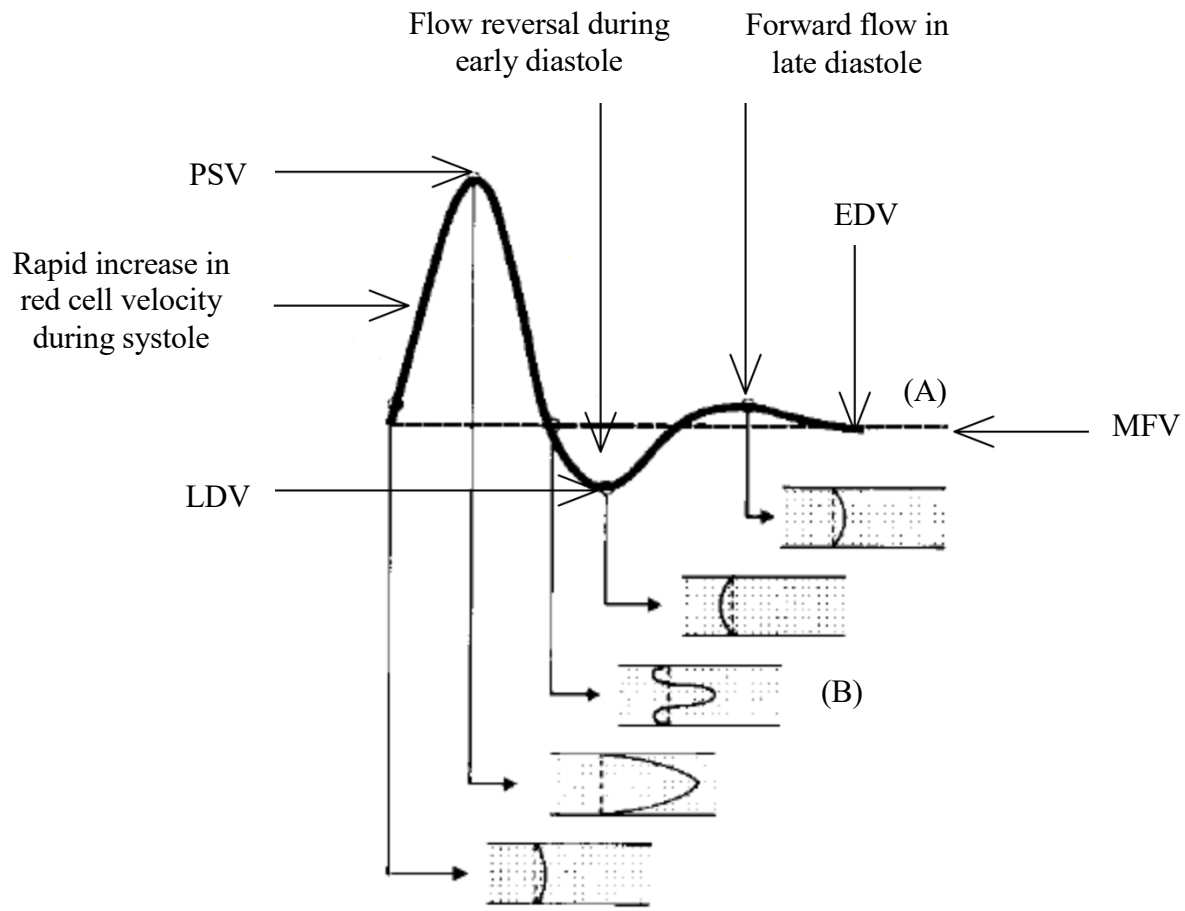


Figure 6.1: Typical appearance of a directional Doppler waveform from a normal common femoral artery (A), showing the flow envelope at various phases of the flow cycle (B) and related velocities. Adapted from (Vowden and Vowden, 2004)

Continuous wave Doppler ultrasound systems like the BV-520T uses continuous transmission and reception of ultrasound to calculate blood flow velocity. Doppler ultrasound signals are obtained from all vessels in the path of the ultrasound beam, until the ultrasound beam becomes sufficiently attenuated due to depth. The BV-520T can determine of the direction of blood flow and designed only to detect pulsatile (arterial) blood flow. Any ultrasound reflections detected from non-pulsatile (venous) blood is negligible or attenuated. In addition, this device can continuously display the blood velocity waveform and PSV in real time. In this study, PSV data acquired from experiment was used to evaluate blood flow change.

6.2.3 Other features and modification

The BV-520T is a bi-directional Doppler ultrasound device, which measures flow in both forward and reverse directions. However, reverse flow represents only the direction of blood flow with respect to the probe. This function should not be confused with the transient flow reversal seen in normal arterial velocity waveforms.

For this study, a mounting for the BV-520T's probe was designed and 3D printed. The mounting provided a fixed 30° angle of insonation, as shown in Figure 6.2. This choice and use of a mount in fixed angle can minimise errors, and more importantly, minimise deviation in measurements and maintain consistency. In addition, it made the probe easier to be held in place during testing.

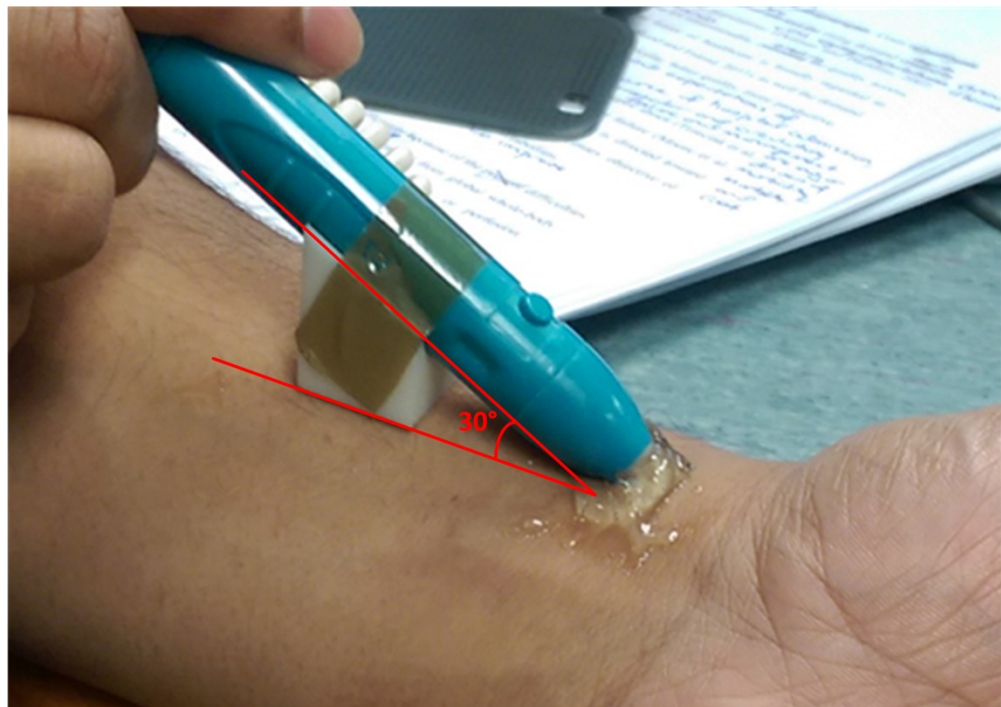


Figure 6.2: Mounting designed to assist in holding the BV-520T probe at fixed 30° angle of insonation

6.2.4 Preliminary tests

Preliminary tests were conducted to understand the BV-520T's functionality and performance. Vascular Doppler ultrasound based flow assessments are typically performed on the radial artery (Bardoň et al., 2010; Rivas et al., 2007; Kim et al., 2015), due strong pulse detection and ease of access. Eight healthy adult volunteers were recruited for this preliminary study. The arterial pulse location was determined manually with the index finger. Where a strong pulse was felt ultrasound gel was applied to that location. PSV was continuously measured for each volunteer in two sets, for duration of 60 s each, giving a total of 40 samples per subject. This initial feasibility and evaluation study was approved by the University of Canterbury, Human Ethics Committee.

Table 6.1 presents the 60 s mean PSV measurements made on this test cohort. The mean PSV measurements matched closely with published PSV values of 54.1 – 59.1 cm/s (Bardoň et al., 2010; Kim et al., 2015; Rivas et al., 2007; Kim et al., 2012). The overall outcome of the preliminary test showed that blood velocity assessments can be achieved with the modified BV-520T sensor. However, it was also observed that a small change in the angle of insonation can produce a significant change in measured PSV, impacting robustness.

Table 6.1: PSV measurements from the preliminary test, S1 means set 1 and S2 means set 2.

	1		2		3		4		5		6		7		8	
	S 1	S 2	S 1	S 2	S 1	S 2	S 1	S 2	S 1	S 2	S 1	S 2	S 1	S 2	S 1	S 2
PSV (cm/s)	63.8	54.1	45.3	52.0	48.1	53.5	68.1	54.5	56.9	57.9	54.2	58.0	54.9	58.6	59.2	60.0
Median PSV (cm/s)	55.9															
Interquartile range (IQR)	53.8 – 58.9															

6.3 Main Study

6.3.1 Ethics Approval

Seven healthy human volunteers (5 males and 2 females) with no pre-existing medical conditions were recruited for the relative blood flow change assessment study. Healthy volunteers are easy to recruit, and are likely to demonstrate understandable responses when a change is induced. In contrast, critically ill-subjects can show changes that are difficult to explain, which can complicate validation for this study.

This study was approved by the HEC, University of Canterbury (Ref: HEC 2016/16/LR-PS). After informed consent was received from each volunteer, they were included in the study. Data were de-identified and securely stored. All documents and details related to this ethics application is provided in Appendix 6.1.

6.3.2 Experimental Protocol

In addition to the PO system and MATLAB processing environment, a conventional sphygmomanometer and pressure cuff was used to perform the vascular occlusion tests. The VOT was designed to induce no and low flow conditions using high and low cuff pressures, respectively. The pressure cuff was wrapped around the upper arm. The BV-520T vascular Doppler ultrasound sensor with the mounting holder was employed for blood flow velocity assessment at the left radial artery.

Subjects were asked to refrain from smoking and strenuous physical activities for at least 2 hours prior to the experiment. This rest time is important to ensure the cardiac activities of the subjects

are normal before the study commences. During the study, subjects were comfortably seated, while resting their left arm on a flat surface, at approximately the same height as their heart, with minimum movement. Subjects were advised to breathe normally for the duration of the experiment. The whole protocol lasted for approximately 6 min.

Ultrasound gel was applied close to the wrist of the left arm, and the radial arterial pulse was detected using the vascular Doppler ultrasound sensor. When the radial arterial pulse was consistently detected, the exact location was marked with a washable marker. The BV-520T sensor was always held on the marked location, for the duration of the experiment to ensure consistency and repeatability. The PO sensor was connected to the middle finger of the subject for the duration of the experiment. Figure 6.3 presents the sensor set ups in this study.

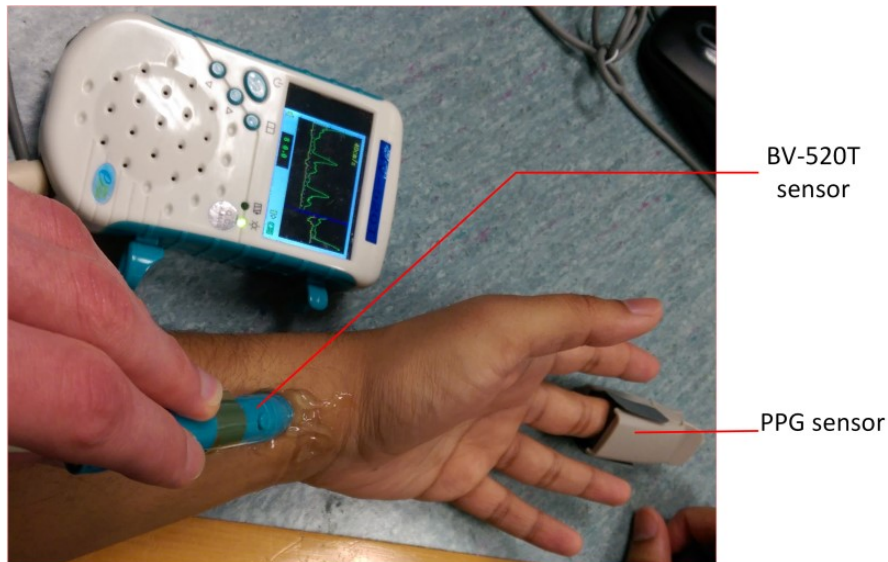


Figure 6.3: The BV-520T and PO sensors set up during the study.

Initially, 60 s of baseline data were recorded. After 60 s, the pressure cuff was inflated to 80 mmHg, which is near the typical diastolic blood pressure. This pressure was maintained for 60 s to induce partial vascular occlusion, and thus reduce arterial flow to the hand during that period. The cuff pressure was further increased to 160 mmHg, which is above the typical systolic blood pressure, and maintained for 60 s. At this stage, the arm was completely occluded with no arterial flow to the hand, confirmed by loss in PPG pulsation. The cuff was then completely deflated by slowly releasing the sphygmomanometer's valve to re-establish blood supply to the hand. The recovery phase PPG was recorded for 120 s, and will be treated as Recovery 1 and 2, each of 60 s duration. The time needed to increase pressure from 0 – 80 mmHg in the cuff was approximately 15 s.

6.3.3 Signal Analysis

All PPG and Doppler ultrasound data were analysed in MATLAB. To estimate the relative blood flow change, amplitude information from the AC signal of the PPG needs to be determined. The peak-trough detection algorithm discussed in Chapter 4 was applied to the extracted AC signal, to determine the amplitudes relating to each heartbeat. Figure 6.4 shows an example of an AC signal with peaks and troughs identified using the algorithm. The difference between each detected peak and trough was the corresponding amplitude for each AC signal pulse.

The Doppler ultrasound velocity data was interpolated using linear interpolation to match the same number of AC signal amplitude samples. A linear model was fitted across the interpolated Doppler ultrasound velocity data and corresponding AC signal amplitude data, and the coefficient of determination (R^2) was computed to assess the strength of their correlation. In addition, the peak-

peak interval time was used to determine heart rate (HR) in beats per minute (bpm). A 5 second block moving average of the HR was also calculated for the complete PPG signal to assess HR for the whole test across each subject.

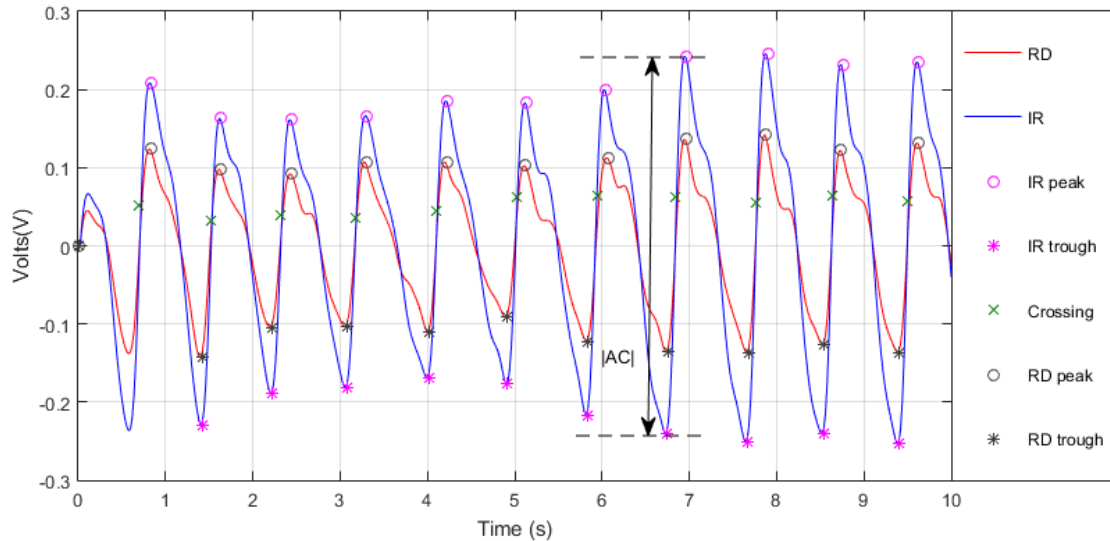


Figure 6.4: Peak-trough detection algorithm, to extract AC amplitude ($|AC|$) information from the AC signal of RD and IR PPGs.

6.4 Results

6.4.1 Blood flow change detection

In this study, only the AC signal of the IR PPG was used for analysis. Tissue cycling of blood volume at high oxygen saturation level has less influence on the detected RD signal in contrast to the IR signal (Staff, 2011). Thus, the IR PPG was assumed to be more responsive to changes in blood flow conditions.

Figure 6.5 shows the blood flow trajectory for one of the subjects detected by the PPG in comparison to the Doppler. The overall flow trends measured by the PPG and Doppler ultrasound

sensors showed good agreement in general, but varied more during the recovery phases. Both sensing methods successfully detected partial and full occlusion phases.

At baseline, no significant change in blood flow was observed by either method. After 60 s, there was a significant drop in both AC signal amplitude and Doppler ultrasound velocity due to partial occlusion. In particular, the PPG sensor showed a relatively more responsive or rapid drop than the Doppler ultrasound sensor. The reduction in flow during this phase was a result of restricted arterial flow to the hand, and the flow remained low without any significant variation. At full occlusion, no flow was detected by either method, as desired. The PO sensor increased LED intensity above baseline level during full occlusion to increase absorption. However, since there was no flow, the AC signal amplitude dropped to zero even at increased light intensity.

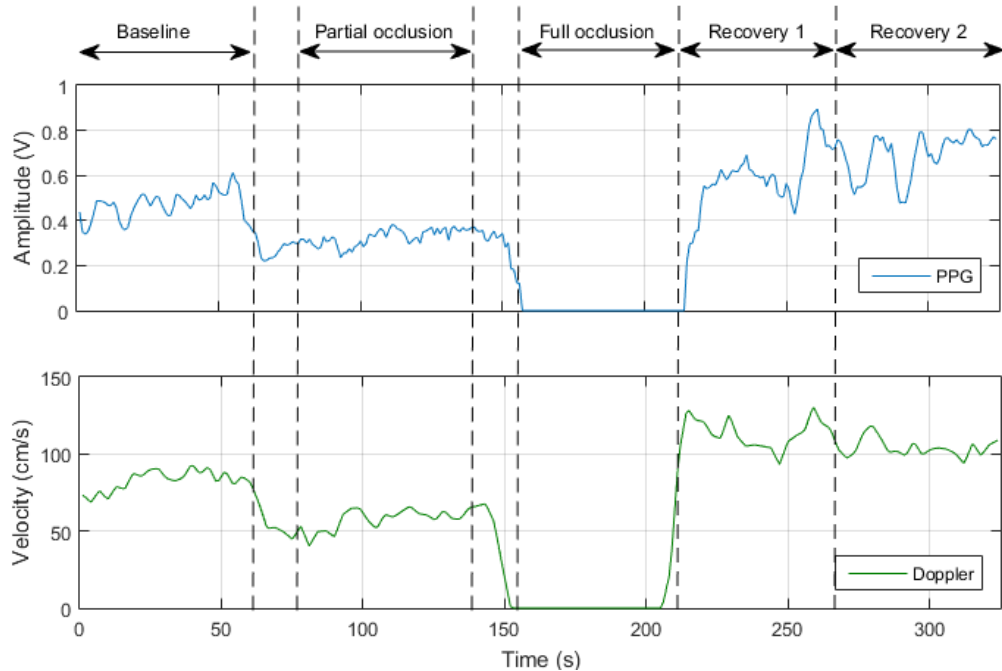


Figure 6.5: Blood flow change trend captured for one subject during the whole experiment with PPG (top) and Doppler (bottom).

Immediately after the cuff pressure was released to zero, re-establishment of flow was detected by both methods. In the first 5 seconds of the recovery phase, the Doppler ultrasound sensor demonstrated reactive hyperemic flow, with measured velocity going up to 2 times to that of baseline. In contrast, the AC signal amplitude was just over baseline level. A spatial effect due to the differences in sensor location led to a small delay (<1 s) in detecting the re-establishement of flow by the PPG sensor. About 60 seconds into the recovery phase, the measured blood velocity declined close to baseline level. In comparison, the AC signal amplitude rose above baseline and remained at an elevated level, even with the PO sensor LED intensity returning to baseline level.

6.4.2 Median PPG and Doppler data analysis

A 60 second block median of AC signal amplitude and Doppler velocity was computed for each protocol to provide the overall median value as a representation of the specific period. Table 6.2 presents the median amplitude and velocity for each subject, per protocol. The median of these subject-specific median values and interquartile (IQR) values for both measurements are also included. Figure 6.6 shows the trajectory of the median AC signal amplitude and Doppler velocity values during each phase for the whole study.

During the partial occlusion phase, both the AC signal amplitude and Doppler ultrasound velocity demonstrated drops of 36% and 37%, respectively, in overall median values from baseline across the cohort. This drop was accompanied with lower IQR values, and thus a more consistent, less variable inter-subject result, compared to baseline. At the full occlusion phase, the value of the two methods decreased to zero from baseline, as expected, for all subjects.

Table 6.2: Median [IQR] AC signal amplitude (V) and Doppler ultrasound velocity (cm/s) data from the study

Subject	Method	Baseline		Partial Occlusion		Full occlusion		Recovery 1		Recovery 2	
1	PPG	0.5	[0.4 - 0.5]	0.1	[0.1 - 0.1]	0.0	[0.0 - 0.0]	0.3	[0.3 - 0.4]	0.6	[0.5 - 0.6]
	Doppler	55.5	[50.8 - 58.7]	24.8	[17.6 - 34.0]	0.0	[0.0 - 0.0]	66.4	[59.4 - 75.7]	58.5	[54.9 - 69.2]
2	PPG	0.5	[0.4 - 0.5]	0.3	[0.3 - 0.4]	0.0	[0.0 - 0.0]	0.6	[0.5 - 0.7]	0.7	[0.6 - 0.8]
	Doppler	84.1	[78.5 - 87.8]	60.6	[57.8 - 64.0]	0.0	[0.0 - 0.0]	111.6	[105.1 - 119.7]	102.7	[100.5 - 106.5]
3	PPG	0.4	[0.3 - 0.4]	0.3	[0.2 - 3]	0.0	[0.0 - 0.0]	0.4	[0.3 - 5]	0.5	[0.5 - 0.6]
	Doppler	85.3	[81.2 - 90.1]	52.5	[48.0 - 58.7]	0.0	[0.0 - 0.0]	109.0	[102.3 - 114.1]	98.4	[94.9 - 105.5]
4	PPG	0.1	[0.1 - 0.1]	0.1	[0.1 - 0.1]	0.0	[0.0 - 0.0]	0.2	[0.2 - 0.2]	0.2	[0.2 - 2]
	Doppler	55.0	[46.5 - 62.3]	39.2	[36.5 - 41.1]	0.0	[0.0 - 0.0]	60.5	[51.7 - 72.1]	53.7	[49.5 - 58.5]
5	PPG	1.3	[1.2 - 1.4]	0.7	[0.6 - 0.7]	0.0	[0.0 - 0.0]	1.2	[1.1 - 1.3]	1.4	[1.3 - 1.4]
	Doppler	105.7	[102.0 - 111.0]	77.6	[72.5 - 83.8]	0.0	[0.0 - 0.0]	137.3	[124.9 - 145.0]	103.0	[99.0 - 107.3]
6	PPG	0.7	[0.7 - 0.8]	0.4	[0.4 - 0.5]	0.0	[0.0 - 0.0]	0.7	[0.6 - 0.7]	0.8	[0.8 - 0.8]
	Doppler	84.0	[81.1 - 86.7]	56.4	[50.3 - 62.4]	0.0	[0.0 - 0.0]	74.5	[57.9 - 83.1]	83.4	[81.3 - 84.8]
7	PPG	0.4	[0.3 - 0.4]	0.3	[0.3 - 0.3]	0.0	[0.0 - 0.0]	0.6	[0.4 - 0.6]	0.7	[0.6 - 0.7]
	Doppler	88.0	[84.3 - 93.9]	52.8	[45.9 - 61.3]	0.0	[0.0 - 0.0]	74.0	[61.8 - 83.6]	82.2	[78.2 - 85.6]
Median [IQR]	PPG	0.5	[0.4 - 0.7]	0.3	[0.1 - 0.4]	0.0	[0.0 - 0.0]	0.6	[0.4 - 0.7]	0.7	[0.6 - 0.8]
	Doppler	84.1	[62.6 - 87.3]	52.8	[42.5 - 59.5]	0.0	[0.0 - 0.0]	74.5	[68.3 - 110.9]	83.4	[64.4 - 101.6]

Interesting observations were made during Recovery 1. Subjects 1 and 5 had median values of 24% and 6% lower, respectively, than median baseline AC signal amplitude. However, their corresponding Doppler ultrasound velocities were 20% and 30% higher, respectively, than median baseline values. In contrast, Subject 7 showed a 16% lower value than the median baseline Doppler ultrasound velocity but exhibited a 38% higher than median baseline AC signal amplitude. Except Subject 6, the other 3 subjects demonstrated both higher AC signal amplitude and Doppler ultrasound velocity median values when compared to median baseline values. Subject 6 provided

7% and 11% lower median values than baseline for AC signal amplitude and Doppler ultrasound velocity, respectively.

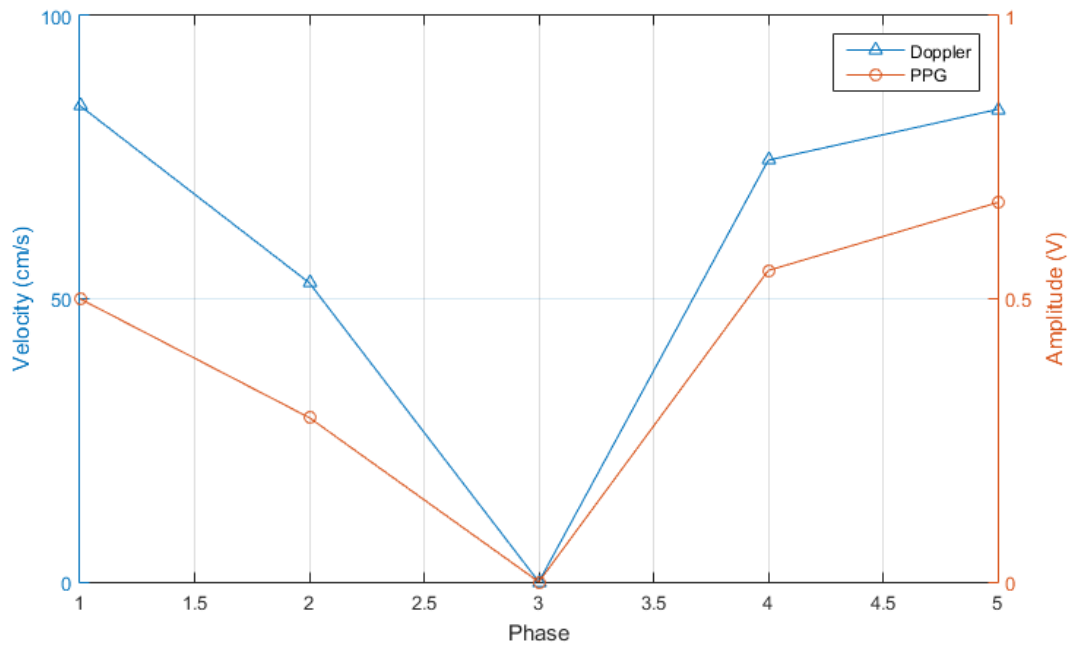


Figure 6.6: Trajectory of the median AC signal amplitude and Doppler velocity values for the whole study; Phase 1 – Baseline, Phase 2 – Partial occlusion, Phase 3 – Full occlusion, Phase 4 – Recovery 1, Phase 5 – Recovery 2.

In Recovery 2, the overall median AC signal amplitude increased by 33% above the overall median baseline values, in general. All subjects, except Subjects 6 and 7, showed a median Doppler ultrasound velocity with little difference (< 7%) compared to baseline values. However, Subjects 2 and 3 showed a median Doppler ultrasound velocity, up to 22%, higher than baseline velocity.

6.4.3 Correlation between the two measurements

Correlation between median AC signal amplitude and median Doppler ultrasound velocity for each subject and phase is shown in Figure 6.7. The linear model fitted through the data points shows a good fit between the two measurements, with a positive gradient. Although the data points are not tightly clustered, a good correlation of $R^2 = 0.69$ was found between the two measurements.

Subject 5 produced 2 out of 5 outlying data points. Subject 5 showed a baseline blood velocity and AC signal amplitude value of 1.5 and 3 times greater, respectively, than the average of the other baseline values. At recovery 2, a large 21% drop was seen in blood velocity, compared to a small 11% rise in AC signal amplitude from Recovery 1. All these differences could be a result of measurement error by either or both sensors in this case.

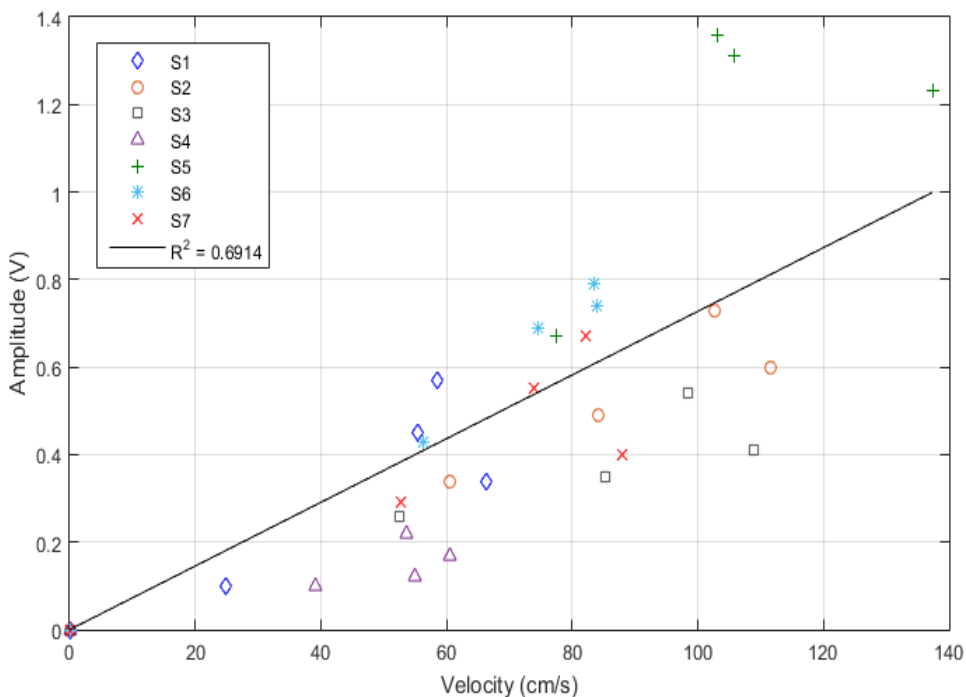


Figure 6.7: Correlation between mean pulse amplitude and velocity of blood flow for the whole cohort

6.4.4 Heart rate assessment

HR was assessed across all subjects to monitor changes in cardiovascular activity at all times during the experiment. Figure 6.8 shows the HR trend recorded for Subject 2 as an example, with a mean HR of 73.5 bpm (SD ± 4.2 bpm). As should be expected, the estimated heart rate dropped to zero during full occlusion phase, which occurs due to failure in detecting any arterial pulse by the finger based PPG sensor. No significant changes in HR across the subjects were recorded throughout the study.

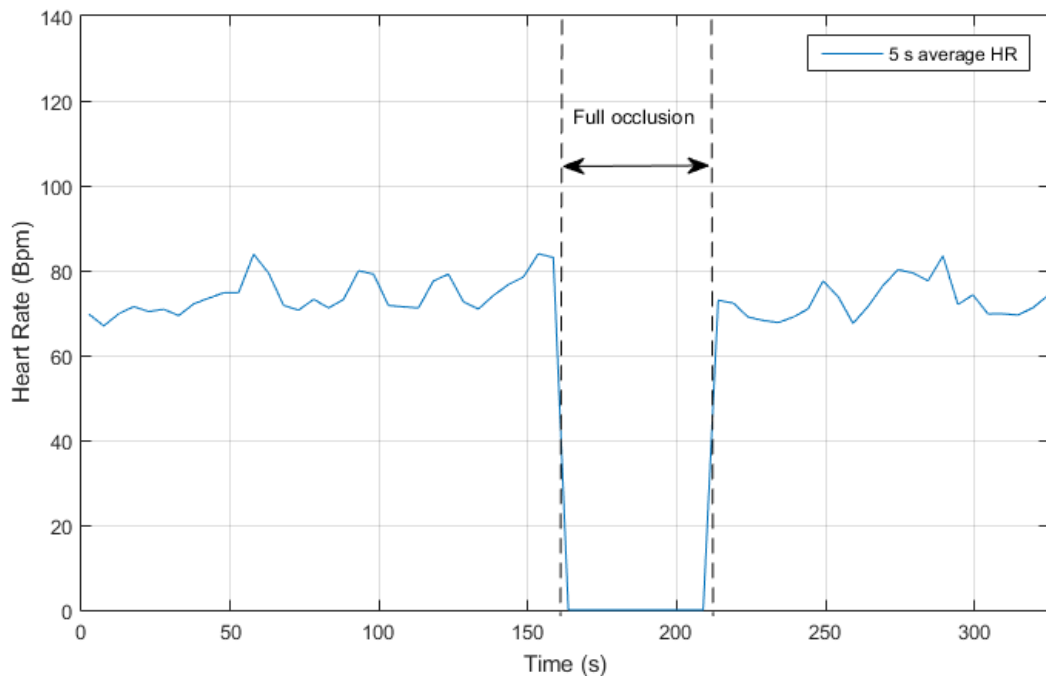


Figure 6.8: Detected HR trend using the PPG sensor trend for Subject 2 during the experiment, with no HR detected during full occlusion.

6.5 Discussion

6.5.1 Blood flow trends

This study presents and evaluates a non-invasive method to assess relative changes in volumetric blood flow in the finger using transmission mode PPG. The measured AC signal amplitude correlates with measured Doppler ultrasound blood velocity. The results indicate the potential for PPG sensor to monitor changes in local tissue blood perfusion and flow, and thus for use as a surrogate for and as an alternative to Doppler ultrasound measurements.

In certain cases, there can be a change in blood flow across a blood vessel without a rise in blood flow velocity (Klabunde, 2011). The blood flow through a blood vessel is defined (Klabunde, 2011):

$$\text{Blood flow} = \text{Velocity} \times \text{CSA} \quad (6.2)$$

Blood flow in a particular vessel is directly proportional to the CSA of the vessel diameter. During partial occlusion, the cross sectional area of the supplying peripheral artery is reduced, which increase the peripheral vascular resistance to incoming flow, and thus decreases overall blood flow to the hand. This reduction in flow is captured by both the Doppler and PPG sensors as a reduction in blood velocity and pulse amplitude, respectively.

Immediately after the pressure cuff was completely deflated at Recovery 1, an increase in perfusion was detected by both methods. The Doppler ultrasound was generally more sensitive to rapid changes in tissue blood flow, such as reactive hyperemia, indicated by a large overshoot in first the 5 s. In contrast, the PPG sensor did not demonstrate any such characteristic and rose more

slowly. It should be noted that the variability among the Doppler velocity measurements, represented by a wide IQR across the cohort during Recovery 1, is an indication of the wide range of subject specific changes in arterial CSA in response to this test.

The Doppler ultrasound velocity is specific to location of the probe, which is the radial artery in this study. The radial artery being a major blood vessel can reflect transient changes in flow dynamics more rapidly than smaller blood vessels further down the arterial tree. In contrast, the AC signal amplitude reflects volumetric flow in the whole region of sensor illumination, which in this case are the palmar fingertip arterioles and capillaries. These much smaller blood vessels in the index finger are branched several generations from the radial artery, and thus result in a significant reduction in overall CSA. Hence, there is a greater resistance to flow and any change in flow is much more dissipated in the whole region, and thus in the PPG sensor. These effects may be explained by a delayed and damped response demonstrated by the AC amplitude in these experiments. Although the AC amplitude is less sensitive to transient flow dynamics than the Doppler ultrasound measurements in the radial artery, it can still capture overall blood velocity changes in the illuminated region.

The measured response to removal of full occlusion in the recovery phases was not as similar for the two methods, as seen in the previous phases. Equally, both technologies showed a significant deviation from baseline during Recovery 1 and 2, indicating greater inter-subject variability in response to the reestablishment of flow after the full occlusion. Unlike the AC amplitude measurements, the Doppler ultrasound velocity measurements showed a wider IQR in comparison

to baseline. However, a good overall agreement between the median trajectory of the two measurements can be seen in Figure 6.6, for all phases of the experiment.

6.5.2 Vasodilation during post occlusion hyperemia

Post occlusion hyperemia has been previously reported to increase CSA in forearm blood vessels (Mollison et al., 2006; Corretti et al., 2002; Kochi et al., 2005; Heffernan et al., 2010). The resulting increase in shear stress on the vascular endothelium due to increase in blood flow causes endothelium-dependent vasodilation (Pyke and Tschakovsky, 2007; Corretti et al., 2002; Kochi et al., 2005), and thus increase in CSA. Such vasodilation effects are also termed as flow-mediated vasodilation. In Recovery 2, the AC signal amplitude rose to an elevated level above baseline level. Since the PPG sensor captures blood flow in terms of volume change, given an increase in blood in-flow and compliant vessels there should be a transient increase in illuminated blood volume before out-flow catches up. The elevated AC signal amplitude level at Recovery 2 indicates increased flow rate and blood volume, which is thus assumed to be due to an increase in CSA of the blood vessel.

The increase in peripheral arterial diameter due to flow-mediated vasodilation is typically not an immediate effect. Previous studies have reported that a gradual increase in blood vessel diameter of up to 22% above baseline can occur approximately 60 s after release of the occlusive pressure cuff, or 45 – 60 s after peak reactive hyperemic blood flow (Uehata et al., 1996; Corretti et al., 1995; Kochi et al., 2005). This fact coincides well with the slow increase in AC signal amplitude in Recovery 2, which is about 60 s after initial cuff release.

The decline of the median blood velocity measurements close to baseline level with hyperemic flow, as seen in Figure 6.6 and Table 6.1, suggests a significant increase in arterial CSA. However, hyperemic blood flow is expected to return to baseline level after 4-5 mins of hyperemia (Corretti et al., 2002; Corretti et al., 1995). Since only 2 mins of recovery phase data was recorded during the study, it was not possible to capture that specific phenomenon.

6.5.3 Overall outcome

Overall, a good positive correlation was found between the median AC signal amplitude and Doppler ultrasound blood velocity measurements across the subjects. The good correlation achieved suggests that one method might be a good surrogate of the other. Equally, it indicates that trends match as well, which is clinically important. Given these differences in rapid transient response during Recovery 1 and 2, the correlation is better for slower changes, as might be seen clinically. In addition, no significant change in HR across the subjects was recorded throughout the study. Such an outcome is expected, since the induced change in blood flow strictly applies to the periphery, and was not due to change in cardiac output or blood pressure.

However, it is expected that the two methods will not always have a strong correlation. Blood velocity is one of the key components that dictate blood flow, while the AC signal amplitude is related to volumetric flow in the illuminated area. Under conditions of possible changes in arterial diameter, such as at Recovery 1 and Recovery 2, the blood velocity and AC signal amplitude may have a weaker correlation. However, the greater inter-subject variability shown by the Doppler ultrasound velocity measurements question the method's reliability in measuring high perfusion status. Results from the recovery phases indicate, the AC signal amplitude may be also associated

with arterial diameter changes, despite the lag between seeing the effect of removing the occlusion at the two different locations.

6.5.4 Study Limitations

The primary limitation of this study was the inability to measure the CSA of the radial artery. Application of a pulsed wave, colour, Doppler ultrasound measurements can provide coloured cross sectional images of the radial artery, from where the arterial diameter can be measured, and thus yielding CSA (Kim et al., 2015; Hosono et al., 2000). Unfortunately, such device was not available during this study. The continuous wave Doppler ultrasound device used only provides blood velocity measurements, in particular PSV. As a result, the CSA of the radial artery could not be determined, and this limitation hindered the possibility to quantitatively determine absolute blood flow. Without absolute blood flow data, the Doppler ultrasound velocity measurements can only be conditionally related to PPG based amplitude measurements. However, it is trends in response to condition and care that are clinically important, and are not affected by this issue.

Another limitation was the difficulty to firmly hold the vascular Doppler ultrasound probe fixed at the marked place due to subtle hand movement of both the subject and investigator. In addition, even with the modified probe mounting the angle of insonation could not always be maintained at 30° with absolute certainty, introducing some error and inconsistency. The Doppler ultrasound sensor is very sensitive to any deviation in angle of insonation (Logason et al., 2001). Such limitations of the probe positioning sometimes resulted in noisy or no signal received by the probe, affecting robustness. Under these circumstances, the erroneous data and its time was identified and excluded from analysis. The corresponding PPG data was also removed to maintain consistency.

6.6 Summary

The AC signal amplitude can be used to monitor relative blood flow changes in the finger. It can successfully identify different flow states, and thus can be used to monitor changes in perfusion. This study presented a method to induce blood flow changes in the forearm using a blood pressure cuff and investigated the relation between blood velocity and AC signal amplitude. The PPG sensor detected these changes in flow with respect to baseline blood flow, when compared to a commercial Doppler ultrasound sensor. A good correlation ($R^2 = 0.69$) was obtained between PPG based median pulse amplitude and Doppler ultrasound determined median velocity, particularly at normal and low flow conditions.

The other key outcome of this study shows that the AC signal amplitude monitoring can be a good alternative to the vascular Doppler ultrasound based peripheral perfusion monitoring. It can provide non-invasive, continuous, and reliable measurements, and is unaffected by an angle at which the probe is attached to the finger, unlike the Doppler ultrasound sensor. Results also indicate that the AC signal amplitude is related to overall blood flow in the region of investigation, while blood velocity is a parameter of overall flow in one particular vessel. However, it should be noted that the AC signal amplitude captures the relative change in volumetric flow and not absolute blood flow. Absolute flow can only be determined from measurement of both the CSA of the radial artery and the relative blood velocity.

Chapter 7: Estimation of peripheral venous saturation and oxygen extraction using a novel pulse oximeter method

7.1 Introduction

The pulse oximeter is one of the most widely accepted non-invasive clinical monitoring systems. However, conventional pulse oximeters are restricted to estimation of SaO_2 only. Coupling estimation of peripheral SvO_2 with estimation of SaO_2 would enable assessment of local oxygen extraction ($\text{O}_2\text{E} = \text{SaO}_2 - \text{SvO}_2$). O_2E information could provide an indicator of the adequacy of local tissue perfusion, to aid in early diagnosis of microcirculatory dysfunction in medical conditions, such as sepsis and shock (Rivers et al., 2001; Spronk et al., 2004; Teboul and Monnet, 2015).

Venous blood in the periphery is typically non-pulsatile in nature, as discussed in Chapter 2, and thus conventional pulse oximetry cannot be used to measure SvO_2 . This chapter presents the proof of concept of a novel pulse oximeter method used for peripheral SvO_2 estimation, employing artificial respiration-like modulations to the peripheral vasculature to utilise the difference in the mechanical properties of arteries and veins. These modulations are then detected by PPG and analysed to assess regional SvO_2 . Successful estimation of SvO_2 will also enable pulse oximeter based estimation of O_2E .

7.2. Artificial venous blood modulation using the compliance difference principle

7.2.1 Arterial-venous compartment compliance difference principle

Arteries and veins have significantly different vessel wall mechanical properties. For example, the femoral artery and vein have elastic modulii of 1.05 N/m^2 and 0.5 N/m^2 , respectively (Caro et al., 2012). Venous walls are significantly thinner and less elastic than arterial walls, as shown in Figure 7.1. Arterial walls have more involuntary muscle and elastic fibers surrounded by a thicker collagen lining. In contrast, veins have a larger lumen, which allows them to hold a greater volume of blood.

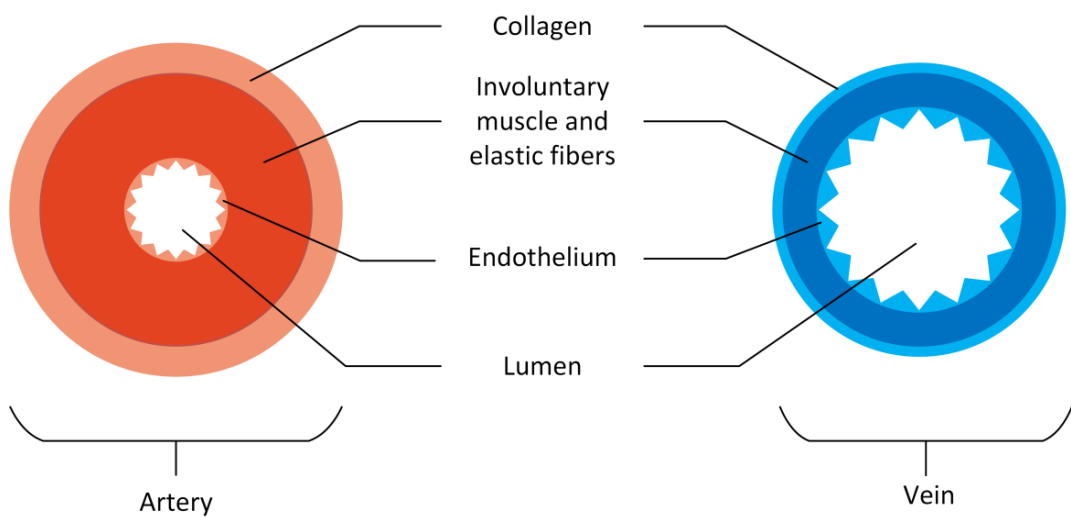


Figure 7.1: Cross section view of a typical artery and vein, depicting the difference in vessel elasticity. Adapted from: Wester et al. (2013).

Due to the significant differences in mechanical properties of the two vessels, under low pressure, the veins are up to 10 – 20 times more compliant compared to arteries (Klabunde, 2011; Caro et al., 2012; Wester et al., 2013). Vessel compliance (C) is the ability of a blood vessel to distend and increase in volume with increasing transmural pressure, as defined:

$$C = \frac{\Delta V}{\Delta P} \quad (7.1)$$

Transmural pressure (ΔP) is the pressure difference between the inside and outside of the vessel wall. With small changes in pressure, the circulating blood inside the veins thus experiences large volume changes compared to the arteries (Wardhan and Shelley, 2009; Caro et al., 2012). This large compliance difference is what causes the respiratory modulations in the venous blood seen in previous studies (Wardhan and Shelley, 2009; Caro et al., 2012), and is illustrated in Fig. 7.2.

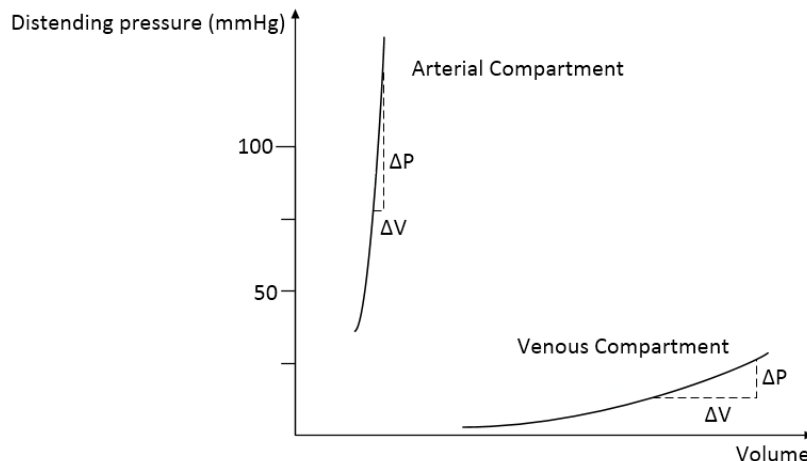


Figure 7.2: The relationship between volume and pressure within both the arterial and venous systems. Adapted from: (Wardhan and Shelley (2009); Mohrman et al. (2006); Klabunde (2011); Wester et al. (2013); Hall (2006)).

Thus, low frequency and low pressure inflation of a pneumatic cuff around a digit or limb can predominantly affect the venous blood, but not the arterial blood (Groothuis et al., 2003). In particular, a small change in cuff pressure will result in a relatively large blood volume change in the venous compartment compared to its arterial counterpart. This compliance difference can be exploited to generate a pulsatile signal in the venous system that can be detected by PPG, without disturbing arterial flow.

7.2.2 Artificial pulse generation system development

An automated artificial pulse generation (APG) system was developed to generate user-defined pulsations that can mechanically modulate blood volumes inside the finger. This system is designed to utilize the arterial-venous compliance difference to induce artificial pulsations predominantly in the venous compartment. The APG system uses a pneumatic UDC1.6 or UDC2.5 (D.E. Hokanson Inc., Bellevue, WA, USA) digit cuff to modulate venous blood inside the finger. Two sizes of cuffs were chosen for the experiment; UDC1.6 (1.6 x 9 cm) was used for small/thin fingers and UDC2.5 (2.5 x 9 cm) was used for large/thick fingers.

The digit cuff was placed at the intermediate phalanges of the middle/index finger, next to the PPG sensor as shown in Figure 7.3. The venous compartment in the periphery has series of valves which provides shielding against peak transient pressure effects (Zervides et al., 2008), and thus, can attenuate any artificial pulsations if the cuff is distant from the sensor. Hence, to provide effective and easily detectable APG pulsations the cuff was positioned close to the sensor.

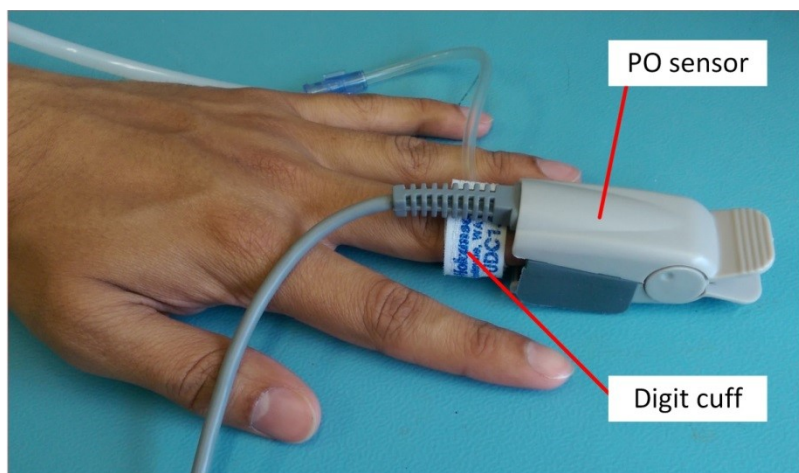


Figure 7.3: PPG sensor and digit cuff placement

7.2.3 APG pressure control and selection test

Inflation/deflation of the digit cuff was controlled by a 3-way solenoid valve (EVT 307-5DZ-02F-Q, SMC, Noblesville, IN, USA). Operation of the solenoid valve was managed by a PC running LabVIEW through a USB6009 (National Instruments, Austin, TX, USA) multifunction data acquisition device (DAQ). A signal generator was developed to generate square pulses to switch the solenoid on/off. Air was supplied to the cuff using a compressor regulated to a maximum pressure of 260 mmHg. When the solenoid valve is turned on, it opens and allows air to flow into the pressure cuff. A precision flow regulator (AS1002F, SMC, Noblesville, IN, USA) was used to control the cuff inflation pressure to a specific value, between a possible maximum range of 10–260 mmHg. For the deflation portion of the pulse, the cuff was exhausted to the atmosphere with the solenoid valve turning off.

The complete APG system is shown schematically in Figure 7.4. By periodically inflating and deflating the digit cuff, an artificial respiration-like pulse can be modulated onto the venous blood of the finger. To find the right modulation pressure, the APG was tested for cuff inflation pressures of 10 – 70 mmHg, which is below typical diastolic pressures of approximately 80 mmHg. No significant modulations in the raw PPG signals were detected for 10 – 30 mmHg. Significant PPG modulations were observed for 40 – 50 mmHg. In contrast, PPG modulations at 60 – 70 mmHg had the highest signal amplitudes. However, this highest pressure range reduced AC signal amplitude of the PPG, suggesting interference with arterial inflow. Therefore, the 40 – 50 mmHg cuff inflation pressure was chosen for this study. Being approximately 50% below typical diastolic pressures, the cuff compression pressure will be almost exclusively be felt in the venous compartment, as illustrated in Figure 7.2.

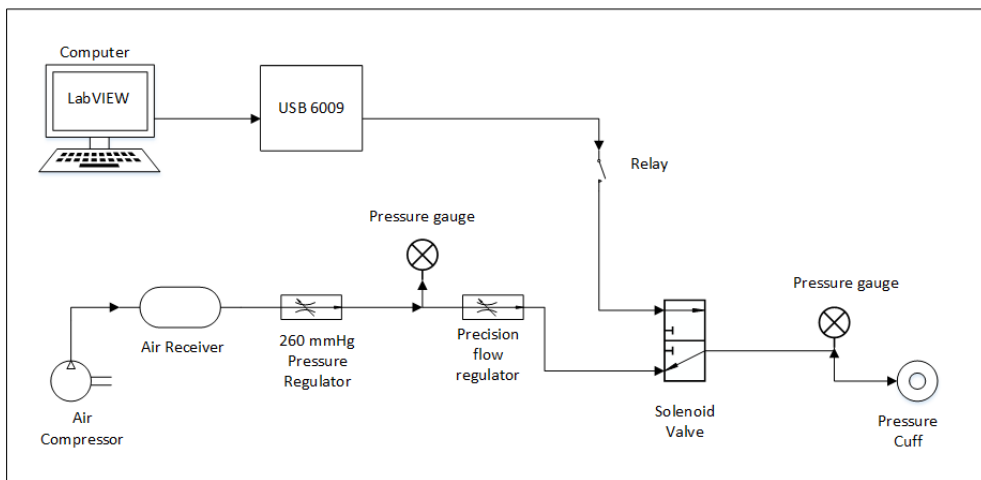


Figure 7.4: APG system functional block diagram illustrating overall operation.

7.2.4 APG frequency selection test

The APG modulation frequency was selected to be 0.2 Hz, with a 50% duty cycle. A 50% duty cycle was used to maintain the same time duration for the cuff inflation and deflation phase. The 0.2 Hz frequency is close to typical respiratory frequencies and should create artificial venous blood modulations, as previously reported by Walton et al. when detecting natural venous blood modulations in the oesophagus using PPG (Walton et al., 2010). In addition, at a 0.2 Hz APG frequency, the designed low frequency extraction filter for this study can capture up to the 2nd harmonic component of APG related frequencies, as discussed in the following sections. Finally, at such a low modulation frequency, the APG generated frequencies are significantly below cardiac frequencies and any overlap is avoided.

Additionally, arteries contain a high amount of elastin in their walls, which provides superior elastic recoil ability (Seifter et al., 2005). Thus, they can withstand higher blood pressures and high frequency pulsatile blood flow. In contrast, veins, with thinner walls and lower elastin content have much less elastic recoil capability. Therefore, high frequency modulations that are greater than

cardiac frequencies for venous blood oscillation, as previously used by Eschiadis et al. (Eschiadis et al., 2007), will not be effective since veins will require a longer recoil time. Equally, the oscillation induced pulses would overlap any mechanically induced response. Clinically, this high frequency approach may damage venous vessel walls and interfere with intravenous access (Walton, 2010).

7.2.5 GUI to operate APG

Figure 7.5 shows a LabVIEW GUI developed to control the APG system solenoid valves. The GUI allows the user to regulate the frequency and duty cycle of artificial pulse generation using graphical dials. The pulse generation system can be turned off anytime using the stop button.

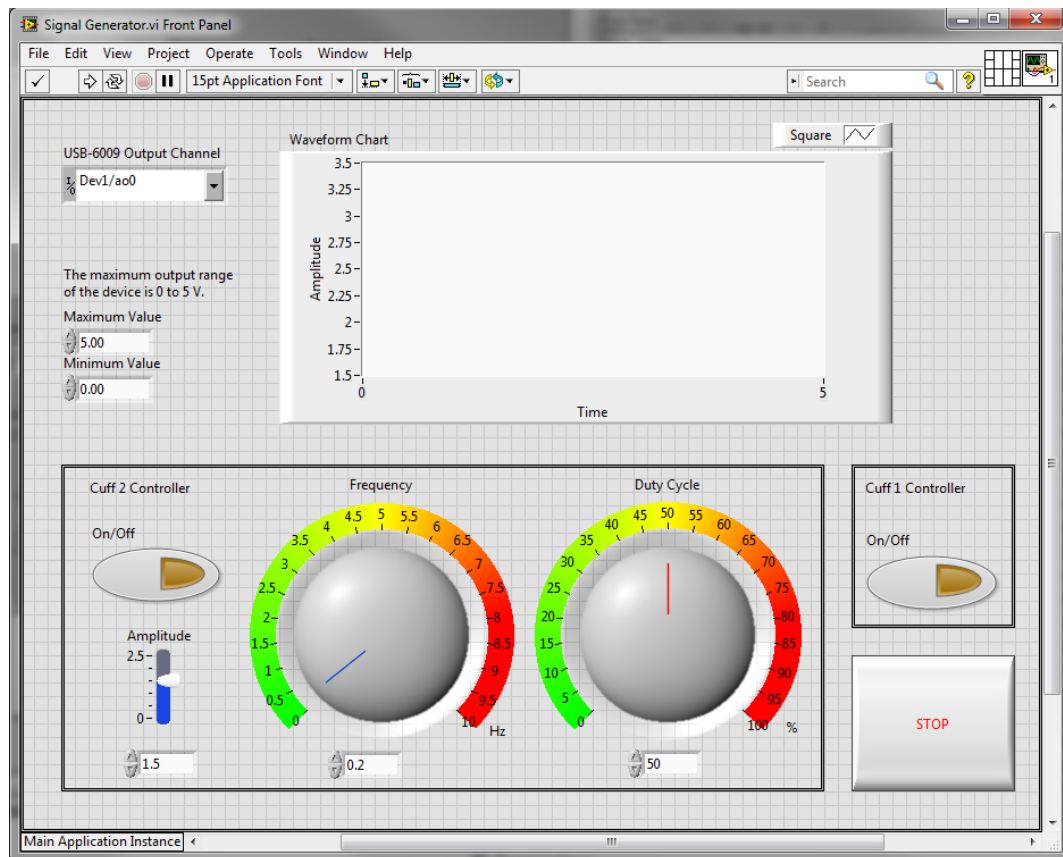


Figure 7.5: LabVIEW GUI used to control the APG system

A built-in signal generator is used to generate continuous square shaped pulses of 0.2 Hz frequency, 0° phase, amplitude of 1.5 V, offset of 2.5 V, and 50% duty cycle, with a sampling rate of 2000 Hz. Output from the signal generator is connected to the NI DAQ digital-to-analog output module. Depending on the square pulses high and low value, the DAQ module supplies an analog voltage of 3.3 V to turn the solenoid valve ON and 0 V to turn it OFF. This GUI is separate to the PPG acquisition and monitoring GUI described in Chapter 3.

7.3 Study protocol and data processing

7.3.1 Ethics approval

Ten healthy subjects were recruited for the proof of concept testing of APG induced venous blood modulation and estimation of SvO_2 from the modulated PPG. Healthy adults are easy to recruit, and are likely to demonstrate responses that can be explained when a change is induced, as part of initial testing of the concept. In contrast, critically ill-subjects can show changes that are difficult to explain, which can make complicate validation for this study.

This study and use of data were approved by the HEC, Ref: HEC 2015/04/LR-PS. A volunteer was included in the study as a subject after informed and signed consent was received. Data were de-identified and securely stored. The information sheet and consent form of this application are included in Appendix 6.1

7.3.2 Study protocol

Subjects were asked to refrain from smoking and strenuous physical activities for at least 1 hour prior to the experiment, to ensure normal cardiac function before commencing the study. During

the study, subjects rested their left hand on a flat surface, at approximately the same height as their heart, with minimal movement. Subjects were asked to breathe normally. The PO sensor was mounted on the subject's middle finger, with the digit cuff adjacent to it as shown in Figure 7.3. PPG data were logged after the PO sensor's LED intensities stabilized.

Initially, one minute of baseline PPG data under resting conditions were obtained for each subject. The APG was activated for two minutes to create modulations with a frequency of 0.2 Hz with a 50% duty cycle at 40 – 50 mmHg compression pressure. As noted earlier, this compression pressure is significantly below typical arterial diastolic pressure, and is thus expected to predominantly modulate venous blood only. As a proof-of-concept only, no blood samples were taken for a blood gas reference measure.

7.3.3 Data processing and analysis

As a result of the APG activation, the original PPG waveform contains an additional pulsatile signal, superimposed on the DC signal. The effect of introducing a pulsatile signal can be considered as an artefact introduced into the PPG signal. This low frequency artefact was spectrally extracted and analysed for SvO_2 . In this study, and throughout this thesis, estimated SaO_2 and SvO_2 using the PO system are denoted as $SpaO_2$ and $SpvO_2$, respectively.

The peak and trough detection algorithm of Section 4.3.1 was modified and applied separately to the extracted AC and DC signals for the RD and IR wavelengths. This algorithm was used to determine the amplitudes relating to each heartbeat and APG pulse as $|AC|$ and $|DC|$ components, respectively, as shown in Figure 7.6. The algorithm checks both the RD and IR for zero-crossings, and applies a windowing technique to accurately identify a complete pulse for the AC and DC

signals. Once the zero crossings are identified, the maximum and minimum between each point are determined as peaks and troughs, respectively. Amplitude is calculated as the difference between each peak and trough.

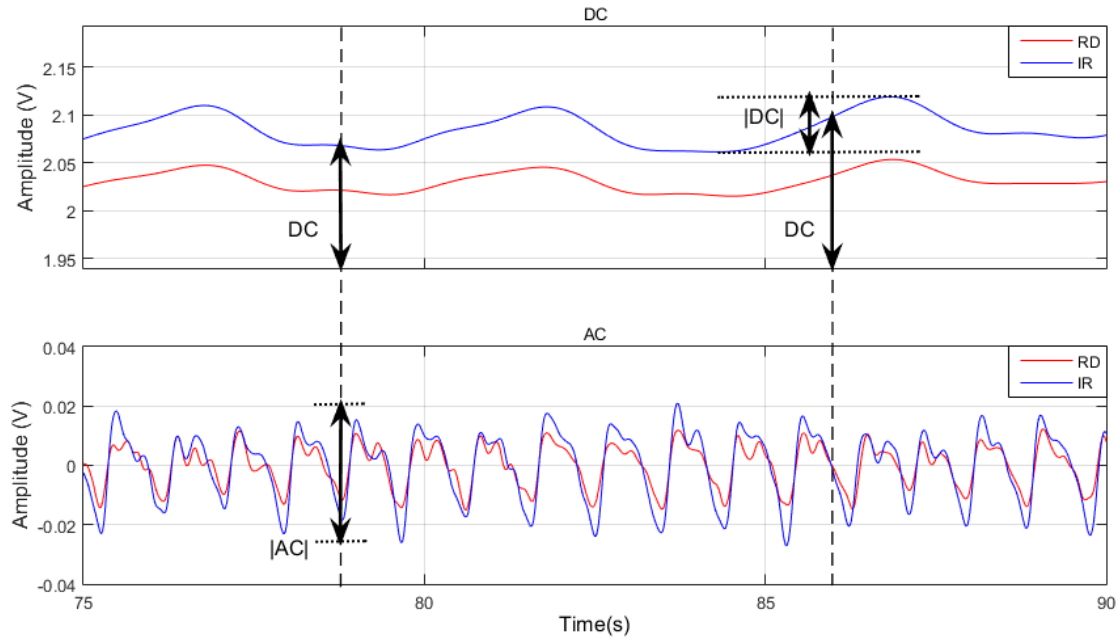


Figure 7.6: Derived components from Walton's time domain equations, in terms of the AC and DC PPG signals.

For every identified wave pulse, the algorithm considered the maximum point of the pulse window as the pulse peak, and the subsequent local maximum as the dicrotic notch peak. For the DC component, the algorithm worked similarly, except the zero-crossing threshold, was replaced by a moving average windowed threshold. Additionally, for each heartbeat and APG pulse, the corresponding mean DC value was also determined, DC_{mean} . Walton's time domain equations (Walton et al., 2010) were used to calculate the ratio of ratios (R values) relating to arterial (R_{Art}) and venous (R_{Ven}) oxygen saturations, defined:

$$R_{Art} = \frac{(|AC|/DC_{mean})_{Red}}{(|AC|/DC_{mean})_{IR}} \quad (7.2)$$

$$R_{Ven} = \frac{(|DC|/DC_{mean})_{Red}}{(|DC|/DC_{mean})_{IR}} \quad (7.3)$$

In Equation 7.2, $|AC|$ is the amplitude of individual RD and IR AC waves. Similarly, in Equation 7.3, $|DC|$ is the amplitude of individual RD and IR DC waves. For both equations, DC is the corresponding mean value from the DC signal's oscillatory cycle. Instantaneous saturation values for both R_{Art} and R_{Ven} values were calculated per Equations 7.2 and 7.3, respectively using the calibration equation described in Section 4.4.2 as follows:

$$SpaO_2 = 110 - 25 * R_{Art} \quad (7.4)$$

$$SpvO_2 = 110 - 25 * R_{Ven} \quad (7.5)$$

The median of these instantaneous saturation estimations, over a 2 min window, was calculated to estimate $SpaO_2$ and $SpvO_2$ per subject. The Wilcoxon signed rank test was used to compare paired median values of $SpaO_2$ and $SpvO_2$ for each subject, where $p < 0.05$ is considered statistically significant. Frequency domain analysis was used to confirm the presence of important frequencies in the raw PPG signals, including HR, APG related frequencies, and other known physiological harmonics or artefacts.

7.4 Results and discussion

7.4.1 Venous pulse detection

Figures 7.7 and 7.8 provide examples of the experimental results for Subjects 6 and 9. During the baseline period, the DC signal was effectively constant, while the AC signal pulsed due to the

cardiac cycle. With the introduction of the APG at approximately 60 s, the DC signal oscillates periodically, as anticipated. Due to the significant contrast in arterial-venous compliance, the low pressure and frequency modulations predominantly effect the venous compartment, with little impact on the arterial system. Thus, observed oscillations in the DC signal are primarily due to venous blood (Walton et al., 2010; Phillips et al., 2012).

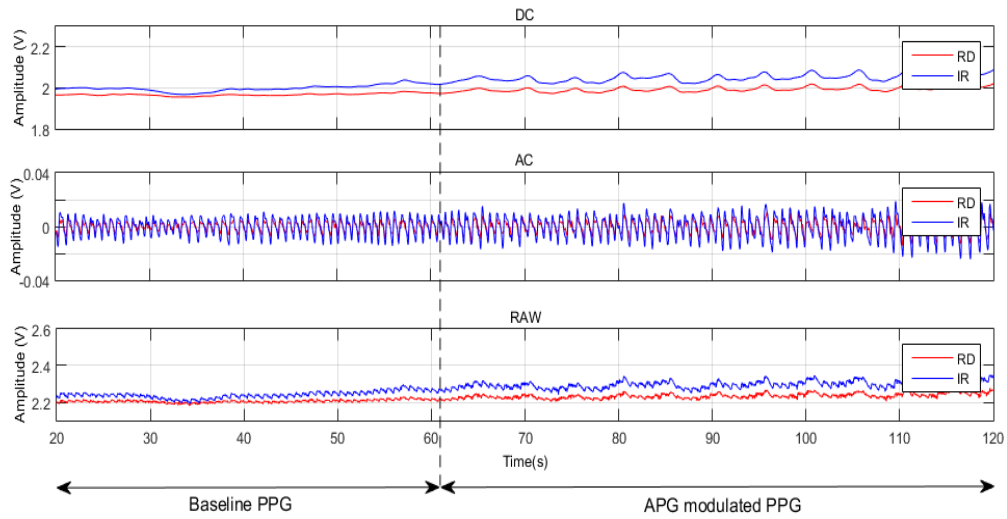


Figure 7.7: PPG signals of Subject 6: DC (top), AC (middle) and RAW (bottom) for each subject.

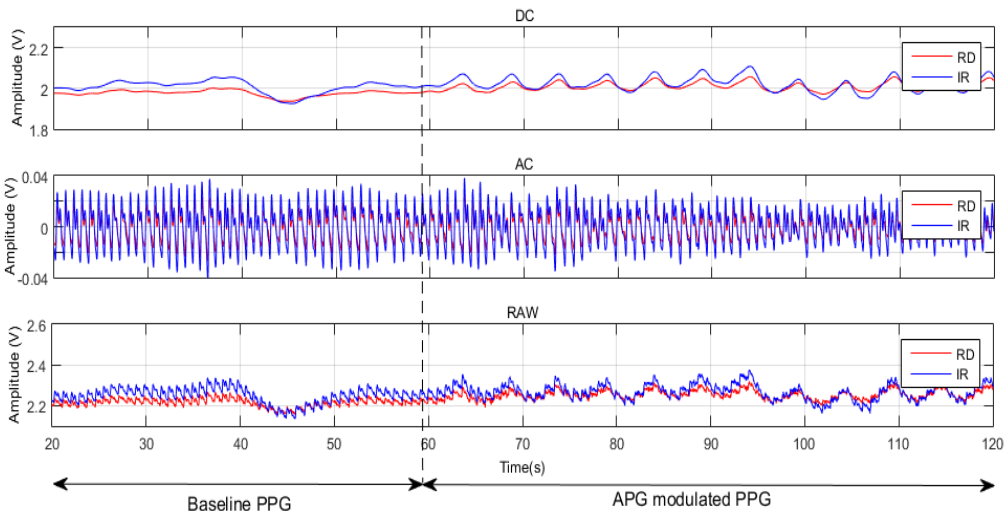


Figure 7.8: PPG signals of Subject 9: DC (top), AC (middle) and RAW (bottom) for each subject.

7.4.2 Instantaneous saturation estimation

The time course of estimated instantaneous SpaO_2 and SpvO_2 for Subjects 6 and 9 is shown in Figure 7.9. Each of these instantaneous saturation points is calculated either from one heart beat or one APG pulse during the baseline and APG modulated time periods, respectively. The number of instantaneous SaO_2 points per minute is significantly greater compared to its SvO_2 counterpart.

This discrepancy occurs because a subject's HR varies between 40 to 120 bpm under resting conditions. In contrast, the APG was controlled to provide 12 pulses per minute or at 0.2 Hz, at all times, yielding fewer pulses. The dashed line represents the median saturation value for the two subjects, as reported in Table 7.1 for the entire period.

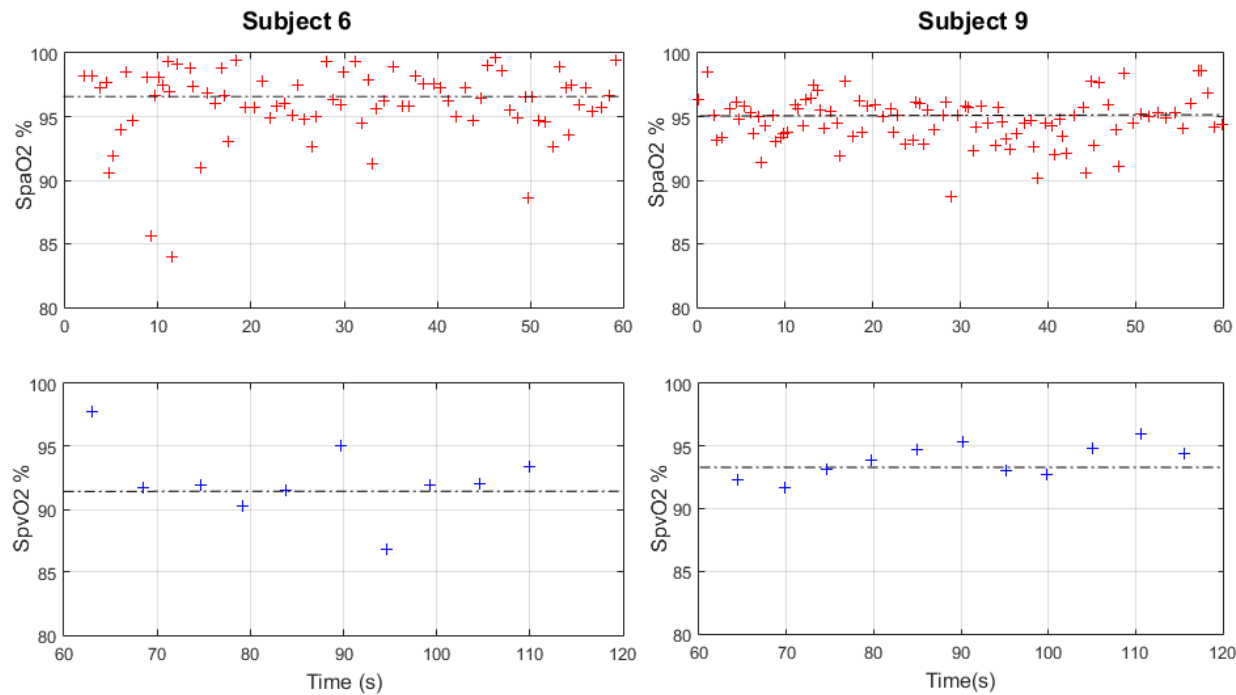


Figure 7.9: Instantaneous SaO_2 and SvO_2 calculated for Subjects 6 and 9, for an illustrative portion of the baseline and APG periods.

7.4.3 SpO_2 assessment by the two pulse oximeters

Prior to the main experiment, SaO_2 estimations were simultaneously recorded from the PO system ($SpaO_2$) and a commercial pulse oximeter (SpO_2) for comparison. The two pulse oximeters showed very good agreement, with a median SpO_2 difference of approximately 1% between pairs of measurements. In addition, these arterial saturation estimations fall in the expected SaO_2 range (95 – 100%) for human adults (Williams, 1998; Crapo et al., 1999). It should be noted that the PO system estimates oxygen saturations using published equations, while the NPB-75 have built in calibration equation for such estimations. In addition, the custom pulse oximeter provides a higher resolution than the commercial one. Thus, reducing the resolution will also reduce the difference in saturation measurements.

Table 7.1: Subject demographics and SaO_2 estimation comparison by two pulse oximeters

Subject	Gender	Age	1SpO_2	2SpaO_2	ΔSpO_2
1	M	25	98	96.6	1.4
2	M	35	97	96.4	0.6
3	M	30	100	98.7	1.3
4	M	21	98	97.1	0.9
5	F	22	98	97.3	0.7
6	F	21	98	96.3	1.7
7	F	23	97	96.9	0.1
8	M	21	99	98.1	0.9
9	M	26	97	95.9	1.1
10	M	22	98	97.5	0.5
Median		22.5	98	97	0.9
IQR[25th-75th]		21 - 26	97 - 98	96.4 - 97.5	0.6 - 1.3

1SpO_2 refers to the Nellcor NPB-75 estimated arterial saturation readings

2SpaO_2 refers to the custom pulse oximeter estimated arterial saturation readings

7.4.4 Main Outcome

Individual data for all the subjects are presented in Table 7.2. Median $SpaO_2$ closely matches published data in the typical SaO_2 range of 95 – 99% (Valdez-Lowe et al., 2009; Nitzan et al.,

2014b; Crapo et al., 1999). Median SpvO₂ agrees with reported SvO₂ ranges of 92% – 95% measured in peripheral regions (Phillips et al., 2012; Shafqat et al., 2012). The median difference between the two saturations was 3.8%, while the difference between pairs of measurements in each subject was statistically significant ($p = 0.002$), and always reported SpvO₂ < SpaO₂, as expected, but not seen in the study by Phillips et al. (2012).

As a result, estimated O₂E was found to be just under 4%. The reason for the small O₂E is that fingers do not contain large quantities of skeletal muscle or other highly metabolic tissues. Therefore, tissue oxygen absorption in fingers is relatively low compared to tissues in organs, such as the liver or brain, where difference SaO₂ and SvO₂ may be up to 30% (Bloos and Reinhart, 2005; Zaja, 2007).

Table 7.2: Subject estimated saturation values from the experiment

Subject	SpaO ₂ (%)	SpvO ₂ (%)	O ₂ E (%)
1	96	90.2	5.8
2	97.6	92.9	4.7
3	98.3	94.7	3.6
4	97.1	93.9	3.2
5	97.4	94.3	3.1
6	96.8	91.9	4.9
7	96.7	93.1	3.6
8	97.4	91.1	6.3
9	95.1	93.9	1.2
10	96.1	93.2	2.9
Median	96.95	93.15	3.6
IQR[25th-75th]	96.1 - 97.4	91.1 - 93.9	3.1 - 4.9

Figure 7.10 shows the frequency domain power spectrum of the PPG data from Subject 4 during APG, as an example. All the key frequencies expected in this study are present. In particular, the APG modulation frequency in the DC signal was verified using amplitude spectrum plots. Cardiac

and other harmonic frequencies could also be clearly identified from these plots, as shown. The cardiac pulses are greatly attenuated by the time they get detected by the PO sensor, and thus have much lower magnitude compared to the APG pulses, which are generated closer to the sensor.

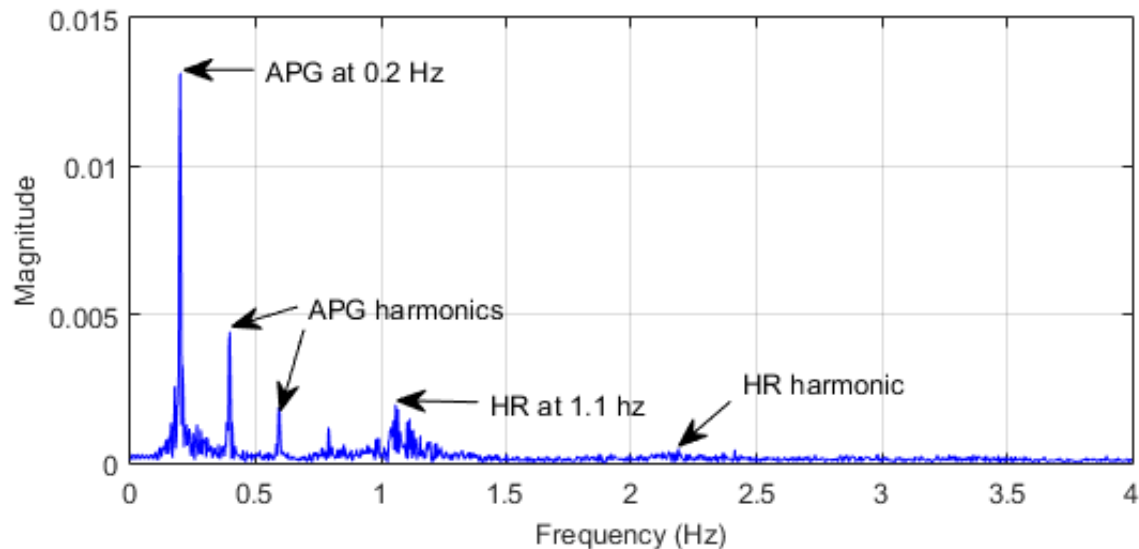


Figure 7.10: Power spectrum of IR PPG signal for Subject 4, with labelled harmonics.

7.4.5 Limitations and future work

The primary limitation of this concept was that the results obtained need to be validated by obtaining reference SaO_2 and SvO_2 measurements via blood gas analysis. Given this proof of concept, prospective trials were planned to perform this validation in a further study, which is presented in Chapter 8. The results from this study justify a more in depth analysis including gold standard blood comparators.

7.5 Summary

This chapter successfully demonstrated an APG system that can be utilized to induce blood volume changes predominantly in the peripheral venous system. Modulation of venous blood is evident from periodic oscillations observed in the DC portion of the PPG signal. The artificially generated pulses in PPG signal can be analysed to estimate local venous saturation. This novel pulse oximeter concept allows reliable, repeatable modulation of venous blood that can be detected by the PPG signal for estimation of SvO_2 , and thus O_2E .

Estimated saturation values lie within the published range of values in the referenced literatures. The median difference in saturations, or O_2E , showed a statistically significant and expected difference ($p = 0.002$) between pairs of measurements in each subject. In addition, the whole system was relatively cost effective, approx. NZ\$ 1000, and easy to implement. The outcomes from this study justify clinical validation trial with whole blood data when assessing SvO_2 and O_2E under normal, low, and no perfusion scenarios. Chapter 8 presents the application of this novel concept in a clinical environment and the clinical validation using blood gas comparators.

Chapter 8: Clinical validation trial of a novel pulse oximeter concept for non-invasive estimation of peripheral venous saturation

8.1 Introduction

SaO_2 and SvO_2 are the basic parameters to assess oxygen delivery process and monitor oxygen consumption, and are integral to the analysis of whole body oxygen circulation. Thus, continuous or semi-continuous measurements of SvO_2 would be useful in hemodynamic and perfusion monitoring in clinical settings according to recent clinical consensus statements (Cecconi et al., 2014). Currently, no commercial equipment provides continuous, non-invasive measurement of SvO_2 . In addition, there are no existing or widely used empirical calibration models to estimate peripheral SvO_2 using the modulation ratio, R values, derived from PPG signals.

This chapter introduces the clinical validation study, the “Monitoring O₂ Saturation for Extraction: The MOOSE Study” (MOOSE) trial, for the novel pulse oximeter concept discussed in Chapter 7. In this study, the correlation between R values derived from APG pulsed venous blood, R_{ven} , and blood gas analyzer measured SvO_2 in the periphery is investigated. In addition, the difference in optical absorption of venous blood compared to arterial blood is also explored. The main outcome of this study should offer a novel, initially validated SvO_2 estimation model and sensor using non-invasive pulse oximetry.

8.1.1 MOOSE trial Background

One of the main goals of the MOOSE study was to develop a calibration model from the correlation between calculated R_{Ven} and measured SvO_2 to estimate $SpvO_2$. To develop a robust calibration model, a wide range of SvO_2 measurements are required. Hence, another important objective of this study was to develop an experimental protocol to induce significant, physiologically realistic changes in SvO_2 levels that could provide high and low saturated samples to ensure a robust model and validation.

Several improvements to the existing APG system were made to meet the goals of this study. These improvements include the implementation of a digital pressure control system and an APG signal extraction digital filter. In addition, a commercial blood gas analyzer and a patient monitor were employed to supply a gold standard blood gas analysis comparator and to monitor cardiac activity, respectively. Finally, several techniques were investigated to induce consistent, realistic drops in peripheral SvO_2 that could be easily measured by the existing PO system. This chapter presents all the equipment, ethics application, methods, and resulting model and validation trial results from the MOOSE study.

8.2 Improvements to the APG system and PPG processing

Several key modifications were made to the APG system to improve cuff pressure control and make the whole system more robust. The manual-tap flow regulator used to control the APG cuff inflation pressure in Chapter 7 is difficult to operate and struggles to precisely maintain a constant pressure. In a clinical setting and for this validation trial, a more robust, reliable, and easy to operate pressure control system is needed. As a result, the manual-tap flow regulator was replaced

by an ITV001 (SMC, Noblesville, IN, USA) electro-pneumatic regulator. This digital regulator can be controlled using a voltage signal and also provides a feedback signal to monitor the supplied pressure. In addition, the LabVIEW pressure control interface in Section 7.3.5 was modified to allow operation of the ITV001. Finally, a second ITV001 was also installed in case the primary one malfunctions.

8.2.1 Pressure regulation with ITV001

The ITV001 can provide continuous control of air pressure proportional to an electrical signal. This digital regulator can provide a set pressure from a minimum of approximately 7.5 mmHg up to a maximum of approximately 750 mmHg. A minimum supply pressure of 1500 mmHg, and supply voltage of 24 V is required to operate the ITV001. Figure 8.1 shows a block diagram illustrating ITV001 operation.

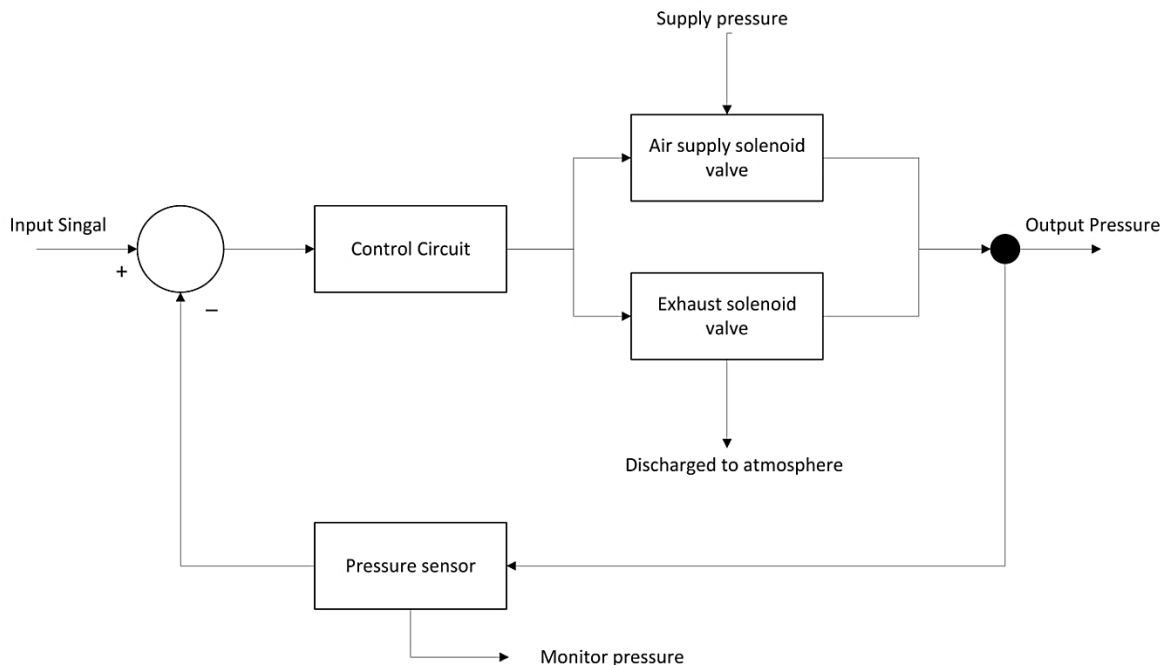


Figure 8.1: Block diagram of the ITV001 pressure regulator working principle.

An increase in the input signal turns ON the air supply solenoid valve. This activation allows part of the supplied pressure to pass through the air supply solenoid valve and change the output pressure. The output pressure provides a feedback signal to the control circuit through the pressure sensor. Pressure corrections are performed in the control circuit until the output pressure becomes proportional to the input signal, enabling output pressure to be proportional to the input signal. During such corrections, excess air is released to the atmosphere via an exhaust solenoid valve.

8.2.2 Pressure regulation interface

Figure 8.2 shows the updated pressure control GUI. The regulators are controlled by a dial which provides a proportional voltage signal using the NI DAQ. When the dial is set to zero, no voltage signal is generated and keeps the regulator off. In particular, a voltage of 0.55 V sets the pressure output by the regulator to approximately 40 mmHg. A chart was also designed to assist in pressure regulation, which displays the pressure values equivalent to the output voltage values.

Output pressure from the digital regulator can be monitored by the pressure gauges shown in Figure 8.2. The IV001 has a pressure sensor output channel which is connected to the DAQ. Output voltage signal from the pressure sensor is converted to equivalent pressure via linear calibration, using the data provided in the ITV001 manufacturer's catalog (Daly and Leahy, 2013). The converted pressure value is displayed in MPa by the pressure gauges.

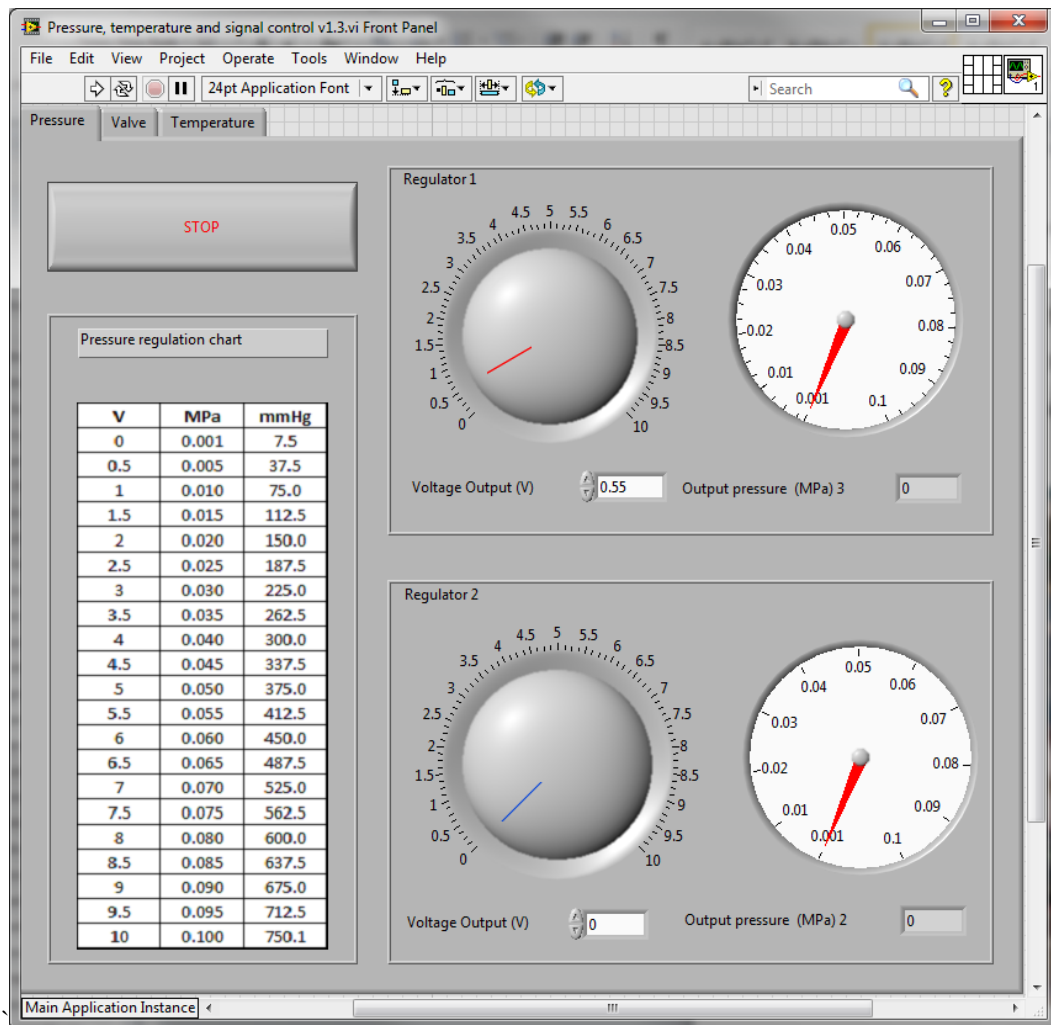


Figure 8.2: LabVIEW based APG pressure control GUI.

8.2.3 Additional filter to extract APG signals

Parallel to the Stage 2 filter configuration described in Section 4.2, an additional bandpass filter was implemented to extract APG related frequencies in the range of 0.15 – 0.67 Hz, from the Stage 1 filtered PPG signal. A 12th order IIR Butterworth design was used to develop this filter. The high order of 12 was used to provide a steeper roll-off slope at cut-off frequency.

This new filter results in <2% loss of the input PPG_{DC} signal amplitude in terms of the attenuation provided. The filter output signal is thus eligible for analysis. Similar to the other implemented filters, zero phase filtering is used to avoid any phase distortion. The output signal from this new filter is treated as the APG signal.

8.3 Ethics approval and study cohort

8.3.1 HDEC ethics approval

The MOOSE trial required blood draws in a clinical environment by registered clinicians and nurses. In this study, the main ethical issues concerned the very low risk of injury from an arterial catheter and venepuncture. All invasive procedures were conducted by the coordinating investigator, Prof G Shaw, who has 29 years of experience as a medical practitioner and over 20 years as an Intensive Care Specialist. The study was approved by the NZ HDEC (Reference: 15/CEN/141) under the project title “The MOOSE study”. All documents related to this ethics approval application, including information sheet and consent form, are included in Appendix 8.2.

8.3.2 Study cohort

The MOOSE study was conducted in the ICU of St George’s Hospital, Christchurch. Eight healthy adult, male, volunteers (aged 23 – 37 years) with no pre-existing medical conditions were recruited for this study. Volunteers were only included as a subject in the study after receiving signed, informed consent. Subject specific data were de-identified and securely stored in a private computer. Healthy adults volunteers are easy to recruit, and are likely to demonstrate understandable responses when a change is induced. In contrast, critically ill-subjects can show changes that are difficult to explain, which can make complicate this validation study.

Subjects were asked to refrain from smoking and strenuous physical activities for at least 4 hours prior to the experiment. This long resting time is necessary to ensure the subjects are well rested and have normal cardiac activity prior to the study. During the study, subjects were comfortably seated, while resting their left arm on a flat surface at approximately the same height as their heart and with minimum movement. Subjects were advised to breathe normally for the duration of the experiment.

8.4 Methodology, trial protocol and modifications

8.4.1 Additional equipment employed

In addition to the PO system and equipment used for the proof-of-concept testing in Chapter 7, several other devices were employed as part of the trial study:

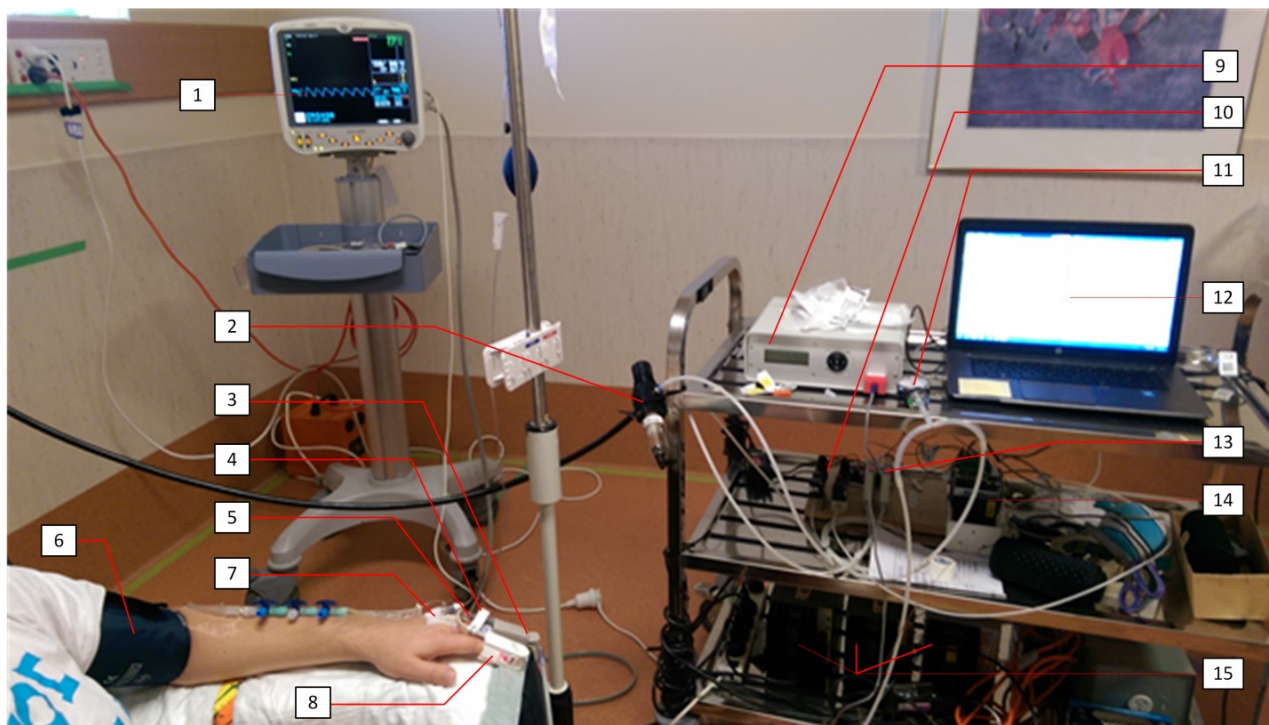
- A portable i-Stat1 blood gas analyzer (Abbott, Princeton, NJ, USA).
- A Masimo SET (Masimo Corporation, Irvine, CA, USA) pulse oximeter sensor to continuously monitor SpO₂, HR, and arterial blood flow for comparison. It also provides a clinically used reference measurement for comparison, in addition to blood gas measurements.
- A portable DASH 5000 (GE Healthcare, Chicago, Illinois, USA) monitoring screen to monitor the Masimo SET sensor output (SpO₂ and HR), and other physiological parameters, such as the arterial pressure waveform from the installed arterial line.
- A conventional blood pressure cuff to conduct vascular occlusion tests as part of the experimental protocol.
- Consumables involved in drawing of blood samples and subject wellbeing, such as arterial and intravenous (IV) catheters, local anaesthetic, and bandages.

8.4.2 Study set up procedure

The following experimental set up procedure was followed:

1. A radial arterial catheter was inserted in the left arm wrist to draw blood samples.
 - a. The catheter (20g or 22g) was inserted under sterile conditions using a small amount (0.2ml) of subcutaneous local anaesthetic (lidocaine 1%).
 - b. The catheter was connected to an ‘intraflow’ device, which delivered about 3 ml per hour of 0.9% saline through the arterial catheter.
2. An IV catheter was inserted in a vein on the back of the hand to draw blood samples.
 - a. The catheter (20g or 22g) was inserted under sterile conditions using a small amount (0.2ml) of subcutaneous local anaesthetic (lidocaine 1%).
 - b. The catheter was connected to an ‘intraflow’ device, which delivered about 3 ml per hour of 0.9% saline through the IV catheter.
3. It was sometimes necessary to repeat some (or all) steps of the procedure if there were any unforeseen technical problems.
 - a. No more than two attempts were made to place the arterial catheter and no more than three attempts for the venous catheter.
4. The PO sensor was clipped to the index/middle finger of the left hand.
5. The Masimo SET pulse oximeter sensor was clipped to the ring of the left hand.
6. A non-invasive, surface mounted, thermocouple was attached next to the PO sensor to continuously monitor digit skin temperature.
7. The pressure cuff was wrapped around the participant’s left forearm to make blood pressure measurements and perform VOT, according to the experimental protocol.

The MOOSE study equipment and set up are labelled in Figure 8.3.



- | | | |
|-------------------------------|-----------------------------|------------------------|
| 1. Dash monitoring screen | 2. Air supply and regulator | 3. PO sensor |
| 4. Thermocouple sensor | 5. Digit pressure cuff | 6. Blood pressure cuff |
| 7. Venous line and catheter | 8. Masimo SET sensor | 9. PO system |
| 10. Solenoid valves | 11. Pressure gauge | 12. PC running LABVIEW |
| 13. ITV001 pressure regulator | 14. NI DAQ system | 15. Power supplies |

Figure 8.3: Typical equipment set up for the MOOSE study. All components are individually labelled.

8.4.3 Experimental protocol

1. At the beginning of the MOOSE study, resting HR and blood pressure of the participants were recorded to ensure they were fit (<80 bpm, approximately 120/80 mmHg blood pressure). In addition, their height, weight, and body temperature were also recorded. Two minutes of baseline PPG data were recorded without any APG activation.
2. The participants were asked to perform the following tests as part of the study protocol:
 - a. Test 1: Hold their left arm at chest level, referred to as baseline.

- b. Test 2: Raise their left arm above the head for 4 min.
 - c. Test 3: Raise their left arm above the head, then exercise the left hand by clenching and releasing a stress ball/toy, periodically, for 4 min until the arm feels tired.
 - d. Test 4: Allow pressure cuff induced vascular occlusions for 4 – 6 min using pressures of 170 mmHg, which are above typical systolic pressures to block all flow to the hand.
3. Blood was drawn during each test as follows:
 - a. Test 1: 1x arterial sample, 1x venous sample after 1 min of APG activation.
 - b. Test 2: 1x arterial sample (Subjects 1 – 5 only) and 1x venous sample at 2 min into the test.
 - c. Test 3: 1x arterial sample (Subjects 1 – 5 only) and 1x venous sample, at 2 min into the test after the exercise was complete.
 - d. Test 4: 1x venous sample immediately before the pressure cuff was released, and 1x venous sample at 30 s into post occlusion.

It should be noted, only 1x arterial sample was drawn as a reference sample for Subjects 6 – 8, as explained in Section 8.4.4. In general, up to a total of 8 blood samples were drawn from each participant. Each blood sample was approximately 2 ml and maximal total blood volume approximately 16 ml. The catheters were flushed with 0.9% saline (1 – 3 ml) after each blood draw.

4. APG was turned on part way through each test to enable SvO_2 assessment until the test ended at the following times:
 - a. Test 1: Turned on after 2 min.
 - b. Test 2: Turned on after 1 min.
 - c. Test 3: Turned on immediately after exercise was complete.

- d. Test 4: Turned on 5 s before pressure cuff release.

The APG was turned off between test intervals.

- 5. The whole study protocol took up to 1 hour to complete.
 - a. Each test lasted for 8 – 10 min.
 - b. A break of 3 min was given between each test for the subject to adjust to the test condition.
 - c. Participants were not asked to complete more than 2x per protocol.

Figure 8.4 shows an example of a venous sample being drawn by clinicians during the study.



Figure 8.4: Clinicians drawing venous blood sample from the peripheral vein of a subject via the venous line IV catheter.

Tests 2 and 3 were investigated for Subjects 1 – 5 only to detect any change in SvO_2 using the PO sensor and APG system. When the arm was raised above heart level, the mean arterial blood pressure and flow is reduced, and thus a drop in SvO_2 can occur. In addition, when the hand is exercised with the arm raised above the heart, the local tissue demand for oxygen is increased. Thus, a significant drop in SvO_2 is expected during Test 3 due to increased extraction of oxygen. Figure 8.5 shows an example of a subject taking part in Test 3, squeezing a stress ball with the hand as exercise until fatigue. All attached sensors needed to be temporarily removed during the protocol manoeuvre to effectively work out the local hand muscles.

Test 3 was not performed with the hand in horizontal position, at chest level, since it will not reduce peripheral arterial flow and pressure. If the arm is exercised at this position to increase tissue O_2E , arterial blood flow can naturally increase to meet this demand. Thus, a significant change in peripheral SvO_2 levels is unlikely to be obtained.



Figure 8.5: A subject exercising the hand using a squishable toy during Test 3.

In contrast to Tests 2 and 3, Test 4 was developed later and applied for Subjects 5 – 8 only. This test was conducted as an alternate technique to cause a more repeatable and more easily induced significant drop in SvO_2 , induced by several minutes of ischemia. It should be noted that Test 4 was repeated for Subjects 6 – 8 for 4 and 6 min of vascular occlusions, in contrast to Subject 5 who was only tested for 4 min of occlusion. Section 8.4.4 explains in details for these changes in the study protocol.

8.4.4 Problems encountered and changes in study procedure

During the first 5 trials, the study protocol was refined with experience to make it more feasible and robust. These amendments include obtaining only 1x arterial sample as a reference SaO_2 and the exclusion of Test 2 and 3 in favor of the more repeatable and robust Test 4 for Subjects 5 – 8.

The ethics application was updated accordingly to inform HDEC about these changes in the study protocol, and these changes were accepted.

SaO₂ is a global parameter, and is highly unlikely to vary with any change in local conditions for a healthy adult. For Subjects 1 – 5, SaO₂ measurements shown to not vary by more than ±1.02% of the baseline measurements (Test 1) for any tests. Therefore, a one off arterial blood sample was drawn during Test 1 as a reference SaO₂ measurement for Subjects 6 – 8. Equally, this change meant no arterial line was used for subjects 6 – 8, reducing risk, cost, and burden. As a result, since continuous monitoring of the arterial pressure waveform was not of interest to this study and was also deemed unnecessary due to removal of the arterial line, this data was no longer collected.

Test 3 was very difficult to execute and maintain consistency, due to the exercise phase involved. During the hand exercise phase, as shown in Figure 8.5, all the sensors had to be removed to allow exercising of the hand and avoid capturing noisy data due to excessive motion artefacts. To draw blood samples, the arm had to be brought down to chest level. When the arm is above the chest, a drop in arterial blood flow occurs, which is accompanied by reduction in venous blood capacitance and volume change, since venous blood pressure is much lower (10 mmHg) compared to arterial blood pressures (e.g. 120/80 mmHg). In addition, the APG system did not function effectively with less venous blood volume change, making it a less robust test to assess the ability to measure large SvO₂ changes.

Finally, a delay of approximately 20 s occurred from having to connect and re-adjust all the sensors when the hand was repositioned to chest level. This process results in loss of valuable

transient physiological data, as reflex mechanisms react quickly in healthy subjects. In particular, a 20 s delay was long enough for local SvO_2 to return to normal levels, and thus the PO sensor could not detect any significant change in SvO_2 . As a result of this experience, Test 3 was not continued due to this lack of robustness in implementation. Hence, data from this test were excluded from any analysis, and are not presented.

8.5 Data processing and Analysis

8.5.1 Data processing

All PPG data were processed and digitally filtered in MATLAB to extract high and low frequency signals from the PPG, as discussed in Chapter 7. However, peak and trough detection algorithms (Section 4.3) were not used to determine amplitude information due to the complexity and reliability of its application. Thus, an FFT based frequency domain analysis was used to determine parameters for R value estimation from both high (AC) and low (APG) frequency signals:

$$R_{Art} = \frac{(|AC|_{HR}/|DC|_{0\ Hz})_{RD}}{(|AC|_{HR}/|DC|_{0\ Hz})_{IR}} \quad (8.1)$$

$$R_{Ven} = \frac{(|APG|_{0.2\ Hz}/|DC|_{0\ Hz})_{RD}}{(|APG|_{0.2\ Hz}/|DC|_{0\ Hz})_{IR}} \quad (8.2)$$

Where,

- $|AC|_{HR}$ is the peak magnitude at HR frequency of the AC signal
- $|APG|_{0.2\ Hz}$ is the peak magnitude at 0.2 Hz of the APG signal
- $|DC|_{0\ Hz}$ is the peak magnitude at 0 Hz frequency of the DC signal

This choice of analysis is a more robust way to compute R_{Art} and R_{Ven} related to the estimation of $SpaO_2$ and $SpvO_2$, respectively, since the driving frequency and their magnitudes can be easily

identified from the frequency power spectrum. The fundamental frequency, which is associated with the peak magnitude, was identified from the frequency power spectrums of AC, APG and DC offset signals and substituted into Equations 8.1 and 8.2 to compute the R_{Art} and R_{Ven} . In addition, the FFT analysis was implemented on PPG data blocks of 20 s, using this selection criterion of 1000 samples at a frequency resolution of 0.025 Hz, corresponding to the blood sampling time for each test. The reason for this time window selection is to efficiently capture and analyse the transient effects in Test 4, as explained later in Section 8.6.3, and to be consistent with all the other activities.

8.5.2 Statistical analysis

A linear model was fitted across the calculated R_{Ven} and measured SvO_2 , and the coefficient of determination was computed to assess the strength of their correlation. The linear model was then used as the calibration curve to estimate $SpvO_2$ for each R_{Ven} . The Wilcoxon signed rank test was used to compare paired median values of measurements, including R_{Ven} and R_{Art} for each subject, over the experimental cohort. P -values of $p < 0.05$ were considered statistically significant.

8.5.3 Error propagation analysis

Every measurement result is associated with an independent amount of error or uncertainty (δ) (Taylor and Kuyatt, 1994). Thus, a comprehensive error propagation analysis was implemented to calculate uncertainties for measured SvO_2 (δSvO_2) and R_{Ven} (δR_{Ven}). The clinical data defined in the Abbott i-Stat1 device manual (Abbott, 2013) were used to calculate δSvO_2 . For this blood gas analyzer, oxygen saturation (SO_2) is calculated based on direct measurements of partial

pressure of oxygen (PaO_2) and acidity (pH), and estimated bicarbonate (HCO_3) values in blood as follows:

$$\text{SO}_2 = \frac{(X^3 + 150X)}{X^3 + 150X + 23400} \times 100 \quad (8.3)$$

$$X = \text{PO}_2 \times 10^{(0.48(\text{pH}-7.4)-0.0013(\text{HCO}_3-25))} \quad (8.4)$$

SO_2 being a calculated parameter does not have a specified uncertainty. In contrast, PO_2 and pH are measured parameters and have specified measurement uncertainties of $\pm 3.12\%$ and $\pm 0.005\%$, respectively, at temperatures of 37°C (Abbott, 2013). Both of these parameters are temperature dependent. For healthy adults, the temperature of blood is typically stable at approximately 37°C . Thus, the manufacturer specified uncertainties for PO_2 and pH were used to calculate the uncertainty SO_2 in this study. However, HCO_3 being an estimated parameter does not have a specified uncertainty, but is dependent on the measured partial pressure of carbon dioxide (PCO_2) and pH:

$$\log \text{HCO}_3 = \text{pH} + \log \text{PCO}_2 - 7.68 \quad (8.5)$$

Manipulating Equation 8.5 for HCO_3 gives:

$$\text{HCO}_3 = \text{PCO}_2 \times 10^{(\text{pH}-7.608)} \quad (8.6)$$

Since the uncertainty of pH is very small, its effect on the uncertainties of HCO₃ and SO₂ can be assumed to be negligible. In addition, PCO₂ has a specific uncertainty of ±1.57% at a blood temperature of 37°C. Thus, the uncertainty of PCO₂ and the mean value of pH = 7.165 (Abbott, 2013) were used to estimate the uncertainty of HCO₃ using error propagations for linear combinations as follows (Starr and Saito, 2014):

$$\delta HCO_3 = \delta PCO_2 \times 10^{(pH - 7.608)} \quad (8.7)$$

$$\delta HCO_3 = 1.57 \times 10^{(7.165 - 7.608)} = 0.566\%$$

The uncertainties of PO₂ and HCO₃ in addition to the mean values of PO₂ (65.1 mmHg), pH (7.165), and HCO₃ (23 mmol/L) were then applied to Equation 8.4 to determine the uncertainty in X using error propagation of non-linear combinations (Starr and Saito, 2014):

$$\delta X = \delta PO_2 \times 10^{0.48(pH - 7.4) - 0.0013(HCO_3 - 25)} \quad (8.8)$$

Calculating the partial derivatives of δX:

$$\frac{dX}{dPO_2} = 10^{0.48(7.165 - 7.4) - 0.0013(23 - 25)} = 0.776 \quad (8.9)$$

$$\frac{dX}{dHCO_3} = 65.1 \times \frac{1}{(0.48(7.165 - 7.4) - 0.0013(23 - 25))ln10} = -256.557 \quad (8.10)$$

Substituting Equations 8.9 and 8.10 into Equation 8.8 gives:

$$\delta X = \sqrt{\left(\frac{dX}{dPO_2}\right)^2 \times (PO_2)^2 + \left(\frac{dX}{dHCO_3}\right)^2 \times (HCO_3)^2} \quad (8.11)$$

$$\delta X = \sqrt{(0.776^2 \times 3.12^2 + (-256.557)^2 \times (0.566)^2)} = 145.231$$

Finally, δX and the calculated mean values for X (50.51) and SO₂ (85.36%) were applied to Equation 8.3 to yield δSO_2 using error propagation of linear combinations:

$$\delta SO_2 = 100 * \frac{3 \times \frac{145.231}{50.51} \times 85.36 + 1500}{3 \times \frac{145.231}{50.51} \times 85.36 + 150 \times 145.231 + 23400} \quad (8.12)$$

$$\delta SO_2 = 4.87\%$$

The uncertainty for SO₂ was thus calculated $\pm 4.87\%$. Hence, $\delta SvO_2 = \delta SO_2$.

The uncertainty of the PO sensor for SpO₂ measurement is $\pm 2\%$ (Batchelder and Raley, 2007; Fouzas et al., 2011), which is the typical error of measurement for pulse oximeters. Error propagation analysis of linear combinations was applied to the empirical calibration equation used to determine SpO₂ (Equation 7.4), and thus calculate δR :

$$\delta R = \frac{110}{25} - \frac{1}{25} \times \delta SpO_2 \quad (8.13)$$

$$\delta R = 4.4 - 0.04 \times 0.02 = 4.40\%$$

The uncertainty for the resulting modulation ratio R is thus estimated to be $\pm 4.40\%$. Hence, $\delta R_{\text{Ven}} = \delta R$.

8.6 Results

8.6.1 Detection of AC and APG signals from PPG

Figure 8.6 shows an example of post processed PPG signals detected by the PO sensor, in the time domain, during the baseline phase of the experimental protocol or Test 1. During the first 120 s of Test 1, the APG signal was effectively constant since the APG system was not activated, while the AC signal pulsed due to the cardiac cycle. Upon activation of the APG system at approximately 130 s, the APG signal showed a period oscillation with an amplitude of up to 0.6 mV, as desired.

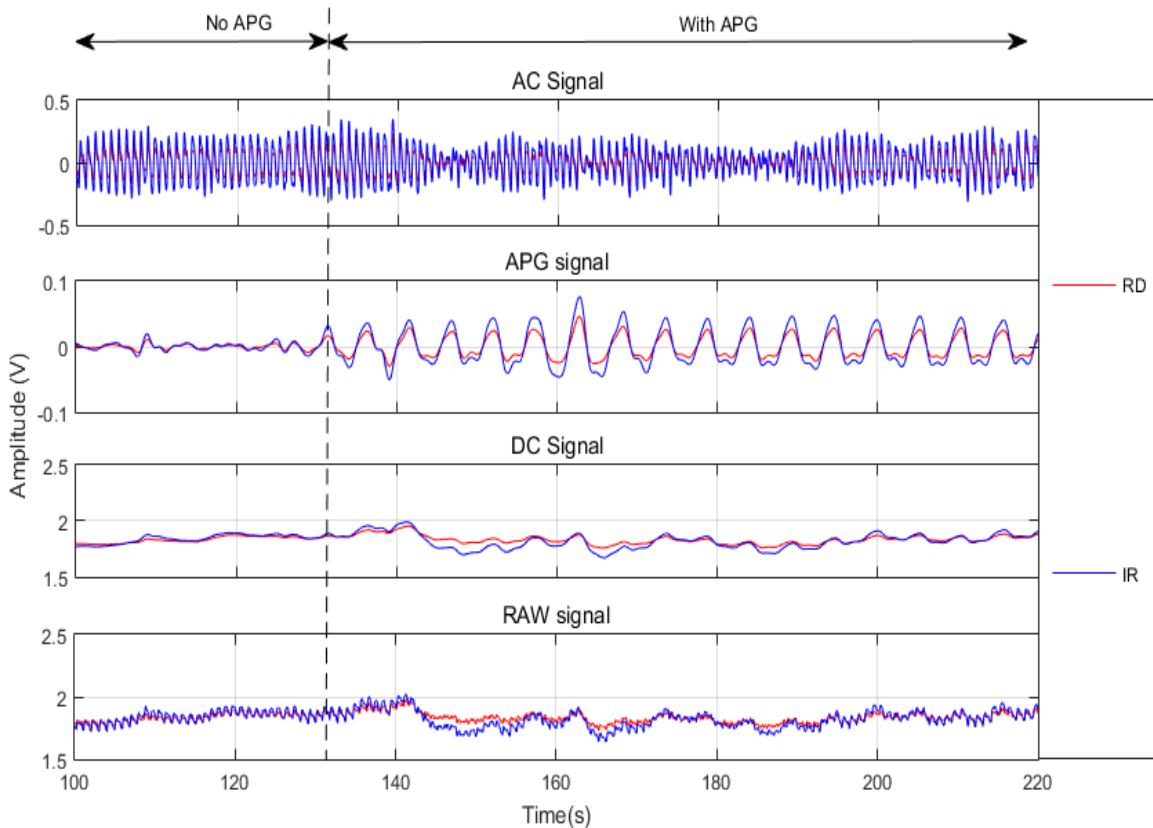


Figure 8.6: Baseline PPG signals showing pre APG and post APG phases for Subject 7; starting from the top 1) AC signal, 2) APG signal, 3) DC Signal, and 4) RAW signal.

These periodic effects due to APG could also been seen on the raw PPG signals when the APG was activated. Due to the significant contrast in arterial-venous compliance, the low pressure and frequency modulations predominantly effect the venous compartment, with little impact on the arterial system or the AC signal. Thus, the observed oscillations in the APG signal are primarily due to venous blood (Walton et al., 2010; Phillips et al., 2012; Khan et al., 2015b).

Immediately after the APG was activated, the AC signal occasionally had a small drop in signal amplitude due to sudden artefacts caused by digit cuff inflation. However, this effect was temporary and the AC amplitude became normal within approximately 10 s. In addition, no significant attenuation of AC signal amplitude was observed due to APG for the duration of the test. These observations in the AC signal are in agreement with those observed in Section 7.5.1.

Figure 8.7 shows an example of the frequency domain magnitudes related to Equations 8.1 and 8.2 determined from the frequency power spectrum for Subject 7. The magnitude for the DC signals at 0 Hz (panels e and f) was the highest due to the large DC offset from scattering and absorption by static tissue components. The magnitude for the AC signals at HR frequency was higher than the APG signals at 0.2 Hz. This difference is due to the amplification of the AC signal by the transimpedance amplifier of the PO system, during signal conditioning, which is recorded from ADC Channel 2. In contrast, the APG signal has no prior amplification since it is extracted from the unamplified raw PPG data acquired from ADC Channel 1. Section 3.3.3 provides more details on the PPG signal conditioning and the ADC Channels.

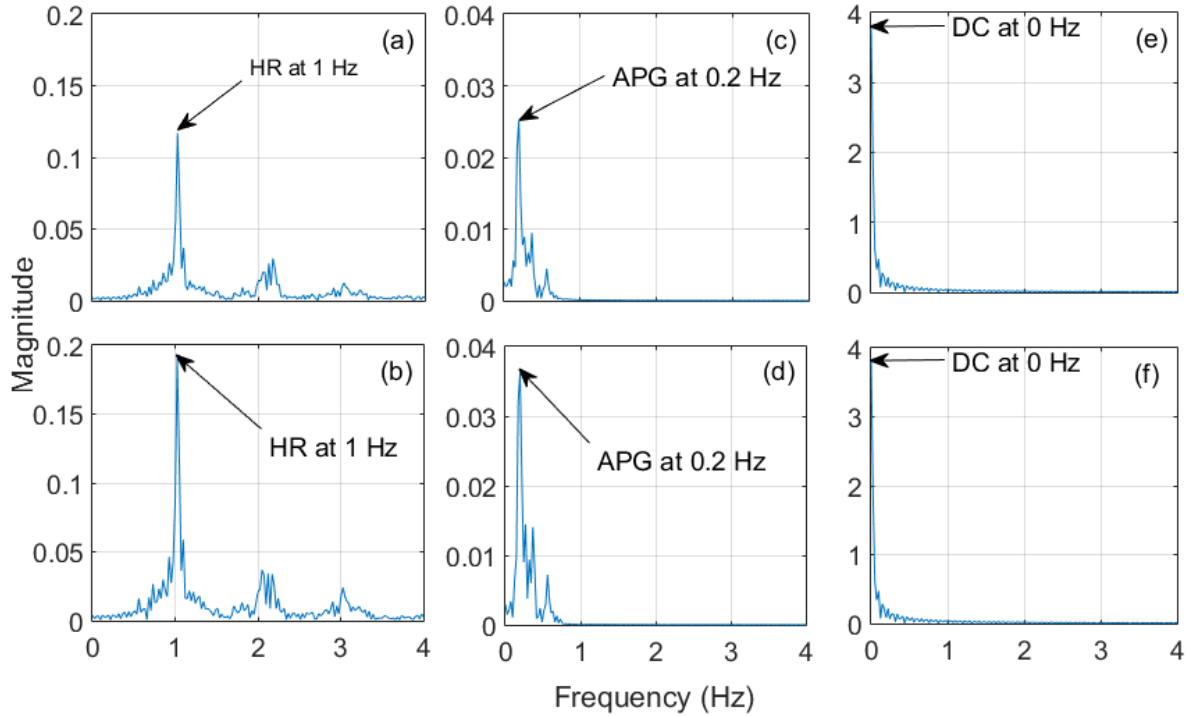


Figure 8.7: Frequency power spectrums for Subject 7 from Test 1 with labelled frequencies; (a) AC signal at RD, (b) AC signal at IR, (c) APG signal at RD, (d) APG signal at IR, (e) DC signal at RD, and (f) DC signal at IR.

8.6.2 Interesting findings in Test 4

Time domain PPG signals detected for Subject 7 during Test 4 is presented in Figure 8.8, as an example. The vascular occlusion phase of this test shows no heart beat was detected when the arm was completely occluded, as expected. Immediately after the pressure cuff was released at approximately 300 s, blood flow to the hand was re-established, enabling HR detection by the AC signals of the PPG.

Interesting features could be seen in the APG signal in the Recovery 1 and 2 phases of Test 4, as labelled in Figure 8.8. At approximately 20 s into re-perfusion or Recovery 1, the APG signal shows that the amplitude of each RD signal pulse was greater than or equal to its IR counterpart,

$RD \geq IR$. During Recovery 2, the amplitude of the IR signal pulses became greater than the RD signal pulses. The overall APG signal attributes at Recovery 2 resembles the respective overall baseline APG signal, as perfusion is restored.

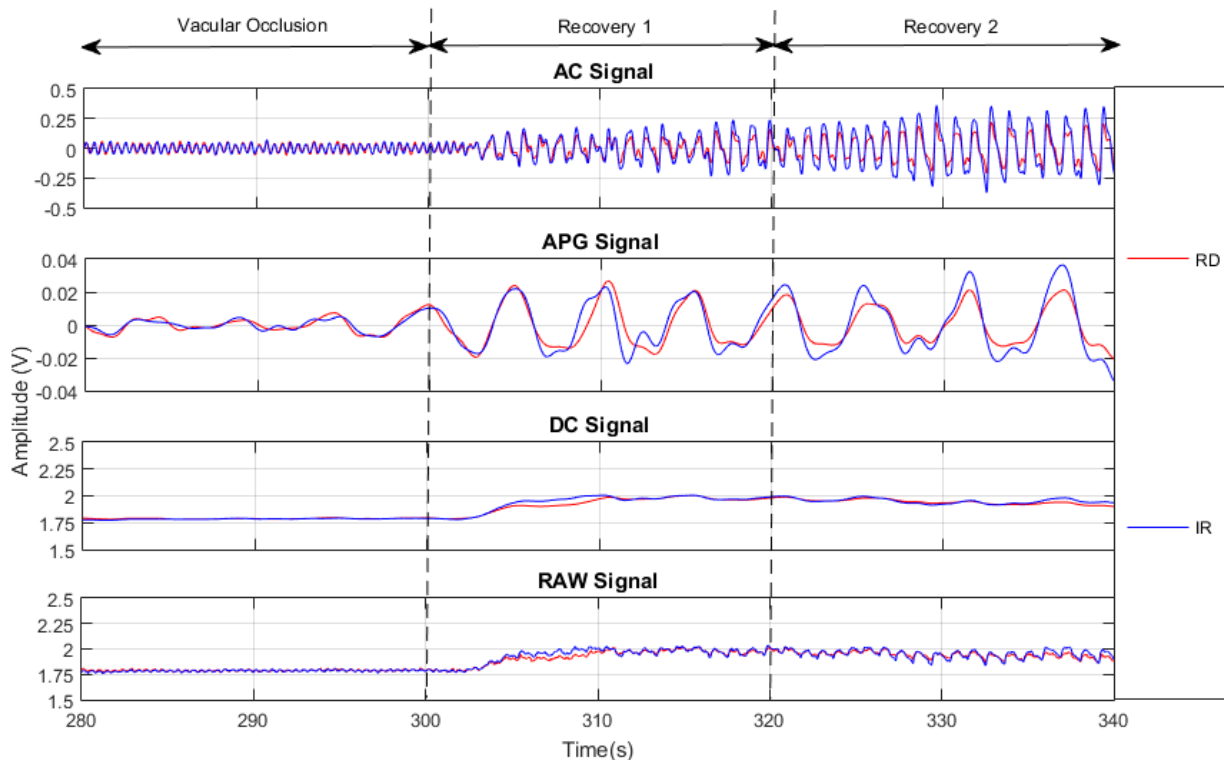


Figure 8.8: PPG signals for Subject 7 in Test 4; starting from the top 1) AC signal, 2) APG signal, 3) DC Signal, and 4) RAW signal.

More specifically, the IR and RD amplitudes were of similar magnitude for the first 6 heart beats, or 6 s, of the AC signal in Recovery 1. In contrast, for the later portion of Recovery 1 and all of Recovery 2, the IR amplitude was greater than the RD amplitude. The overall AC signal amplitudes for both IR and RD signals at Recovery 2 was close or equal to baseline level, in contrast to the overall AC signal amplitudes in Recovery 1.

8.6.3 Correlation between R_{Ven} and SvO_2

Table 8.1 presents all the estimated R_{Ven} values and measured SvO_2 samples, including their estimated uncertainties, for each subject in all the tests ($n = 21$). The correlation between these two measurements is shown in Figure 8.9. A strong, negative correlation is found between the two measurements, with $R^2 = 0.95$. The linear model fitted through the data points shows a good association between R_{Ven} and SvO_2 and explains all but 5% of the variation. In addition, the gradient (-40.5%) of this model is different to the gradient (-25.0%) of the empirical SaO_2 estimation model in Section 4.4.2.

Table 8.1: Estimated R_{Ven} , measured SvO_2 , and related uncertainties for each subject from the whole study

Subject	R_{Ven}	δR_{Ven}	$\text{SvO}_2 \%$	δSvO_2
1	0.64	0.03	82.00	3.99
	0.70	0.03	79.00	3.85
2	0.55	0.02	91.00	4.43
3	0.63	0.03	82.00	3.99
	0.52	0.02	91.00	4.43
4	0.87	0.04	76.00	3.70
	0.97	0.04	74.00	3.60
5	0.43	0.02	94.00	4.58
	0.46	0.02	93.00	4.53
	1.07	0.05	64.00	3.12
6	0.68	0.03	82.00	3.99
	1.23	0.05	59.00	2.87
	1.70	0.07	42.00	2.05
7	0.71	0.03	83.00	4.04
	0.62	0.03	85.00	4.14
	0.79	0.03	78.00	3.80
	1.24	0.05	66.00	3.21
8	0.67	0.03	88.00	4.29
	0.47	0.02	92.00	4.48
	0.99	0.04	77.00	3.75
	1.17	0.05	59.00	2.87

Most of the data points are in close proximity of the fitted linear model. However, the data point at $R = 1.7$, $SvO_2 = 42\%$ is expected to be distant from the other data points, since it is much lower than the median SvO_2 value. However, such distant outlying points can skew the R^2 value to be relatively greater than expected. In this case, exclusion of this potential outlier still shows a strong correlation ($R^2 = 0.92$) between the two measured and calculated values, indicating the point does not significantly affect the overall correlation.

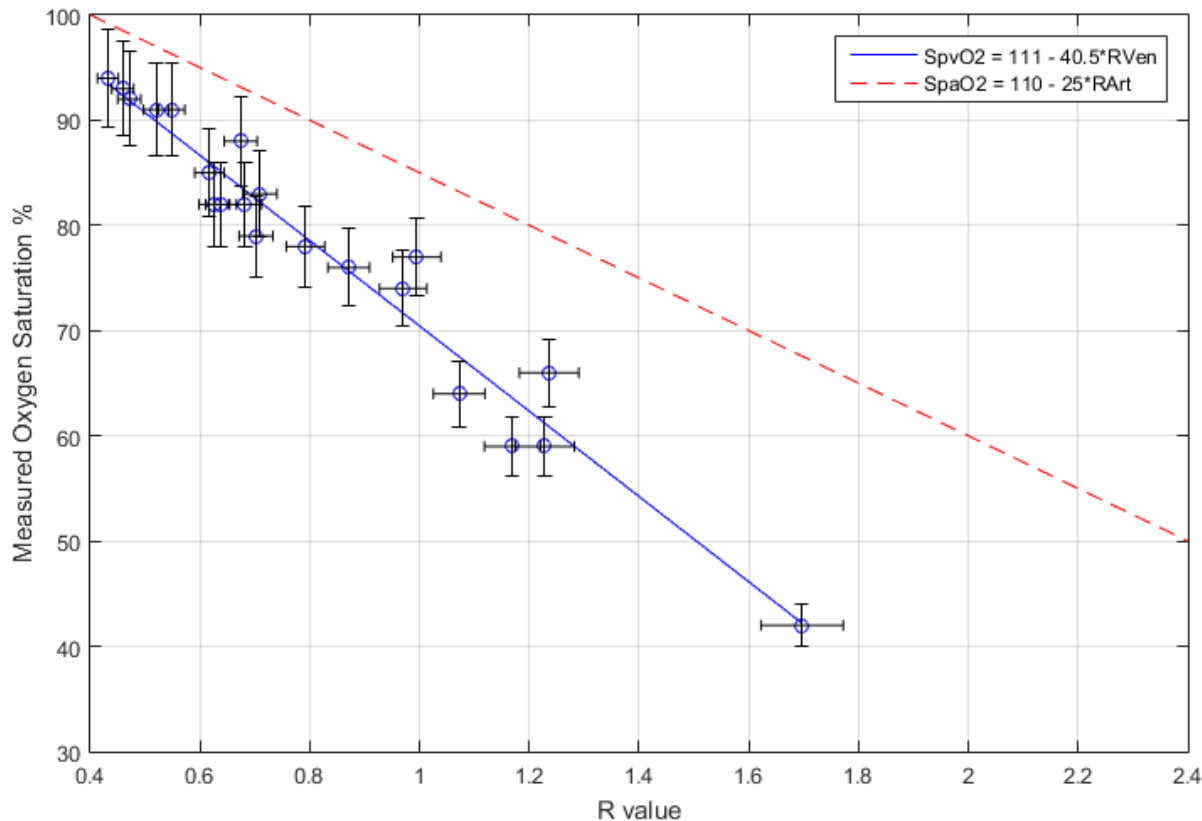


Figure 8.9: Correlation ($R^2 = 0.9515$) between all estimated R_{Ven} and measured SvO_2 samples across the whole cohort from the 3 tests. The solid blue line is the proposed $SpvO_2$ calibration model and the dashed red line is the empirical SpO_2 calibration model (Webster, 2002).

8.6.4 Study Measurements

PPG based and blood gas measurements for each subject from Test 1 are shown in Table 8.2. Tables 8.3 and 8.4 present these measurements across the whole cohort for Tests 2 and 4, respectively. All 3 tables include SpvO₂ values estimated using the fitted linear SvO₂ estimation model. In addition, PPG estimated O₂E ($O_2Ep = SpaO_2 - SpvO_2$) and O₂E calculated from blood gas measurements ($O_2E = SaO_2 - SvO_2$) are also presented in the tables.

Table 8.2: Baseline PPG and blood gas measurements for all the subjects

Subject	R _{Ven}	SpvO ₂ %	SvO ₂ %	R _{Art}	SpaO ₂ %	SaO ₂ %	O ₂ Ep %	O ₂ E %
1	0.64	84.97	82.00	0.56	96.02	97.00	11.05	15.00
2	0.55	88.60	91.00	0.52	96.91	98.00	8.30	7.00
3	0.63	85.45	82.00	0.58	95.62	98.00	10.17	16.00
4	0.87	75.50	76.00	0.55	96.16	96.00	20.65	20.00
5	0.43	93.32	94.00	0.48	98.00	97.00	4.68	3.00
6	0.68	83.20	82.00	0.47	98.16	97.00	14.96	15.00
7	0.71	82.08	83.00	0.63	94.34	97.00	12.26	14.00
	0.62	85.83	85.00	0.58	95.40	97.00	9.57	12.00
8	0.67	83.50	88.00	0.57	95.74	97.00	12.24	9.00
	0.47	91.71	92.00	0.53	96.68	97.00	4.96	5.00
Median	0.63	85.21	84.00	0.56	96.09	97.00	10.61	13.00
Interquartile	0.57- 0.68	83.27- 87.91	82.00- 90.25	0.53- 0.57	95.65- 96.85	97.00- 97.00	8.62- 12.26	7.50- 15.00

The R_{Ven} determined across all the subjects for each protocol are significantly different ($p < 0.001$) to the corresponding R_{Art}, as expected. In addition, the overall median difference between estimated SpaO₂ and SpvO₂ across the 3 tests is 13.8%, and positive as expected. In addition, the difference between pairs of measurements in each subject is statistically significant ($p < 0.001$).

For Test 1, the median SpvO₂ is close to the measured SvO₂, with a median percentage difference of 1.4%. In addition, paired SpvO₂ and SvO₂ values for each subject did not show any statistically significant difference ($p \approx 1.0$). The estimated median SpaO₂ agrees well with measured median SaO₂, with a percentage difference of 0.94%, and the difference between pairs of measurements in each subject is not statistically significant ($p = 0.11$).

Table 8.3: PPG and blood gas measurements for all the subjects from Test 2

Subject	R _{Ven}	SpvO ₂ %	SvO ₂ %	R _{Art}	SpaO ₂ %	SaO ₂ %	O ₂ Ep %	O ₂ E %
1	0.70	82.35	79.00	0.53	96.87	99.00	14.52	20.00
3	0.52	89.73	91.00	0.47	98.20	97.00	8.47	6.00
4	0.97	71.53	74.00	0.52	97.02	96.00	25.49	22.00
5	0.46	92.20	93.00	0.48	97.91	97.00	5.71	4.00
Median	0.61	86.04	85.00	0.50	97.47	97.00	11.43	12.00
IQR	0.51-0.77	79.64-90.35	77.75-91.50	0.48-0.52	96.98-97.98	96.75-97.50	7.78-17.27	5.50-20.00

The individual SvO₂ measurements in Test 4 across all the subjects are significantly smaller, up to 0.48x, than their corresponding baseline values. In addition, the calculated O₂E is found to be up to 3.67x greater than at the baseline level. Thus, the estimated SpvO₂ and O₂Ep values are also significantly lower and higher, respectively, than their respective baseline counterparts for each subject in this test. However, Test 4 shows a large difference of 3.93% between median SaO₂ and SpaO₂. It should be noted that no separate SaO₂ measurements were made during Test 4, as explained in Section 8.4.4. Hence, it is not possible to fully confirm the accuracy of the estimated SpaO₂ values in this test.

Table 8.4: PPG and blood gas measurements for all the subjects from Test 4

Subject	R _{Ven}	SpvO ₂ %	SvO ₂ %	R _{Art}	SpaO ₂ %	SaO ₂ %	O ₂ Ep %	O ₂ E %
5	1.07	67.39	64.00	0.69	92.83	97.00	25.44	33.00
6	1.23	61.05	59.00	0.70	92.44	97.00	31.39	38.00
	1.70	42.08	42.00	0.68	93.07	97.00	50.99	55.00
7	0.79	78.73	78.00	0.52	96.98	97.00	18.26	19.00
	1.24	60.75	66.00	0.76	91.03	97.00	30.28	31.00
8	0.99	70.50	77.00	0.55	96.31	97.00	25.81	20.00
	1.17	63.46	59.00	0.62	94.63	97.00	31.16	38.00
Median	1.17	63.46	64.00	0.68	93.07	97.00	29.61	33.00
IQR	1.03- 1.23	60.90- 68.94	59.00- 71.50	0.58- 0.70	92.64- 95.47	97.00- 97.00	2.63- 31.28	25.50- 38.00

* SaO₂ is within ±1.02% of the measured baseline value

No data is presented for Subject 2 in Table 8.3, as no APG signal was detected during Test 2 for that subject. The digit cuff for Subject 2 was lightly attached to the digit throughout Test 2. This loose attachment affected the APG system's performance and is a set up failure, rather than a sensor concept failure. In addition, Test 4 was conducted only once for 4 min for Subject 5. Hence, the results from only one test are presented in Table 8.3 for that subject.

Table 8.5 summarizes all the measured and estimated oxygen saturation values, including their paired differences, for the three tests. Using the empirical pulse oximeter calibration equation for SpaO₂, shown in Figure 8.9, the median difference between SaO₂ and SpaO₂ was 0.65 [IQR: -0.98 – 1.51] %. The median difference between SvO₂ and SpvO₂, determined using the calibration equation for SvO₂ developed in this study, was just 0.29 [IQR: -2.05 – 1.27] %.

Table 8.5: Measured and estimated oxygen saturation differences for all subjects, across the three tests. No measured or estimated arterial oxygen saturations for some subjects are presented as explained in Section 8.4.4.

Subject	SpvO ₂ %	SvO ₂ %	SvO ₂ – SpvO ₂ %	SpaO ₂ %	SaO ₂ %	SaO ₂ – SpaO ₂ %
1	84.97	82.00	-2.97	96.02	97.00	0.98
	82.35	79.00	-3.35	96.87	99.00	2.13
2	88.60	91.00	2.40	96.91	98.00	1.09
3	85.45	82.00	-3.45	95.62	98.00	2.38
	89.73	91.00	1.27	98.20	97.00	-1.20
4	75.50	76.00	0.50	96.16	96.00	-0.16
	71.53	74.00	2.47	97.02	96.00	-1.02
5	93.32	94.00	0.68	98.00	97.00	-1.00
	92.20	93.00	0.80	97.91	97.00	-0.91
	67.39	64.00	-3.39	-	-	-
6	83.20	82.00	-1.20	98.16	97.00	-1.16
	61.05	59.00	-2.05	-	-	-
	42.08	42.00	-0.08	-	-	-
7	82.08	83.00	0.92	94.34	97.00	2.66
	85.83	85.00	-0.83	-	-	-
	78.73	78.00	-0.73	-	-	-
	60.75	66.00	5.25	-	-	-
8	83.50	88.00	4.50	95.74	97.00	1.26
	91.71	92.00	0.29	-	-	-
	70.50	77.00	6.50	-	-	-
	63.46	59.00	-4.46	-	-	-
Median	82.35	82.00	0.29	96.77	97.00	0.65
IQR	70.50-85.83	74.00-88.00	-2.05-1.27	95.81-97.69	97.00-97.00	-0.98-1.51

8.7 Discussion

8.7.1 Main outcome

This study demonstrates that peripheral SvO₂ can be reliably and accurately measured using the APG system and the developed calibration curve with its very high R^2 value. Using the APG system, peripheral venous blood can be pulsed like arterial blood, exploiting the significant arterial-venous compliance difference. Results from the study shows R_{Ven}, derived from the APG and DC signals, can be correlated to the SvO₂.

Overall, a good correlation is found between estimated R_{Ven} and measured SvO₂ across all the subjects in the 3 tests, as shown in Figure 8.9. The negative correlation is expected and in

accordance to the empirically derived R value and measured SaO_2 in other studies (Tremper and Barker, 1989; Ross, 1999; Webster, 2002). This relationship allows determination of SvO_2 from R_{Ven} , which can be obtained from using the APG system. Thus, the linear fit and very high $R^2 = 0.95$ indicates the applicability of the metric in assessment of SvO_2 in future studies.

Using the model developed in this study, the median difference between pairs of measured and estimated venous oxygen saturation values was calculated to be 0.29%, with IQR of -2.05 – 1.27 %, which shows the high degree of accuracy of the model. The median difference between pairs of measured and estimated arterial oxygen saturation values was calculated to be just 0.65 %, with similar IQR of -0.98 – 1.51 %, using the empirical pulse oximeter calibration model. Thus, venous oxygen saturation accuracies from this pulse oximeter system are expected to be similar to those commonly obtained for arterial oxygen saturations.

In addition, the study introduced a robust potential experimental method to induce changes in peripheral SvO_2 levels and detect these changes using the PO sensor and the APG system. Two tests were implemented in this study to induce change in SvO_2 level and use APG system modulated PPG signal (APG signal) to capture those changes. Out of all the 3 tests, including baseline, Test 4 is the most important to meet the goals of this study, as it induced large consistent and reliably obtained changes in saturation from baseline physiological values.

8.7.2 Difference between R_{Art} and R_{Ven} modulation ratios

The characteristic of the relationship between the RD to IR modulation ratio, or R value, and the oxygen saturation is associated with the bulk tissue's optical properties. Perturbation induced

artefacts can have a measurable impact on the relative optical properties of the tissue medium being investigated using PPG (Casciani et al., 2008). Such artefacts in a limb may simulate the effects of tissue hemoglobin concentration variations of the tissues medium. These variations can result in different R values derived from PPG measurements when compared to non-perturbed PPG measurements, as seen in previous studies (Mannheimer et al., 1997; Casciani et al., 2008).

Outcomes of this study suggest the low pressure external modulations caused by the APG system predominantly impacted only the venous system, and not the arterial system, due to the significant arterial-venous compliance difference. Figures 8.6 and 8.8 show these perturbation effects were only visible in the APG signals and not in the AC signals, as indicated by no significant interference with the AC signal. Therefore, R_{Ven} values derived from the APG and DC offset signals are different to R_{Art} values derived from the AC and DC offset signals.

8.7.3 Low oxygen saturation detection using PPG

When the arm is completely occluded above systolic blood pressures, arterial blood supply to the arm is stopped. During Test 4, the arm was occluded and blood flow to the arm was restricted for several minutes. Without any perfusion it is expected that the occluded blood will slowly desaturate oxygen overtime (Skarda et al., 2007; Lima and Bakker, 2011; Futier et al., 2011; Gómez et al., 2008). The oxygen present in the occluded blood will gradually diffuse out to the nearby tissues due to the hypoxic condition created by low oxygen tension or PO_2 in the occluded region. This effect can be explained by the reduction of PO_2 in venous blood (PvO_2), measured via blood gas analysis but not presented in this research, across all the subjects in Test 4 indicating reduced oxygen saturation of venous blood.

In Test 4, a venous sample was taken immediately before the arm pressure cuff was completely deflated to get a measure of the true ischemic, oxygen desaturated blood. The APG was activated just before releasing the pressure cuff, and thus, the immediate few APG pulses will refer to the true ischemic blood. The APG pulse amplitude of the RD signal is expected to be greater than the IR signal during such low saturation phase (NTS, 2011; Mannheimer, 2007), which agrees with the time domain observations in Figure 8.8. This effect in the time domain PPG signals also has an equal effect to the PPG signals in the frequency domain. Thus, higher than baseline R_{Ven} values are observed in the Recovery 1 phase of Test 4. In addition, due to the greater inaccuracy of the wavelengths used at saturation <70% (Mannheimer et al., 1997), the error in measurement is also large for those R_{Ven} values.

During the occlusion phase of Test 4, the local tissue was being deprived of oxygen by the lack of perfusion. Previous studies have shown that tissues will temporarily increase extraction of oxygen from blood to return to normal tissue saturation level after ischemia (Derdeyn et al., 1998; Lima and Bakker, 2011; Lipcsey et al., 2012). Thus, when the cuff is released after brief ischemia the local tissues and muscles in the arm increased extraction of oxygen, which is evident across all the subjects in Test 4, and as can be seen in Table 8.3.

The recovery of oxygen desaturated blood to baseline oxygen saturation level after ischemia is very rapid during reactive hyperemia in healthy adults (Skarda et al., 2007; Gómez et al., 2008). For Subjects 5 and 6, a venous sample was taken approximately 30 s after blood flow was restored to the arm. Blood gas analysis of those samples revealed the SvO_2 to have already returned to

baseline level. Thus, it can be concluded that the change from low saturation to normal oxygen saturation level during reactive hyperemia is very rapid, and can occur in less than 30 s. This finding is in agreement with the observations made in the APG signal of Figure 8.8.

When the arm is completely occluded, the oxygen saturation of arterial blood is also expected to drop like venous blood. Restoration of perfusion should allow SaO_2 to return to normal levels faster than the venous blood, since arteries are the oxygen supplying blood vessels. Previously, two studies have shown that the restoration of tissue oxygens saturation after 4 min of brief ischemia in the arm of healthy adults is approximately 5 s (Gomez et al., 2008; Lima and Bakker, 2011), and depends on the duration of the occlusion. Thus, it can take approximately 5 seconds for the peripheral arteries to return to normal SaO_2 levels after brief ischemia, as desaturated blood are quickly flushed with freshly supplied, highly saturated, arterial blood.

Therefore, the initial few AC signal pulses, with low IR amplitudes compared to RD amplitudes, may demonstrate lower SaO_2 levels (Mannheimer, 2007; NTS, 2011), in agreement to Figure 8.8 and the SpaO_2 estimates in Table 8.4. However, due to this very short, rapid recovery time and resource constraints while conducting Test 4, it was not possible to draw any arterial blood samples and investigate this very interesting rapid recovery effect in more detail. It should also be noted that the primary interest of this study is to measure desaturated SvO_2 and not desaturated SaO_2 blood.

No significant changes in SvO_2 from baseline were observed due to lifting the arm in Test 2. These findings suggest that variation in peripheral SvO_2 and O_2E is not influenced by reduction in peripheral arterial blood flow induced in this test. In particular, one subject in Test 2 showed

elevated SvO_2 and PvO_2 levels, for causes yet to be determined. However, possible reasons include; 1) increased temperature of the hand to arterialise the venous blood, 2) increased vasodilation of peripheral arteries to improve blood flow conditions. Test 2 was also difficult to execute in several ways. First, it was difficult to draw blood when the hand was held up. Second, a tourniquet needed to be used to increase venous blood volume for sampling, and thus, obstruct venous flow in the periphery. However, these results are not unexpected, since this maneuver changes flow but does not imply a significant enough perturbation to oxygen supply, as in Test 4, to see a significant change in SvO_2 and O_2E .

8.7.4 Limitations

One of the primary limitations of the MOOSE study is the small number ($n = 21$) of data points or samples used to develop the SpvO_2 calibration curve. In addition, no very dark skinned or female subjects were recruited in this study. More data points from a larger, diverse, and healthy cohort will enable development of a more robust R_{Ven} vs SvO_2 correlation plot, and thus, a more reliable SpvO_2 calibration curve. Following the outcomes of this study, a further study is planned to include a large cohort of critically ill patients with potentially low SvO_2 levels. However, the very strong correlation obtained between the two measurements indicates the concept will likely generalize well.

The PO sensor uses wavelengths of 660 nm and 940 nm that can provide less accurate measurements at low saturations. Mannheimer et al. (Mannheimer et al., 1997) used two mathematical models to numerically explore the effect emitter wavelengths have on pulse oximeter accuracy at low oxygen saturations. It was reported that sensors fabricated with 735 and 890 nm

emitters read more accurately at low saturations ($\leq 70\%$) under a variety of conditions than sensors made with conventionally used 660 and 940 nm emitters. This information matches the slightly larger R_{Ven} errors observed in Test 4 at low saturations. A multi-wavelength sensor could be implemented to overcome this issue and determine R values from PPG signals at different wavelengths.

The APG signals presented in this study are not amplified or conditioned by any transimpedance amplifier. This is because the APG signals are extracted from the raw PPG signals. Such shortcomings may result in poor APG signals with low SNR under different conditions, such as at low skin temperatures (Khan et al., 2016). Signal processing and amplification of the APG signals in the analog end may result in a more reliable signal, as it is done in case of the AC signal. However, several modifications to the PO system's hardware need to be made to implement these changes, and the results obtained without it are still very good.

8.8 Summary

This clinical validation study presents a novel way to non-invasively estimate SvO_2 and O_2E using a novel pulse oximeter and APG system. Results suggest the APG system can modulate the venous system periodically. These periodic effects can be successfully detected by the PPG, extracted as APG signals, and analysed for SvO_2 . FFT analysis of 20 s long PPG signals were used to determine the fundamental frequency information from the APG, AC, and DC signals, and thus, R value and oxygen saturations. A strong, negative, linear correlation ($R^2 = 0.95$) is found between estimated R_{Ven} and measured SvO_2 , with the median difference of 0.29% between pairs of measurement. In addition, the estimated R_{Ven} values are significantly smaller ($p < 0.001$) than the

estimated R_{Art} , resulting in significantly different $SpvO_2$ and SpO_2 estimates, respectively, as desired. Overall, the main outcome of this study is a novel calibration curve that can be used to estimate peripheral SvO_2 .

The proposed $SpvO_2$ estimation model can be used as a potential metric and indicator for low O_2E , consumption, and tissue hypoxia. Real-time estimation of peripheral SvO_2 using this novel pulse oximeter and APG method will enable real-time monitoring of these physiological conditions. Thus, improvement and application of this novel concept could aid in diagnosis of medical conditions related to microcirculation dysfunction, such as sepsis and cardiac failure, which are both common in the ICU, as well as length of stay, cost, and mortality.

Chapter 9: Conclusions

9.1 Outcomes from Thesis: Part 1

Part 1 of this thesis discusses the development of a novel pulse oximeter system and PPG processing environment. In comparison to commercial pulse oximeters, the PO system was developed to provide access to all the signals of interest, in particular the raw and amplified PPG signals, for post processing and analysis. All PPG signals are digitally processed and analysed in MATLAB to estimate physiological parameters of interest.

Chapter 3 presents the basic design and hardware specifications of the pulse oximeter system used in this research. The IR and RD PPG signals are sampled at 50 Hz and separated during signal conditioning and processing to allow independent logging. A finite state machine was developed for automatic or manual LED intensity control of the sensor, providing the user greater flexibility and allowing scope for repeatable measurements. The PPG acquisition GUI enables logging, real-time monitoring, and storing of PPG data for post processing in MATLAB or other tool. In addition, the GUI can be used to operate the FSM and time protocols. Overall, the end product is a complete, flexible, and customisable PPG acquisition and monitoring system.

Chapter 4 presented the PPG signal processing and analysis techniques used in this research to assess SpO₂ and HR. A two stage filtering system was designed and implemented to extract signals below 0.67 Hz and in the range of 0.67 – 4.5 Hz as DC and AC PPG components, respectively. In

addition, a robust peak and trough detection algorithm was developed and tested to determine signal amplitude from the extracted PPG signals. Published time domain algorithms and empirical calibration equations are used to calculate the modulation ratio (R value) and estimate SpO₂, respectively. Furthermore, two PPG based methods to assess HR over time from PPG in the time and frequency domains are also discussed and compared.

The effect of different digit skin temperatures on transmittance pulse oximetry, which is the mode of sensor used in this research, were investigated in Chapter 5. In one study, three tests were conducted at cold, normal, and warm skin temperatures to test the hypothesis that cold temperatures can significantly degrade PPG signal quality, and thus, measurement accuracy. A further study was conducted to validate the hypothesis using reference blood gas measurements. Results from both studies show that cold temperature conditions significantly reduce PPG signal quality and waveform shape, demonstrated by reduced signal RMS and amplitude, and thus affecting the accuracy of SpO₂ estimation. This deterioration in PPG signal quality is correlated with decreases in blood volume and blood flow, due to induced vasoconstriction. Overall, the main outcome is a tri-linear model quantifying PPG signal quality as a function of temperature.

Warm temperature conditions significantly improved the quality of the PPG signals, up to 4 times from baseline, as well as the reliability in SpO₂ estimation. This improvement in signal quality can be associated with increase in blood volume and blood flow, due to increased vasodilation. The overall experimental outcomes from this research suggest that warm skin temperature conditions of approximately 33°C should to be maintained for reliable transmittance pulse oximetry, and any

further clinical use of these signals in monitoring or measuring parameters related to peripheral oxygen extraction and circulation.

9.2 Outcomes from Thesis: Part 2

Part 2 of this thesis investigated the use of PPG signals for continuous, non-invasive peripheral perfusion monitoring. In particular, this part of the thesis describes a pneumatic pressure cuff and control system to assess venous blood oxygen saturation and resulting oxygen extraction, O₂E. In addition, monitoring changes in volumetric blood flow using the PO sensor is also presented in this part of the thesis. Thus, all three major aspects of tissue perfusion monitoring in circulatory failure and/or microvascular dysfunction are assessed.

Chapter 6 demonstrated PPG signal amplitude can be used to monitor peripheral volumetric blood flow changes in the finger. It can successfully identify different flow states induced by vascular occlusions, when compared to the measurements made by a commercial vascular Doppler ultrasound device, and thus can be used to monitor changes in peripheral perfusion. A good correlation ($R^2 = 0.69$) and trend agreement was obtained between median PPG amplitude and Doppler ultrasound velocity, particularly at normal and clinically important low flow conditions. The other key outcome of this study shows that the PPG amplitude monitoring can be a surrogate or alternative to the vascular Doppler ultrasound based blood velocity monitoring, and can provide continuous and reliable measurements.

Proof of concept testing of a novel pulse oximeter and APG system that can assess peripheral SvO₂ and O₂E is presented in Chapter 7. The APG system can generate low frequency and low pressure

modulations to make the venous blood pulsatile without interfering with the arterial blood, exploiting the significant arterial-venous compliance difference. These periodic modulations can be detected by PPG signals and analysed to assess SvO_2 . Outcomes from this study show that the estimated SaO_2 and SvO_2 values lie within published ranges of values in the literatures. In addition, the median difference in saturation, or O_2E , showed a statistically significant and expected differences ($p = 0.002$) between pairs of measurements in each subject. Thus, the concept is preliminarily validated.

The outcomes from Chapter 7 justified clinical validation trial with whole blood data from blood gas analysis as a reference standard in a further study detailed in Chapter 8. Arterial and venous bloods can have different optical properties under perturbations, and thus, can provide different modulation ratios. Hence, the empirical calibration equation used to estimate $SpaO_2$ cannot be used to estimate $SpvO_2$. In addition, frequency domain analysis of PPG signals was found to be more robust and easy to implement compared to time domain PPG analysis for assessing the pulsatile responses.

The MOOSE study described in Chapter 8 developed a novel pulse oximeter calibration model to estimate SvO_2 using the modulation ratio R_{Ven} , derived from APG and DC offset signals, and blood gas measured SvO_2 . This calibration model was based on a robust experimental protocol that was developed to induce a range of SvO_2 values, and thus a range of R_{Ven} values. The results show a strong, expected negative, linear correlation ($R^2 = 0.95$) between estimated R_{Ven} and measured SvO_2 . In addition, the calculated R_{Ven} values are significantly smaller ($p < 0.001$) than the calculated R_{Art} , resulting in significantly different $SpvO_2$ and $SpaO_2$ estimates, respectively, as

expected. Overall, the main outcome of the MOOSE study is an SvO_2 estimation model that can be used as a sensor to assess peripheral O_2E , and thus, perfusion. Thus, this sensor may potentially detect peripheral perfusion alterations in real-time during microvascular and/or overall circulatory dysfunctions, such as in sepsis or cardiac failure.

9.3 Overall outcome

Knowing the tissue oxygen delivery and absorption are necessary to assess tissue perfusion. This thesis presents a novel, non-invasive pulse oximeter based concept to assess peripheral perfusion in terms SpaO_2 , SpvO_2 , O_2E , and volumetric blood flow changes. It also demonstrated that pulse oximetry can be applied in overall perfusion monitoring, and not restricted to conventional SpO_2 monitoring. Such pulse oximetry based overall perfusion monitoring meets a key clinical endpoint or goal in monitoring circulatory function and its response to care during circulatory management and resuscitation.

Light energy absorbed by venous blood, typically represented as the DC component of the PPG signal, is usually ignored to improve SNR for SpO_2 estimation. Due to the typical non-pulsatile nature of venous blood, conventional pulse oximeter sensors fail to assess SvO_2 . This thesis presents a feasible, low cost, and reliable method to transform the venous system into a dynamic system. A novel SpvO_2 calibration curve is developed in this research that can be used by pulse oximeters to estimate local SvO_2 . As a result, peripheral SvO_2 can be similarly estimated like SaO_2 by pulse oximetry.

In addition, this thesis discusses a novel method to monitor blood flow in terms of relative volumetric changes using the PPG signal amplitude. Thus, clinically important flow limited states can be reliably identified in comparison to normal or high flow states. Equally, any changes in perfusion can be continuously monitored. This PPG amplitude metric can also be used a reliable surrogate measurement to vascular Doppler ultrasound based blood velocity measurement.

In general, this thesis suggests several non-invasive methods with good clinical accuracy in assessing the four key parameters associated with peripheral perfusion. The sensor developed in this research can be used as indicator of increased oxygen consumption and inadequate oxygen delivery in critically ill patients. Thus, with further validation of these methods, their application in clinical settings can significantly aid in early-goal directed therapy in sepsis and circulatory failure, thereby, can reduce cost, burden, and improve healthcare.

Chapter 10: Future Work

The research presented in this thesis presents a novel pulse oximeter system that can be used for non-invasive perfusion monitoring in terms of SvO_2 , O_2E and volumetric blood flow changes. In addition, the robustness and accuracy of pulse oximeter sensors at different digit skin temperatures was investigated. However, the potential future work of this research includes improving the overall reliability, robustness, and versatility of the technology. First, several improvements can be made to the pulse oximeter hardware and sensing technology. Second, the perfusion monitoring methods can be further developed, including more comprehensive investigations and analysis of the PPG signals.

10.1 Improvements to the PO system

Currently, the PO system hardware is only configured to amplify the DC corrected PPG signal, denoted as the amplified PPG signal, at the transimpedance amplifier stage. Amplification results in a more reliable signal, with high SNR, to be sampled by the ADC. Similarly, amplification of the APG signals can also provide a more reliable signal to be sampled by the ADC. However, to make such modification several changes need to be made at the transimpedance amplifier stage. In addition, application of analog amplifiers is necessary to extract the APG signals, using the filter specifications discussed in Section 8.2.3, from the raw PPG signals.

Other improvements are also desired in the PPG acquisition interface. In particular, development of the LED intensity control algorithm of the firmware is necessary to increase the sensitivity, and thereby, improve the intensity adjustment process to changes in blood flow or haemoglobin absorption conditions. This improvement can aid in detecting rapid changes in peripheral perfusion.

10.2 Modifications to the sensor and clinical applicability

Chapter 8 demonstrated that the current pulse oximeter sensor with wavelengths 660 nm (RD) and 940 nm (IR) can perform inaccurately at low saturations. The outcome of the MOOSE study showed larger δR_{ven} at lower SvO_2 levels. It is suggested 735 and 890 nm wavelength emitters can perform more accurately at oxygen saturations below 70% (Mannheimer et al., 1997). Thus, implementation of two additional LEDs of 735 nm and 890 nm wavelengths can improve accuracy of the PO sensor. In addition, haemoglobin absorption information will be acquired from a wide band of wavelengths, allowing room for exploration and estimation of other physiological metabolites. However, such modifications will require disassembly and re-development of the PO sensor, since no commercially available pulse oximeter sensor provides more than 2 LEDs, and thus wavelengths.

Several other improvements can be made to the current sensor to ensure reliability and robustness. First, the current sensor can be improved to provide more comfort and less tight attachment. This sensor was found to be relatively tighter than the commercial Masimo SET sensor used in the clinical part of this research. More specifically, a tightly attached sensor may also lead to inaccurate measurements and necrosis (Philips, 2003). Second, the sensor cable can be

repositioned to minimize motion artefacts and improve sensor reliability. Third, a temperature controllable small heating element, such as a high resistance coil, can also be added inside the sensor to provide localized heating and promote blood flow in cold fingers. Finally, the sensor can be made waterproof to enable continuous PPG measurements under water, such as during the Cold test in Chapter 5.

10.3 Assessment of absolute blood flow

Detection of peripheral volumetric blood flow changes by PPG can be compared with a more reliable reference measurement, such as laser Doppler, for further change in flow trend analysis. In addition, extending the relative blood flow change measurement to absolute blood flow measurement can be very useful, especially when baseline blood flow is unknown, and is expected to correlate better with PPG based measurements. Measurement of the local vessel diameter using colour Doppler ultrasound images can enable estimation of the vessel CSA, and thus, absolute blood flow. Finally, associating absolute blood flow with O₂E can allow estimation of oxygen extraction rate of local tissues, which can be a more robust indicator for perfusion changes.

10.4 Further testing and application of the SvO₂ estimation model

One of the primary limitations of the MOOSE study, discussed in Chapter 8, was the small number of samples ($n = 21$) used to develop the SvO₂ estimation model. The MOOSE study was composed of a male cohort ($n = 8$), and vascular occlusion induced low saturations was tested on only 4 subjects. Female subjects were not recruited in this validation study because they generally have colder fingers, and potentially lower peripheral perfusion, in comparison to male subjects and thus, could result in poor PPG signals. The complexity and resource constraints of the study did not

allow the experiment to be repeated on the same subjects, considering the MOOSE study recruitment was done from a small group of people. Finally, none of the subjects had very dark digit skin pigmentation which can have an effect on pulse oximeter accuracy at low saturations (Feiner et al., 2007).

Recruitment of volunteers from a larger and diverse population will allow more samples from a wider SvO_2 range to be acquired to improve the robustness of the SvO_2 estimation model. In addition, a further study is planned to include critically ill patients, preferably with sepsis or septic shock, with potentially low SvO_2 levels. Bland-Altman analysis of the SvO_2 model based estimations, SpvO_2 , against reference blood gas measurements from that study will allow more a comprehensive test of correlation between the two methods. Therefore, application of the model in such a study will enable the proposed model to be applied in clinical settings and other studies.

References

- Abbott. 2013. i-STAT®1 System Manual. Available: <https://www.abbottpointofcare.com/en-int/support/technical-documentation/istat-system-manuals> [Accessed 25/04/2016].
- Aburahma, A. & Bandyk, D. 2012. *Noninvasive vascular diagnosis: a practical guide to therapy*, Springer Science & Business Media. 1447140052.
- Adhikari, N. K., Fowler, R. A., Bhagwanjee, S. & Rubenfeld, G. D. 2010. Critical care and the global burden of critical illness in adults. *The Lancet*, 376, 1339-1346.
- Ait-Oufella, H., Lemoinne, S., Boelle, P., Galbois, A., Baudel, J., Lemant, J., Joffre, J., Margetis, D., Guidet, B. & Maury, E. 2011. Mottling score predicts survival in septic shock. *Intensive care medicine*, 37, 801-807.
- Alberti, C., Brun-Buisson, C., Burchardi, H., Martin, C., Goodman, S., Artigas, A., Sicignano, A., Palazzo, M., Moreno, R., Boulme, R., Lepage, E. & Le Gall, R. 2002. Epidemiology of sepsis and infection in ICU patients from an international multicentre cohort study. *Intensive Care Med*, 28, 108-21.
- Alian, A. A. & Shelley, K. H. 2014. Photoplethysmography. *Best Practice & Research Clinical Anaesthesiology*, 28, 395-406.
- Allen, J. 2007. Photoplethysmography and its application in clinical physiological measurement. *Physiol Meas*, 28, R1-39.
- Alnaeb, M. E., Alobaid, N., Seifalian, A. M., Mikhailidis, D. P. & Hamilton, G. 2007. Optical techniques in the assessment of peripheral arterial disease. *Curr Vasc Pharmacol*, 5, 53-9.
- Alty, S. R., Angarita-Jaimes, N., Millasseau, S. C. & Chowienczyk, P. J. 2007. Predicting arterial stiffness from the digital volume pulse waveform. *Biomedical Engineering, IEEE Transactions on*, 54, 2268-2275.
- Angus, D. C., Linde-Zwirble, W. T., Lidicker, J., Clermont, G., Carcillo, J. & Pinsky, M. R. 2001a. Epidemiology of severe sepsis in the United States: analysis of incidence, outcome, and associated costs of care. *Crit Care Med*, 29, 1303-10.
- Angus, D. C., Linde-Zwirble, W. T., Lidicker, J., Clermont, G., Carcillo, J. & Pinsky, M. R. 2001b. Epidemiology of severe sepsis in the United States: analysis of incidence, outcome, and associated costs of care. *Critical Care Medicine-Baltimore-*, 29, 1303-1310.
- Aoyagi, T. 2003. Pulse oximetry: its invention, theory, and future. *Journal of anesthesia*, 17, 259-266.
- Aoyagi, T. & Miyasaka, K. 2002. Pulse oximetry: its invention, contribution to medicine, and future tasks. *Anesth Analg*, 94, S1-3.
- Astiz, M. E., Degent, G. E., Lin, R. Y. & Rackow, E. C. 1995. Microvascular function and rheologic changes in hyperdynamic sepsis. *Crit Care Med*, 23, 265-71.
- Astiz, M. E., Tilly, E., Rackow, E. D. & Weil, M. H. 1991. Peripheral vascular tone in sepsis. *Chest*, 99, 1072-5.
- Awad, A. A., Haddadin, A. S., Tantawy, H., Badr, T. M., Stout, R. G., Silverman, D. G. & Shelley, K. H. 2007. The relationship between the photoplethysmographic waveform and systemic vascular resistance. *Journal of clinical monitoring and computing*, 21, 365-372.

- Bagha, S. & Shaw, L. 2011. A real time analysis of PPG signal for measurement of SpO₂ and pulse rate. *International journal of computer applications*, 36, 45-50.
- Barcroft, H. & Edholm, O. G. 1943. The effect of temperature on blood flow and deep temperature in the human forearm. *The Journal of Physiology*, 102, 5-20.
- Bardoň, P., Školoudík, D., Langová, K., Herzig, R. & Kaňovský, P. 2010. Changes in blood flow velocity in the radial artery during 1-hour ultrasound monitoring with a 2-MHz transcranial probe—A pilot study. *Journal of Clinical Ultrasound*, 38, 493-496.
- Barnato, A. E., Alexander, S. L., Linde-Zwirble, W. T. & Angus, D. C. 2008. Racial variation in the incidence, care, and outcomes of severe sepsis: analysis of population, patient, and hospital characteristics. *American journal of respiratory and critical care medicine*, 177, 279-284.
- Batchelder, P. B. & Raley, D. M. 2007. Maximizing the laboratory setting for testing devices and understanding statistical output in pulse oximetry. *Anesthesia & Analgesia*, 105, S85-S94.
- Bateman, R. M., Sharpe, M. D. & Ellis, C. G. 2003. Bench-to-bedside review: microvascular dysfunction in sepsis--hemodynamics, oxygen transport, and nitric oxide. *Crit Care*, 7, 359-73.
- Bateman, R. M., Sharpe, M. D., Jagger, J. E. & Ellis, C. G. 2015. Sepsis impairs microvascular autoregulation and delays capillary response within hypoxic capillaries. *Critical Care*, 19, 1-14.
- Bateman, R. M., Tokunaga, C., Kareco, T., Dorscheid, D. R. & Walley, K. R. 2007. Myocardial hypoxia-inducible HIF-1 α , VEGF, and GLUT1 gene expression is associated with microvascular and ICAM-1 heterogeneity during endotoxemia. *American Journal of Physiology-Heart and Circulatory Physiology*, 293, H448-H456.
- Bauer, P. R. 2002. Microvascular responses to sepsis: clinical significance. *Pathophysiology*, 8, 141-148.
- Bennett, N. P. 1998. Technology Overview: SpO₂ Monitors with Oxismart Advanced Signal Processing and Alarm Management Technology. *Pleasanton, CA*.
- Bergstrand, S., Lindberg, L. G., Ek, A. C., Linden, M. & Lindgren, M. 2009. Blood flow measurements at different depths using photoplethysmography and laser Doppler techniques. *Skin Research and Technology*, 15, 139-147.
- Bloomfield, E. L. 2003. The impact of economics on changing medical technology with reference to critical care medicine in the United States. *Anesth Analg*, 96, 418-25.
- Bloos, F. & Reinhart, K. 2005. Venous oximetry. *Intensive Care Med*, 31, 911-3.
- Boerma, E. C., Kuiper, M. A., Kingma, W. P., Egbers, P. H., Gerritsen, R. T. & Ince, C. 2008. Disparity between skin perfusion and sublingual microcirculatory alterations in severe sepsis and septic shock: a prospective observational study. *Intensive care medicine*, 34, 1294-1298.
- Boerma, E. C., Van Der Voort, P. H. J. & Ince, C. 2005. Sublingual microcirculatory flow is impaired by the vasopressin-analogue terlipressin in a patient with catecholamine-resistant septic shock. *Acta anaesthesiologica scandinavica*, 49, 1387-1390.
- Bohnhorst, B., Lange, M., Bartels, D. B., Bejo, L., Hoy, L. & Peter, C. 2012. Procalcitonin and valuable clinical symptoms in the early detection of neonatal late-onset bacterial infection. *Acta Paediatrica*, 101, 19-25.
- Bonanno, F. G. 2011. Clinical pathology of the shock syndromes. *Journal of emergencies, trauma, and shock*, 4, 233.

- Bone, R., Balk, R., Cerra, F., Dellinger, R., Fein, A., Knaus, W., Schein, R., Sibbald, W., Abrams, J. & Bernard, G. 1992. American-College of Chest Physicians Society of Critical Care Medicine Consensus Conference-definitions for sepsis and organ failure and guidelines for the use of innovative therapies in sepsis. *Critical care medicine*, 20, 864-874.
- Bornmyr, S., Svensson, H., Lilja, B. & Sundkvist, G. 1997. Skin temperature changes and changes in skin blood flow monitored with laser Doppler flowmetry and imaging: a methodological study in normal humans. *Clinical Physiology*, 17, 71-81.
- Braun, L., Riedel, A. A. & Cooper, L. M. 2004. Severe sepsis in managed care: analysis of incidence, one-year mortality, and associated costs of care. *Journal of Managed Care Pharmacy*, 10, 521-530.
- Briers, J. D. 2001. Laser Doppler, speckle and related techniques for blood perfusion mapping and imaging. *Physiological measurement*, 22, R35.
- Budidha, K. & Kyriacou, P. A. 2014. The human ear canal: investigation of its suitability for monitoring photoplethysmographs and arterial oxygen saturation. *Physiol Meas*, 35, 111-28.
- Cannesson, M., Desebbe, O., Hachemi, M., Jacques, D., Bastien, O. & Lehut, J. J. 2007. Respiratory variations in pulse oximeter waveform amplitude are influenced by venous return in mechanically ventilated patients under general anaesthesia. *Eur J Anaesthesiol*, 24, 245-51.
- Cannesson, M. & Talke, P. 2009. Recent advances in pulse oximetry. *F1000 Medicine Reports*, 1, 66.
- Caro, C. G., Pedley, T., Schroter, R., Seed, W. & Parker, K. 2012. *The mechanics of the circulation*, Cambridge University Press, New York 978-0-521-15177-1.
- Carpentier, P. 1998. New techniques for clinical assessment of the peripheral microcirculation. *Drugs*, 58, 17-22.
- Carrigan, S. D., Scott, G. & Tabrizian, M. 2004. Toward resolving the challenges of sepsis diagnosis. *Clin Chem*, 50, 1301-14.
- Casciani, J. R., Mannheimer, P. D., Nierlich, S. L. & Ruskewicz, S. J. 2008. Pulse oximeter and sensor optimized for low saturation. Google Patents.
- Cecconi, M., De Backer, D., Antonelli, M., Beale, R., Bakker, J., Hofer, C., Jaeschke, R., Mebazaa, A., Pinsky, M. R. & Teboul, J. L. 2014. Consensus on circulatory shock and hemodynamic monitoring. Task force of the European Society of Intensive Care Medicine. *Intensive care medicine*, 40, 1795-1815.
- Cennini, G., Arguel, J., Akşit, K. & Van Leest, A. 2010. Heart rate monitoring via remote photoplethysmography with motion artifacts reduction. *Optics express*, 18, 4867-4875.
- Chan, F.-C. D. 2002. *Non-invasive venous oximetry through venous blood volume modulation*. Doctor of Philosophy, PhD Thesis, Loughborouh University.
- Chan, F. C. D., Hayes, M. J. & Smith, P. R. 2007. *Venous pulse oximetry*. US 10/502,758.Grant. US7263395B2.
- Chan, T. & Gu, F. 2011. Early diagnosis of sepsis using serum biomarkers. *Expert Rev Mol Diagn*, 11, 487-96.
- Chuang, C.-C., Ye, J.-J., Lin, W.-C., Lee, K.-T. & Tai, Y.-T. 2015. Photoplethysmography variability as an alternative approach to obtain heart rate variability information in chronic pain patient. *Journal of clinical monitoring and computing*, 29, 801-806.

- Chung, C.-S., Yang, S., Song, G. Y., Lomas, J., Wang, P., Simms, H. H., Chaudry, I. H. & Ayala, A. 2001. Inhibition of Fas signaling prevents hepatic injury and improves organ blood flow during sepsis. *Surgery*, 130, 339-345.
- Cloete, G., Fourie, P. R. & Scheffer, C. 2013. Development and testing of an artificial arterial and venous pulse oximeter. *Conf Proc IEEE Eng Med Biol Soc*, 2013, 4042-5.
- Cohn, S. M., Nathens, A. B., Moore, F. A., Rhee, P., Puyana, J. C., Moore, E. E. & Beilman, G. J. 2007. Tissue oxygen saturation predicts the development of organ dysfunction during traumatic shock resuscitation. *J Trauma*, 62, 44-54; discussion 54-5.
- Colquhoun, D. A., Tucker-Schwartz, J. M., Durieux, M. E. & Thiele, R. H. 2012. Non-invasive estimation of jugular venous oxygen saturation: a comparison between near infrared spectroscopy and transcutaneous venous oximetry. *Journal of clinical monitoring and computing*, 26, 91-98.
- Cooke, E. D., Bowcock, S. A. & Smith, A. T. 1985. Photoplethysmography of the distal pulp in the assessment of the vasospastic hand. *Angiology*, 36, 33-40.
- Corretti, M. C., Anderson, T. J., Benjamin, E. J., Celermajer, D., Charbonneau, F., Creager, M. A., Deanfield, J., Drexler, H., Gerhard-Herman, M., Herrington, D., Vallance, P., Vita, J. & Vogel, R. 2002. Guidelines for the ultrasound assessment of endothelial-dependent flow-mediated vasodilation of the brachial arteryA report of the International Brachial Artery Reactivity Task Force. *Journal of the American College of Cardiology*, 39, 257-265.
- Corretti, M. C., Plotnick, G. D. & Vogel, R. A. 1995. Technical aspects of evaluating brachial artery vasodilatation using high-frequency ultrasound. *American Journal of Physiology-Heart and Circulatory Physiology*, 268, H1397-H1404.
- Crapo, R. O., Jensen, R. L., Hegewald, M. & Tashkin, D. P. 1999. Arterial Blood Gas Reference Values for Sea Level and an Altitude of 1,400 Meters. *American Journal of Respiratory and Critical Care Medicine*, 160, 1525-1531.
- Croner, R. S., Hoerer, E., Kulu, Y., Hackert, T., Gebhard, M.-M., Herfarth, C. & Klar, E. 2006. Hepatic platelet and leukocyte adherence during endotoxemia. *Critical Care*, 10, R15.
- Cutolo, M., Ferrone, C., Pizzorni, C., Soldano, S., Seriolo, B. & Sulli, A. 2010. Peripheral blood perfusion correlates with microvascular abnormalities in systemic sclerosis: a laser-Doppler and nailfold videocapillaroscopy study. *The Journal of rheumatology*, 37, 1174-1180.
- Daly, S. M. & Leahy, M. J. 2013. 'Go with the flow': a review of methods and advancements in blood flow imaging. *Journal of biophotonics*, 6, 217-255.
- Dassel, A., Graaff, R., Aardema, M., Zijlstra, W. & Aarnoudse, J. 1997. Effect of location of the sensor on reflectance pulse oximetry. *BJOG: An International Journal of Obstetrics & Gynaecology*, 104, 910-916.
- De Backer, D., Creteur, J., Preiser, J. C., Dubois, M. J. & Vincent, J. L. 2002. Microvascular blood flow is altered in patients with sepsis. *Am J Respir Crit Care Med*, 166, 98-104.
- De Backer, D., Donadello, K., Sakr, Y., Ospina-Tascon, G., Salgado, D., Scolletta, S. & Vincent, J. L. 2013. Microcirculatory alterations in patients with severe sepsis: impact of time of assessment and relationship with outcome. *Crit Care Med*, 41, 791-9.
- De Backer, D., Orbegozo Cortes, D., Donadello, K. & Vincent, J.-L. 2014. Pathophysiology of microcirculatory dysfunction and the pathogenesis of septic shock. *Virulence*, 5, 73-79.
- De Kock, J. P. & Tarassenko, L. 1993. Pulse oximetry: Theoretical and experimental models. *Medical and Biological Engineering and Computing*, 31, 291-300.
- Dellinger, R. P., Levy, M. M., Carlet, J. M., Bion, J., Parker, M. M., Jaeschke, R., Reinhart, K., Angus, D. C., Brun-Buisson, C., Beale, R., Calandra, T., Dhainaut, J. F., Gerlach, H.,

- Harvey, M., Marini, J. J., Marshall, J., Ranieri, M., Ramsay, G., Sevransky, J., Thompson, B. T., Townsend, S., Vender, J. S., Zimmerman, J. L. & Vincent, J. L. 2008. Surviving Sepsis Campaign: international guidelines for management of severe sepsis and septic shock: 2008. *Intensive Care Med*, 34, 17-60.
- Demeulenaere, S. 2007. Pulse oximetry: uses and limitations. *The Journal for Nurse Practitioners*, 3, 312-317.
- Derdeyn, C. P., Yundt, K. D., Videen, T. O., Carpenter, D. A., Grubb, R. L. & Powers, W. J. 1998. Increased oxygen extraction fraction is associated with prior ischemic events in patients with carotid occlusion. *Stroke*, 29, 754-758.
- Di Giantomasso, D., May, C. N. & Bellomo, R. 2003. Vital organ blood flow during hyperdynamic sepsis*. *CHEST Journal*, 124, 1053-1059.
- Dickson, J. L., Gunn, C. A. & Chase, J. G. 2014. Humans are horribly variable. *International Journal of Clinical and Medical Imaging*, 1.
- Diniz, P. S., Da Silva, E. A. & Netto, S. L. 2010. *Digital signal processing: system analysis and design*, Cambridge University Press. 1139491571.
- Doerschug, K. C., Delsing, A. S., Schmidt, G. A. & Haynes, W. G. 2007. Impairments in microvascular reactivity are related to organ failure in human sepsis. *American Journal of Physiology - Heart and Circulatory Physiology*, 293, H1065-H1071.
- Dombrovskiy, V., Martin, A., Sunderram, J. & Paz, H. 2007. Occurrence and outcomes of sepsis: influence of race. *Critical care medicine*, 35, 763-768.
- Donnelly, R., Hinwood, D. & London, N. J. M. 2000. Non-invasive methods of arterial and venous assessment. *BMJ : British Medical Journal*, 320, 698-701.
- Dorlas, J. C. & Nijboer, J. A. 1985. Photo-electric plethysmography as a monitoring device in anaesthesia. Application and interpretation. *Br J Anaesth*, 57, 524-30.
- Dorman, T. & Pauldine, R. 2007. Economic stress and misaligned incentives in critical care medicine in the United States. *Crit Care Med*, 35, S36-43.
- Drucker, E. & Krapfenbauer, K. 2013. Pitfalls and limitations in translation from biomarker discovery to clinical utility in predictive and personalised medicine. *Epmaj*, 4, 7.
- Dyszkiewicz, A. & Tendera, M. 2006. Vibration syndrome diagnosis using a cooling test verified by computerized photoplethysmography. *Physiological measurement*, 27, 353.
- Eberhardt, R. T. & Raffetto, J. D. 2005. Chronic venous insufficiency. *Circulation*, 111, 2398-2409.
- Echiadis, A. S., Crabtree, V. P., Bence, J., Hadjinikolaou, L., Alexiou, C., Spyf, T. J. & Hu, S. 2007. Non-invasive measurement of peripheral venous oxygen saturation using a new venous oximetry method: evaluation during bypass in heart surgery. *Physiological Measurement*, 28, 897-911.
- Elgendi, M. 2012. On the Analysis of Fingertip Photoplethysmogram Signals. *Current Cardiology Reviews*, 8, 14-25.
- Ellis, C. G., Bateman, R. M., Sharpe, M. D., Sibbald, W. J. & Gill, R. 2002. Effect of a maldistribution of microvascular blood flow on capillary O₂ extraction in sepsis. *Am J Physiol Heart Circ Physiol*, 282, H156-64.
- Episepsis & Group, S. 2004. EPISEPSIS: a reappraisal of the epidemiology and outcome of severe sepsis in French intensive care units. *Intensive care medicine*, 30, 580-588.
- Esper, A. M., Moss, M., Lewis, C. A., Nisbet, R., Mannino, D. M. & Martin, G. S. 2006. The role of infection and comorbidity: Factors that influence disparities in sepsis. *Critical care medicine*, 34, 2576.

- Fahy, B., Lareau, S. & Sockrider, M. 2007. Patient Information Series: Pulse Oximetry. Available: <http://patients.thoracic.org/information-series/en/resources/ats-patient-ed-pulse-oximetry.pdf>.
- Farquhar, I., Martin, C. M., Lam, C., Potter, R., Ellis, C. G. & Sibbald, W. J. 1996. Decreased Capillary Density in Vivo in Bowel Mucosa of Rats with Normotensive Sepsis. *Journal of Surgical Research*, 61, 190-196.
- Feiner, J. R., Severinghaus, J. W. & Bickler, P. E. 2007. Dark Skin Decreases the Accuracy of Pulse Oximeters at Low Oxygen Saturation: The Effects of Oximeter Probe Type and Gender. *Anesthesia & Analgesia*, 105, S18-S23 10.1213/01.ane.0000285988.35174.d9.
- Finfer, S., Bellomo, R., Lipman, J., French, C., Dobb, G. & Myburgh, J. 2004. Adult-population incidence of severe sepsis in Australian and New Zealand intensive care units. *Intensive care medicine*, 30, 589-596.
- Flaatten, H. 2004. Epidemiology of sepsis in Norway in 1999. *Critical care*, 8, R180.
- Fluck, R. R., Jr., Schroeder, C., Frani, G., Kropf, B. & Engbretson, B. 2003. Does ambient light affect the accuracy of pulse oximetry? *Respir Care*, 48, 677-80.
- Fouzas, S., Priftis, K. N. & Anthracopoulos, M. B. 2011. Pulse oximetry in pediatric practice. *Pediatrics*, 128, 740-752.
- Franceschini, M. A., Boas, D. A., Zourabian, A., Diamond, S. G., Nadgir, S., Lin, D. W., Moore, J. B. & Fantini, S. 2002. Near-infrared spiroximetry: noninvasive measurements of venous saturation in piglets and human subjects. *Journal of Applied Physiology*, 92, 372-384.
- Fu, T.-H., Liu, S.-H. & Tang, K.-T. 2008. Heart rate extraction from photoplethysmogram waveform using wavelet multi-resolution analysis. *Journal of medical and biological engineering*, 28, 229-232.
- Futier, E., Christophe, S., Robin, E., Petit, A., Pereira, B., Desbordes, J., Bazin, J.-E. & Vallet, B. 2011. Use of near-infrared spectroscopy during a vascular occlusion test to assess the microcirculatory response during fluid challenge. *Critical Care*, 15, 1-10.
- Gallen, I. W. & Macdonald, I. A. 1990. Effect of two methods of hand heating on body temperature, forearm blood flow, and deep venous oxygen saturation. *Am J Physiol*, 259, E639-43.
- Gil, E., Orini, M., Bailón, R., Vergara, J., Mainardi, L. & Laguna, P. 2010. Photoplethysmography pulse rate variability as a surrogate measurement of heart rate variability during non-stationary conditions. *Physiological Measurement*, 31, 1271.
- Gill, R. W. 1985. Measurement of blood flow by ultrasound: Accuracy and sources of error. *Ultrasound in Medicine & Biology*, 11, 625-641.
- Ginosar, Y., Weiniger, C., Meroz, Y., Kurz, V., Bdolah-Abram, T., Babchenko, A., Nitzan, M. & Davidson, E. 2009. Pulse oximeter perfusion index as an early indicator of sympathectomy after epidural anesthesia. *Acta Anaesthesiologica Scandinavica*, 53, 1018-1026.
- Goldman, J. M., Petterson, M. T., Kopotic, R. J. & Barker, S. J. 2000. Masimo signal extraction pulse oximetry. *Journal of Clinical Monitoring and Computing*, 16, 475-483.
- Gomez, H., Torres, A., Polanco, P., Kim, H. K., Zenker, S., Puyana, J. C. & Pinsky, M. R. 2008. Use of non-invasive NIRS during a vascular occlusion test to assess dynamic tissue O₂ saturation response. *Intensive Care Med*, 34, 1600-7.
- Gómez, H., Torres, A., Polanco, P., Kim, H. K., Zenker, S., Puyana, J. C. & Pinsky, M. R. 2008. Use of non-invasive NIRS during a vascular occlusion test to assess dynamic tissue O₂ saturation response. *Intensive care medicine*, 34, 1600-1607.
- Gottrup, F. 1994. Physiology and measurement of tissue perfusion. *Ann Chir Gynaecol*, 83, 183-9.

- Graaff, R., Dassel, A., Koelink, M., De Mul, F., Aarnoudse, J. & Zijlstra, W. 1993. Optical properties of human dermis in vitro and in vivo. *Applied optics*, 32, 435-447.
- Gregson, W., Black, M. A., Jones, H., Milson, J., Morton, J., Dawson, B., Atkinson, G. & Green, D. J. 2011. Influence of cold water immersion on limb and cutaneous blood flow at rest. *Am J Sports Med*, 39, 1316-23.
- Groothuis, J. T., Van Vliet, L., Kooijman, M. & Hopman, M. T. E. 2003. *Venous cuff pressures from 30 mmHg to diastolic pressure are recommended to measure arterial inflow by plethysmography*.
- Gutierrez, J. & Theodorou, A. 2012. Oxygen Delivery and Oxygen Consumption in Pediatric Critical Care. In: LUCKING, S. E., MAFFEI, F. A., TAMBURRO, R. F. & THOMAS, N. J. (eds.) *Pediatric Critical Care Study Guide*. Springer London.
- Guyancourt, F. 2014. Type T Reference Tables N.I.S.T Monograph 175 Revised to ITS-90. Available: <http://www.omega.com/temperature/z/pdf/z207.pdf> [Accessed 23/06/2015].
- Hall, J. E. 2006. *Guyton and Hall textbook of medical physiology*, Philadelphia, Elsevier Saunders. 0721602401.
- Hanning, C. D. & Alexander-Williams, J. M. 1995. Pulse oximetry: a practical review. *BMJ : British Medical Journal*, 311, 367-370.
- Hart, D. W., Chinkes, D. L. & Gore, D. C. 2003. Increased tissue oxygen extraction and acidosis with progressive severity of sepsis. *Journal of Surgical Research*, 112, 49-58.
- Hartmut Gehring, M., Me, H. M. & Schmucker, P. 2002. The effects of motion artifact and low perfusion on the performance of a new generation of pulse oximeters in volunteers undergoing hypoxemia. *Respiratory Care*, 47, 48-60.
- Haynes, A. B., Weiser, T. G., Berry, W. R., Lipsitz, S. R., Breizat, A.-H. S., Dellinger, E. P., Herbosa, T., Joseph, S., Kibatala, P. L., Lapitan, M. C. M., Merry, A. F., Moorthy, K., Reznick, R. K., Taylor, B. & Gawande, A. A. 2009. A Surgical Safety Checklist to Reduce Morbidity and Mortality in a Global Population. *New England Journal of Medicine*, 360, 491-499.
- Heck, A. & Hall, V. 1974. An on-line system for measurement of opacity pulse propagation times in atraumatic screening of patients for occlusive vascular disease. *Medical instrumentation*, 9, 88-92.
- Heffernan, K. S., Karas, R. H., Mooney, P. J., Patel, A. R. & Kuvvin, J. T. 2010. Pulse wave amplitude is associated with brachial artery diameter: implications for gender differences in microvascular function. *Vasc Med*, 15, 39-45.
- Hertzman, A. B. 1938. The blood supply of various skin areas as estimated by the photoelectric plethysmograph. *American Journal of Physiology--Legacy Content*, 124, 328-340.
- Higgins, J. L. & Fronek, A. 1986. Photoplethysmographic evaluation of the relationship between skin reflectance and skin blood volume. *J Biomed Eng*, 8, 130-6.
- Hoa, N. T. T., Diep, T. S., Wain, J., Parry, C. M., Hien, T. T., Smith, M. D., Walsh, A. L. & White, N. J. 1998. Community-acquired septicaemia in southern Viet Nam: the importance of multidrug-resistant *Salmonella typhi*. *Transactions of the Royal Society of Tropical Medicine and Hygiene*, 92, 503-508.
- Hood, L. & Friend, S. H. 2011. Predictive, personalized, preventive, participatory (P4) cancer medicine. *Nat Rev Clin Oncol*, 8, 184-7.
- Hosono, M., Suehiro, S., Shibata, T., Sasaki, Y., Kumano, H. & Kinoshita, H. 2000. Duplex scanning to assess radial artery suitability for coronary artery bypass grafting. *The Japanese Journal of Thoracic and Cardiovascular Surgery*, 48, 217-221.

- Huang, F.-H., Yuan, P.-J., Lin, K.-P., Chang, H.-H. & Tsai, C.-L. 2011. Analysis of reflectance photoplethysmograph sensors. *world academy of science, engineering and technology*, 59, 1266-1269.
- Huizenga, C., Zhang, H., Arens, E. & Wang, D. 2004. Skin and core temperature response to partial- and whole-body heating and cooling. *Journal of Thermal Biology*, 29, 549-558.
- Humeau, A., Steenbergen, W., Nilsson, H. & Strömborg, T. 2007. Laser Doppler perfusion monitoring and imaging: novel approaches. *Medical & biological engineering & computing*, 45, 421-435.
- Ifeachor, E. C. & Jervis, B. W. 2002. *Digital Signal Processing: A Practical Approach*, Pearson Education. 0201596199.
- Ince, C. 2005. The microcirculation is the motor of sepsis. *Crit Care*, 9 Suppl 4, S13-9.
- Jacobs, M. J., Jörning, P. J., Beckers, R. C., Ubbink, D. T., Van Kleef, M., Slaaf, D. W. & Reneman, R. S. 1990. Foot salvage and improvement of microvascular blood flow as a result of epidural spinal cord electrical stimulation. *Journal of vascular surgery*, 12, 354-360.
- Jonsson, A. 2006. *New sensor design made to discriminate between tissue blood flow at different tissue depths at the sacral area*.
- Jubran, A. 2009. Pulse oximetry. In: HEDENSTIerna, G., MANCEBO, J., BROCHARD, L. & PINSKY, M. R. (eds.) *Applied Physiology in Intensive Care Medicine*. Springer Berlin Heidelberg.
- Jubran, A. 2015. Pulse oximetry. *Crit Care*, 19, 272.
- Kamat, V. 2002. Pulse oximetry. *Indian J. Anaesth*, 46, 261-268.
- Kamshilin, A. A., Nippolainen, E., Sidorov, I. S., Vasilev, P. V., Erofeev, N. P., Podolian, N. P. & Romashko, R. V. 2015. A new look at the essence of the imaging photoplethysmography. *Scientific reports*, 5.
- Keane, M. & Toole, M. 2003. Miller-Keane Encyclopedia and Dictionary of Medicine, Nursing, and Allied Health, Seventh Edition. *Miller-Keane Encyclopedia and Dictionary of Medicine, Nursing, and Allied Health, Seventh Edition*. . Seventh Edition ed.: Saunders.
- Khan, M., Pretty, C. G., Amies, A. C., Elliott, R., Chiew, Y. S., Shaw, G. M. & Chase, J. G. 2016. Analysing the effects of cold, normal, and warm digits on transmittance pulse oximetry. *Biomedical Signal Processing and Control*, 26, 34-41.
- Khan, M., Pretty, C. G., Amies, A. C., Elliott, R., Shaw, G. M. & Chase, J. G. 2015a. Investigating the Effects of Temperature on Photoplethysmography. *IFAC-PapersOnLine*, 48, 360-365.
- Khan, M., Pretty, C. G., Amies, A. C., Elliott, R. B., Suhaimi, F. M., Shaw, G. M. & Chase, J. G. 2015b. Peripheral venous blood oxygen saturation can be non-invasively estimated using photoplethysmography. Engineering in Medicine and Biology Society (EMBC), 2015 37th Annual International Conference of the IEEE, 25-29 Aug. 2015 6405-6408.
- Kim, J. U., Lee, Y. J., Lee, J. & Kim, J. Y. 2015. Differences in the Properties of the Radial Artery between Cun, Guan, Chi, and Nearby Segments Using Ultrasonographic Imaging: A Pilot Study on Arterial Depth, Diameter, and Blood Flow. *Evidence-Based Complementary and Alternative Medicine*.
- Kim, S., Lee, J., Kim, W., Sun, J., Kwon, M. & Kil, H. 2012. Evaluation of radial and ulnar blood flow after radial artery cannulation with 20-and 22-gauge cannulae using duplex Doppler ultrasound. *Anaesthesia*, 67, 1138-1145.

- Kirschenbaum, L. A., Astiz, M. E., Rackow, E. C., Saha, D. C. & Lin, R. 2000. Microvascular response in patients with cardiogenic shock. *Crit Care Med*, 28, 1290-4.
- Klabunde, R. 2011. *Cardiovascular physiology concepts*, Lippincott Williams & Wilkins. 1451113846.
- Kochi, K., Hojyo, H., Ban, K. & Sueda, T. 2005. A novel endothelial function test using Doppler flow: the snuff-box technique. *Heart Vessels*, 20, 207-11.
- Kunz, A. 2012. Underrated disease keeps killing – World Sepsis Day 2012. NBHAP.
- Kuttila, K. & Niinikoskii, J. 1989. Peripheral perfusion after cardiac surgery. *Critical Care Medicine*, 17, 217-220.
- Kvernebo, K., Megerman, J., Hamilton, G. & Abbott, W. M. 1989. Response of skin photoplethysmography, laser Doppler flowmetry and transcutaneous oxygen tensiometry to stenosis-induced reductions in limb blood flow. *European journal of vascular surgery*, 3, 113-120.
- Kyriacou, P. A., Powell, S., Langford, R. M. & Jones, D. P. 2002. Investigation of oesophageal photoplethysmographic signals and blood oxygen saturation measurements in cardiothoracic surgery patients. *Physiol Meas*, 23, 533-45.
- Laing, R. A., Danisch, L. A. & Young, L. R. 1975. The choroidal eye oximeter: an instrument for measuring oxygen saturation of choroidal blood in vivo. *Biomedical Engineering, IEEE Transactions on*, 183-195.
- Lee, Q., Redmond, S., Chan, G., Middleton, P., Steel, E., Malouf, P., Critoph, C., Flynn, G., O'lane, E. & Lovell, N. 2013. Estimation of cardiac output and systemic vascular resistance using a multivariate regression model with features selected from the finger photoplethysmogram and routine cardiovascular measurements. *BioMedical Engineering OnLine*, 12, 1-15.
- Leung, T. S., Tisdall, M. M., Tachtsidis, I., Smith, M., Delpy, D. T. & Elwell, C. E. 2008. Cerebral tissue oxygen saturation calculated using low frequency haemoglobin oscillations measured by near infrared spectroscopy in adult ventilated patients. *Oxygen Transport to Tissue XXIX*. Springer.
- Levy, M. M., Fink, M. P., Marshall, J. C., Abraham, E., Angus, D., Cook, D., Cohen, J., Opal, S. M., Vincent, J.-L. & Ramsay, G. 2003. 2001 sccm/esicm/accp/ats/sis international sepsis definitions conference. *Intensive care medicine*, 29, 530-538.
- Lifesciences, E. 2002. Understanding Continunous Mixed Venous Oxygen Saturation (SvO₂) monitoring with the Swan-Ganz Oximetry TD System. 2nd ed.: Edwards Lifesciences LLC.
- Lima, A. & Bakker, J. 2005. Noninvasive monitoring of peripheral perfusion. *Intensive Care Med*, 31, 1316-26.
- Lima, A. & Bakker, J. 2011. Near-infrared spectroscopy for monitoring peripheral tissue perfusion in critically ill patients. *Rev Bras Ter Intensiva*, 23, 341-351.
- Lima, A. & Bakker, J. 2015. Clinical assessment of peripheral circulation. *Current Opinion in Critical Care*, 21, 226-231.
- Lima, A., Jansen, T. C., Van Bommel, J., Ince, C. & Bakker, J. 2009. The prognostic value of the subjective assessment of peripheral perfusion in critically ill patients. *Critical care medicine*, 37, 934-938.
- Lima, A., Van Bommel, J., Sikorska, K., Van Genderen, M., Klijn, E., Lesaffre, E., Ince, C. & Bakker, J. 2011. The relation of near-infrared spectroscopy with changes in peripheral circulation in critically ill patients*. *Critical care medicine*, 39, 1649-1654.

- Lima, A. P., Beelen, P. & Bakker, J. 2002. Use of a peripheral perfusion index derived from the pulse oximetry signal as a noninvasive indicator of perfusion. *Critical care medicine*, 30, 1210-1213.
- Lindberg, L.-G. & Oberg, P. A. 1993. Optical properties of blood in motion. *Optical Engineering*, 32, 253-257.
- Lipcsey, M., Woinarski, N. C. & Bellomo, R. 2012. Near infrared spectroscopy (NIRS) of the thenar eminence in anesthesia and intensive care. *Ann Intensive Care*, 2, 11.
- Logason, K., Bärlin, T., Jonsson, M. L., Boström, A., Hårdemark, H. G. & Karacagil, S. 2001. The Importance of Doppler Angle of Insonation on Differentiation Between 50–69% and 70–99% Carotid Artery Stenosis. *European Journal of Vascular and Endovascular Surgery*, 21, 311-313.
- Lu, S., Zhao, H., Ju, K., Shin, K., Lee, M., Shelley, K. & Chon, K. H. 2008. Can photoplethysmography variability serve as an alternative approach to obtain heart rate variability information? *Journal of clinical monitoring and computing*, 22, 23-29.
- Lush, C. W. & Kvietys, P. R. 2000. Microvascular dysfunction in sepsis. *Microcirculation*, 7, 83-101.
- Lynch, J. M., Buckley, E. M., Schwab, P. J., Busch, D. R., Hanna, B. D., Putt, M. E., Licht, D. J. & Yodh, A. G. 2014. Noninvasive Optical Quantification of Cerebral Venous Oxygen Saturation in Humans. *Academic Radiology*, 21, 162-167.
- Mannheimer, P. D. 2007. The light-tissue interaction of pulse oximetry. *Anesth Analg*, 105, S10-7.
- Mannheimer, P. D., Cascini, J., Fein, M. E. & Nierlich, S. L. 1997. Wavelength selection for low-saturation pulse oximetry. *Biomedical Engineering, IEEE Transactions on*, 44, 148-158.
- Markandey, V. 2010. Pulse Oximeter Implementation on the TMS320C5515 DSP Medical Development Kit (MDK). Available: <http://www.ti.com/lit/an/sprab37a/sprab37a.pdf> [Accessed 1 November 2013].
- Martin, G. S., Mannino, D. M., Eaton, S. & Moss, M. 2003. The epidemiology of sepsis in the United States from 1979 through 2000. *New England Journal of Medicine*, 348, 1546-1554.
- Masimo. 2007. Clinical Applications of Perfusion Index. Available: <http://www.masimo.fi/pdf/whitepaper/LAB3410F.pdf> [Accessed 29/11/2014].
- Matson, A., Soni, N. & Sheldon, J. 1991. C-reactive protein as a diagnostic test of sepsis in the critically ill. *Anaesth Intensive Care*, 19, 182-6.
- Mayr, F. B., Yende, S., Linde-Zwirble, W. T., Peck-Palmer, O. M., Barnato, A. E., Weissfeld, L. A. & Angus, D. C. 2010. Infection rate and acute organ dysfunction risk as explanations for racial differences in severe sepsis. *Jama*, 303, 2495-2503.
- Mendelson, Y. 1992. Pulse oximetry: theory and applications for noninvasive monitoring. *Clinical Chemistry*, 38, 1601-7.
- Mendelson, Y. 2003. Pulse oximeter and method of operation. US Patent 20,030,144,584.
- Mendelson, Y. & Kent, J. C. 1989. Variations in optical absorption spectra of adult and fetal haemoglobins and its effect on pulse oximetry. *Biomedical Engineering, IEEE Transactions on*, 36, 844-848.
- Mendelson, Y. & Ochs, B. D. 1988. Noninvasive pulse oximetry utilizing skin reflectance photoplethysmography. *Biomedical Engineering, IEEE Transactions on*, 35, 798-805.
- Mesquida, J., Gruartmoner, G., Martinez, M. L., Masip, J., Sabatier, C., Espinal, C., Artigas, A. & Baigorri, F. 2011. Thenar oxygen saturation and invasive oxygen delivery measurements in critically ill patients in early septic shock. *Shock*, 35, 456-9.

- Miller, F. P., Vandome, A. F. & Mcbrewster, J. 2009. *Beer-Lambert Law*, VDM Publishing. 9786130200602.
- Millikan, G. A. 1942. The oximeter, an instrument for measuring continuously the oxygen saturation of arterial blood in man. *Review of scientific Instruments*, 13, 434-444.
- Mohrman, D. E., Heller, L. J. & Heller, L. J. 2006. *Cardiovascular physiology*, New York, McGraw-Hill Medical. 0071701206.
- Mollison, H. L., Mckay, W. P., Patel, R. H., Kriegler, S. & Negraeff, O. E. 2006. Reactive hyperemia increases forearm vein area. *Canadian Journal of Anesthesia*, 53, 759-763.
- Moore, F. A., Haenel, J. B., Moore, E. E. & Whitehill, T. A. 1992. Incommensurate oxygen consumption in response to maximal oxygen availability predicts postinjury multiple organ failure. *Journal of Trauma and Acute Care Surgery*, 33, 58-66.
- Moore, J. X., Donnelly, J. P., Griffin, R., Safford, M. M., Howard, G., Baddley, J. & Wang, H. E. 2015. Black-white racial disparities in sepsis: a prospective analysis of the REasons for Geographic And Racial Differences in Stroke (REGARDS) cohort. *Critical Care*, 19, 1-10.
- Moran, J., Myburgh, J., Syres, G., Jones, D., Cameron, P., Higgins, A., Finfer, S., Webb, S., Delaney, A. & Cross, A. 2007. The outcome of patients with sepsis and septic shock presenting to emergency departments in Australia and New Zealand.
- Moss, M. 2005. Epidemiology of sepsis: race, sex, and chronic alcohol abuse. *Clinical infectious diseases*, 41, S490-S497.
- Murray, W. B. & Foster, P. A. 1996. The peripheral pulse wave: information overlooked. *J Clin Monit*, 12, 365-77.
- Myint, C., King Hann, L., Kiing Ing, W., Gopalai, A. A. & Min Zin, O. Blood Pressure measurement from Photo-Plethysmography to Pulse Transit Time. Biomedical Engineering and Sciences (IECBES), 2014 IEEE Conference on, 8-10 Dec. 2014 2014. 496-501.
- Nakajima, K., Tamura, T. & Miike, H. 1996. Monitoring of heart and respiratory rates by photoplethysmography using a digital filtering technique. *Med Eng Phys*, 18, 365-72.
- Nakajima, Y., Mizobe, T., Takamata, A. & Tanaka, Y. 2000. Baroreflex modulation of peripheral vasoconstriction during progressive hypothermia in anesthetized humans. *Am J Physiol Regul Integr Comp Physiol*, 279, R1430-6.
- Naslund, J., Pettersson, J., Lundeberg, T., Linnarsson, D. & Lindberg, L. G. 2006. Non-invasive continuous estimation of blood flow changes in human patellar bone. *Med Biol Eng Comput*, 44, 501-9.
- Natalini, G., Rosano, A., Franceschetti, M. E., Facchetti, P. & Bernardini, A. 2006. Variations in arterial blood pressure and photoplethysmography during mechanical ventilation. *Anesthesia & Analgesia*, 103, 1182-1188.
- Neviere, R., Mathieu, D., Chagnon, J. L., Lebleu, N., Millien, J. P. & Wattel, F. 1996. Skeletal muscle microvascular blood flow and oxygen transport in patients with severe sepsis. *American Journal of Respiratory and Critical Care Medicine*, 153, 191-195.
- Nilsson, L., Johansson, A. & Kalman, S. 2003. Macrocirculation is not the sole determinant of respiratory induced variations in the reflection mode photoplethysmographic signal. *Physiol Meas*, 24, 925-37.
- Nioka, S., Kime, R., Sunar, U., Im, J., Izzetoglu, M., Zhang, J., Alacam, B. & Chance, B. 2006. A novel method to measure regional muscle blood flow continuously using NIRS kinetics information. *Dynamic Medicine*, 5, 5.

- Nitzan, M., Babchenko, A., Khanokh, B. & Landau, D. 1998. The variability of the photoplethysmographic signal--a potential method for the evaluation of the autonomic nervous system. *Physiol Meas*, 19, 93-102.
- Nitzan, M., Babchenko, A., Khanokh, B. & Taitelbaum, H. 2000. Measurement of oxygen saturation in venous blood by dynamic near infrared spectroscopy. *J Biomed Opt*, 5, 155-62.
- Nitzan, M., Noach, S., Tobal, E., Adar, Y., Miller, Y., Shalom, E. & Engelberg, S. 2014a. Calibration-free pulse oximetry based on two wavelengths in the infrared - a preliminary study. *Sensors (Basel)*, 14, 7420-34.
- Nitzan, M., Patron, A., Glik, Z. & Weiss, A. T. 2009. Automatic noninvasive measurement of systolic blood pressure using photoplethysmography. *BioMedical Engineering OnLine*, 8, 1-8.
- Nitzan, M., Romem, A. & Koppel, R. 2014b. Pulse oximetry: fundamentals and technology update. *Med Devices (Auckl)*, 7, 231-9.
- Nitzan, M. & Taitelbaum, H. 2008. The measurement of oxygen saturation in arterial and venous blood. *Instrumentation & Measurement Magazine, IEEE*, 11, 9-15.
- Njoum, H. & Kyriacou, P. A. 2013. Investigation of finger reflectance photoplethysmography in volunteers undergoing a local sympathetic stimulation. *Journal of Physics: Conference Series*, 450, 012012.
- Nts, N. T. S. 2011. A Technology Overview of the Nellcor™ OxiMax Pulse Oximetry System. Available:
http://www.covidien.com/imageServer.aspx/doc226941.1.2.3_OxiMax%20whitepaper.pdf?contentID=25496&contenttype=application/pdf [Accessed 22/06/2015].
- O'brien, C. & Montain, S. J. 2003. Hypohydration effect on finger skin temperature and blood flow during cold-water finger immersion. *J Appl Physiol (1985)*, 94, 598-603.
- Oak, S. & Aroul, P. 2015. How to Design Peripheral Oxygen Saturation (SpO₂) and Optical Heart Rate Monitoring (OHRM) Systems Using the AFE4403. Available:
<http://www.ti.com/lit/an/slaa655/slaa655.pdf> [Accessed 10-10-2015].
- Optoelectronics, O. 2013. Dual Emitter / Matching Photodector Series. OSI Optoelectronics
- Ortega, R., Hansen, C. J., Elterman, K. & Woo, A. 2011. Pulse Oximetry. *New England Journal of Medicine*, 364, e33.
- Osmundson, P. J., O'fallon, W. M., Clements, I. P., Kazmier, F. J., Zimmerman, B. R. & Palumbo, P. 1985. Reproducibility of noninvasive tests of peripheral occlusive arterial disease. *Journal of vascular surgery*, 2, 678-683.
- Padkin, A., Goldfrad, C., Brady, A. R., Young, D., Black, N. & Rowan, K. 2003. Epidemiology of severe sepsis occurring in the first 24 hrs in intensive care units in England, Wales, and Northern Ireland. *Critical care medicine*, 31, 2332-2338.
- Pareznik, R., Knezevic, R., Voga, G. & Podbregar, M. 2006. Changes in muscle tissue oxygenation during stagnant ischemia in septic patients. *Intensive Care Med*, 32, 87-92.
- Patton, K. T. 2015. *Anatomy and physiology*, Elsevier Health Sciences. 0323316875.
- Petrov, I., Petrov, Y., Prough, D., Deyo, D., Cicenaite, I. & Esenaliev, R. 2012. Optoacoustic monitoring of cerebral venous blood oxygenation through extracerebral blood. *Biomedical optics express*, 3, 125-136.
- Petterson, M. T., Begnoche, V. L. & Graybeal, J. M. 2007. The effect of motion on pulse oximetry and its clinical significance. *Anesth Analg*, 105, S78-84.

- Philips. 2003. Understanding Pulse Oximetry SpO₂ Concepts. Available: http://incenter.medical.philips.com/doclib/enc/fetch/586262/586457/Understanding_Pulse_Oximetry.pdf?nodeid%3D586458%26vernum%3D2 [Accessed 24/02/2016].
- Phillips, J. P., Belhaj, A., Shafqat, K., Langford, R. M., Shelley, K. H. & Kyriacou, P. A. 2012. Modulation of finger photoplethysmographic traces during forced respiration: venous blood in motion? *Conf Proc IEEE Eng Med Biol Soc*, 2012, 3644-7.
- Podbregar, M. & Mozina, H. 2007. Skeletal muscle oxygen saturation does not estimate mixed venous oxygen saturation in patients with severe left heart failure and additional severe sepsis or septic shock. *Crit Care*, 11, R6.
- Pyke, K. E. & Tschakovsky, M. E. 2007. Peak vs. total reactive hyperemia: which determines the magnitude of flow-mediated dilation? *Journal of Applied Physiology*, 102, 1510-1519.
- Reddy, K. A., George, B., Mohan, N. M. & Kumar, V. J. 2011. A Novel Method for the Measurement of Oxygen Saturation in Arterial Blood. *2011 Ieee International Instrumentation and Measurement Technology Conference (I2mtc)*, 364-368.
- Rheineck-Leyssius, A. T. & Kalkman, C. J. 1999. Advanced pulse oximeter signal processing technology compared to simple averaging. II. Effect on frequency of alarms in the postanesthesia care unit. *J Clin Anesth*, 11, 196-200.
- Rivas, A., Samón, R., Ibrik, O., Martínez-Cercós, R. & Viladoms, J. 2007. Noninvasive assessment of forearm vessels by color Doppler ultrasonography (CDU) before and after creation of radiocephalic fistula (RCF). *Nefrologia*, 27.
- Rivers, E., Nguyen, B., Havstad, S., Ressler, J., Muzzin, A., Knoblich, B., Peterson, E., Tomlanovich, M. & Early Goal-Directed Therapy Collaborative, G. 2001. Early goal-directed therapy in the treatment of severe sepsis and septic shock. *N Engl J Med*, 345, 1368-77.
- Roberts, V. 1982. Photoplethysmography-fundamental aspects of the optical properties of blood in motion. *Transactions of the Institute of Measurement and Control*, 4, 101-106.
- Roggan, A., Friebel, M., Do'Rschel, K., Hahn, A. & Mu"ller, G. 1999. Optical Properties of Circulating Human Blood in the Wavelength Range 400–2500 nm. *Journal of Biomedical Optics*, 4, 36-46.
- Ross, F. 1999. Noninvasive Optical Monitoring. *The Biomedical Engineering Handbook, Second Edition. 2 Volume Set*. CRC Press.
- Rostand, S. G., Kirk, K. A. & Rutsky, E. A. 1984. Dialysis-associated ischemic heart disease: Insights from coronary angiography. *Kidney International*, 25, 653-659.
- Rusch, T. L., Sankar, R. & Scharf, J. E. 1996. Signal processing methods for pulse oximetry. *Comput Biol Med*, 26, 143-59.
- Sair, M., Etherington, P. J., Peter Winlove, C. & Evans, T. W. 2001. Tissue oxygenation and perfusion in patients with systemic sepsis. *Crit Care Med*, 29, 1343-9.
- Sakr, Y., Dubois, M. J., De Backer, D., Creteur, J. & Vincent, J. L. 2004. Persistent microcirculatory alterations are associated with organ failure and death in patients with septic shock. *Crit Care Med*, 32, 1825-31.
- Sandberg, M., Zhang, Q., Styf, J., Gerdle, B. & Lindberg, L. G. 2005. Non-invasive monitoring of muscle blood perfusion by photoplethysmography: evaluation of a new application. *Acta physiologica scandinavica*, 183, 335-343.
- Schnapp, L. M. & Cohen, N. H. 1990. PULSE oximetry. uses and abuses. *Chest*, 98, 1244-1250.
- Schoevers, J., Scheffer, C. & Dippenaar, R. 2009. Low-oxygen-saturation quantification in human arterial and venous circulation. *IEEE Trans Biomed Eng*, 56, 846-54.

- Secor, D., Li, F., Ellis, C. G., Sharpe, M. D., Gross, P. L., Wilson, J. X. & Tyml, K. 2010. Impaired microvascular perfusion in sepsis requires activated coagulation and P-selectin-mediated platelet adhesion in capillaries. *Intensive care medicine*, 36, 1928-1934.
- Seifert, J., Sloane, D. & Ratner, A. 2005. *Concepts in medical physiology*, Lippincott Williams & Wilkins. 078174489X.
- Selvaraj, N., Jaryal, A., Santhosh, J., Deepak, K. K. & Anand, S. 2008. Assessment of heart rate variability derived from finger-tip photoplethysmography as compared to electrocardiography. *Journal of medical engineering & technology*, 32, 479-484.
- Severinghaus, J. W. 2007. Takuo Aoyagi: discovery of pulse oximetry. *Anesth Analg*, 105, S1-4, tables of contents.
- Shafique, M. 2011. *Investigation of photoplethysmography and arterial blood oxygen saturation during artificially induced peripheral hypoperfusion utilising multimode photometric sensors*. PhD Thesis, City University.
- Shafqat, K., Langford, R. & Kyriacou, P. 2015. Estimation of instantaneous venous blood saturation using the photoplethysmograph waveform. *Physiological Measurement*, 36, 2203.
- Shafqat, K., Langford, R. M., Pal, S. K. & Kyriacou, P. A. 2012. Estimation of venous oxygenation saturation using the finger Photoplethysmograph (PPG) waveform. *Conf Proc IEEE Eng Med Biol Soc*, 2012, 2905-8.
- Shelley, K. & Shelley, S. 2001. Pulse oximeter waveform: photoelectric plethysmography. *Clinical Monitoring, Carol Lake, R. Hines, and C. Blitt, Eds.: WB Saunders Company*, 420-428.
- Shelley, K. H. 2007. Photoplethysmography: beyond the calculation of arterial oxygen saturation and heart rate. *Anesthesia & Analgesia*, 105, S31-S36.
- Shelley, K. H., Alian, A. A., Shelley, A. J., Walton, Z. D. & Silverman, D. G. 2011. A Method for Determining the Peripheral Venous/Arterial Compliance Ratio. Department of Anesthesiology, Yale University School of Medicine, New Haven, CT 06520.
- Shelley, K. H., Silverman, D. G. & Shelley, A. J. 2014. Volume status monitor: peripheral venous pressure, hypervolemia and coherence analysis. Google Patents.
- Sherebrin, M. H. & Sherebrin, R. Z. 1990. Frequency analysis of the peripheral pulse wave detected in the finger with a photoplethysmograph. *Biomedical Engineering, IEEE Transactions on*, 37, 313-317.
- Silva, E., Pedro, M. A., Sogayar, A. C., Mohovic, T., Silva, C. L., Janiszewski, M., Cal, R. G., De Sousa, É. F., Abe, T. P. & De Andrade, J. 2004. Brazilian sepsis epidemiological study (BASES study). *Critical Care*, 8, R251.
- Sinex, J. E. Pulse oximetry: Principles and limitations. *The American Journal of Emergency Medicine*, 17, 59-66.
- Sinex, J. E. 1999. Pulse oximetry: Principles and limitations. *The American Journal of Emergency Medicine*, 17, 59-66.
- Skarda, D. E., Mulier, K. E., Myers, D. E., Taylor, J. H. & Beilman, G. J. 2007. Dynamic near-infrared spectroscopy measurements in patients with severe sepsis. *Shock*, 27, 348-53.
- Song, S., Cho, J., Oh, H., Lee, J. & Kim, I. Estimation of blood pressure using photoplethysmography on the wrist. *Computers in Cardiology*, 2009, 2009. IEEE, 741-744.
- Sørensen, H., Secher, N. H. & Rasmussen, P. 2013. A note on arterial to venous oxygen saturation as reference for NIRS-determined frontal lobe oxygen saturation in healthy humans. *Frontiers in Physiology*, 4, 403.

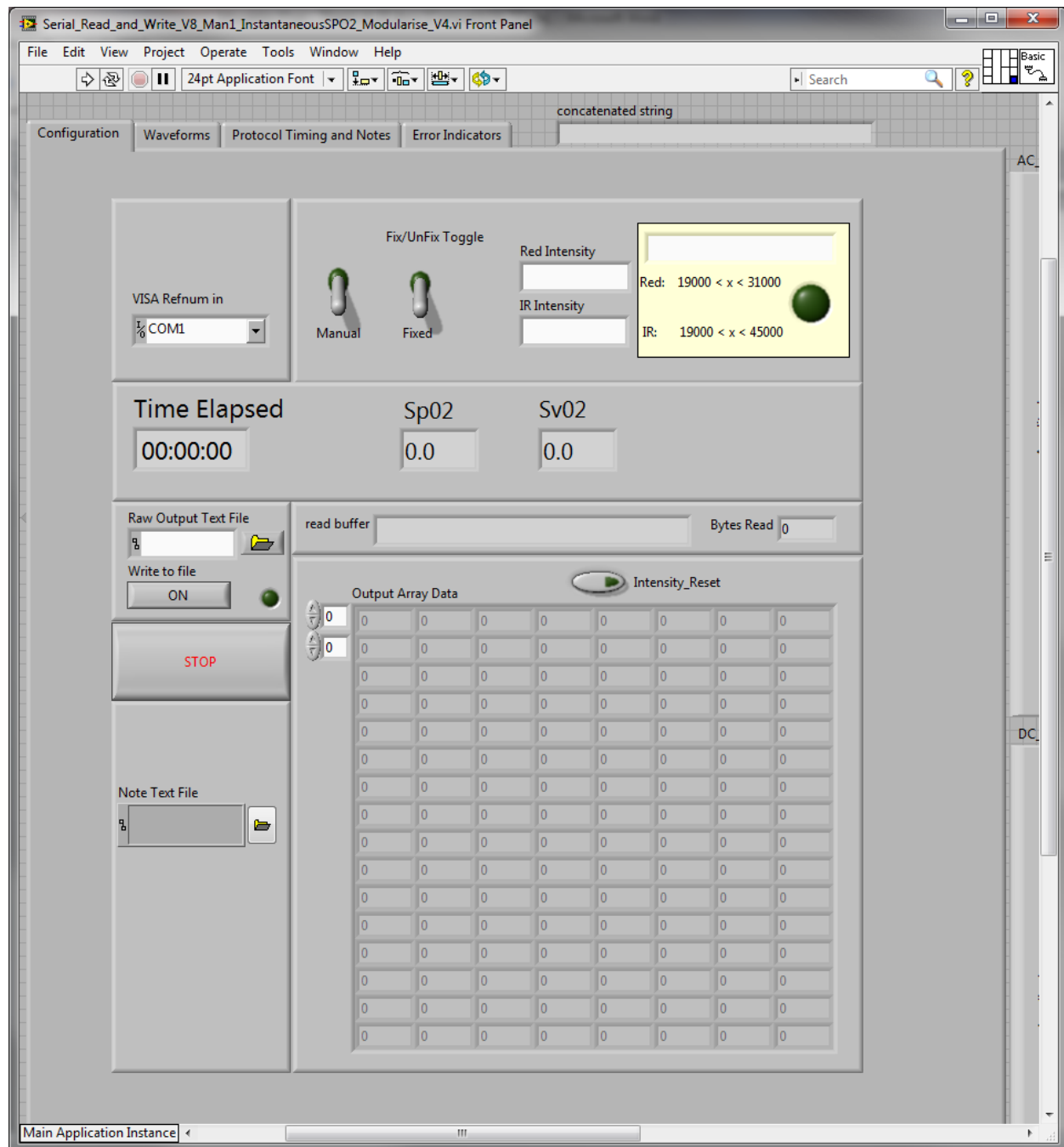
- Spronk, P. E., Zandstra, D. F. & Ince, C. 2004. Bench-to-bedside review: sepsis is a disease of the microcirculation. *Crit Care*, 8, 462-8.
- Squire, J. 1940. Instrument for measuring quantity of blood and its degree of oxygenation in web of the hand. *Clin Sci*, 4, 331-339.
- Staff, N. T. 2011. A Technology Overview of the Nellcor™ OxiMax Pulse Oximetry System. Available:
http://www.covidien.com/imageServer.aspx/doc226941.1.2.3_OxiMax%20whitepaper.pdf?contentID=25496&contentType=application/pdf [Accessed 12/1/2015].
- Starr, M. E. & Saito, H. 2014. Sepsis in Old Age: Review of Human and Animal Studies. *Aging Dis*, 5, 126-36.
- Talke, P. & Stapelfeldt, C. 2006. Effect of peripheral vasoconstriction on pulse oximetry. *J Clin Monit Comput*, 20, 305-9.
- Tamura, T., Maeda, Y., Sekine, M. & Yoshida, M. 2014. Wearable Photoplethysmographic Sensors—Past and Present. *Electronics*, 3, 282-302.
- Taylor, B. N. & Kuyatt, C. E. 1994. *Guidelines for evaluating and expressing the uncertainty of NIST measurement results*, US Department of Commerce, Technology Administration, National Institute of Standards and Technology Gaithersburg, MD.
- Teboul, J. L. & Monnet, X. 2015. Assessing Global Perfusion During Sepsis: SvO₂, Venoarterial PCO₂ Gap or Both? In: VINCENT, J.-L. (ed.) *Annual Update in Intensive Care and Emergency Medicine 2015*. Springer International Publishing.
- Thiele, R. H., Tucker-Schwartz, J. M., Lu, Y., Gillies, G. T. & Durieux, M. E. 2011. Transcutaneous Regional Venous Oximetry: A Feasibility Study. *Anesthesia & Analgesia*, 112, 1353-1357 10.1213/ANE.0b013e3182166a26.
- Thorsson, O., Lilja, B., Ahlgren, L., Hemdal, B. & Westlin, N. 1985. The effect of local cold application on intramuscular blood flow at rest and after running. *Medicine and science in sports and exercise*, 17, 710-713.
- Thrush, A. & Hartshorne, T. 1999. *Peripheral Vascular Ultrasound: How, Why and When*, Churchill Livingstone. 9780443060496.
- Thrush, A. & Hartshorne, T. 2009. *Vascular Ultrasound: How, why and when*, Elsevier Health Sciences. 0080982573.
- Tic, T. I. C. S. 1997. Standards for Intensive Care Units. Available:
http://www.md.ucl.ac.be/didac/hosp/architec/UK_Intensive_care.pdf [Accessed 25/06/2015].
- Tremper, K. K. & Barker, S. J. 1989. Pulse Oximetry. *Anesthesiology*, 70, 98-108.
- Trzeciak, S. & De Backer, D. 2007. Modulation of the sepsis inflammatory response by resuscitation: The missing link between cytopathic and hypoxic hypoxia? *Crit Care Med*, 35, 2206-7.
- Trzeciak, S., Dellinger, R. P., Parrillo, J. E., Guglielmi, M., Bajaj, J., Abate, N. L., Arnold, R. C., Colilla, S., Zanotti, S., Hollenberg, S. M., Microcirculatory Alterations In, R. & Shock, I. 2007. Early microcirculatory perfusion derangements in patients with severe sepsis and septic shock: relationship to hemodynamics, oxygen transport, and survival. *Ann Emerg Med*, 49, 88-98, 98 e1-2.
- Uehata, A., Lieberman, E., Gerhard, M., Anderson, T., Ganz, P., Polak, J., Creager, M. & Yeung, A. 1996. Noninvasive assessment of endothelium-dependent flow-mediated dilation of the brachial artery. *Vascular medicine (London, England)*, 2, 87-92.

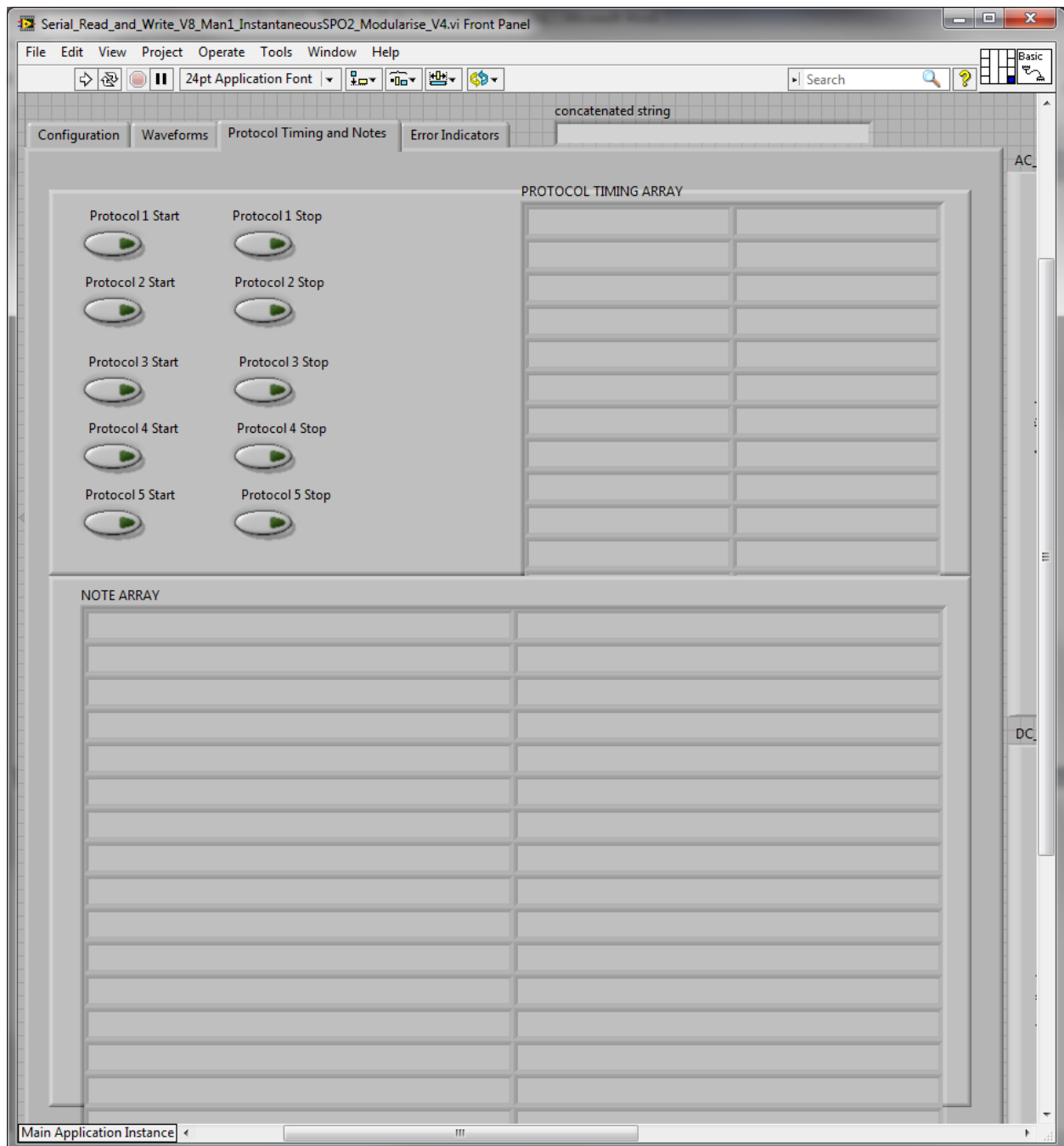
- Uzzan, B., Cohen, R., Nicolas, P., Cucherat, M. & Perret, G. Y. 2006. Procalcitonin as a diagnostic test for sepsis in critically ill adults and after surgery or trauma: a systematic review and meta-analysis. *Crit Care Med*, 34, 1996-2003.
- Valdez-Lowe, C., Ghareeb, S. A. & Artinian, N. T. 2009. Pulse oximetry in adults. *AJN The American Journal of Nursing*, 109, 52-59.
- Van Beekvelt, M. C., Colier, W., Wevers, R. A. & Van Engelen, B. G. 2001. Performance of near-infrared spectroscopy in measuring local O₂ consumption and blood flow in skeletal muscle. *Journal of Applied Physiology*, 90, 511-519.
- Van Den Bruel, A., Haj-Hassan, T., Thompson, M., Buntinx, F., Mant, D. & Investigators, E. R. N. O. R. S. I. 2010. Diagnostic value of clinical features at presentation to identify serious infection in children in developed countries: a systematic review. *The Lancet*, 375, 834-845.
- Van Genderen, M. E., Lima, A., Akkerhuis, M., Bakker, J. & Van Bommel, J. 2012a. Persistent peripheral and microcirculatory perfusion alterations after out-of-hospital cardiac arrest are associated with poor survival. *Critical care medicine*, 40, 2287-2294.
- Van Genderen, M. E., Paauwe, J., De Jonge, J., Van Der Valk, R. J., Lima, A., Bakker, J. & Van Bommel, J. 2014. Clinical assessment of peripheral perfusion to predict postoperative complications after major abdominal surgery early: a prospective observational study in adults. *Critical Care*, 18, 1.
- Van Genderen, M. E., Van Bommel, J. & Lima, A. 2012b. Monitoring peripheral perfusion in critically ill patients at the bedside. *Curr Opin Crit Care*, 18, 273-9.
- Verdant, C. L., De Backer, D., Bruhn, A., Clausi, C. M., Su, F., Wang, Z., Rodriguez, H., Pries, A. R. & Vincent, J.-L. 2009. Evaluation of sublingual and gut mucosal microcirculation in sepsis: A quantitative analysis*. *Critical care medicine*, 37, 2875-2881.
- Vincent, J.-L., Moraine, J.-J. & Van Der Linden, P. 1988. Toe temperature versus transcutaneous oxygen tension monitoring during acute circulatory failure. *Intensive care medicine*, 14, 64-68.
- Vincent, J., Sakr, Y., Sprung, C. L., Ranieri, V. M., Reinhart, K., Gerlach, H., Moreno, R., Carlet, J., Le Gall, J. & Payen, D. 2006. Sepsis in European intensive care units: results of the SOAP study. *CRITICAL CARE MEDICINE-BALTIMORE-*, 34, 344.
- Vincent, J. L. & De Backer, D. 2004. Oxygen transport-the oxygen delivery controversy. *Intensive Care Med*, 30, 1990-6.
- Vincent, J. L., Macias, W. L., Levy, M. M., Russell, J. A., Trzaskoma, B. L. & Eliezer, S. 2003. Early response to therapy predicts eventual survival in severe sepsis. *Intensive Care Medicine*, 29, S74-S74.
- Vowden, K. & Vowden, P. 2004. Hand-held Doppler Ultrasound: the assessment of lower limb arterial and venous disease. *Cardiff: Huntleigh Healthcare*.
- Walley, K. R. 1996. Heterogeneity of oxygen delivery impairs oxygen extraction by peripheral tissues: theory. *Journal of Applied Physiology*, 81, 885-894.
- Walton, Z. D. 2010. Measuring Venous Oxygen Saturation Using the Photoplethysmograph Waveform.
- Walton, Z. D., Kyriacou, P. A., Silverman, D. G. & Shelley, K. H. 2010. Measuring venous oxygenation using the photoplethysmograph waveform. *J Clin Monit Comput*, 24, 295-303.
- Wang, L., Pickwell-Macpherson, E., Liang, Y. P. & Zhang, Y. T. 2009. Noninvasive cardiac output estimation using a novel photoplethysmogram index. *Conf Proc IEEE Eng Med Biol Soc*, 2009, 1746-9.

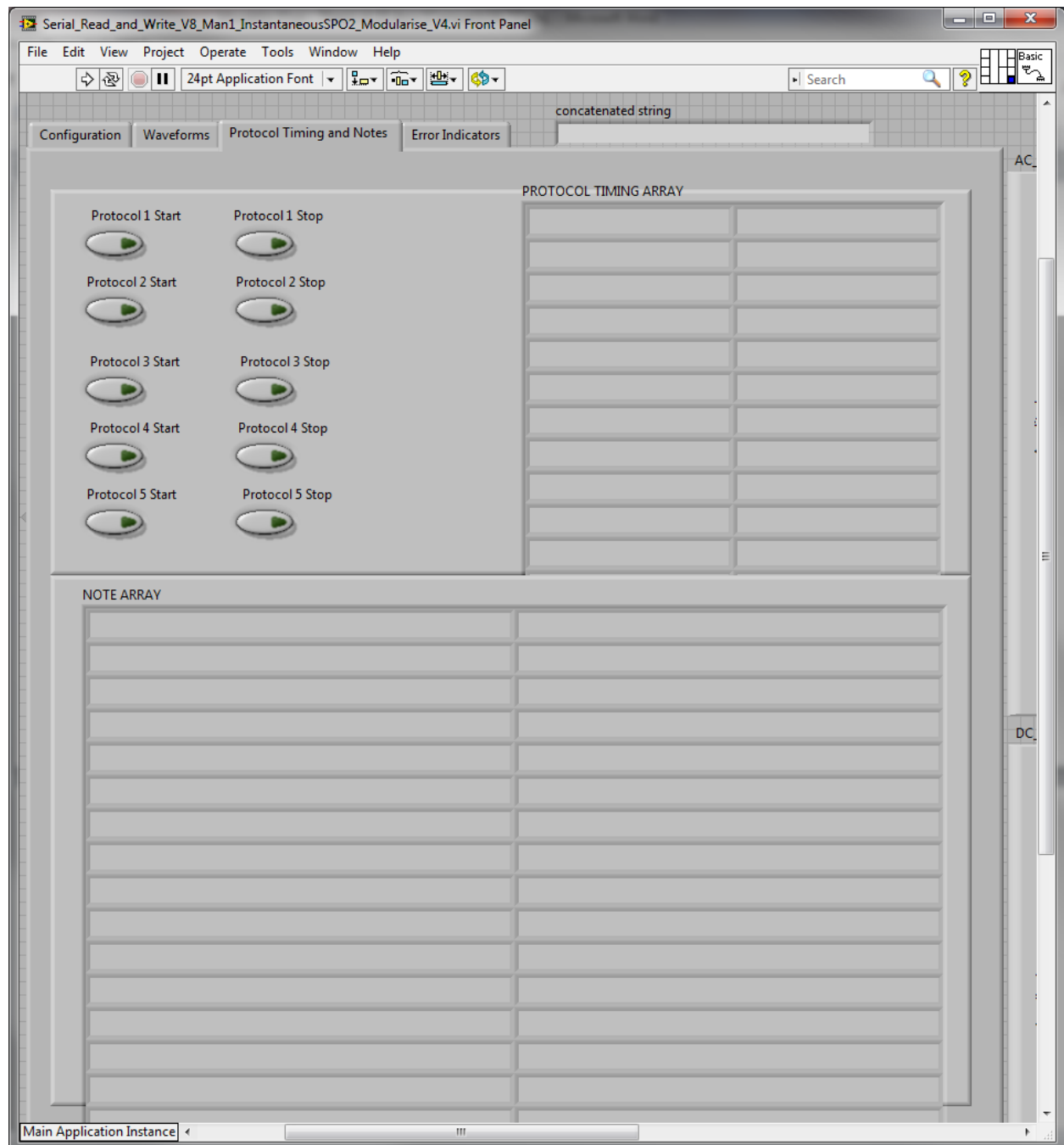
- Wang, L., Poon, C. C. & Zhang, Y. T. 2010. The non-invasive and continuous estimation of cardiac output using a photoplethysmogram and electrocardiogram during incremental exercise. *Physiol Meas*, 31, 715-26.
- Wang, P., Ba, Z. F., Cioffi, W. G., Bland, K. I. & Chaudry, I. H. 1998. The pivotal role of adrenomedullin in producing hyperdynamic circulation during the early stage of sepsis. *Archives of Surgery*, 133, 1298-1304.
- Wang, P. & Liu, Q. 2011. *Biomedical sensors and measurement*, Springer Science & Business Media. 3642195253.
- Wardhan, R. & Shelley, K. 2009. Peripheral venous pressure waveform. *Curr Opin Anaesthesiol*, 22, 814-21.
- Webster, J. G. 2002. *Design of pulse oximeters*, CRC Press. 1420050796.
- Wester, A. L., Dunlop, O., Melby, K. K., Dahle, U. R. & Wyller, T. B. 2013. Age-related differences in symptoms, diagnosis and prognosis of bacteremia. *BMC Infect Dis*, 13, 346.
- Wieben, O. 1997. Light absorbance in pulse oximetry. *Design of pulse oximeters*, 4, 40-55.
- Williams, A. J. 1998. ABC of oxygen: assessing and interpreting arterial blood gases and acid-base balance. *British Medical Journal*, 317, 1213.
- Wood, E. H., Sutterer, W. & Cronin, L. 1950. Oximetry. *Medical physics*, 2, 664-680.
- Yang, Y. X., Xie, B. S., Zhou, Z. X., Liu, J. N., Xue, Y. Y. & Lv, G. L. 1998. Computer analysis system of blood oxygen saturation in an animal hypoxia model. *Medical and Biological Engineering and Computing*, 36, 355-358.
- Young, J. D. & Cameron, E. M. 1995. Dynamics of skin blood flow in human sepsis. *Intensive Care Med*, 21, 669-74.
- Yousef, Q., Reaz, M. & Ali, M. a. M. 2012. The analysis of PPG morphology: investigating the effects of aging on arterial compliance. *Measurement Science Review*, 12, 266-271.
- Yoxall, C. & Weindling, A. 1997. Measurement of venous oxyhaemoglobin saturation in the adult human forearm by near infrared spectroscopy with venous occlusion. *Medical and Biological Engineering and Computing*, 35, 331-336.
- Zaja, J. 2007. Venous oximetry. *Signa Vitae*, 2, 6-10.
- Zervides, C., Narracott, A. J., Lawford, P. V. & Hose, D. R. 2008. The role of venous valves in pressure shielding. *Biomed Eng Online*, 7, 10.1186.
- Zhang, Q., Andersson, G., Lindberg, L. G. & Styf, J. 2004. Muscle blood flow in response to concentric muscular activity vs passive venous compression. *Acta Physiol Scand*, 180, 57-62.
- Zhang, Q., Lindberg, L. G., Kadefors, R. & Styf, J. 2001. A non-invasive measure of changes in blood flow in the human anterior tibial muscle. *Eur J Appl Physiol*, 84, 448-52.

Appendix

Appendix 3.1: PPG acquisition interface tabs







Appendix 5.1: Ethics application information sheet, consent form, and approval

Telephone: +64 22 120 2606 (Musabbir Khan)
+64 3 364 2987 ext 7224 (Geoff Chase)
Email: musabbir.khan@pg.canterbury.ac.nz
geoff.chase@canterbury.ac.nz



Investigate the effect of heat and caffeine on pulse oximeter accuracy for people with cold fingers

INFORMATION SHEET FOR PARTICIPANTS

My name is Musabbir Khan, and I am doing a PhD in Bio-engineering at the University of Canterbury. My research involves use of pulse oximeters. Pulse oximeters are widely used in clinical settings to monitor blood oxygen saturation and heart rate non-invasively. Cold fingers give erroneous pulse oximeter readings because of poor peripheral blood flow. Prior studies have demonstrated that drinking hot tea or coffee improves pulse oximeter accuracy by increasing peripheral blood flow and thus the strength of the signal. Hot water bottle also produced similar affects. To use pulse oximeters clinically for other purposes, it is necessary to know whether it is the caffeine or the temperature of the liquid or increase in skin surface temperature was responsible.

I would like to invite you to participate in this research project.

This means that you understand the following:

- You need to allow the following equipment attached to your hand during the duration of the experiment:
 - i. A non-invasive sensor in the middle finger of your left hand.
 - This will perform data acquisition for non-invasive saturation assessment.
 - Task will be accomplished by Musabbir
 - ii. A surface mount thermocouple probe taped to finger close to the sensor:
 - This will non-intrusively gather temperature reading from the surface of your skin
- You will be asked to consume three common everyday beverages in random order and rest your arm on a hot water bag:
 - Hot water (same temperature as tea/coffee) - *hot liquid with no caffeine*
 - Hot tea/coffee (e.g. Dilmah Ceylon tea) – *hot liquid with caffeine*
 - Cold energy drink (e.g. Red Bull) – *cold liquid with caffeine*

- Hot water bottle (standard supermarket bottles) – *direct heat from contact*
- You should avoid any smoking and/or alcohol consumption at least 4 hours prior to the trial.
- You need to refrain from any physical or strenuous activities at least 1 hour before the experiment.
- You will be seated in a comfortable chair/sofa inside a temperature controlled room (maintained at 20°C – 30°C)
- You have to rest your right arm on a flat surface and make minimum movement with it during the experiment unless advised so.
- You need to stay for the duration of the experiment, approximately 60 min. However you are allowed to take breaks in between if necessary.
- You have the right discontinue anytime during the experiment, subjected to any emergency or distress.

Taking part in this project is voluntary and you can leave at any time if you want, without penalty. The results of this project may be published at a conference and/or journal, and will be publically available through the University of Canterbury library. You will be assigned a number when undertaking the trial so your data will not be identifiable in anyway except to my supervisors and I. I will send you a summary of your data from the trial if you wish.

Data will be stored in an encrypted drive on a secure computer at the University premises. It will be kept for 10 years and then destroyed.

If you have any questions about the study, please contact me (details above) or my senior supervisor Geoff Chase (details above).

If at any time you are unhappy or have concerns about the project, you or your parents can contact the Chair of the University of Canterbury Humans Ethics Committee, University of Canterbury, Private Bag 4800, Christchurch, Email: human-ethics@canterbury.ac.nz

If you would like to take part in this project, please fill out the attached CONSENT FORM on the next page.

Yours sincerely,

Musabbir Khan

Telephone: +64 22 120 2606 (Musabbir Khan)
+64 3 364 2987 ext 7224 (Geoff Chase)

Email: musabbir.khan@pg.canterbury.ac.nz
geoff.chase@canterbury.ac.nz



Investigate the effect of heat and caffeine on pulse oximeter accuracy for people with cold fingers

- Musabbir has explained the experiment to me and answered my questions about it.
- I understand that it is my choice to be part of the project and that I may pull out at any stage.
- I understand that non-invasive data from my finger will also be obtained via finger sensor.
- I understand that temperature reading will be recorded from the skin surface using a non-invasive thermocouple probe.
- I understand that I have to refrain from alcohol consumption or smoking at least 4 hours prior to the study.
- I understand that I should avoid any strenuous physical activity at least 1 hour before the study.
- I understand that I have to follow the designated protocols during the trial.
- I understand that the experiment can take up to 60 min.
- I understand that all the information collected for this project will be kept safe at the University of Canterbury and destroyed after 10 years.
- I understand if I require further information I can contact Musabbir or his supervisor Geoff Chase (details above).
- I note that this project has been reviewed and approved by the University of Canterbury Human Ethics Committee.
- I understand that if I have any complaints, I can contact the Chair of the University of Canterbury Human Ethics Committee, Private Bag, 4800, Christchurch (human-ethics@canterbury.ac.nz)

I would like to request a copy of my results

Yes No

By ticking the above boxes and signing below, I confirm that I understand the project and I am willing to be a participant for it.

Name: _____

Date: _____

Signature: _____

Phone number: _____

Email address: _____



HUMAN ETHICS COMMITTEE

Secretary, Lynda Griffioen
Email: human-ethics@canterbury.ac.nz

Ref: HEC 2015/04/LR-PS

16 February 2015

Musabbir Khan
Department of Mechanical Engineering
UNIVERSITY OF CANTERBURY

Dear Musabbir

Thank you for forwarding to the Human Ethics Committee a copy of the low risk application you have recently made for your research proposal "Investigate the effect of heat and caffeine on pulse oximeter accuracy for people with cold fingers".

I am pleased to advise that this application has been reviewed and I confirm support of the Department's approval for this project.

Please note that this approval is subject to the incorporation of the amendments you have provided in your email of 13 February 2015.

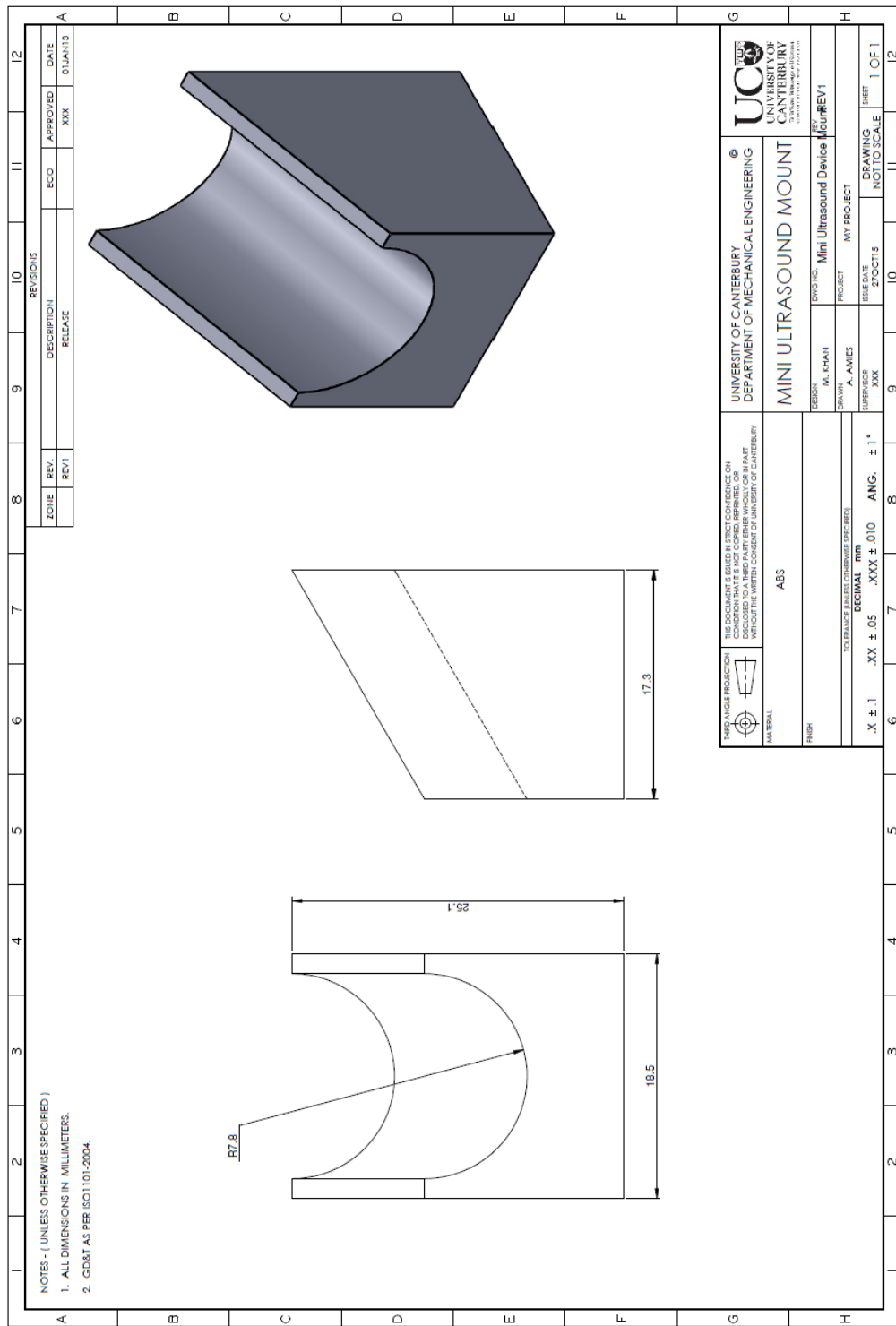
With best wishes for your project.

Yours sincerely

A handwritten signature in black ink, appearing to read 'L. MacDonald'.

Lindsey MacDonald
Chair, Human Ethics Committee

Appendix 6.1: Manufacturing schematic for the BV-520T probe mount



Appendix 6.1: Ethics application information sheet, consent form, and approval



Department of Mechanical Engineering
Telephone: +64 3 364 2987 ext 7276
Email: musabbir.khan@pg.canterbury.ac.nz
23-02-2016

Monitoring peripheral blood flow using photoplethysmography Information Sheet for participants

My name is Musabir Khan, and I am doing a PhD in Bio-engineering at the University of Canterbury. My research uses pulse oximeters, which are the ubiquitous sensors clipped over the finger. Pulse oximeters are widely used in hospitals to monitor blood oxygen level and heart rate non-invasively. The sensor makes measurement using light transmission through the finger, so no physical harm or puncture is caused.

Pulse oximeters produce photoplethysmograph (PPG) waveform which is rich in physiological information. Recent researches have shown that the PPG can be used to extract blood flow information. This study will help me to assess blood flow changes in the human forearm using PPG by conducting a specific forearm blood flow occlusion test. Another non-intrusive device, a vascular ultrasound Doppler, will be used as a reference measurement and comparison.

If you choose to take part in this study, your involvement in this project will be:

- 1) You must be a healthy adult (18+ years of age) with no pre-existing medical conditions.
- 2) You need to refrain from smoking and strenuous physical activity for 2 hours.
- 3) You will be comfortably seated while resting your left arm on a flat surface, at approximately the same height as your heart, with minimum movement, and breathe normally.
- 4) You need to allow the following equipment to be used on you during the duration of the experiment:
 - a. A non-invasive PPG sensor will be worn on the middle/index of your left hand.
 - b. Application of ultrasound gel and a commercial, non-invasive, vascular Doppler probe to assess blood flow velocity from the radial artery close to the wrist.
 - c. Wear a conventional blood pressure cuff on the left upper arm:
 - i. The cuff will not be inflated during baseline measurement.
 - ii. The cuff pressure will be raised to a very high pressure to prevent blood flow to the arm for a period of 1 min.
 - iii. The pressure will be reduced to from high pressure to low pressure to allow low blood flow for a period of 1 min.
 - iv. The cuff pressure will be completely deflated to allow normal blood flow.
- 5) All PPG and Doppler data will be saved on a secured computer
- 6) The duration of the experiment will be approximately 10 min.

In the performance of the tasks and application of the procedures there are no known significant risks involved. The tightness produced by the pressure cuff in the arm, when it will be inflated, may cause some temporary discomfort ('pins and needles' sensation). If necessary, we will refer you to the University of Canterbury Health Centre. However, any related injury is highly unlikely.

Participation is voluntary and you have the right to withdraw at any stage without penalty. You may ask for your raw data to be returned to you or destroyed at any point. If you withdraw, I will remove information relating to you. However, once analysis of raw data starts on April 2016, it will become increasingly difficult to remove the influence of your data on the results. The results of the project



may be published, but you may be assured of the complete confidentiality of data gathered in this investigation: your identity will not be made public.

To ensure anonymity and confidentiality, you will be assigned a number when undertaking the trial so your data will not be identifiable in anyway except to my supervisors and I. No personal information, video, or audio recordings will be taken. All data will be stored in an encrypted hard disk on a computer, located in a secure office space at the University premises, and destroyed after 10 years. Back up of the data will be stored in an external encrypted hard drive. Identities of participants will not be revealed.

The results of this project may be published at a conference and/or journal, and will be publically available through the University of Canterbury library. The results will also form a chapter of my PhD thesis, which is a public document and will be available through the UC Library.

Please indicate to the researcher on the consent form if you would like to receive a copy of the summary of results of the project via email.

The project is being carried out as part of the PhD research by *Musabbir Khan* under the supervision of *Dist. Prof. Geoffrey Chase*, who can be contacted at geoff.chase@canterbury.ac.nz. He will be pleased to discuss any concerns you may have about participation in this project.

This project has been reviewed and approved by the University of Canterbury Human Ethics Committee, and participants should address any complaints to The Chair, Human Ethics Committee, University of Canterbury, Private Bag 4800, Christchurch (human-ethics@canterbury.ac.nz).

If you agree to participate in the study, you are asked to complete the consent form and return to Musabbir Khan personally or through email at musabbir.khan@pg.canterbury.ac.nz.

Musabbir Khan

Department of Mechanical Engineering
Telephone: +64 3 364 2987 ext 7276
Email: musabbir.khan@pg.canterbury.ac.nz

**Monitoring peripheral blood flow using photoplethysmography
Consent Form for participants**

- I have been given a full explanation of this project and have had the opportunity to ask questions.
- I read and understood the project details provided in the participant's information sheet.
- I understand the pressure cuff inflation on the arm may cause minor discomfort.
- I understand what is required of me if I agree to take part in the research.
- I understand that participation is voluntary and I may withdraw at any time without penalty.
Withdrawal of participation will also include the withdrawal of any information I have provided should this remain practically achievable.
- I understand that any information or opinions I provide will be kept confidential to the researcher and that any published or reported results will not identify the participants. I understand that a thesis is a public document and will be available through the UC Library.
- I understand that all data collected for the study will be kept in locked and secure facilities and/or in password protected electronic form and will be destroyed after 10 years.
- I understand the risks associated with taking part and how they will be managed.
- I understand that I am able to receive a report on the findings of the study by contacting the researcher at the conclusion of the project.
- I understand that I can contact the primary researcher Musabbir Khan at musabbir.khan@pg.canterbury.ac.nz or his supervisor Geoff Chase at geoff.chase@canterbury.ac.nz for further information. If I have any complaints, I can contact the Chair of the University of Canterbury Human Ethics Committee, Private Bag 4800, Christchurch (human-ethics@canterbury.ac.nz)
- I would like a copy of the results of the project via email at _____
- By signing below, I understand the project and agree to participate in this research project.

Name: _____ Signed: _____ : Date: _____

To return the consent form, you can either hand it to me personally at Room E209, Department of Mechanical Engineering, University of Canterbury, or email me the form at musabbir.khan@pg.canterbury.ac.nz

Musabbir Khan



HUMAN ETHICS COMMITTEE

Secretary, Rebecca Robinson
Telephone: +64 03 364 2987, Extn 45588
Email: human-ethics@canterbury.ac.nz

Ref: HEC 2016/16/LR-PS

9 March 2016

Musabbir Khan
Mechanical Engineering
UNIVERSITY OF CANTERBURY

Dear Musabbir

Thank you for submitting your low risk application to the Human Ethics Committee for the research proposal titled "Blood Flow Monitoring Using Photoplethysmography".

I am pleased to advise that this application has been reviewed and approved.

Please note that this approval is subject to the incorporation of the amendments you have provided in your email of 9th March 2016.

With best wishes for your project.

Yours sincerely

A handwritten signature in black ink, appearing to read 'Lindsey MacDonald'.

Lindsey MacDonald
Chair, Human Ethics Committee

Appendix 8.1: Ethics application information sheet, consent form, and approval



District Health Board

Te Poari Hauora o Waitaha



Information Sheet for Participants

The MOOSE Study: Non-invasive Monitoring of O₂ Saturation for Extraction in the peripheral region

Co-ordinating Investigator
Prof Geoffrey M Shaw Intensive Care Specialist, MBChB Department of Intensive Care Medicine Christchurch Hospital

Co-investigators
Dist. Prof J. Geoffrey Chase Professor at University of Canterbury Department of Mechanical Engineering University of Canterbury

Mr Musabbir Khan
PhD Student
Department of Mechanical Engineering
University of Canterbury

Dr Christopher G Pretty
Senior lecturer at University of Canterbury
Department of Mechanical Engineering
University of Canterbury

Introduction

The MOOSE Study focuses to non-intrusively monitor blood oxygen saturation in the peripheral blood vessels, such as in the finger, and estimate the amount of oxygen absorption (extraction) by muscles. Our research uses pulse oximeters, which are the ubiquitous sensors clipped over the finger. Pulse oximeters are widely used in hospitals to monitor arterial blood oxygen level and heart rate non-invasively. The sensor measures how light passes through the finger, so no physical harm or puncture is caused.

We have recently developed a concept that extends the pulse oximeter's ability to estimate both arterial and venous blood oxygen level non-invasively, including their difference (oxygen extraction), and blood flow from fingers. Monitoring of these parameters can potentially help in diagnosis and treatment of early microcirculation dysfunction, sepsis and other cardiovascular clinical disease.

Currently, this concept seeks validation with an established method. To achieve this goal, gas content of blood from real blood samples is required to be known, in order to get a true reference of oxygen level in both arteries and veins. Comparison with whole blood data will help validate this concept.

It is important that you read and understand this information sheet. It describes the purpose, procedures, risks, and your right to participate or withdraw.

The Study Protocol

To participate in this study you need to carefully read and understand the following:

- The subject needs to allow the following equipment attached to your hand during the duration of the experiment:
 - a. Insertion of peripheral arterial (in the radial artery, close to the wrist) and IV catheters (in the dorsal digital vein, located in the top side of the finger) for blood sample collection:
 - All blood samples will be drawn ONLY by a professional medical doctor (Prof G Shaw, Intensive Care Specialist, MBChB, Christchurch hospital, New Zealand).
 - A mild discomfort might be caused due to the insertion of catheters in the hand.
 - b. A custom non-invasive pulse oximeter sensor in the index/middle finger of your left hand.
 - Data will be acquired for non-invasive blood oxygen level and blood flow assessment.
 - All non-invasive data will be collected by Musabir Khan (PhD Candidate, University of Canterbury).
 - c. A commercial non-invasive pulse oximeter sensor in the ring finger of your left hand
 - Heart rate, arterial blood inflow, and oxygen saturation data will be monitored on a screen.
 - d. A non-invasive, surface mount thermocouple probe needs to be taped to the corresponding finger, next to the sensor:
 - This probe will continuously record temperature reading from the surface of your skin.
 - e. An air filled digit pressure cuff around your finger, adjacent to the finger sensor.
 - The digit cuff will be automatically inflated and deflated using an artificial pulse generation system and pressurized air supply
- You will be asked to perform the following procedures in sequence with the above equipment attached to your hand:
 - i. Hold arm at chest level
 - ii. Raise arm above head
 - iii. Allow pressure cuff induced vascular occlusion for 2 min
 - iv. Allow pressure cuff induced vascular occlusion for 4 min
 - v. Allow pressure cuff induced vascular occlusion for 6 min
- a. Arterial blood will ONLY be drawn once at the beginning of (i) for a reference measurement.
- b. During each of the above activities, two blood samples (approximately 2 ml per sample) will be drawn from the venous line.
- c. After each of the above activities, you will be given 5-10 minutes before the next procedure
- d. A total of 11 blood samples will be drawn.
 - 10x venous blood draw will be made with the IV catheters
 - 1x arterial blood draw will be made with peripheral arterial
- e. The study protocol can take up to 1 hour to complete.
 - Each activity will last for ~10 mins.
 - A break of ~3 min will be given between each activity

Canterbury

District Health Board

Te Poari Hauora o Waitaha



- Your resting heart rate (HR) and blood-pressure will be measured to ensure you are fit (<80 beats per minute) before the study commences. In addition, your height, weight and body temperature will also be recorded.
- You will be seated in a comfortable chair/sofa with both of your arms rested on a flat surface and make minimum movement during the experiment (approx. 15-60 mins).
- You should avoid any smoking, alcohol consumption, and strenuous physical activities at least 4 hours prior to the trial.

Other Information

Study Approval

This study has received ethical approval from the Health and Disability Ethics Committee, New Zealand.

Location of Study

The study is proposed to be carried out in an intensive care facility (St Georges Hospital ICU, Christchurch), where the participants will have continuous recordings of their blood pressure during the procedure. Prof G Shaw and a nurse will be immediately available in the unlikely event of any adverse reaction.

Selection of Participants

Healthy adult participants with no cardiovascular dysfunction or other pre-existing medical conditions are recruited for this study. You must inform the investigators about any medical conditions you have. However, no restriction on gender or ethnicity applies.

Risks

The risks applied to you for participating in this study are minimal. Insertion of catheters in the hand may cause some discomfort or minor injury. These risks are mitigated by performing the study in a suitable clinical environment with nursing support. The procedure will be carried out by the coordinating investigator, Prof G Shaw, who has 29 years of experience as a medical practitioner, and over 20 years as a specialist intensive care clinician.

Stopping participation in this study

Taking part in this project is voluntary. You can leave at any time if you want, without penalty. This is most likely if there is a technical failure of the equipment or difficulties in obtaining arterial or venous access. The investigators will seek permission to use any data collected up to that time, otherwise it will be destroyed.

Confidentiality

If you participate in this study, your National Health Information (NHI) number or any personal details that could identify you will not be used. You will not be personally identified in any reports on this study. A unique number will be assigned to you when undertaking the trial, so that your data will not be identifiable in anyway except to the investigators. Your medical information will be processed on a secured computer. All related data will be stored in an encrypted hard drive for up to 20 years,

Canterbury

District Health Board

Te Poari Hauora o Waitaha

and then destroyed. However, no sensitive information will be collected, discussed or shared even amongst the research team. Only information that is directly relevant to this study will be used.



De-identified information may be shared amongst other researchers in this field. Results of this study will be presented at conferences and submitted for publication in medical and bioengineering journals. By signing the accompanying form, you agree to participate in this research, the record review, information storage, and data transfer described above.

Contact Details

For any questions or concerns about the study, feel free to contact any of the study investigators using the following contact information:

Co-ordinating Investigator

Professor Geoffrey M Shaw
Intensive Care Specialist, MBChB
Department of Intensive Care Medicine
Christchurch Hospital
Phone: (03) 364 1077
Email: Geoff.Shaw@cdhb.health.nz

Co-ordinating Investigator 1

Dist. Prof J. Geoffrey Chase
Professor at University of Canterbury
Department of Mechanical Engineering
University of Canterbury
Phone: (03) 364 2987 ext. 7224
Email: geoff.chase@canterbury.ac.nz

Co-ordinating Investigator 2

Dr Christopher G Pretty
Senior lecturer at University of Canterbury
Department of Mechanical Engineering
University of Canterbury
Phone: (03) 364 2987 ext. 7234
Email: chris.pretty@canterbury.ac.nz

Co-ordinating Investigator 3

Mr Musabbir Khan
PhD Student
Department of Mechanical Engineering
University of Canterbury
Phone: (02) 212 02606
Email: musabbir.khan@pg.canterbury.ac.nz

If you would like to take part in this project, please fill out the attached CONSENT FORM.

Thank you for considering participation in this study.

Canterbury

District Health Board

Te Poari Hauora o Waitaha



Geoff Shaw,

Co-ordinating Investigator

Consent Form for Participants**The MOOSE Study: Non-invasive Monitoring of O₂ Saturation for Extraction in the peripheral region**

Lay title:	The MOOSE Study
Co-ordinating investigator:	Prof Geoffrey M Shaw
Participant's name:	

I have read and I understood the information sheet dated (____/____/____) for people taking part in the MOOSE study. I have had the opportunity to discuss this study. I am satisfied with the answers I have been given.

I have had the opportunity to use family support or a friend to help me ask questions and understand the study.

I understand that taking part in this study is voluntary and I can withdraw from the study at any time I wish.

I understand that my participation in this study is confidential and that no material which could identify me will be used in any reports on this study.

I understand that the study will be stopped if it should appear to be harmful.

I know whom to contact if I have any questions about the study.

This study has been given ethical approval by the Health and Disability Ethics Committee, New Zealand. This means that the Committee may check at any time that the study is following appropriate ethical procedures.

I understood the risks involved in this study Yes No

I agree to participate in this study under my own consent Yes No

I wish to receive a copy of my results. Yes No

Signature:

Printed name:

Date:

 / / 201__

Canterbury

District Health Board

Te Poari Hauora o Waitaha



Address for results:

Full names of researchers:

Prof Geoffrey M Shaw
Dist. Prof J Geoffrey Chase
Dr Christopher G Pretty
Mr Musabir Khan

Contact phone number for researchers:

(03) 364 1077, (03) 364 2987, (02) 212 02606

Project explained by:

Date:

/ / 201__

Signed:

Date:

(Co-ordinating Investigator)

**Health and Disability Ethics Committees**

Ministry of Health
Freyberg Building
20 Aitken Street
PO Box 5013
Wellington
6011

04 816 3985

hdecs@moh.govt.nz

25 September 2015

Professor Geoffrey Shaw
Department of Intensive Care
Christchurch Hospital
Private Bag 4710
Christchurch 8011

Dear Professor Shaw

Re:	Ethics ref:	15/CEN/141
	Study title:	Non Invasive Monitoring of Peripheral Oxygen Extraction

I am pleased to advise that this application has been approved by the Central Health and Disability Ethics Committee. This decision was made through the HDEC-Expedited Review pathway.

Summary of Study

- The Committee notes that the Participant Information Sheet names the Southern Health and Disability Ethics Committee as the approving committee, however this application has been approved by the Central committee.

Conditions of HDEC approval

HDEC approval for this study is subject to the following conditions being met prior to the commencement of the study in New Zealand. It is your responsibility, and that of the study's sponsor, to ensure that these conditions are met. No further review by the Central Health and Disability Ethics Committee is required.

Standard conditions:

1. Before the study commences at *any* locality in New Zealand, all relevant regulatory approvals must be obtained.
2. Before the study commences at *any* locality in New Zealand, it must be registered in a WHO-approved clinical trials registry (such as the Australia New Zealand Clinical Trials Registry, www.anzctr.org.au).
3. Before the study commences at a *given* locality in New Zealand, it must be authorised by that locality in Online Forms. Locality authorisation confirms that the locality is suitable for the safe and effective conduct of the study, and that local research governance issues have been addressed.

After HDEC review

Please refer to the *Standard Operating Procedures for Health and Disability Ethics Committees* (available on www.ethics.health.govt.nz) for HDEC requirements relating to amendments and other post-approval processes.

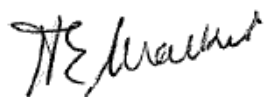
Your next progress report is due by 25 September 2016.

Participant access to ACC

The Central Health and Disability Ethics Committee is satisfied that your study is not a clinical trial that is to be conducted principally for the benefit of the manufacturer or distributor of the medicine or item being trialled. Participants injured as a result of treatment received as part of your study may therefore be eligible for publicly-funded compensation through the Accident Compensation Corporation (ACC).

Please don't hesitate to contact the HDEC secretariat for further information. We wish you all the best for your study.

Yours sincerely,



Mrs Helen Walker
Chairperson
Central Health and Disability Ethics Committee

Encl: appendix A: documents submitted
appendix B: statement of compliance and list of members

Appendix A
Documents submitted

<i>Document</i>	<i>Version</i>	<i>Date</i>
PIS/CF: Participant Information and consent form	2.0	09 September 2015
Evidence of scientific review: Scientific review form Professor Scott Parkes	1.0	20 July 2015
CV for CI: Updated CV for GM Shaw	20-08-2015	20 August 2015
Covering Letter	1.0	04 September 2015
Protocol	1.0	04 September 2015
Application	1	10 September 2015

Appendix B
Statement of compliance and list of members

Statement of compliance

The Central Health and Disability Ethics Committee:

- is constituted in accordance with its Terms of Reference
- operates in accordance with the *Standard Operating Procedures for Health and Disability Ethics Committees*, and with the principles of international good clinical practice (GCP)
- is approved by the Health Research Council of New Zealand's Ethics Committee for the purposes of section 25(1)(c) of the Health Research Council Act 1990
- is registered (number 00008712) with the US Department of Health and Human Services' Office for Human Research Protection (OHRP).

List of members

Name	Category	Appointed	Term Expires
Mrs Helen Walker	Lay (consumer/community perspectives)	01/07/2012	01/07/2015
Dr Angela Ballantyne	Lay (ethical/moral reasoning)	01/07/2015	01/07/2018
Dr Melissa Cragg	Non-lay (observational studies)	01/07/2015	01/07/2018
Dr Peter Gallagher	Non-lay (health/disability service provision)	01/07/2015	01/07/2018
Mrs Sandy Gill	Lay (consumer/community perspectives)	01/07/2015	01/07/2018
Dr Patries Herst	Non-lay (intervention studies)	01/07/2012	01/07/2015
Dr Dean Quinn	Non-lay (intervention studies)	01/07/2012	01/07/2015
Dr Cordelia Thomas	Lay (ethical/moral reasoning)	19/05/2014	19/05/2017

Unless members resign, vacate or are removed from their office, every member of HDEC shall continue in office until their successor comes into office (HDEC Terms of Reference)

<http://www.ethics.health.govt.nz>